Arc bk

RAPID THERMAL CALIBRATION OF HOUSES

R.Everett

ERG 055 1944

This work has been funded by the Science and Engineering Research Council under two contracts:-

Accelerated Thermal House Calibration (GR/C/36773)

Monitoring Implications of the Pennyland and Linford Projects (GR/D/44997).

This report describes the development of a method for determining the basic thermal properties of a house, its fabric heat loss, basic air infiltration characteristics and response to solar gains in a short period of intensive measurement, typically two to three weeks. The relation of these results with occupied house measurements is also discussed and the work is illustrated by data from three housing field trials in Milton Keynes.

ACKNOWLEDGEMENTS

The author would like to thank the following people for their help:-

John Wiltshire of S.E.R.C. for his funding help in sustaining the Pennyland and Linford projects.

David Bartholomew of ETSU for the use of the Linford test house facility.

Bob Lowe who has given much statistical help and was responsible for the analysis of the Pennyland data.

Alan Horton, who carried out the Linford air infiltration measurements, analysed the Linford occupied house data and designed the D.I.Y. heat flux sensors.

Brian Ford, who set up the Spencer St. conservatory project.

John Butler for his contribution on the automatic ventilation rate measurement rig.

David Etheridge of British Gas who supplied the basic air infiltration model and many measurements.

Jack Siviour of E.C.R.C. who has provided the basic thermal calibration method and much practical sound advice.

Alan Reddish for his help in checking the final report.

PREFACE

When Brian Ford first enticed me to try out Jack Siviour's thermal calibration technique on his greenhouse project in 1981, I thought for a while that it might be possible to speed up and simplify house thermal testing dramatically. It might even have been possible to get architects to test their own house designs!

Alas, the Linford project has shown that if you want to know one thing about a house (such as the solar gains), you have to know everything else. Some things, such as the floor heat loss, have turned out to be totally mystifying. Others, like air infiltration are mind-bogglingly complicated but do make a kind of sense.

This report aims to give advice to those fool enough to want to test the thermal performance of a house. I have attempted to describe the various topics as simply as possible, but some, such as the statistical theory, remain resolutely fuzzy, a sure sign that further work is needed.

Happy Reading,

Bob Everett August 1985

CONTENTS

The projects mentioned in this report all have individual full monitoring reports and this is, in effect, a common technical appendix to all of them.

Project reports:-

Thermal performance monitoring of a terrace house with conservatory, New Bradwell, Milton Keynes, Brian Ford, Royal College of Art Dept. of Design Research, December 1982.

Linford Low Energy Houses, R.Everett, A.Horton, J.Doggart & J.Willoughby, Open University Energy Research Group, Jan 1985 (ERG 050).

The Pennyland Project, Dr.R.Lowe, Prof.J.Chapman, R.Everett, O.U.E.R.G., July 1985 (ERG 053).

1. INTRODUCTION

CONTENTS

This chapter outlines the three housing projects that have supplied data used in this report and outlines the contents of the other chapters.

CHAPTER 1

INTRODUCTION

This report initially just set out to describe the development of a method for the rapid thermal calibration of houses, i.e. empirically determining the total house fabric loss and its response to passive solar gains. However, because good agreement was achieved between thermal calibration results and analysis of occupied house data, the report has been extended to cover comparisons of occupied house and experimental test house results.

The basic thermal calibration method was originally used by J.Siviour of the Electricity Council Research Centre as a way of determining the fabric heat loss of a house alone, given at least six weeks measurements. A description of this method was presented as a paper to a conference in Liege in 1981 (see Appendix 1).

The method has been used in two passive solar projects in Milton Keynes, the Spencer St. conservatory project and the Linford direct gain project. It has been extended to determine the effects of passive solar gains on space heating and also to reduce the time period required. The length of time necessary to obtain a reasonable thermal calibration is highly dependent on the weather, especially the mix of sunny and dull days. Given typical winter conditions in central/ southern U.K. a period of two weeks is sufficient, though three weeks should be allowed for worst-case conditions.

The method has been extended to occupied houses in the Linford and Pennyland housing projects.

1.1 Spencer St. Project

In October 1981, the method was tried out on a small terraced house with attached conservatory in New Bradwell in the north of Milton Keynes. This was one of a street of 19th Century houses which were refurbished by Milton Keynes Development Corporation in 1977. This involved dry lining and insulating the solid brick walls with 75 mm insulation as well as the provision of 75 mm roof insulation. (see figure 1.1). The conservatory was added in 1979.

The house was the subject of design studies with a view to improving the performance of the conservatory. It was monitored in detail over the winter of 1980/81 and the autumn of 1981 by Brian Ford of the Royal College of Art, with assistance from the Alternative Technology Group of the Open University. The work was funded by the Energy Technology Support Unit at Harwell as part of the Department of Energy's programme of passive solar energy research.

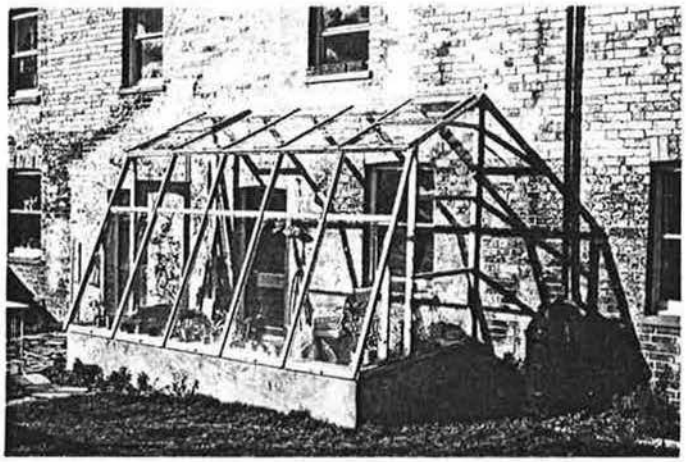

View from the back garden

Figure 1.1 Terraced House With Attached Conservatory, Spencer St.,Milton Keynes.

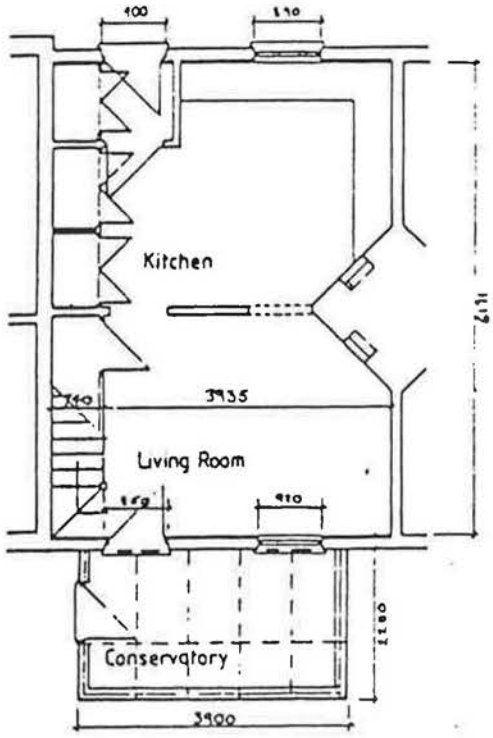

Ground floor plan

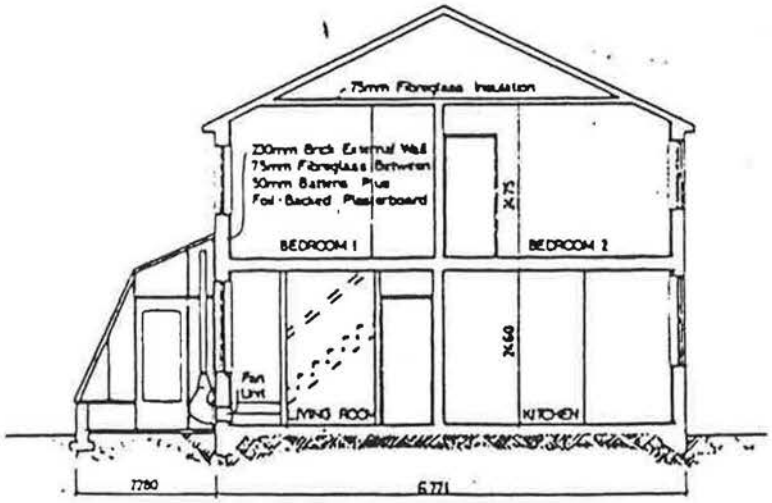

SECTION THROUGH TEST HOUSE, NEW BRADWELL, MILTON KEYNES

Section through test house

Although the house was available for detailed experiments for three weeks in October 1981 while the occupants were on holiday, only seven days actual measurements resulted. The other two weeks were taken up with sorting out (and making) monitoring equipment. However, these seven days data were sufficient to determine the effects of solar radiation on the house heating demand and give a certain amount of information about the mechanisms of heat storage and transfer through the conservatory. It was not possible to determine the fabric loss of the house because of various omissions in the measurements, notably the floor heat loss and losses into the adjacent terraced houses.

The results of this test showed considerable promise for a rapid method of experimentally determining the thermal properties of houses. They were used in support of the research proposal to S.E.R.C. submitted in April 1982. This was for two years work to study the problems of the method and in particular applying it to another passive solar project in Milton Keynes at Great Linford. This funding was granted and started in January 1983, though much of the experimentation and analysis documented here actually predates this.

1.2 The Linford Project

This is a scheme of eight direct gain passive solar houses, also funded by the Department of Energy's Passive Solar Programme. They have a large area of south-facing glazing and a high standard of insulation. They have 100 mm cavity wall insulation, 150 mm roof insulation and double glazing.(see figure 1.2).

The houses were built during 1980 and 81 and were monitored during the winters of 81/82 and 82/83 by the Energy Research Group of the Open University. One house was designated a test house and equipped with a wide range of sensors including an automatic air infiltration measurement rig.

The project has allowed 10 months of detailed testing, over the period March 1982 to May 1983, during which time various modifications were made to the test house, including insulating over the floor with 50 mm polystyrene and altering the effective transmissivity of the windows. These thermal calibration tests have served not only to evaluate the performance of this house design but also to examine the validity and consistency of the method itself, whether it is capable of producing the same answers from successive short-run data sets.

Fortunately, the method appears to work quite well and answers from successive two-week periodsare consistent within the measurement accuracy of the raw data. Surprisingly, further measurements have shown that the test house results are a good description of the performance of at least three of the adjacent occupied houses, which suggests both a uniformity of house construction as well as of experimental method, though considerable assumptions have had to be made in the process.

Great Linford houses: North (top) and South (above) elevations

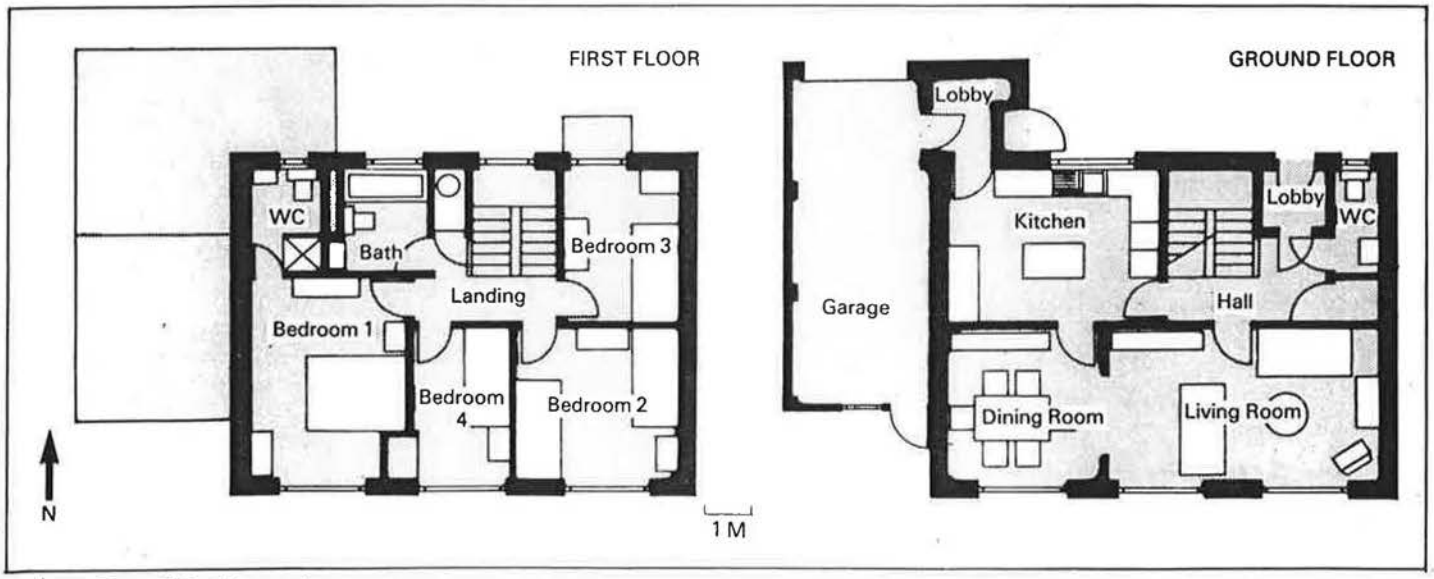

Great Linford house plans

Fig. 1.2 Great Linford passive solar houses

The test house measurements discovered considerable problems in the determination of heat losses through solid floors. This has led to a requirement for them to be measured separately. These difficulties are described briefly in Chapter 3, but are dealt with in greater detail in the main Linford project report.

Air infiltration measurements have turned out to be very important. Much of the Linford test house analysis has been devoted to the development of an air infiltration model allowing missing measurements to be filled in from calculations using measured weather data. This process is described briefly in Chapter 4 but again readers are referred to the main Linford report for full details. A brief section on pressure leakage tests is included, since although they are not part of the thermal calibration method, they have proved very quick and effective in assessing the likely air infiltration of houses.

An important part of a rapid thermal calibration process is to have measuring equipment that is simple, reliable and preferably not excessively expensive. Chapter 5 deals with logging and measurement equipment, given the experience of these and other projects.

Fortunately over the past five years datalogging has become a lot simpler with more reliable loggers and a flood of microcomputers which can easily be interfaced to sensors. Chapter 5 describes practical equipment, including cheap heat flux sensors made for the Linford project and the conversion of the air infiltration rig to automatic operation. It also describes the practical thermographic survey carried out at Linford which gave very rapid information on thermal defects.

Chapter 6 deals with the statistics of weather, the availability of a suitable mix of sunny and dull days throughout the year. It also looks at the self-consistency of the basic method, the problems of covariance between solar radiation and air temperature and at a slightly different method of analysing the measurements. These topics have a certain bearing on the analysis of data from occupied houses, in particular those of the large scale Pennyland field trial.

1.3 The Pennyland Project

This is another passive solar project, adjacent to the Linford houses in north Milton Keynes. This has been jointly funded by the Department of Energy and Department of Environment. It involved over 200 houses and took the basic form of comparisons of energy consumptions for houses at four levels of insulation and three levels of 'solar design'.

The Pennyland Estate was built during 1980 and was monitored over the winters of 1981/82 and 82/83 by the Energy Research Group, in parallel with the Linford project.

Pennyland Single Aspect House: North (top) and South (above) elevations

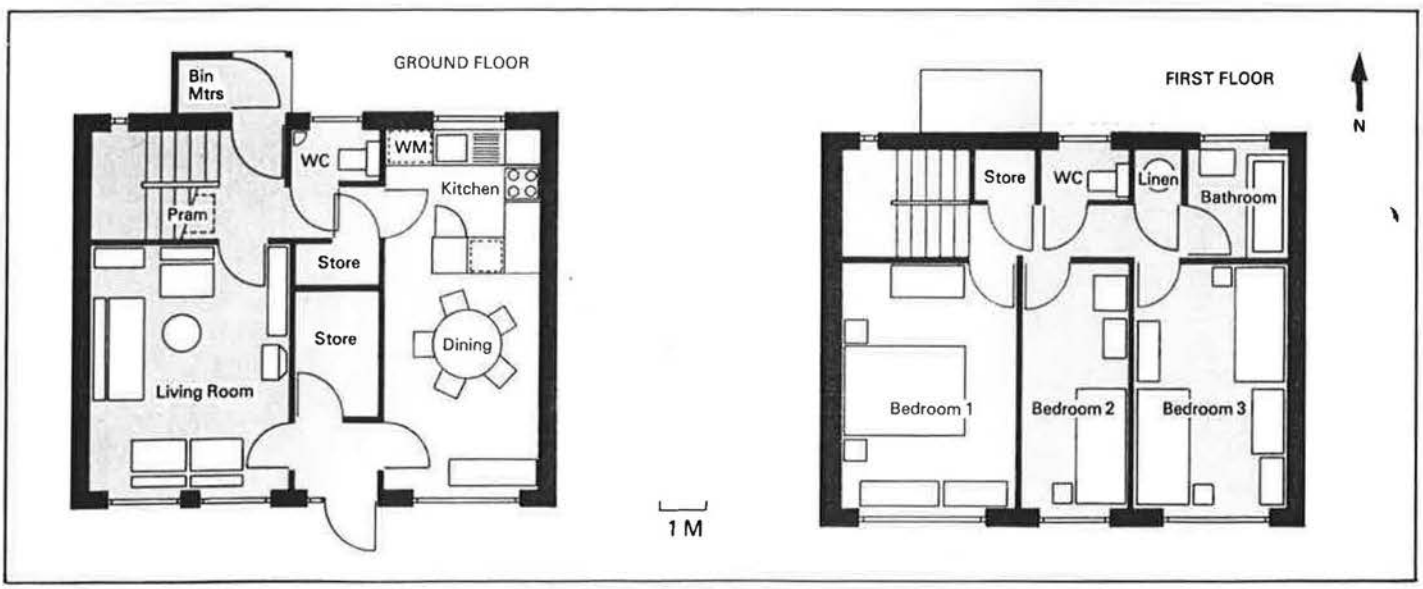

Pennyland house plans

Figure 1.3 Typical Pennyland House Design

It was realised during the design of the project that crude energy comparisons would not be very informative because of the spreads of occupants' behaviour. Thus 80 of the houses were equipped with simple monitoring operating on a weekly average basis. It was hoped that using this data set a degree of 'house characterisation' could be acheived, i.e. extracting a house heat loss coefficient and one for the degree of solar performance, though there was no information on the statistical problems of doing this.

After much careful analysis work, also funded by S.E.R.C., it appears that it is possible to extract rough estimates of house heat loss coefficients, sufficient to show that one house is better insulated than another. Attempts to show that one house design is more 'solar' than another have only met with marginal success and detailed thermal calibration tests are really necessary. The statistical problems of this analysis are discussed in Chapter 6, though for other details of the Pennyland project readers are referred to the main project report.

Chapter 7 deals briefly with methods for coping with thermal timelags due to thermal mass in the basic daily regressions. This involves the use of 'weighting factors' derived from response factor modelling theory, to be used with measured internal and external temperatures. Although these timelag problems seemed important at the outset of the project, they have rather paled into insignificance compared with the practical problems of errors in the measurement of air infiltration rates and floor heat losses. However, they may still be of use in the assessment of well insulated houses with long thermal time constants.

Chapter 8 draws together the conclusions of this report and outlines possibilities for a thermal calibration kit that could possibly go on tour testing a different house every month.

Since this report covers several projects, each graph has been labelled with an identifying picture, to avoid confusion:-

LINFORD 

PENNYLAND 

SPENCER ST. 

2. BASIC METHOD

CONTENTS

This chapter describes the basic thermal calibration procedure with examples from the Spencer St. and Linford projects.

CHAPTER 2

BASIC METHOD

This consists essentially of constructing a careful energy balance for an unoccupied house. By measuring the space heating energy and the resulting house inside-outside temperature difference, the total fabric heat loss of the house can be deduced. The method is complicated by the presence of solar gains of a generally unknown magnitude plus a continuously varying air infiltration loss and, if the house has a solid slab floor, a floor heat loss with curious dynamic properties.

The energy balance can be written as:-

$$Q + R.S = (\Sigma A.U)\Delta T + C_V.\Delta T + F$$

Space heating + Solar Gains = Fabric Heat Loss + Air Infiltration + Floor Loss

In the case of a terrace house there will be an extra term due to heat losses through the party walls into the adjacent houses.

In order to build a proper energy balance, it is necessary to look at each of these terms in detail, as well as at the statistics required to extract the unknowns in the equation, the fabric heat loss and the coefficient of solar gains. The fabric heat loss is essentially determined by looking at the energy balance on dull days and the solar performance by comparing the performance on dull and sunny ones.

2.1 Space Heating

For ease of control and monitoring the test houses have been heated with electric fan heaters with individual electronic thermostats (see Chapter 5). This allows the house to be maintained as far as possible at a uniform constant internal temperature. This tends to minimise the effects of day-to-day energy storage in the building fabric and makes it easier to work out a genuine 'average' house internal temperature. For the Spencer St. house only one heater was used, but two (one upstairs and one downstairs) would have been much better. For the larger Linford house, a total of five were used. The outputs of the five individual controllers were separately monitored, showing the distribution of solar gains throughout the house, though this is not essential to the method.

The house should be run at as high an internal temperature as is feasible (25°C was used in the Linford house). This has several beneficial effects:-

1. The resultant inside-outside temperature difference is large compared to the errors in temperature measurement.
2. The solar gains are less likely to totally displace the space heating during the day, thus upsetting the constant internal temperature.
3. A high ΔT reduces the variation of air infiltration with wind speed, making it easier to fill in missing values.

The house should be heated up to the test internal temperature for at least two and preferably three whole days before measurements begin. This can be done while other equipment is being set up.

2.2 Solar Gains

All houses are to a certain extent solar heated and the magnitudes of solar gains can be quite significant. For a normal house solar gains enter through windows on all sides plus a certain amount which is conducted through the opaque fabric of the walls and roof. For passive solar designs such as those tested here, most of the glazing is concentrated on the south side of the house, with glazing on other facades reduced to a minimum. This simplifies calculations considerably and it has been assumed that solar gains on a daily basis are a linear function of solar radiation on the south-facing vertical surface outside the house. This choice of solar variable, rather than the more normal horizontal solar radiation is a reasonable compromise between a 'meteorological' quantity and something that related only to one house on one site.

Figure 2.1 shows calculated solar gains transmitted through both south and north-facing windows of a Linford type house as a function of south-facing vertical solar radiation, both quantities having been calculated from hourly values of horizontal solar radiation. The relation between the two is fortunately very linear and the coefficient relating them defines an equivalent clear south-facing solar aperture, in this case of approximately 13 m^2.

This 'solar aperture' is purely a tool of convenience and is only roughly related to the actual window areas and transmissivities. Given that typically solar radiation on the north-facing surface of a building is about one third of that on the south-facing surface, the solar aperture can be calculated as:-

$$\text{Solar Aperture} = (A_s + A_n/3) \times \tau\alpha$$

where A_s = Net area of south-facing glazing (i.e. excluding frames)

A_n = Net area of north-facing glazing

τ = transmission of glazing including the effects of obstructions (net curtains, etc)

α = absorptivity of room (taking into account colour of paint, etc.)

Solar gains through the opaque fabric have been ignored, but are likely to amount to an extra 5% or so.

For a more complex house, such as one with an attached conservatory, the solar aperture may be almost impossible to calculate simply and may really only exist as a rough experimental relation between solar radiation and solar gains to the house.

The solar aperture defined here is similar in function to the solar 'recuperation factor' used in the 'temperature without heating' method of analysis developed in Belgium (ref. 2.1). As a result the symbol R has been adopted.

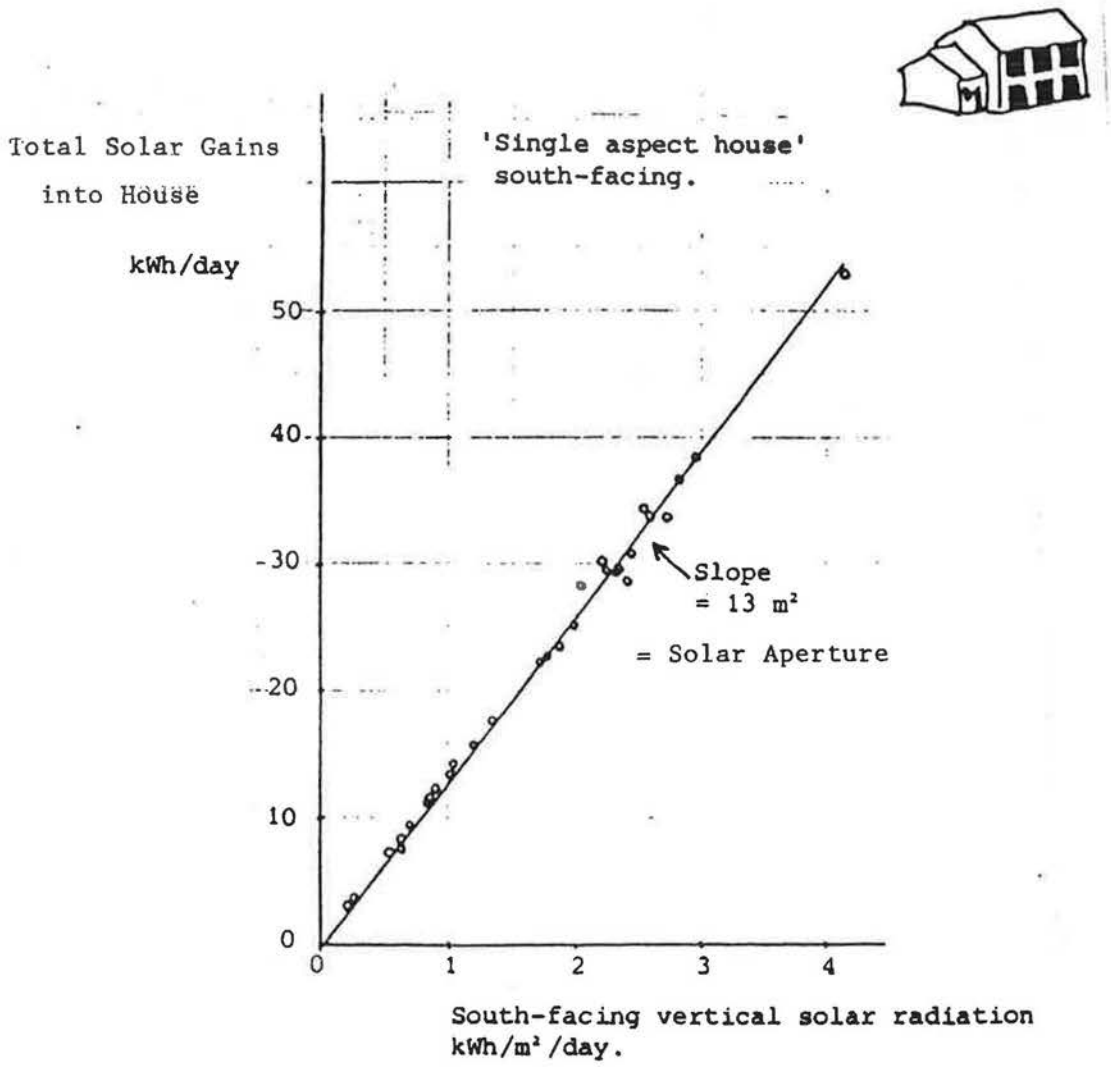

Figure 2.1 The ratio of calculated solar gains into the house through both south and north facing windows is a linear function of solar radiation on the south-facing vertical surface outside the house.

For houses of a more normal design with windows on several sides, it is recommended that the calculations be carried out using a composite solar aperture based on a weighted average of measured solar radiation on the various surfaces according to the relative window areas. This does, however, make it a little difficult to compare the relative solar performance of different houses, though in this case it may not be very important.

2.3 Fabric Heat Loss

This is the main unknown that has to be determined, essentially the heat loss of the walls, windows and roof and also the floor if this is of suspended timber construction. As such it is the product of the individual areas and U-values of the components plus the effects of various cold bridges.

Although the individual U-values of components can be easily determined in test cells using heat flux sensors, what we are concerned with here is the practical sum of all these components in a real house with possible design or construction defects. These defects can be easily judged qualitatively using thermographic techniques (see Chapter 5), but they also need to be assessed quantitatively.

2.4 House Temperature Difference

The accuracy of the determination of the fabric heat loss depends largely on the accuracy of the measurement of the temperature difference between the inside and outside of the house. Having attempted to keep the internal temperature as constant as possible, the external temperature must be determined accurately.

The practical problems of temperature measurement are dealt with in Chapter 5, but there are also theoretical problems concerning the effects of solar radiation.

The external air temperature at Linford was measured in a normal Stevenson Screen. This is essentially a louvred wooden box, but can be thought of as a crude passive solar test cell with a certain amount of solar gains of its own. These solar gains may upset the determination of a solar aperture for a house, as is described in Chapter 6. It would seem best that external temperature measurements are made with an aspirated temperature sensor, in order to get a true air temperature. These solar effects are unlikely to change the estimate of fabric heat loss, though, since this is dependent on the house performance on dull days.

2.5 Air Infiltration Loss

This may vary considerably from hour to hour and thus must be measured continuously. The relation of air infiltration to house ΔT, wind speed and direction is very complex and is discussed in chapter 4.

2.6 Floor Loss

Measurements on the solid concrete floor at Linford showed that this had curious dynamic thermal properties and was not related to the same ΔT and the rest of the building fabric. The details of this are given in chapter 3.

The effects of changing floor heat loss had a disturbing effect on initial analysis regressions for the whole house, producing overestimates of the solar aperture. This kind of effect is discussed in chapter 6.

For practical purposes it thus seems necessary to measure the floor heat loss as a total unknown with heat flux sensors and enter it separately into the house energy balance.

2.7 Losses Through Party Walls

For a terraced house, especially if it is being run at a high internal temperature, there will be appreciable heat losses into adjacent houses. These can easily be overlooked, as was the case with the Spencer St. house, even though the datalogger was actually in one of them.

Fortunately these losses do not pose really serious problems of massive variation or strange dynamics and could probably be estimated with only two heat flux sensors in each party wall. The main problem is really that of the desirablility of measuring temperatures in the adjacent houses and any inconvenience that this might cause.

2.8 Analytic Methods

Having drawn up a house energy balance:-

$$Q + R.S = (\Sigma A.U + C_V).\Delta T + F$$

we can look at it in two possible ways.

One is to treat R, the solar aperture, $\Sigma A.U$, the fabric heat loss and F, the floor loss, as unknown constants.

By regressing measured Q against S and ΔT we can attempt to extract these coefficients. This is equivalent to fitting a mathematical plane surface through data plotted in a 3-dimensional space bounded by the Q,S and ΔT axes as shown in figure 2.2.

This method has various statistical problems which are discussed in Chapter 6. It has not been very fruitful for test house work directly, but has been more useful for the analysis of occupied house data from the Pennyland project. It has been useful for looking at the effects of experimental errors in test house measurements for the second method below.

$$Q = F + (\Sigma A.U + C_v).\Delta T - R.S$$

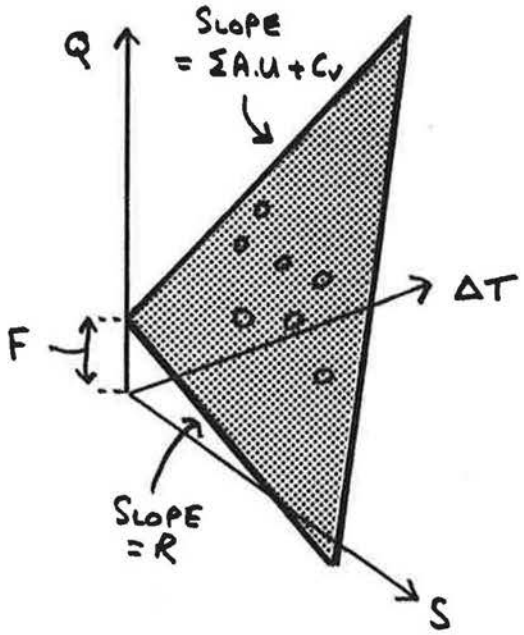

Figure 2.2 3-Dimensional Regression Plot

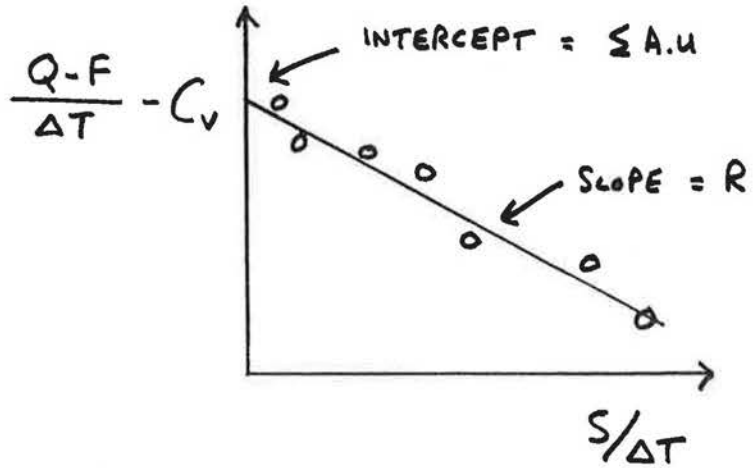

$$\frac{Q-F}{\Delta T} - C_v = \Sigma A.U - R.S/\Delta T$$

Figure 2.3 2-Dimensional Form

Two ways of plotting out house heat balance data

Alternatively, we can take F and C_v as measured known quantities and the heat balance equation can be rewritten:-

$$\frac{Q - F}{\Delta T} - C_v = \Sigma A.U - R.S$$

Thus by plotting $(Q-F)/\Delta T - C_v$ against $S/\Delta T$, we get a graph whose Y-intercept is $\Sigma A.U$ and whose slope is R, the solar aperture. This plot is shown in figure 2.3.

This graph, suggested by J.Siviour of the E.C.R.C., has been used for the determinationnof the solar apertures and fabric heat losses of both the Linford test house, and by including free heat gains from cooking, lights, etc. in Q, also for the occupied houses.

Although this is a mathematical transformation of the 3-dimensional plot, it can be thought of as being roughly equivalent to a projection of the data, edge on to the fitted plane, back on to the surface bounded by the Q and S axes in figure 2.2. If ΔT does not vary over the data set, which is almost the case in short runs of data, it is exactly equivalent.

2.9 Choice of Timescale

It is fairly obvious from figure 2.3 that in order to get a good estimate of $\Sigma A.U$ we need a fair number of data points hard up against the Y-axis, i.e. some dull weather, and also to get a good fix on R, we need a good spread of values of $S/\Delta T$, i.e. some sunny weather as well. As originally suggested by Siviour, using weekly data averages, this involved at least six weeks measurements in order to get enough appropriate weather.

Measurements on the Linford house during the spring of 1982 produced a data set of ten weeks, none of which were very dull and which had a poor scatter of values of $S/\Delta T$. Thus despite careful measurements over a long period of time, it was not really possible to extract hard estimates of $\Sigma A.U$ and R.

Switching to a daily basis for analysis produced a wider spread of values of $S/\Delta T$, including a large number of very dull days. This is illustrated by comparing figures 2.4 and 2.5 from the Linford winter 1983 dataset. The two plots do,in fact,give very similar results, but this is only because care was taken over the determination of the floor heat loss. For the spring 1982 dataset the comparison of small changes in weekly average space heating with small changes in weekly average solar radiation were completely upset by a large change in floor heat loss, which was completely unsuspected.

The price that is paid for switching to a daily, rather than weekly basis, is that of having to attend to thermal timelags from day to day, especially in the storage of solar radiation. For this it is necessary to look at the effects of solar gains on space heating on an hourly basis.

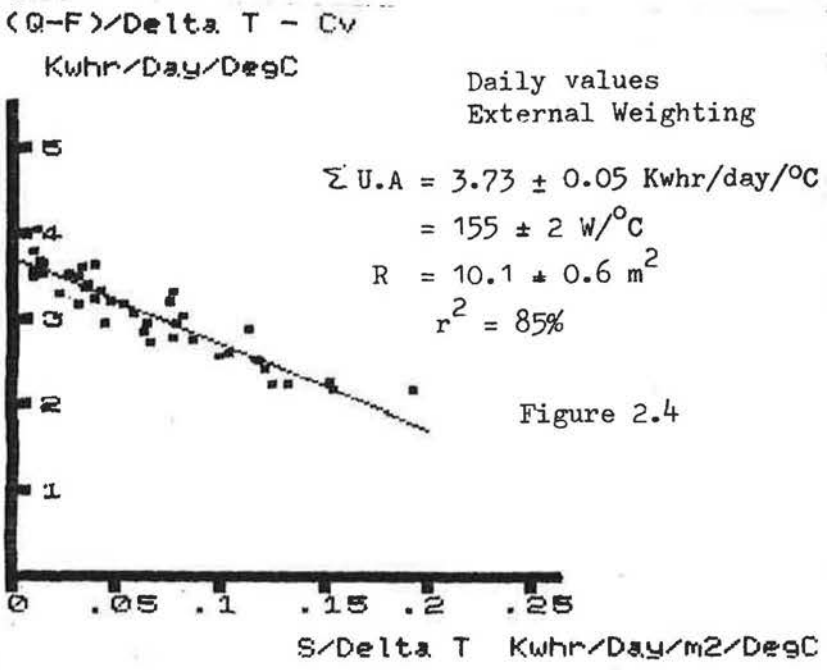

Figure 2.4

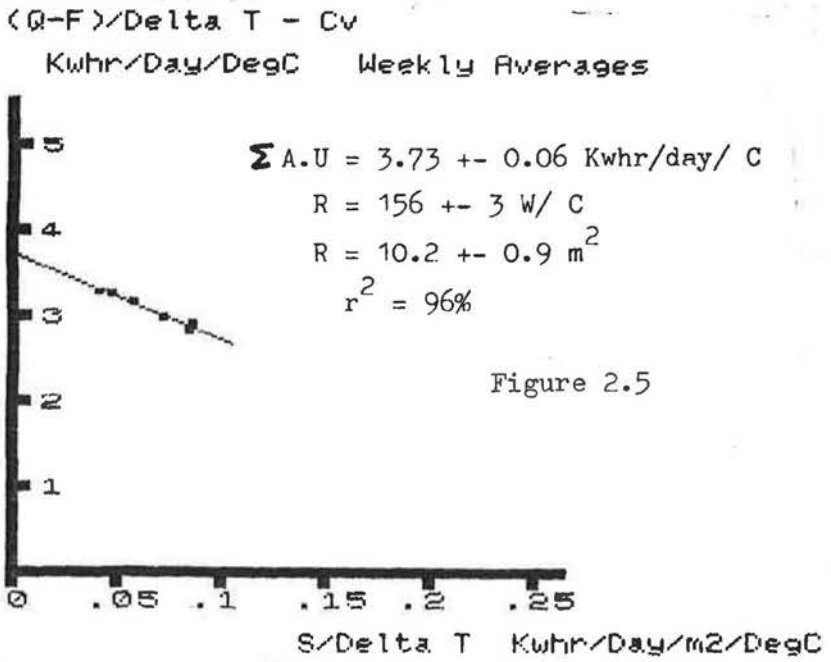

Figure 2.5

Daily averages of data show a wider spread of values of $S/\Delta T$ than weekly averages. The results are similar, though the daily data gives smaller error limits.

2.10 Daily Cycle - Direct Gain House

Figure 2.6 shows a plot of measured space heating for the Linford test house for a dull day followed by two sunny ones. It also shows measured inside surface heat fluxes at four points, two on the floor just inside the window (the sun actually shone on the floor over them) and two on the inside wall surfaces.

The daily pattern of events on a sunny day is roughly as follows:-

1. The sun rises.

2. The external air temperature begins to rise rapidly.

3. Solar radiation enters the windows, striking the floor.

4. A small proportion of this radiation penetrates the carpet and is absorbed in the floor beneath.

5. The remainder of the radiation is dispersed in the air inside the house.

6. This energy, together with the rapid reduction window and ventilation losses due to the rising external temperature leads to a slight rise in internal temperature.

7. This rise in temperature affects the thermostat(s) allowing solar gains to displace space heating immediately.

8. Once the space heating has been totally displaced the internal temperature rises more rapidly.

9. This rise in internal temperature causes a rapid flow of energy into storage in the walls.

10. Towards sunset the solar radiation drops off and the external temperature begins to fall, increasing 'massless' heat losses such as the windows, ventilation loss and to a certain extent, the roof.

11. The internal temperature falls slowly back to the thermostat setting. During this period the space heating is supplied from stored solar energy flowing back out from the walls.

12. Once the thermostat setting is reached the space heating comes on again, but relatively slowly.

13. Although the 'massless' heat losses increase in the evening with the falling external temperature, the heat loss through the thermally massive walls lags about 8 hours behind the daily swing in air temperature, reaching a minimum in the evening.

14. Throughout the evening, although the internal air temperature is constant, heat still flows out of the walls, displacing space heating energy as the deeper wall layers return to equilibrium. This state continues until dawn when the cycle repeats.

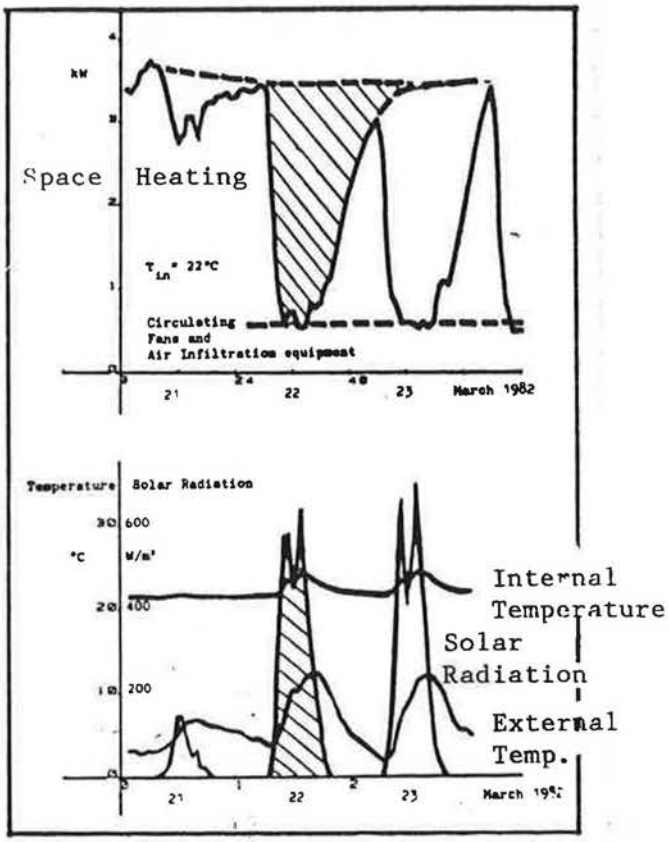

Figure 2.6.

The solar radiation entering the south-facing windows causes a massive reduction in space heating demand on sunny days and large flows of energy into storage in the floor and walls.

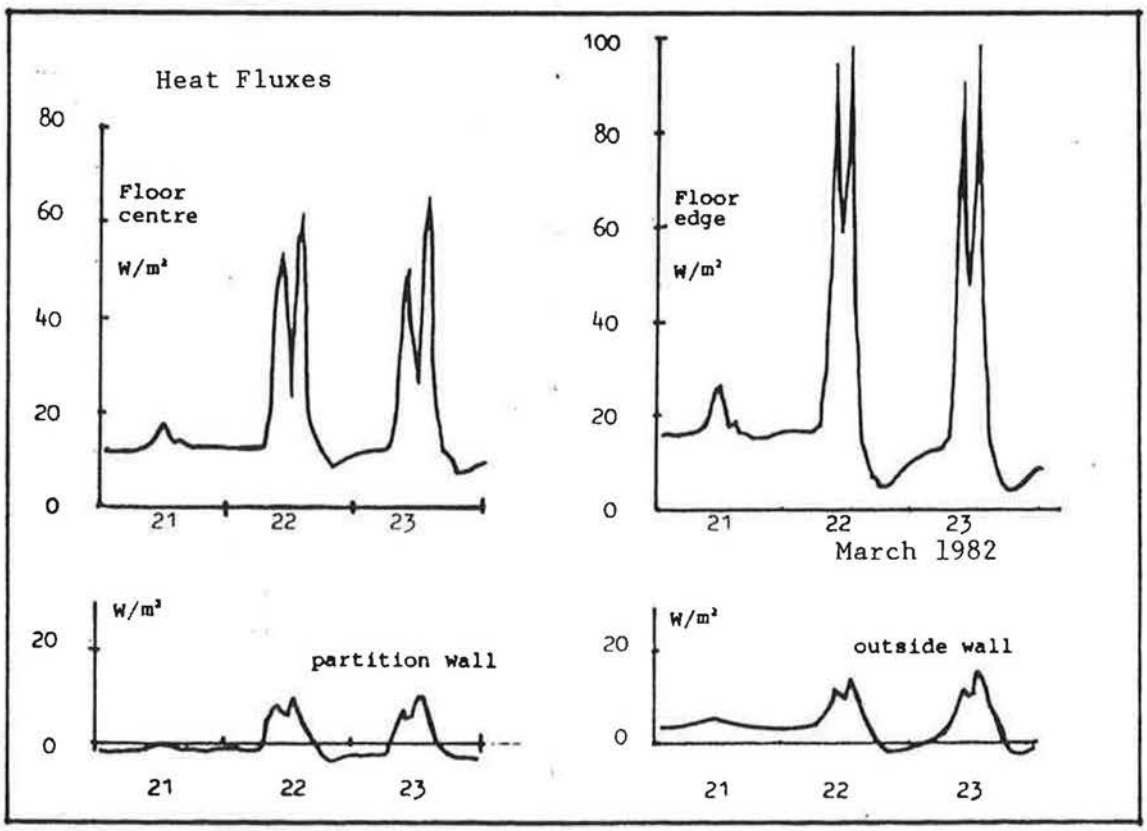

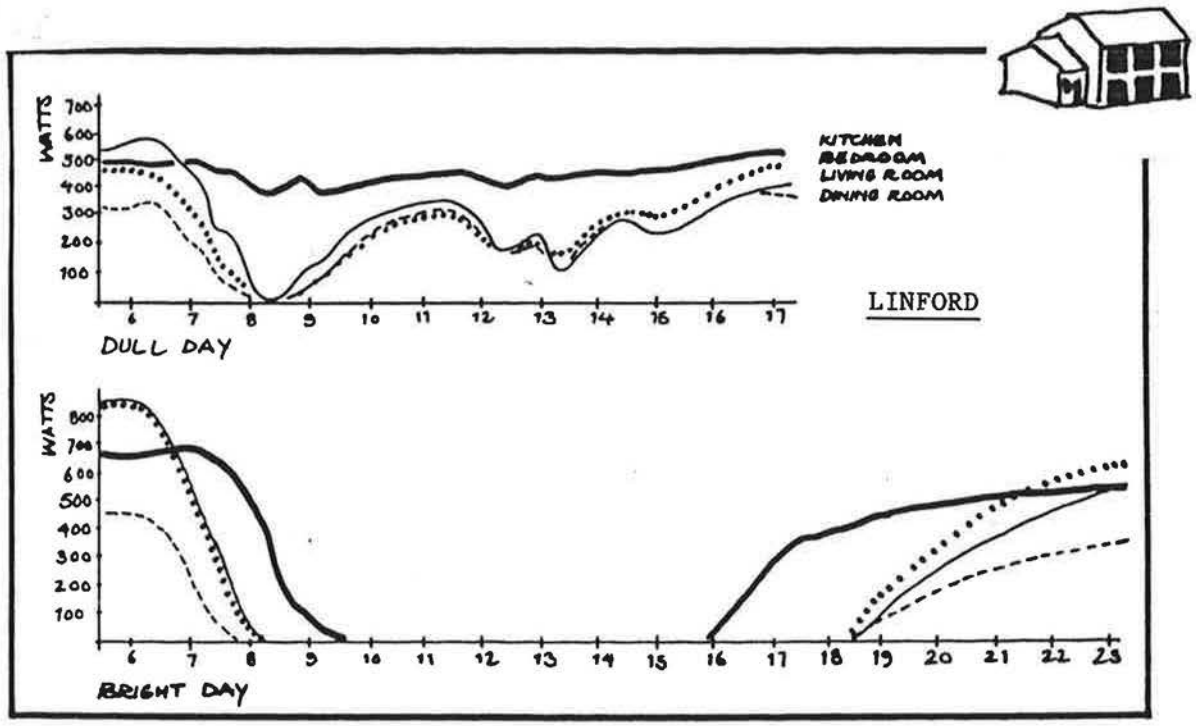

Figure 2.7 Individual power traces of the fan heaters show how solar gains displace space heating in the south-facing rooms, not penetrating very well into the north-facing kitchen.

On dull days the solar radiation may not be enough to totally displace the space heating and the cycle skips stages 8-12.

The process is further complicated by the fact that the solar gains are not evenly distributed over the house, each room responding to the solar gains to a greater or lesser extent. This is illustrated in figure 2.7 which shows the outputs of four of the five fan heaters used in the Linford house.

On a sunny day it is clear that the solar gains affect all the south-facing rooms fairly equally, though the kitchen on the north side is the last room to be affected in the morning, and the first in the evening to require space heating. On a dull day, the kitchen is simply not affected at all and the solar gains simply go to displacing instantaneous space heating in the south-facing rooms.

2.11. Daily Cycle - House With Conservatory

In this case the cycle of events is just as complicated. There are two zones to consider instead of one, though the moderating effect of the conservatory on solar gains means that midday internal overheating in the house is less likely.

Figure 2.8 shows plots of space heating, external air and greenhouse temperatures and the internal wall surface temperature on the greenhouse/house partition wall. It is clear from these plots that the solar radiation produces a massive swing in conservatory temperature as well as a large immediate reduction in house space heating with considerable storage effects into the evening.

The daily cycle is as follows:-

1. The sun rises.

2. The external air temperature begins to rise.

3. Solar radiation penetrates the conservatory striking the floor and the rear wall.

4. Some radiation is absorbed in these surfaces, the remainder being dispersed into the air in the conservatory.

5. This energy, together with the rapidly falling glazing losses starts a massive rise in conservatory temperature.

6. This rise in temperature acting on the south side of the house together with the rise in external temperature acting on the rest of it, causes a reduction in heat losses through the house windows, roof and by air infiltration.

7. This causes an immediate reduction in space heating demand.

8. Just after midday, the greenhouse temperature peaks (at about 40°C in this case).

FIGURE 2.8 - Daily Cycle - House With Conservatory

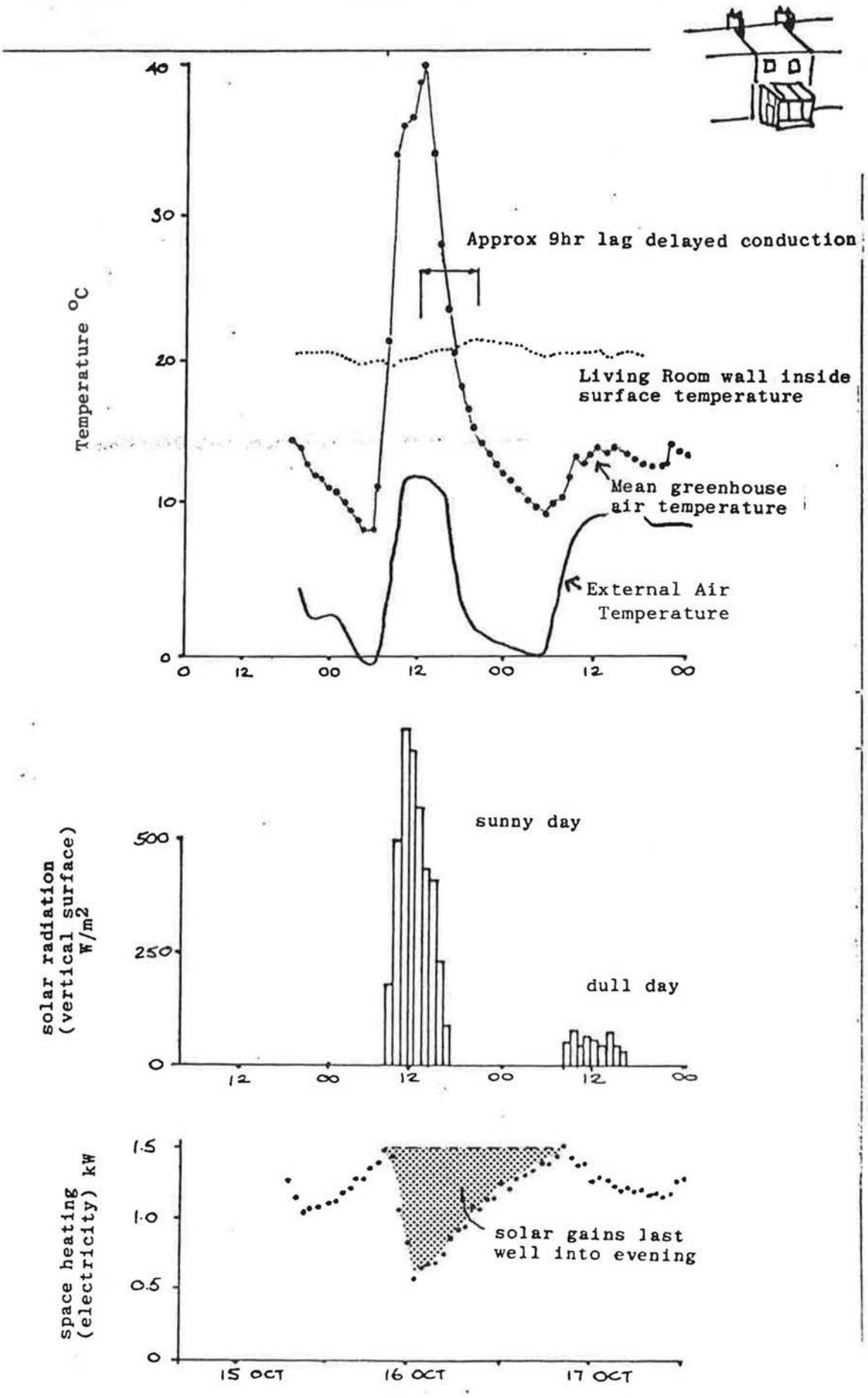

9. Both external air and conservatory temperatures fall rapidly during the afternoon, thus increasing window and air infiltration heat losses in the house. The fall in conservatory temperature is slightly slowed by the effects of stored solar radiation reemerging from the walls and floor.

10 Direct solar gains into the house also fall off towards sunset increasing house heat demand.

11. The effects of the midday peak in external and conservatory temperatures are delayed through the house walls, peaking about 9 hours later. This effect considerably slows the evening rise in house space heating demand.

12. During the night the conservatory and house wall temperatures fall back to equilibrium, but some stored energy in the house/conservatory wall is carried over to the next day.

13. At dawn the cycle repeats again.

Thus for both house types there is a picture of a substantial substitution of space heating by solar gains during the day plus appreciable storage of solar energy in the building fabric. This energy is released mostly in the early evening, but a small amount is carried through beyond midnight and even beyond dawn the next day. For this reason, it is suggested that energy accounting for 'days' should run from dawn to dawn in order to allow the maximum amount of time for stored solar gains to reemerge and displace space heating energy.

2.12 Initial Spencer St. Test

The Spencer St. house was unoccupied for a period of three weeks in October 1981. This seemed a good opportunity to try Siviour's thermal calibration method. Unfortunately, repairs to the logging system and the need to make new equipment meant that only one week's data finally resulted.

The house was heated with a single 2kW fan heater under the control of an electronic thermostat positioned in the centre of the living room. This appeared to maintain the whole house at about 20°C with the extremities of the upstairs bedrooms being about 1°C cooler. Two heaters would have been more appropriate but time did not permit the construction of further equipment.

Measurements were made of the electric heating energy, internal and external air temperatures and solar radiation on the south-facing vertical surface. No air infiltration measurements were made or measurements of the floor heat loss or losses through the party walls into the adjacent houses. The plot of space heating clearly shows the effects of the substitution of solar radiation for electric heating. The precise quantification was not so easy, since it is not clear how far the solar effects last into the next day, nor how much of the trough in the space heating consumption is due to the rise in external air temperature that accompanies a sunny day. (see fig.2.9).

It was thus necessary to separate out the solar and temperature effects. A daily energy balance was drawn up:-

$$Q = (\Sigma A.U + C_v).\Delta T - R.S + F + P$$

where Q = Daily total space heating
Σ A.U = Total fabric heat loss, excluding floor and party walls
C_v = Ventilation loss, assumed constant.
ΔT = Daily average inside-outside temperature difference
R = Solar aperture
S = Daily total solar radiation on the south-facing vertical surface
F = Floor heat loss
P = Party Wall heat loss

Initially analysis was done using a triaxial regression method, using data summed from dawn to dawn and with a weighted external air temperature to compensate for thermal timelags through the building fabric (see Chapter 7).

By regressing Q against ΔT and S it was hoped to produce values for $\Sigma A.U + C_v$, R and F+P, all assumed to be constants. The results were an excellent fit to a plane surface, but the value of F+P was rather too high and the value of $\Sigma A.U + C_v$ rather low. Subsequent work on the Linford house suggested that this type of regression should be treated with great caution, and that the production of a good fit is no guarantee of the right answer.

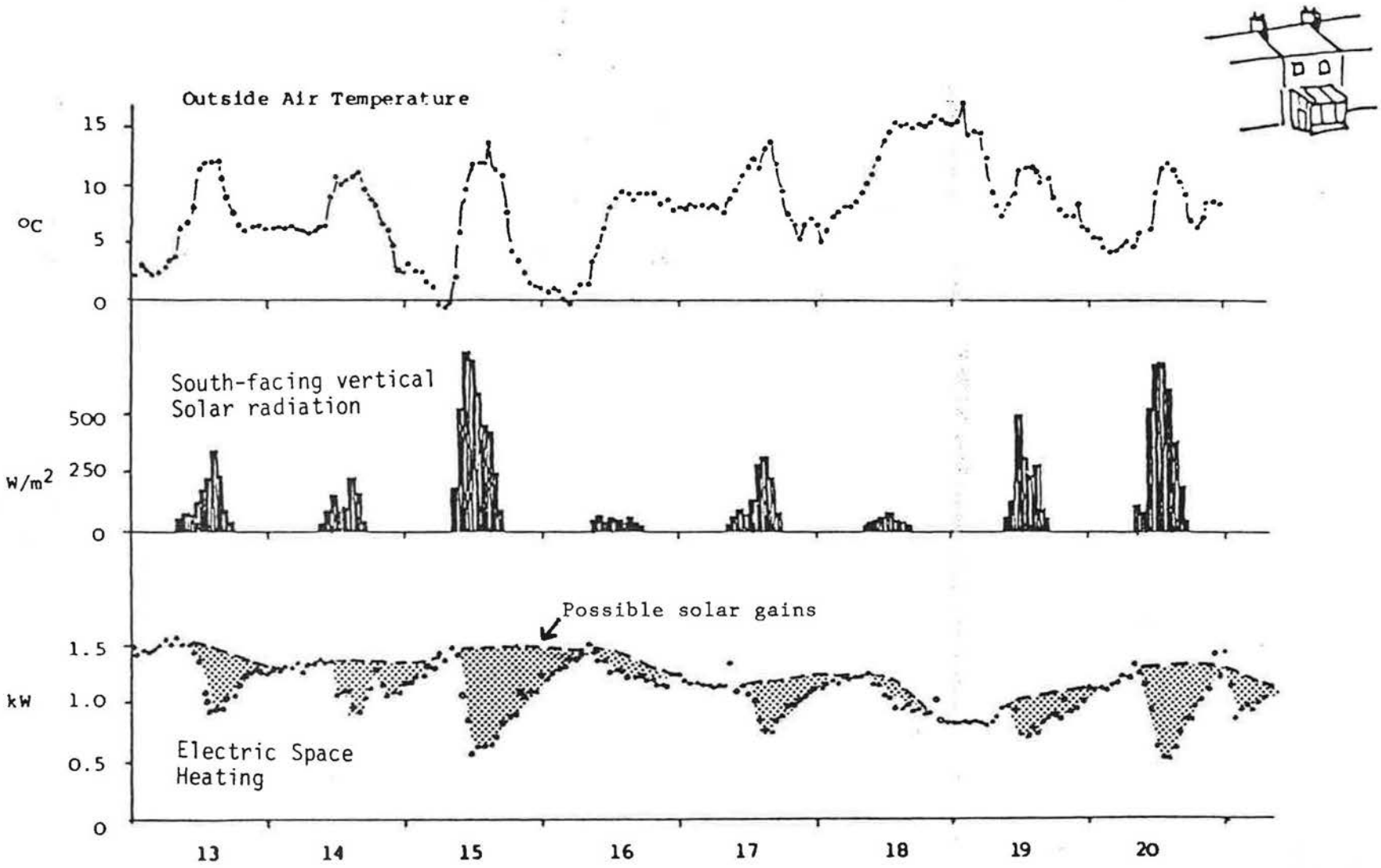

Figure 2.9 Plots of External Air Temperature, Solar Radiation and Space Heating over the period of the constant temperature test clearly show the effects of solar gains into the house.

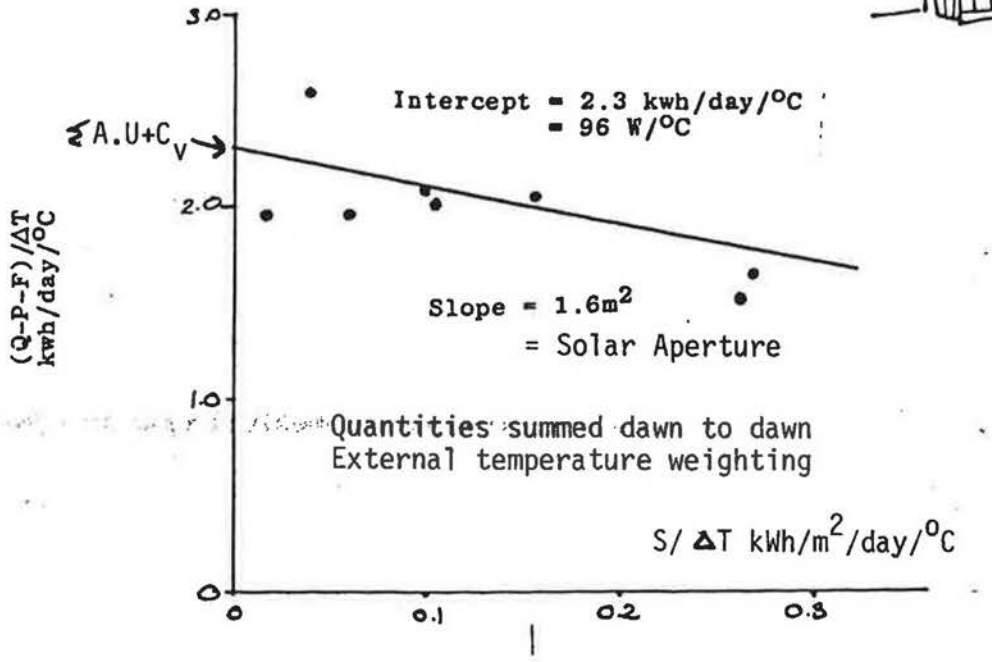

Figure 2.10 Determination of house heat loss and solar aperture

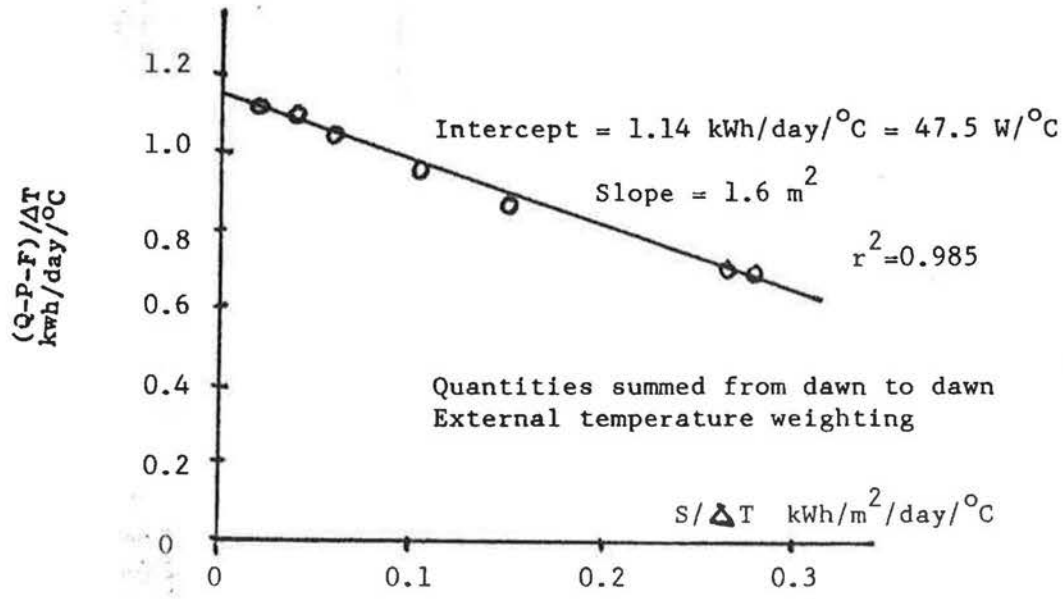

Figure 2.11 'Best fit' from triaxial regression shown in 2-dimensional form

In particular it was found that the value of $\Sigma A.U + C_v$ would be very dependent on the degree of temperature weighting used. The spread of values of ΔT over the data set is fairly small, about 7^oC, and the temperature weighting tends to affect the extreme values by about 1.5^oC. Also there were rather too many parameters assumed to be constant to get a really clear answer.

Changing to the two-dimensional form of the regression, using an estimated value for the floor loss and assuming the party wall loss to be zero, the heat balance equation can be written:-

$$\frac{Q - F}{\Delta T} = \Sigma A.U + C_v - R.\ S/\Delta T$$

We can plot $(Q-F)/\Delta T$ against $S/\Delta T$ as in figure 2.10, giving a Y-intercept of $\Sigma A.U+C_v$ and a slope R.

The value of $\Sigma A.U+C_v$ of 96 $W/^oC$ seems quite compatible with a calculated value of 110 $W/^oC$, assuming an air change rate of 1 ac/h, equivalent to 50 $W/^oC$. An air change rate of 1.4 ac/h had been measured in tests during the previous December but insufficient analysis was carried out to extrapolate the results to this data set.

The plot of figure 2.10 is not the 'best fit' graph. Assuming higher floor and party wall losses and a lower ventilation rate produces the superb straight line of figure 2.11. However, as mentioned above, there are not enough other measurements to interpret this result in terms of actual energy flows.

This test did show, though, that the thermal calibration method was viable on a daily basis and the results were used to support the research proposal for further work on the Linford houses.

The week's data was actually more fruitful in describing the conservatory performance. Given the short thermal time-constant (about four hours) it was possible to fit a very simple descriptive model relating hourly greenhouse temperature to incident solar radiation, external air temperature, and the previous hour's greenhouse temperature. This model allowed the greenhouse performance to be extrapolated over a whole year and some assessment made of the annual energy saving to the house. This is described in the Spencer St. House Project Report.

2.13 A Sample Linford Regression

The Linford test house was ready for thermal calibration experiments in March 1982. It was kept at a constant internal temperature of 22°C by five electric fan heaters with electronic thermostats and air infiltration measurements were made continuously. Analysis of weekly data for March and April 1982 using the triaxial regression method was not very fruitful. The data set suffered from small spreads of both ΔT and solar radiation, and worst of all, a large and rapidly varying floor heat loss (see Chapter 3). This changing floor loss led to a very high estimate of the solar aperture and illustrated the problems of using statistics without really understanding either the statistical method or the physical processes at work in the house.

More detailed work on a two-week segment of this dataset has been more forthcoming. The raw data for part of this period in March 1982 is shown in Figure 2.12 and includes the days shown in figure 2.6, giving a longer time perspective. The actual period was chosen to give the best mix of sunny and dull days, since it is by comparing space heating on the two that the solar aperture is essentially determined.

Measured air infiltration rate is shown as well as space heating, solar radiation and temperatures. It has been expressed as six-hour averages for ease of calculation, since the actual time period of measurement depends on the air change rate (see Chapter 4). The infiltration rate is almost constant over the dataset at about 0.5 ac/hr but does briefly rise to 1 ac/hr on a windy day.

Although there are wide excursions of external air temperature during the day, actual daily average temperatures are almost all the same, about 7°C. Obviously there is not much hope of determining the house heat loss by comparing space heating on warm and cold days.

Largely as a result of studying this dataset, a series of data requirements have been drawn up in order to carry out a thermal calibration. Briefly it would appear that it is possible to get a reasonable estimate of the fabric heat loss of a house and its solar aperture given two weeks data provided that:-

1. There is a good mix of sunny and dull days. The dull days give a good fix on $\Sigma U.A$ and the sunny ones allow the calculation of the solar aperture. The need for dull days tends to limit the whole process to the months October to March, since sunny days seem available all year round, but dull ones are rare in summer.

2. Air infiltration should be measured, since it can vary widely over the experimental period.

3. The floor heat loss should be estimated separately, since it is not directly related to measured external air temperature.

4. 'Days' should run from dawn to dawn rather than midnight to midnight in order to allow any solar gains that have gone into storage in the building fabric the maximum amount of time to emerge and displace space heating.

These four requirements on their own are fairly easy to implement and likely to give reasonable results. In addition, there are three others of a more mathematical nature. They are, in order of decreasing importance:-

5. Corrections should be made for thermal time-lags in the house to changes in external temperature. This involves calculating

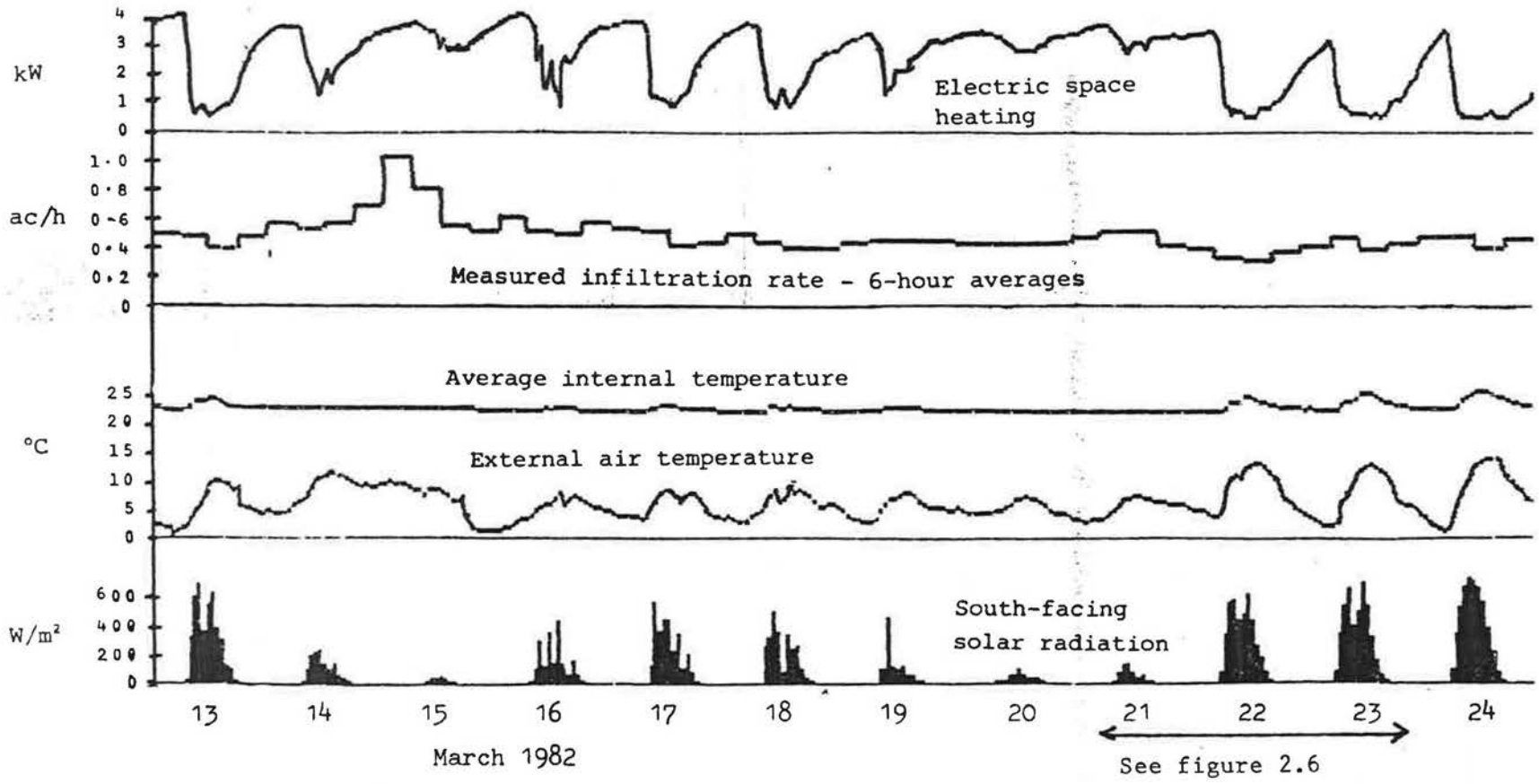

Figure 2.12 **Space Heating, Infiltration, Temperatures and Solar Radiation**

13.3.82 - 24.3.82

LINFORD

the daily average external air temperature incorporating air temperatures from the previous day. This 'external weighting' involves an assumed response factor model of the building fabric.

6. Corrections should also be made in a similar fashion for the slight day-to-day changes in internal temperature, notably the mid-day rises in temperature that accompany a very sunny day, forcing solar radiation into storage in the walls. This 'internal weighting' process involves assuming a model of the thermal mass of the house as it interacts with solar gains and is consequently rather dubious in practice. Also, for day-to-day solar energy storage reasons, it is desirable to delete from the dataset very dull days that are preceded by a run of sunny days.

7. The co-variance of solar radiation and ΔT should be restricted in order to prevent errors in determining the floor heat loss or the infiltration rate appearing as solar aperture. This problem is unlikely to be serious in practice since short-run datasets seem to exhibit little variation in ΔT. In summer sunny days tend to be warmer than dull days, in winter the reverse is true. During spring and autumn there is little difference.

These more abstruse mathematical requirements are discussed in Chapters 6 and 7.

Figures 2.13 to 2.17 show the progressive improvement of fit of the data as various corrections are applied to a crude regression.

Figure 2.13 starts with a simple plot of $Q/\Delta T$ vs. $S/\Delta T$ for the data of figure 2.12, with the energy sums totalled from midnight to midnight. Figure 2.14 shows the same data summed from dawn to dawn. The net result is an increase in apparent solar aperture, since more time has been allowed for solar gains absorbed during the day to reemerge and displace space heating on the same'day'.

Figure 2.15 shows the plot corrected for variations in air infiltration rate and floor heat loss. The plot is now of $(Q-F)/\Delta T - C_v$ against $S/\Delta T$. The effect of this change is to considerably increase the quality of fit, raising the correlation ratio r^2 from 83% to 93%. This is almost entirely due to the proper handling of the sudden peak in air infiltration rate that occurs on the night of March 14/15.

Corrections for thermal timelags in the response of the house to changes in external temperature are incorporated in figure 2.16 . This gives a further improvement in fit, raising r^2 to 96%. Much of this is due to the improved handling of the sudden temperature drop on the night of March 15th, due to the passage of a cold weather front.

Finally, correction for the slight rises in internal temperature on sunny days, and the energy storage that they imply, raises the apparent solar aperture again, as more solar gains are properly translated into displaced space heating.

Q/Delta T Kwhr/Day/Deg C Midnight to Midnight

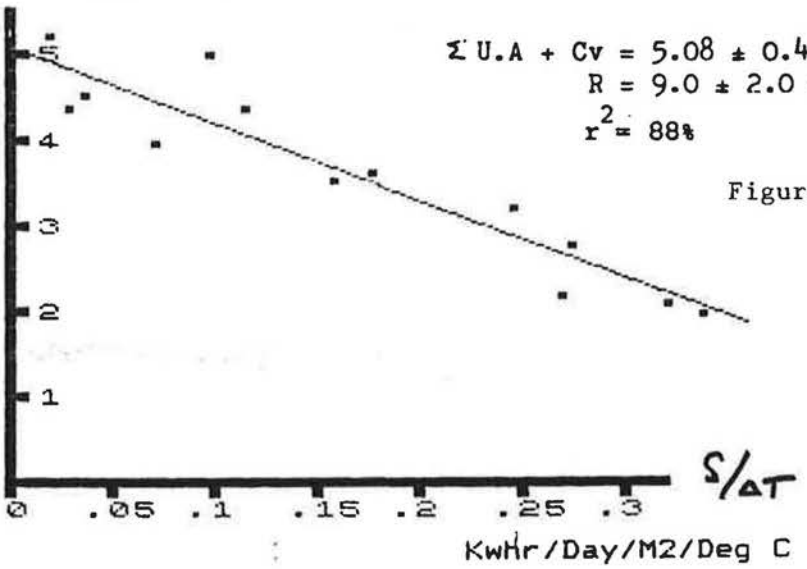

Figure 2.13

Q/Delta T Kwhr/Day/Deg C Dawn to Dawn

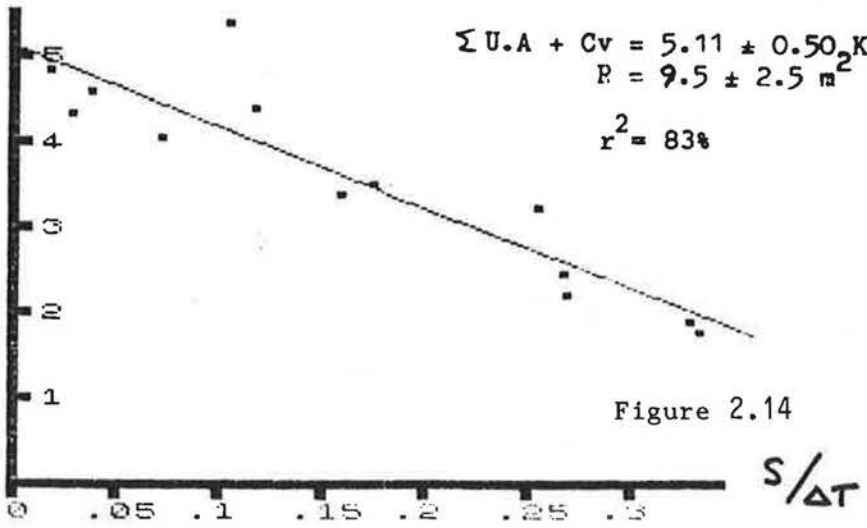

Figure 2.14

Changing the summation of data from midnight to midnight to dawn to dawn increases the apparent solar aperture, as solar gains are allowed more time to emerge from storage and displace space heating.

(Q-F)/Delta T-Cv Kwhr/Day/Deg C

Dawn to Dawn

Figure 2.15

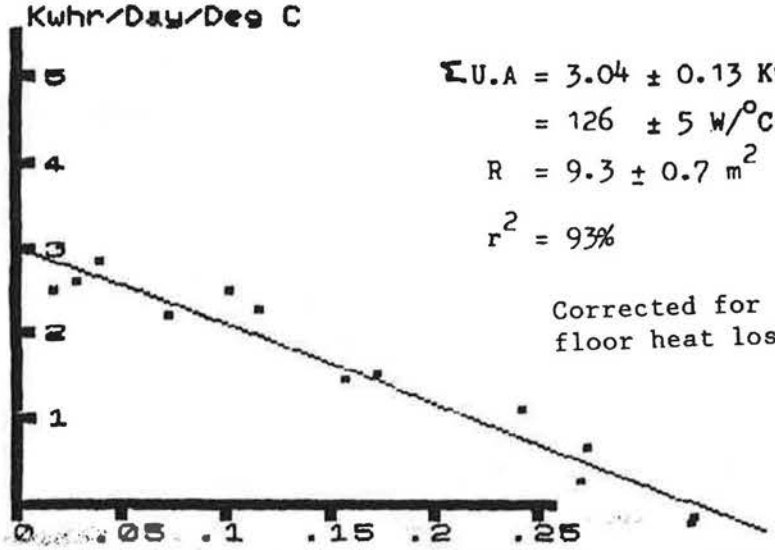

$\Sigma U.A = 3.04 \pm 0.13$ Kwhr/day/°C

$= 126 \pm 5$ W/°C

$R = 9.3 \pm 0.7$ m²

$r^2 = 93\%$

Corrected for variations in floor heat loss and air infiltration

(Q-F)/Delta T-Cv Kwhr/Day/Deg C

Dawn to Dawn Plus External Weighting

Figure 2.16

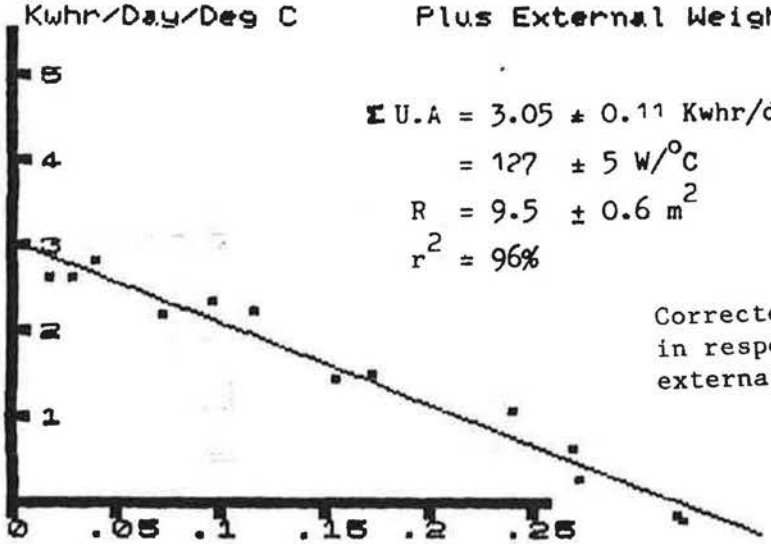

$\Sigma U.A = 3.05 \pm 0.11$ Kwhr/day/°C

$= 127 \pm 5$ W/°C

$R = 9.5 \pm 0.6$ m²

$r^2 = 96\%$

Corrected for thermal lags in response to changes in external temperature

$(Q-F)/\Delta T-C_v$ kWh/day/°C

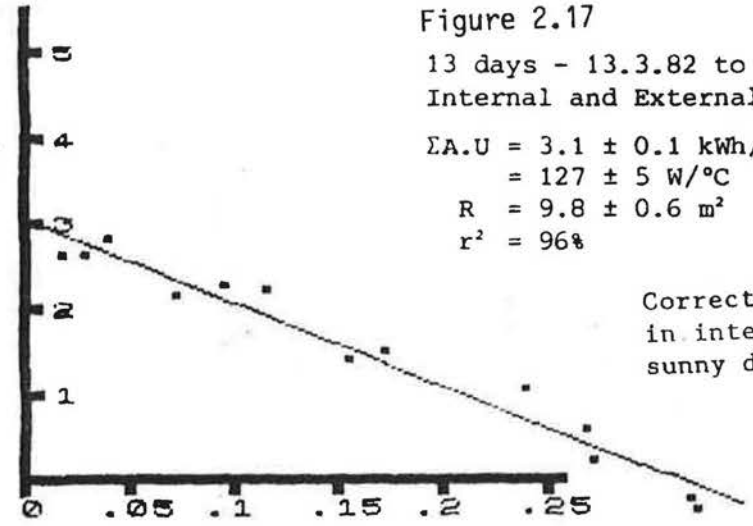

Figure 2.17

13 days - 13.3.82 to 25.3.82
Internal and External Weighting

$\Sigma A.U = 3.1 \pm 0.1$ kWh/day/°C

$= 127 \pm 5$ W/°C

$R = 9.8 \pm 0.6$ m²

$r^2 = 96\%$

Corrected for variations in internal temperature on sunny days.

2.14 Experimental Errors

The final product of this sequence, figure 2.17, gives a fabric heat loss of 127 W/°C ± 5 W/°C and a solar aperture of 9.8 ± 0.6 m^2. The error bars denote the range over which there is a 68% probability that the true answer lies. The 90% confidence levels are approximately double this.

These error limits are, however, merely errors of interpretation of the data and do not include basic measurement errors. The thermal calibration process can determine the total house heat loss fairly accurately, with typical errors of ± 5%, mainly due to errors in temperature measurement. The disaggregation into separate components, though, is rather imprecise because of the larger experimental errors involved.

For example, air infiltration measurements made with the O.U. rig are likely to have errors of ± 20% or more, equivalent to about 8 W/°C. The empirical model for predicting infiltration rate from wind and temperature conditions is even worse, giving errors of ± 13 W/°C. Errors in the determination of floor heat loss in the Linford house are also quite large, probably of the order of ± 10 W/°C, mainly due to the inadequate number of heat flux sensors deployed.

Any figure for the house fabric heat loss excluding the floor should thus be given fairly generous error bars of around 20 W/°C, since it has to include all these errors (though they do tend to add as the square root of the sums of squares).

2.15 Linford 82/83 Experimental Programme

The thermal calibration process was extended over the winter of 1982/83. The internal temperature was raised to 25°C to extend the heating season as far as possible. This high internal temperature also had beneficial effects in reducing mid-day overheating and consequent energy storage effects, enabling 'internal weighting' and its dubious assumptions about the thermal mass of the house to be dispensed with.

Two modifications were made to the floor surface over the period. At the end of October 1982 the floor was covered with carpet tiles to bring test house conditions more into line with those in the occupied houses. In mid-December the floor was insulated over with 50 mm polystyrene. The prime reason for doing this was to obtain estimates for the test house solar aperture free from interference from changing floor heat losses, though as described in Chapter 3, it has provided an interesting experiment in its own right.

In addition to these floor insulation variations three solar variants were tried out:

1. Full clear window area.

2. Full net curtains.

3. Half net curtains, half white card.

These were run in a cyclic fashion of approximately two-week periods as shown in Table 2.1, allowing assessments over a wide range of temperatures and solar inputs. Air infiltration measurements were only made for a part of the time. It was not fully realised how important these measurements are to accurate thermal calibration and the lack of them has led to some data sets being abandoned. However, as second best, there were sufficient measurements to create a model relating air infiltration to wind speed, direction and measured house ΔT, as described in chapter 4.
This did allow the prediction of infiltration rates for any hour of the year from measured weather variables, although of limited accuracy, typically ±30%.

Results

The ten separate periods of the 82/83 season obviously provide enough data for pages of graphs. These have, indeed been produced in order to test the self-consistency of the thermal calibration method, whether or not it can produce the same answers for a given house variant given different weather conditions. Fortunately the data sets for the first two solar variants consistently gave similar values of solar aperture. The data for the last variant, half net curtain, half white card had to be abandoned as containing too much windy weather for the infiltration predictions to be reliable.

Successive estimates of fabric heat loss were not altogether consistent and this appears to be due to errors in determining the floor heat loss. This problem is discussed in Chapter 6.

Table 2.1 Linford 82/83 Constant Temperature Heating Tests

Period	Floor Condition	Window Condition	Ventilation	Internal Temp.
25/2/82 - 4/5/82	Uninsulated Bare	Full Area No curtains	Measured* 52 Days	22°C
11/10/82 - 27/10/82	Uninsulated Bare	Full Area No Curtains	Predicted	25°C
30/11/82 - 10/11/82	Uninsulated Carpet	Full Area No Curtains	Predicted	25°C
12/11/82 - 13/12/82	Uninsulated Carpet	Full Area Net Curtains	Predicted Measured 13 Days	25°C
16/12/82 - 1/1/83 26/1/83 - 10/2/83	Insulated	Full Area No Curtains	Predicted Measured 6 Days	25°C
2/1/83 - 13/1/83 11/2/83 - 3/3/83 4/4/83 - 31/5/83	Insulated	Full Area Net Curtains	Predicted Measured 14 days Predicted	25°C
14/1/83 - 25/1/83 4/3/83 - 15/3/83	Insulated	Half area Net curtains Half area white card	Predicted	25°C

*only included where there are more than 4 samples/day

The solar performance of the test house can thus be summarised in four graphs showing solar apertures with and without net curtains, and with and without floor insulation. Including Figure 2.17 already shown, the remaining variants are plotted in Figures 2.18 to 2.20.

Variant	Apparent Fabric Loss	Solar Aperture
Floor uninsulated no curtains	127 ± 5 W/°C	9.8 ± 0.6 m²
Floor uninsulated (with carpet) net curtains	137 ± 3 W/°C	8.1 ± 0.6 m²
Floor insulated no curtains	155*± 2 W/°C	10.1 ± 0.6 m²
Floor insulated net curtains	148*± 3 W/°C	8.0 ± 0.6 m²

*probably overestimates due to errors in floor loss measurement.

The essential conclusions from these results are that:-

1. Insulating the floor makes no apparent difference to the solar aperture. This is not particularly surprising since it was found that only a small amount of the incident solar radiation was absorbed in the floor surface.
2. The solar aperture without net curtains is about 10 m² and with net curtains about 8 m². The error margins on these are fairly large. The quoted errors are the interval over which there is a 68% confidence that the true answer lies. The 90% confidence interval is about ± 1 m².

The figure of 10 m² for clear windows is considerably less than the calculated solar aperture of 13 m² produced from measured glass areas (see Figure 2.1). Even this figure does not include possible solar gains through the opaque building fabric. The discrepancy can be attributed to three reasons:-

1. Shading effects of the roof eaves and window reveals, not included in the original calculation.

2. Reflection of radiation back from the interior of the house.

3. A problem of definition of air temperature.

This last reason requires a little explanation. The thermal calibration process assumes that a house loses heat to some kind of measured external air temperature. The measured temperature used for the calculations is a Stevenson Screen temperature. Although this is normal practice it is not a true air temperature and will vary with incidental solar radiation. It is possible that this effect could account for 0.5-1 m² of the discrepancy in solar apertures (see Appendix 2).

Test House Correlations

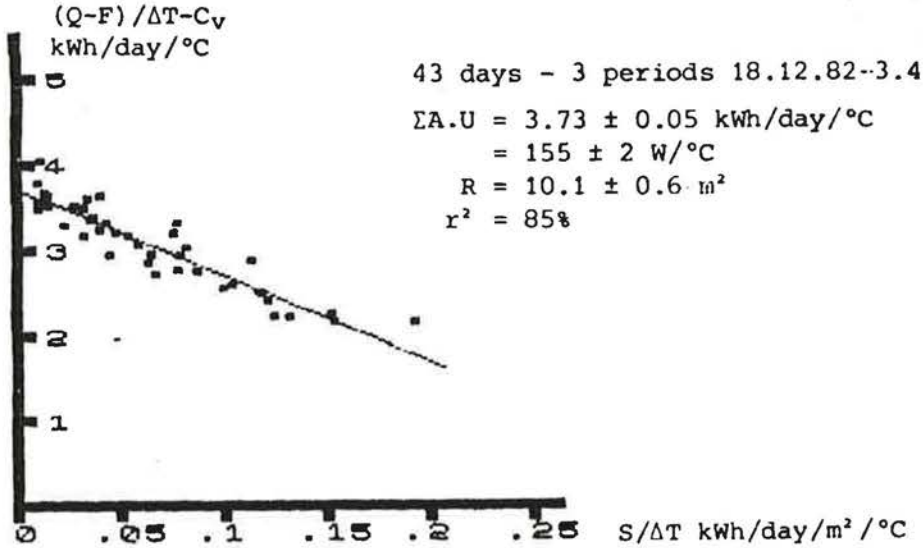

43 days - 3 periods 18.12.82-3.4.83

ΣA.U = 3.73 ± 0.05 kWh/day/°C
= 155 ± 2 W/°C
R = 10.1 ± 0.6 m²
r^2 = 85%

Figure 2.18 No Curtains - Floor Insulated

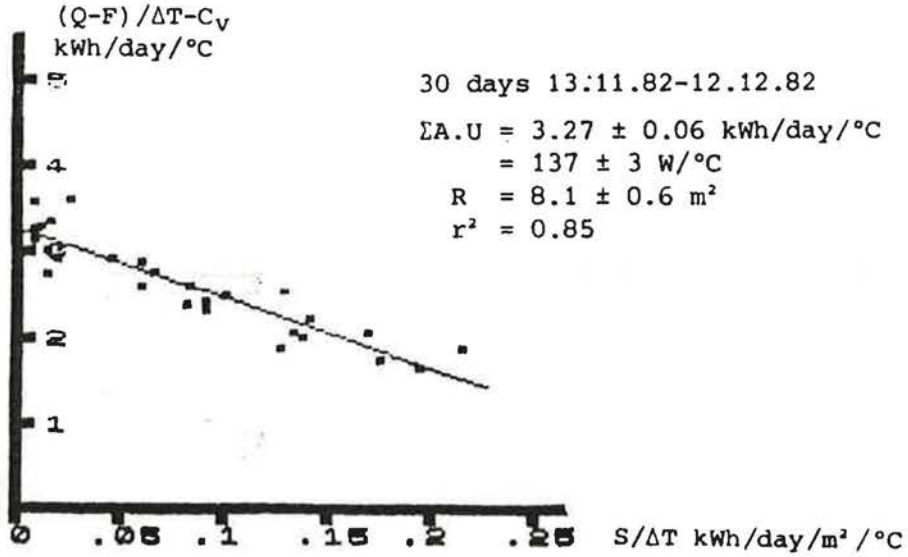

30 days 13.11.82-12.12.82

ΣA.U = 3.27 ± 0.06 kWh/day/°C
= 137 ± 3 W/°C
R = 8.1 ± 0.6 m²
r^2 = 0.85

Figure 2.19 Net Curtains - Floor Uninsulated

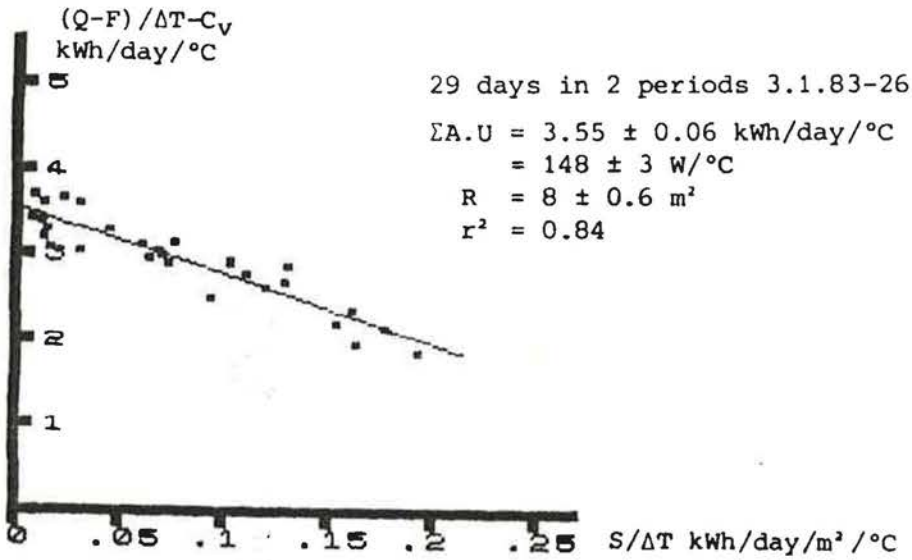

29 days in 2 periods 3.1.83-26.2.83

ΣA.U = 3.55 ± 0.06 kWh/day/°C
= 148 ± 3 W/°C
R = 8 ± 0.6 m²
r^2 = 0.84

Figure 2.20 Net Curtains - Floor Insulated

2.16 Comparisons with Linford Occupied Houses

The regression procedure has been extended to the Linford occupied houses. Here, lacking actual measurements, the floor and ventilation losses have been estimated are careful account has been taken of free heat gains. Also given slight day-to-day variations in internal temperature, a longer regression timescale has been used.

Free heat gains

These have included gains from electricity use, occupants' body heat, hot water cylinder heat losses, boiler casing heat losses and gains from hot water use. The details will be found in the main Linford project report.

Floor heat loss

This has been taken as equivalent to a U-value of 0.9 $W/m^2/^oC$ between the measured living room temperature and the assumed sinusoidal ground temperature suggested in Chapter 3.

Ventilation loss

The hourly air infiltration model of the test house which will be described in Chapter 4 has been extrapolated to the occupied houses by scaling by their measured pressure test air leakages. In addition corrections have been added proportional to measured window opening to give the overall hour by hour ventilation rate. This process is also described in detail in the main Linford report.

Regression timescale

Studied of test house data show that once the floor and ventilation losses are properly dealt with regression timescale is not such a problem. Consistent answers can be obtained from daily, 2-daily and weekly regressions. The timescale used for the occupied houses has been six-day averages, chosen to give the best trade-off between day-to-day energy storage effects and a good spread of $S/\Delta T$ values.

Co-variance of S and ΔT

As will be described in Chapter 6 it can be desirable to restrict the covariance of S and ΔT. Fortunately, given fast computer graphics, it has been easy to visually check this and to split the plots into 'bands' of different ΔT's to see if the regression line differs.

Results

The regression lines for four of the occupied houses are shown in figures 2.21-2.24. Given the large number of assumptions about free heat gains, etc., the quality of fit is extremely good, in fact as good as the short-run test house data. The solar apertures and apparent fabric heat loss figure are given in Table 2.3 below.

LINFORD OCCUPIED
HOUSE CORRELATIONS

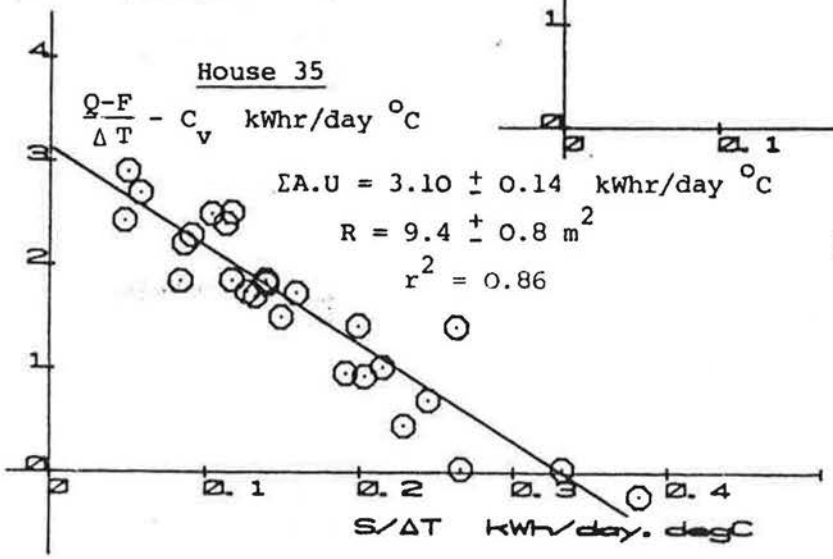

Figure 2.22

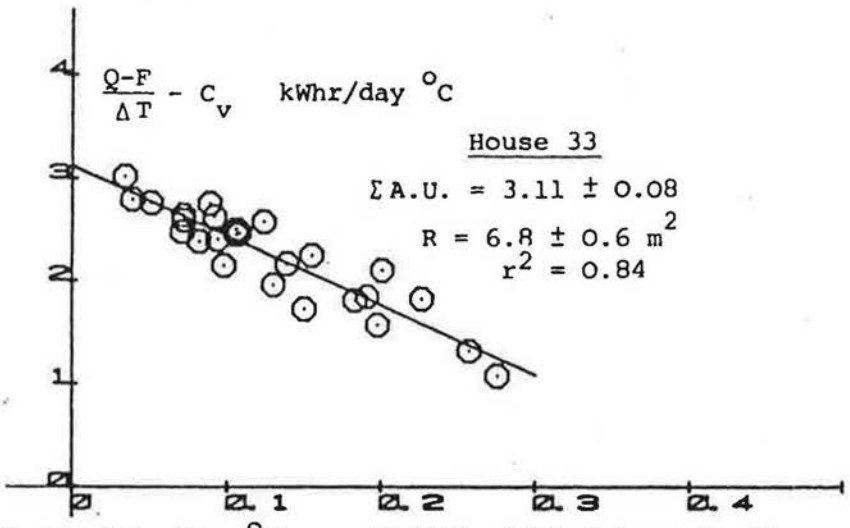

Figure 2.21

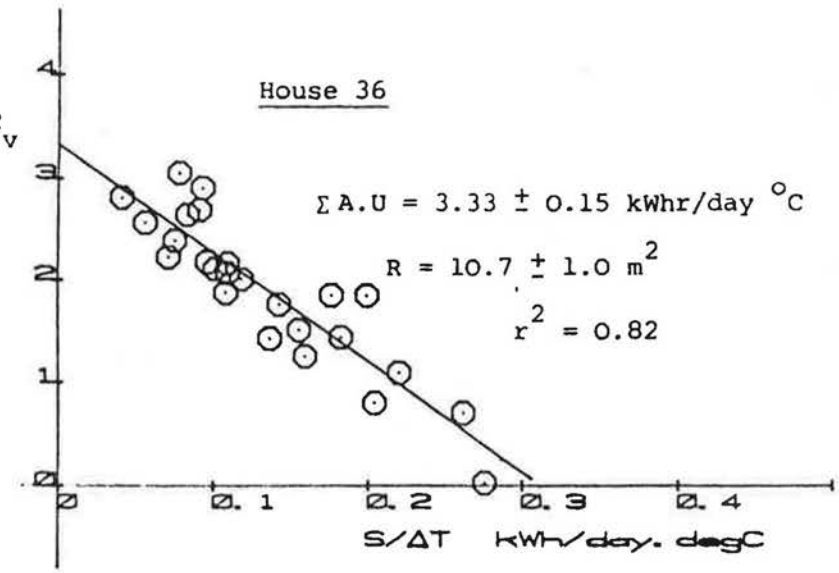

Figure 2.23

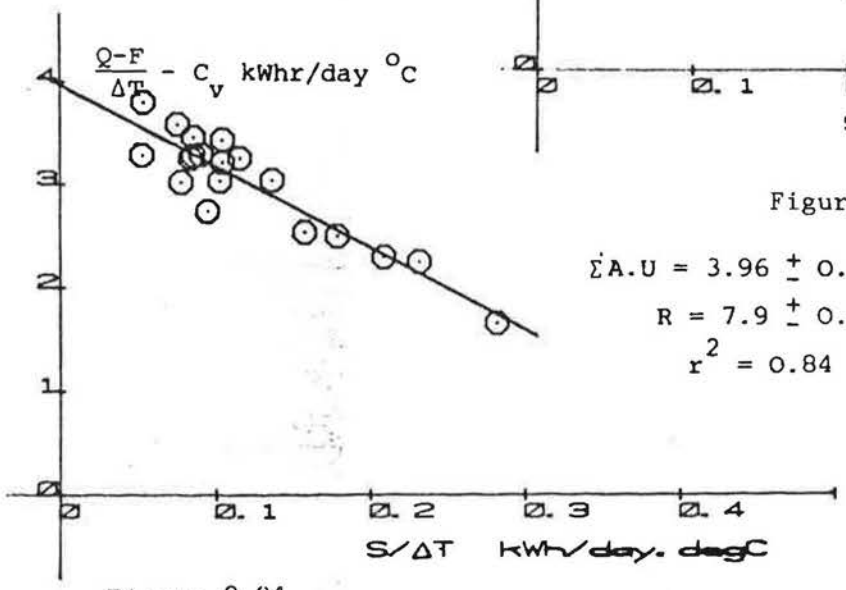

Figure 2.24

Table 2.3 **Occupied House Results**

House No.	Window Condition	Apparent Fabric Heat Loss kWhr/day °C	Apparent Fabric Heat Loss W/°C	Solar Aperture m^2
33	Full net curtains	3.11 ± 0.08	130 ± 3	6.8 ± 0.6
35	Clear - moderate curtain use	3.10 ± 0.14	129 ± 6	9.4 ± 0.8
36	Clear - moderate curtain use	3.33 ± 0.15	139 ± 7	10.7 ± 1.0
38	Full net curtains	3.96 ± 0.11	165 ± 5	7.9 ± 0.8

The apparent solar apertures are quite compatible with the test house results of 8 m^2 for a house with net curtains (see fig. 2.19) and 10 m^2 for one without (see figure 2.17), and agree fairly well with the observed levels of window clutter.

The apparent fabric losses for three of the houses are quite in agreement with the test house value of just over 130 W/°C (see fig.2.25). This suggests a certain uniformity of construction, as well as of experimental method.

The value for house 38 is significantly larger, though this may be due to errors in determining the ventilation loss or free heat gains rather than any genuine difference in thermal performance.

This process of fitting a simple U-value model to occupied house data is in a way mildly revolutionary, since it has been widely held that it is impossible to make 'sense' of occupied house energy consumptions. This topic is revisited in Chapter 6, showing how the progressive addition of more detail (floor loss, ventilation loss, etc.) improves the quality of fit, from the crude measurements made at Pennyland up to the detailed Linford test house results.

Finally the Linford project does hold out the possibility that occupied house data could be sensibly analysed on a daily basis. Figure 2.26 shows a graph using daily averages (midnight to midnight) for one of the houses over a period of a month from January to February 1983. Although the fit is not as good as the six-day averages, it is still quite reasonable.

Attempts to do this with the Spencer St. data were disasterous, since it was not appreciated how important data cleaning was, especially in removing days with unusual occupant behaviour. This resulted in large apparent solar apertures simply due to the fact that the occupants went out on sunny days and stayed in to bake large quantities of bread on dull ones!

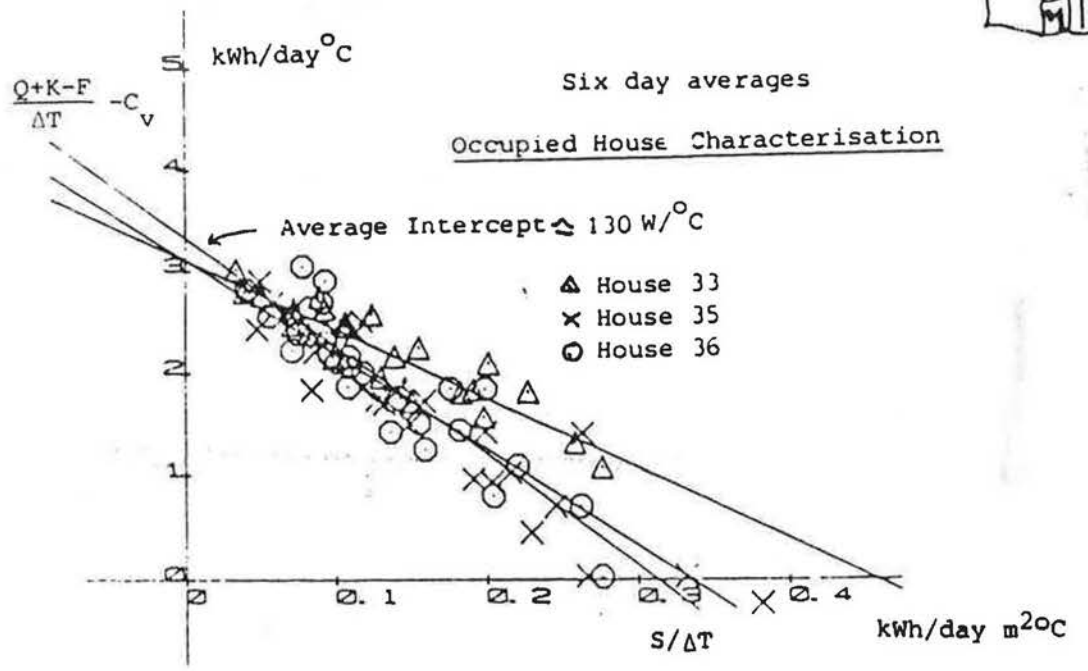

Figure 2.25 Three of the occupied houses show very similar fabric heat losses, approximately equal to that determined for the test house.

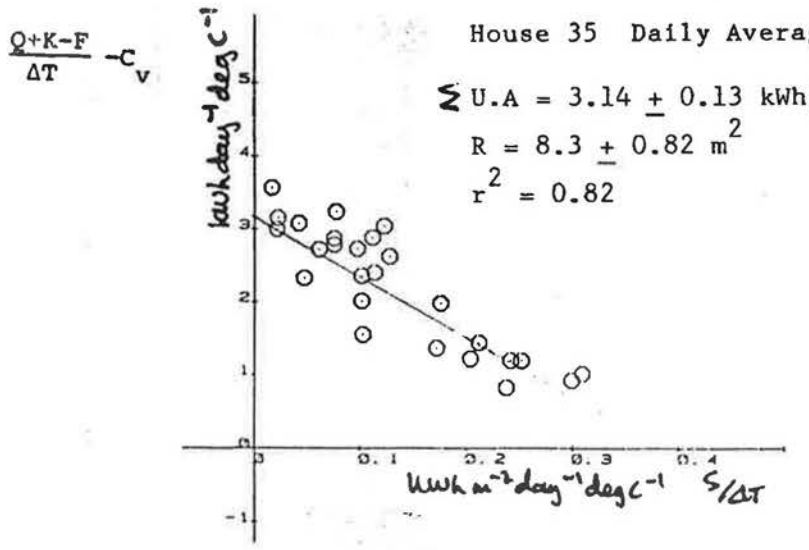

Figure 2.26 A regression using daily average occupied house data still produces good results

3. FLOOR HEAT LOSS

CONTENTS

This chapter summarises the floor heat loss findings from the Linford project which lead to a requirement to measure floor heat loss separately in thermal calibrations.

CHAPTER 3

FLOOR HEAT LOSS

Although it would appear that suspended timber floors with adequate underfloor ventilation can be treated as building fabric in the same way as the walls. windows and roof. solid concrete floors need to be treated separately, since they appear to have curious dynamic properties.

The heat loss is not directly proportional to the short-term difference between internal and external air temperatures, but is more related to the difference between the internal temperature and a slowly moving subsoil temperature. How this ground temperature is related to the external air temperature or to possible groundwater flow is not really clear,though.

Nor is the heat loss uniform over the floor surface. The heat loss is governed by the thermal resistance of the long thermal path down through the soil to the outside air and so most of the heat loss is concentrated at the perimeter. The effect of edge insulation of the floor slab is to extend the necessary path length and thus reduce the overall heat flow.

Fig. 3.1.

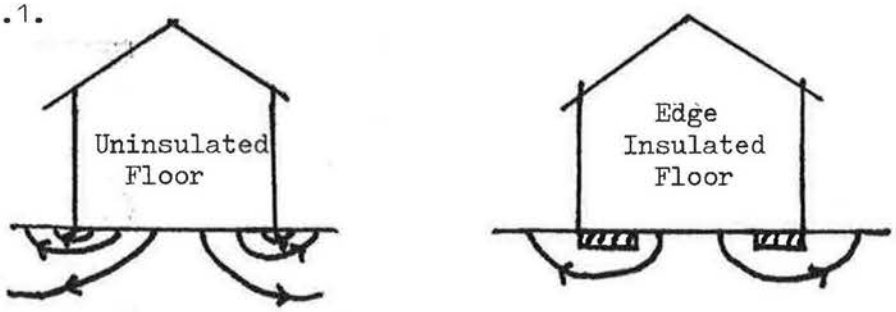

High heat loss around perimeter

Heat is forced to take longer path through ground

The heat loss of a solid floor is thus dependent on the thermal conductivity of the underlying soil, which in turn depends a lot on its water content. The tables of solid floor U-values that appear in the I.H.V.E. and C.I.B.S. Guides are values computed for a clay soil of medium water content (conductivity 1.4 W/m/^{o}C). Values for other soil conditions should be scaled by their conductivity.

The only thing that can be said for certain about the heat loss is that given the large amount of thermal mass of the ground, it only likely to vary very slowly, and for short calibration periods is likely to be almost constant.

3.1. Linford Measurements

The Linford houses have solid concrete floor slabs, edge insulated with 25 mm thick insulation tucked in for almost a metre around the perimeter (see figure 3.2).

The heat flux measurements at the test house can only be described as rather mystifying. Unfortunately, only two heat flux sensors were installed and these were directly lit by the sun's rays shining through the south-facing windows. This involved a certain amount of unravelling of solar and steady state heat loss effects. This process is described in the Linford project report.

Initial analysis showed that the heat loss was about double that expected, given a floor U-value of about 0.5 $W/m^2{}^oC$ predicted from the I.H.V.E. Guide tables. Worse still, it was changing in a way not related either to outside air temperature or solar radiation, creating statistical havoc for the regression process attempting to extract the solar aperture of the house. In order to get round this problem the floor was insulated over with 50 mm polystyrene in December 1983, primarily to improve the estimates of solar performance. However, it has proved very interesting in its own right.

Figure 3.4 shows the measured floor heat loss (with solar effects removed) for the entire test period from March 1982 to June 1983. The most that can be said about the heat loss prior to full insulation is that it falls in the spring and rises in the autumn, and in a way that is not immediately dependent on the external air temperature. After insulation the heat loss is simply constant.

Measurements by D.Spooner at the Cement and Concrete Association have suggested that the floor loss is best expressed in terms of a ground temperature under the house (ref. 3.1). No ground temperature measurements were made at Linford and so a sinusoidally varying temperature has been assumed based on various published cold water main temperatures. Figures 3.5 and 3.6 show the daily floor heat loss values before full insulation plotted against daily average external air temperature and assumed ground temperature. Obviously the latter seems to make better sense. The difference between the apparent U-values for spring and autumn in figure 3.6 may be illusory and simply due to the wrong choice of ground temperature.

After full insulation the floor loss recorded by the two sensors is simply constant and bears no relation to either air temperature or the assumed ground temperature. This curious result does not appear to be a monitoring fault, since it is shown by both sensors and they continue to respond to solar radiation. It is possible that they are responding to a ground temperature at a deeper level, which is likely to be more constant over the year, though why this should be so is a mystery.

Figure 3.2

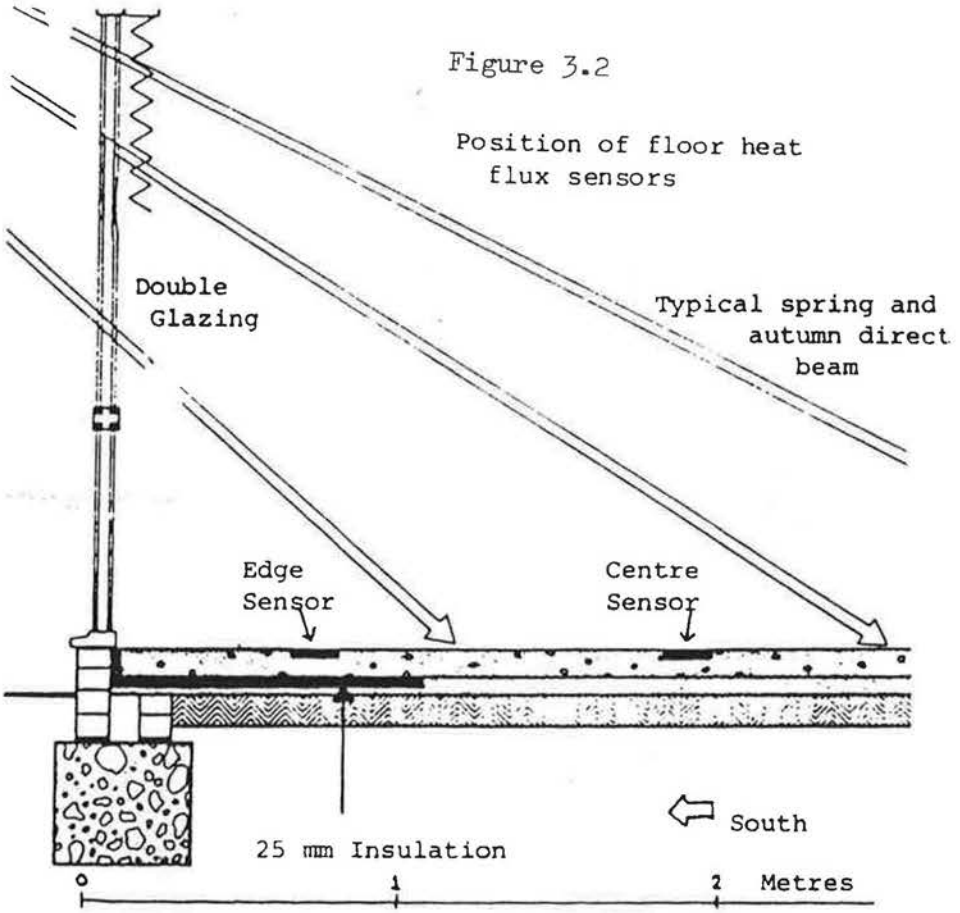

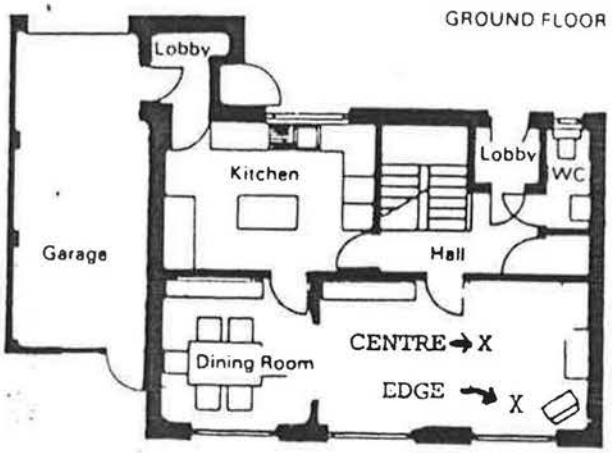

Figure 3.3 Positions of floor heat flux sensors

Figure 3.4

Variation of floor heat flux over the year

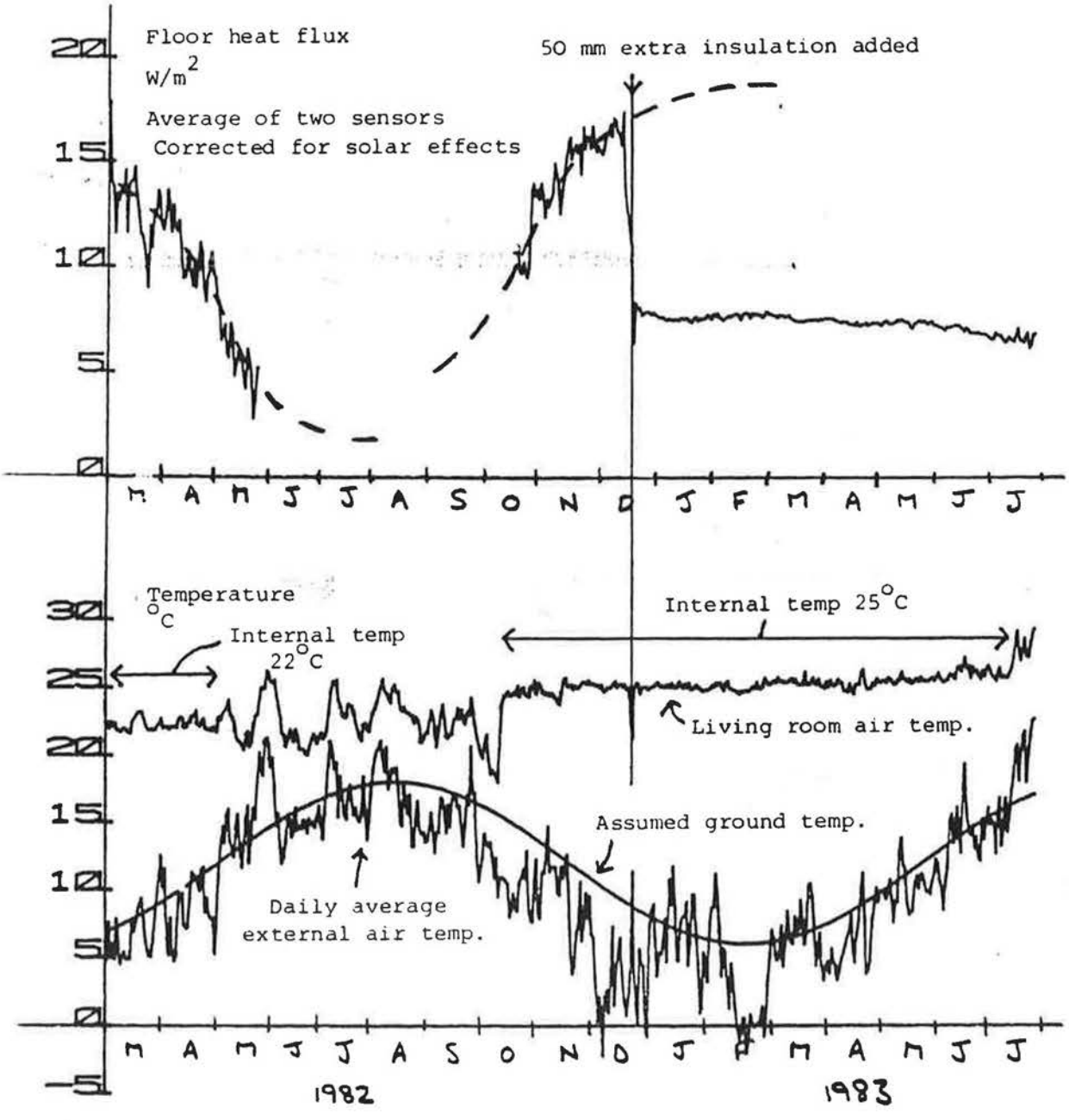

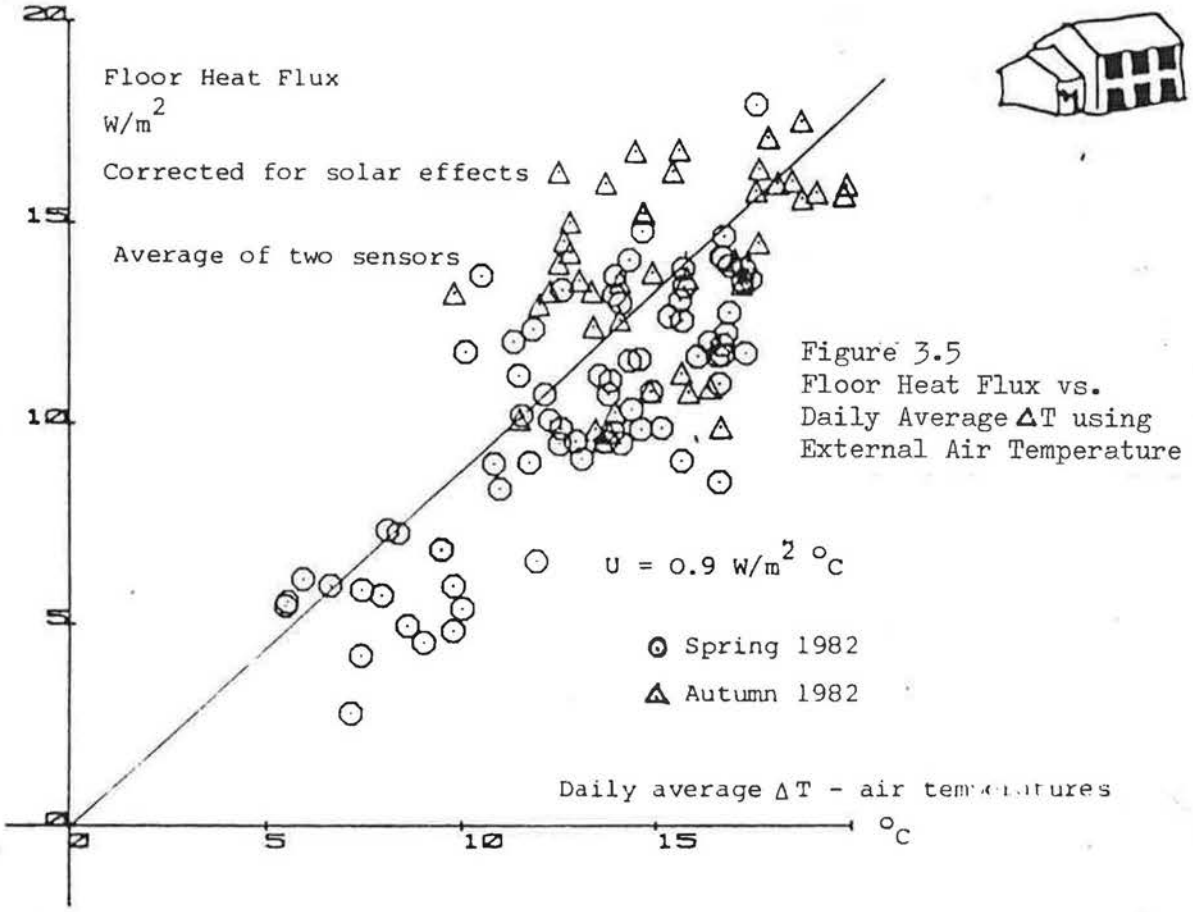

Figure 3.5
Floor Heat Flux vs.
Daily Average ΔT using
External Air Temperature

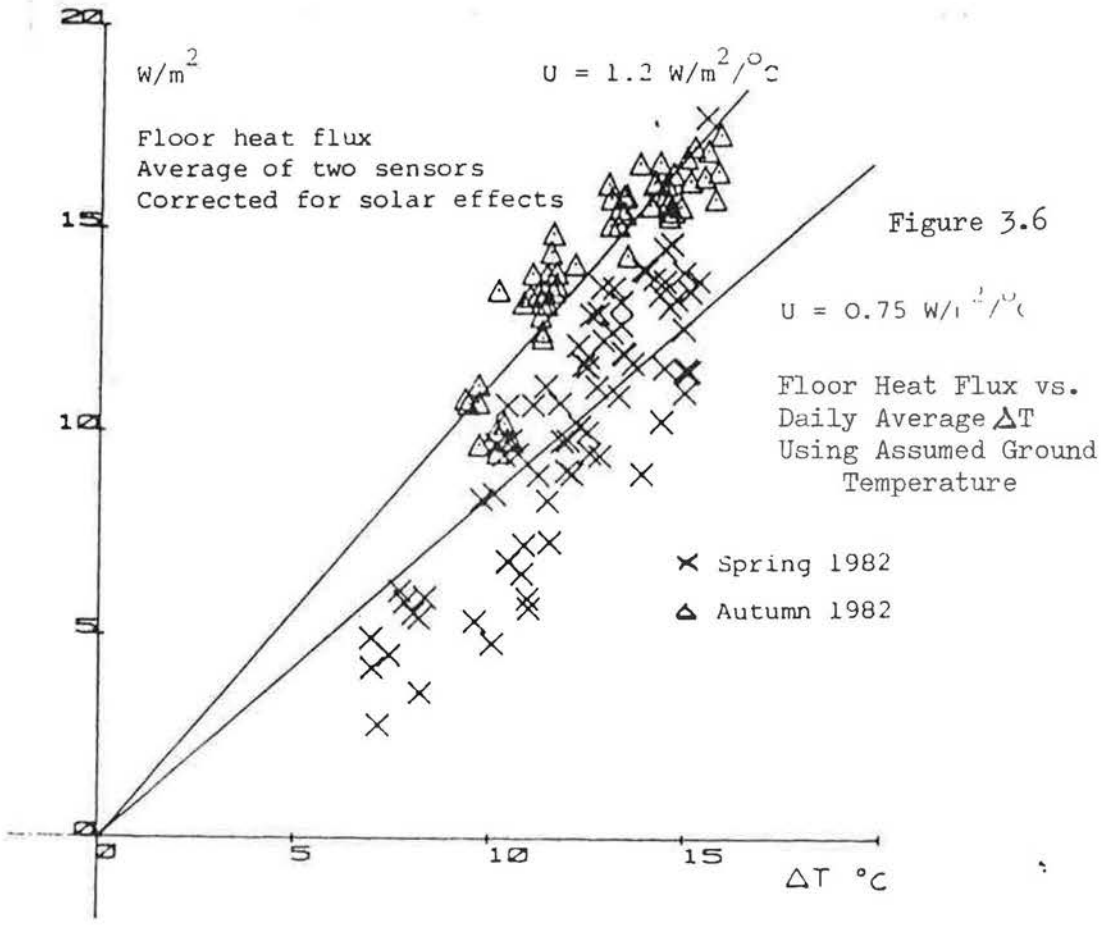

Figure 3.6

Floor Heat Flux vs.
Daily Average ΔT
Using Assumed Ground
Temperature

Daily average ΔT calculated from living room temp. and assumed ground temp.

These floor measurements are, however, only extrapolated from two spot values. Examination of the consistency of the thermal calibration method suggests that the floor heat loss may not actually be constant after December 1983 but may be changing (see chapter 6). The two sensors are immediately below the 50 mm insulation but this is penetrated by large cold bridges in the form of the partition walls, made of dense concrete. Thus it is not really valid to extrapolate from the two sensors to the total floor loss in this case.

No floor measurements were made at the Spencer St. house since the researchers were then sufficiently naive to believe that because there was very little written about floor heat loss, that it was not a problem. In fact, the lack of literature on the subject reflects a genuine lack of knowledge in the area and especially a lack or real experimental measurements. Apart from Spooner's experiments there appears to be no actual published measured data in the U.K. The tables of heat loss in the I.H.V.E. and C.I.B.S. Guides are computed estimates produced around 1950 by N.Billington using an analogue computer. His book 'The Thermal Properties of Buildings', published in 1954 (ref. 3.2.), makes it clear that no measurements had been carried out in the U.K. then, and only a few in the U.S.A. Even those were on constructions with a fairly poor level of insulation. It was also clear that the thermal dynamics of floor heat loss were not understood. This history, including Macey's equation, which deserves revival, is dealt with in the Linford monitoring report.

Thus for practical experimental purposes it seems desirable just to treat the floor loss as a complete unknown, measuring it with as many heat flux sensors as can be spared to the task. About five would seem reasonable for the Linford test house, one in the centre and four spaced around the perimeter, though more would have been useful in exploring the cold bridges caused by the partition walls after full insulation. A thermographic survey can be useful in pinpointing cold bridges and defects, but these are not as likely to be visible in the floor as in other parts of the building structure (see chapter 5).

Floor heat loss is obviously an area where further research is urgently needed, but given the slow timescale of thermal response any practical serious project is likely to take several years to carry out.

References

3.1 D.Spooner, Heat Loss Measurements through an Insulated Domestic Ground Floor, Building Services Engineering Research and Technology, Volume 3, No. 4, 1982

3.2 N.Billington, The Thermal Properties of Buildings, Cleaver Hulme Press, 1954.

4. AIR INFILTRATION

CONTENTS

This chapter describes the air leakage and infiltration measurements on the Linford test house and their consequences for rapid house testing.

CHAPTER 4

AIR INFILTRATION

This has turned out to be the most expensive and complex part of the thermal calibration process. The accuracy to which the house fabric heat loss can be determined is largely limited by the errors in measuring the infiltration loss. Fortunately this is an area where much research is going on in the development of simpler methods which may bear fruit in a few years.

Firstly, it is necessary to distinguish between three different terms that tend to get confused: air leakage, air infiltration and ventilation.

Leakage
The air leakage of a house is a measure of the total number of cracks in the structure and their size. It is measured by pressurizing the house with large fans and measuring the resulting air flow.

Infiltration
This is the air flow through the house under the normal influence of wind and temperature, measured with all the external doors and windows shut. It is measured with a tracer gas technique.

Ventilation
This is effectively air infiltration plus the effects of window and door opening by the occupants. It is difficult to measure directly because of the presence of the people in the house, but methods using carbon dioxide are being developed.

4.1. Pressure Tests

For practical purposes of thermal assessment of buildings, pressure tests give a very rapid indication of the overall leakiness of a building. The equipment, although cumbersome, is simple and relatively cheap (see figure 4.1).

Tests were made by British Gas on all of the Linford houses and some from the Pennyland project. The fans were connected to a substitute window pane that could easily be fitted, allowing a house to be tested in 3-4 hours.

Because the pressure tests involve a fair amount of upheaval in the house and a massive increase in air change rate, they cannot be carried out during the thermal calibration period proper, but must be done either before or after.

The fans are used to pressurise the house and the air flow rate is measured using a precalibrated nozzle in the fan outlet. The difference in pressure between the inside and outside of the house is measured using a manometer (essentially a sloping glass tube full of water). The air flow rates at various pressure differences can then be plotted as in figure 4.2. From this the flow rate at some

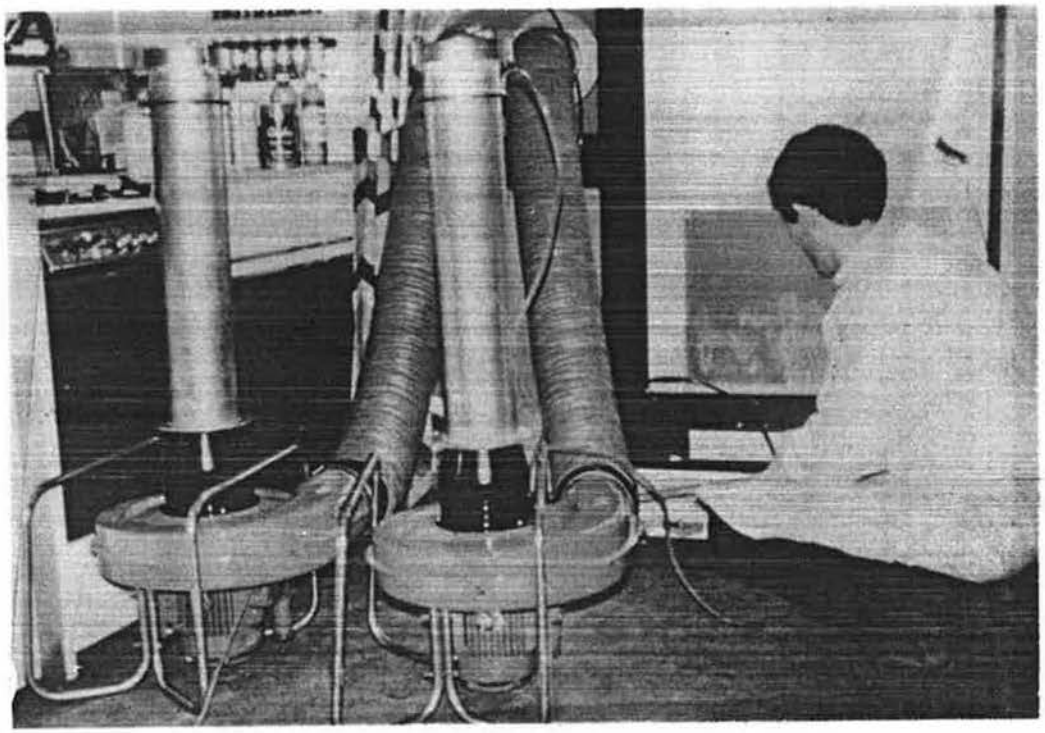

Figure 4.1. Fans being used to pressurise a house

Photo courtesy British Gas

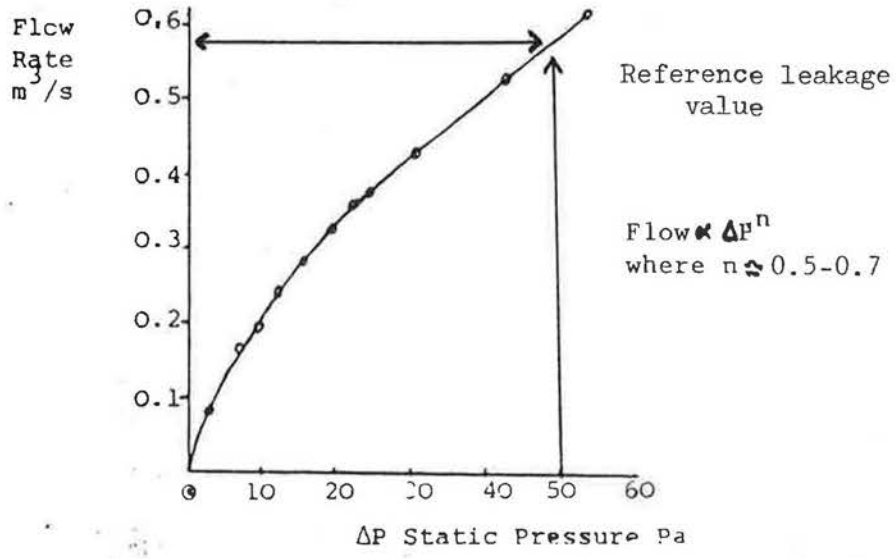

Figure 4.2 Air flow as a function of house inside-outside pressure difference.

standard pressure, usually 50 Pascals, can be worked out. When expressed in terms of the house volume as ac/h this value can be used to compare the results with tests on other houses. Figures 4.3 and 4.4 show the Linford and Pennyland results compared to some modern Canadian and Swedish houses and a sample of 'normal' U.K. houses.

The standard of 50 Pascals does correspond to hurricane force wind conditions and some researchers in the U.S.A. have adopted 10 Pa as a standard and attempted to relate the leakage at this pressure to a seasonal average infiltration rate. This process is discussed later.

Pressurising the house does also allow the identification of individual leakage paths using smoke tests (a large cigar is useful).

4.2. Air Infiltration

For both the Spencer St. and Linford test-houses air infiltration was measured using nitrous oxide as a tracer gas using a decay time method. This involves injecting a known concentration of tracer gas into the house, ensuring that it is evenly mixed throughout with plenty of circulating fans. The concentration is then measured over the next few hours. It decreases as the air/gas mixture leaks out of the house and outside air replaces it. The decay takes an exponential form, and from this the house air infiltration rate can be worked out. This is described in detail in the Linford project report. (See also Appendix 1).

An alternative approach and one that is really more suitable for houses with very low air change rates is to use a system that maintains a constant concentration of tracer gas in the house by steady topping up. This method was used by British Gas in their 'Autovent' system which was used for a brief period in the Linford test house. The system was very versatile and could be used to simultaneously measure individual room infiltration rates. Obviously this system would be the best for any practical house thermal calibration work, but the price for the system of about £40,000 is beyond most pockets.

For the long-term Linford measurements a decay-curve system was modified for continuous automatic operation, providing a much cheaper alternative at around £10,000. Details of this system are given in the equipment section.

For best results it would seem that continuous infiltration rate measurements are desirable, since the wind can pick up quite suddenly increasing the infiltration rate. Automatic operation would seem to be a requirement of any system for two reasons. First, it is desirable not to have researchers continually entering the house under test, disturbing the air infiltration with door opening and supplying extra body heat. Second, nitrous oxide is an anaesthetic gas. Although the concentrations used are well below any published danger level, researchers from both the Spencer St. and Linford projects complained of various symptoms, including dry throats, headaches, confusion and loss of memory after prolonged exposure.

* 50 Pa $\triangleq$ 1 lb/ft^2 $\triangleq$ 5 mm H_2O pressure

Figure 4.3

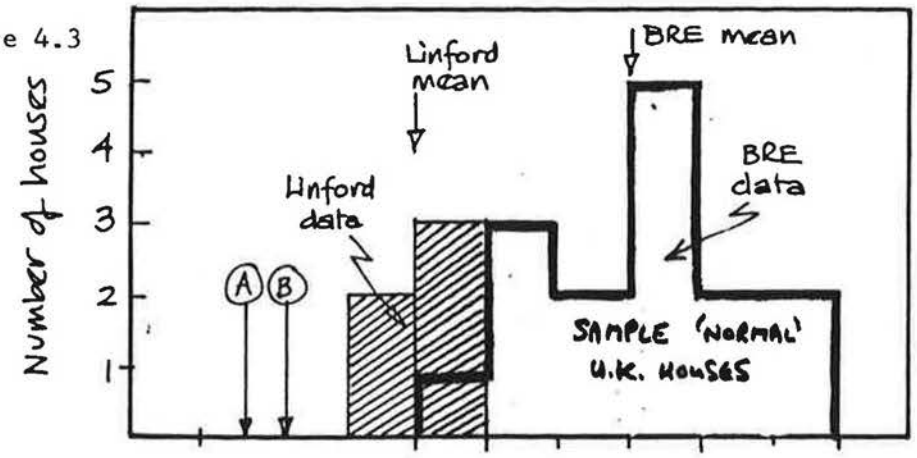

(A) Swedish dwellings (mean of 320 houses)

(B) Canadian dwellings (mean of 50 houses)

Figure 4.4

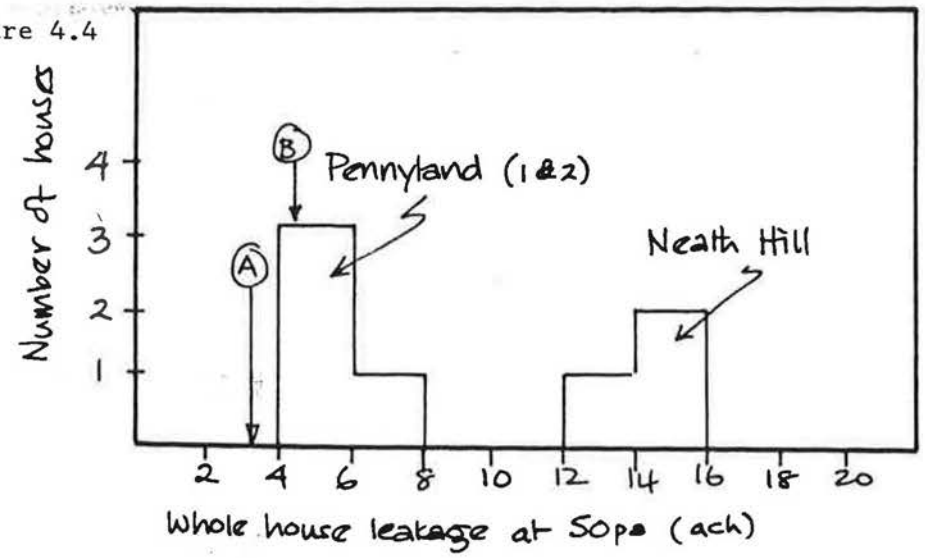

Results of the pressure tests at Neath Hill and Pennyland compared to the Linford results, BRE measurements and Swedish and Canadian results.

Data from ref.4.1 and ref. 4.2

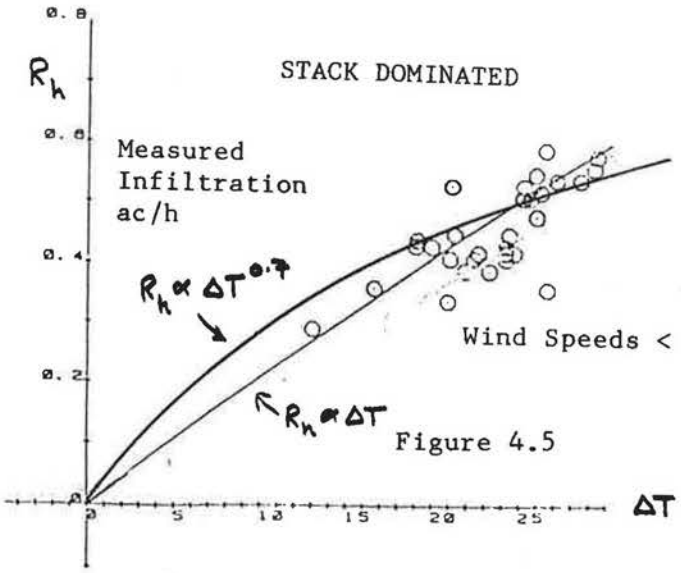

Figure 4.5

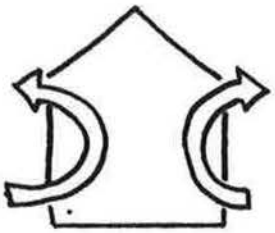

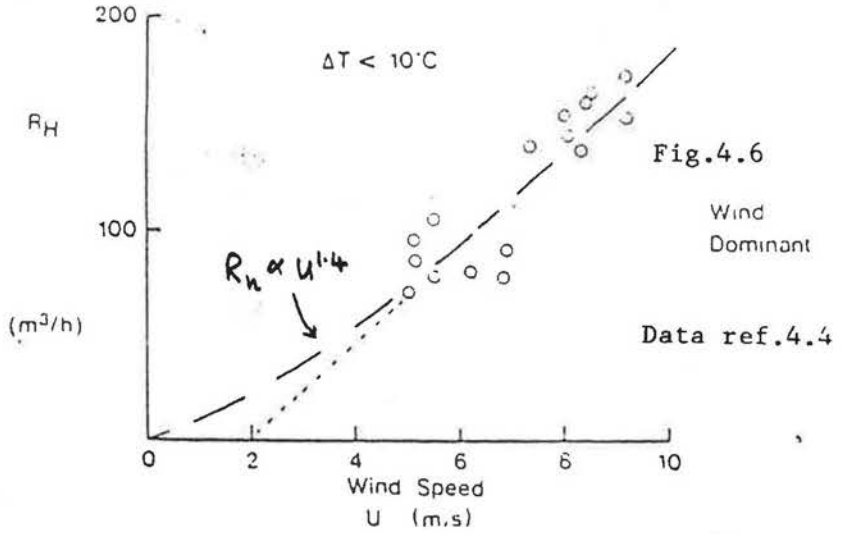

Fig.4.6

Wind
Dominant

Data ref.4.4

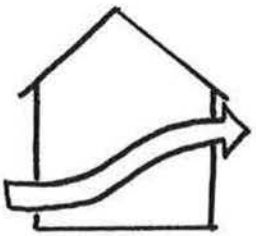

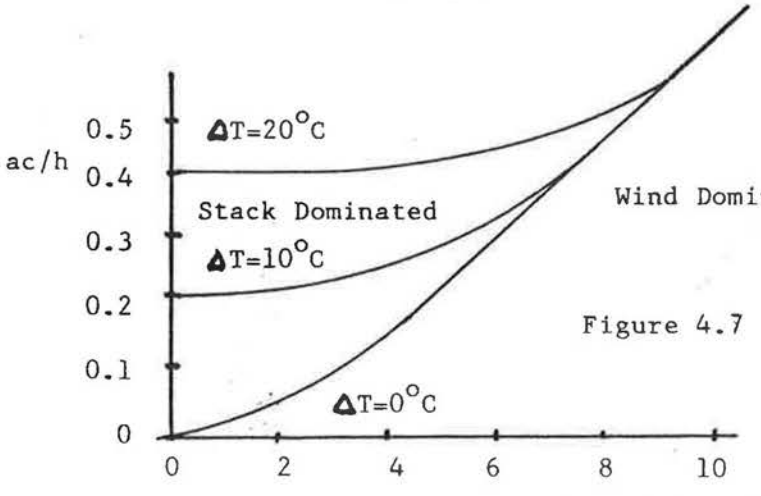

Wind Dominated Zone

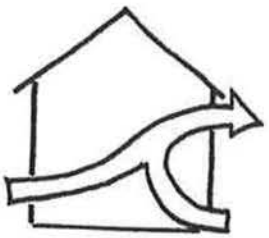

Figure 4.7 Combined Response

4.3. Air Infiltration Theory

Given the relative importance of the air infiltration measurements to the thermal calibration process, and the likelyhood of the equipment needing periodic attention, it is necessary to explain a little of the theory relating infiltration to ΔT, wind speed and direction, so that missing measurements can be filled in with estimates. For the Linford test house actual infiltration measurements were not available over the full experimental period and so missing values were filled in from an infiltration model and measured weather data.

The model is fairly complex and was originally supplied by British Gas as a result of their tests made with the 'Autovent' system. For practical short thermal calibrations it is unlikely that such a full model could be built up, but some basic understanding would allow the filling in of some missing data points.

Air normally moves through a building under both the influence of wind and temperature. There are two driving forces, the stack or buoyancy effect and wind pressure.

4.3.1. Stack Effect

The air inside a house is for the most part warmer than the outside air and hence lighter. It thus tends to rise, in the same manner as a hot air balloon. The stack driving force is proportional to both the height of the house and the inside-outside temperature difference.

Against this driving force is set the resistance to air movement of the cracks in the building fabric. For long thin cracks, such as through walls, the air flow rate is proportional to the applied pressure. For shorter, wider cracks it is proportional to the square root of the pressure. Thus the overall house infiltration rate under stack dominated conditions can be expressed as:-

$$\text{Flow} = K.\Delta T^{n}$$

where K and n are constants.

Figure 4.5 shows a plot of measured infiltration vs. ΔT for low wind speeds for the Linford test house over a period of several months. This shows that, taking typical measurement errors into account, it is really very difficult to assign a precise value to the exponent n. Given the limited range of ΔT's that we would be likely to encounter in any short test, it is probably simplest just to take the infiltration to be proportional to $T^{0.7}$. The exponent can be estimated from pressure test results, though the extreme pressures used may not give representative values for more gentle natural conditions.

4.3.2. Wind Pressure Effects

In addition to the stack effect, the wind pressure exerts a driving influence. The effect on air infiltration is approximately proportional to the wind speed at high values and somewhat non-linear at low speeds (see figure 4.6). In the theory suggested

by Warren (ref. 4.6) the wind response is taken to be proportional to U^{2n}, or typically $U^{1.4}$. This gives a reasonable approximation to the observed response. The effects of ΔT actually take over at low wind speeds giving a series of possible curves as shown in figure 4.7..

Warren and Sondereger (ref.4.5) both suggest taking this combined response as the vector sum of the stack dominated response and the wind response:-

$$\text{Total Infiltration} = \sqrt{(\text{Stack Response})^2 + (\text{Wind Response})^2}$$

$$\text{or} \quad \sqrt{(A.\Delta T^n)^2 + (B.U^{2n})^2}$$

where $n \simeq 0.7$

The effect of wind is not likely to be equal in all directions. For the Linford test house, there seemed to be a pronounced sheltering by the garage and the adjacent house to the south-west (see figure 4.8) and a terrace house is likely to be considerably sheltered by the neighbouring houses (figure 4.9). This added dimension of wind direction, which in practice tends to change continuously with the passing cyclones and anti-cyclones, makes it difficult to build up a total picture of the infiltration response to wind given only a short measurement period.

For the Linford test house the British Gas tests were sufficient to produce a partial model of the house infiltration response to winds from the south-west, with a conjectured response in other directions. The O.U. measurements, covering over two months were sufficient to extend this model to winds from the north-east, but even then the lack of strong winds from the north-west and south-east still left gaps in measuring the full response.

The full model built up, including both wind and temperature effects was sufficiently accurate to predict the measured infiltration rate to within $\pm$ 0.15 ac/h or, in heat loss terms $\pm$ 13 W/°C. The offset of 15% between the model and the measurements (see figure 4.10) may simply be due to the fact the the British Gas measurements were made with the internal doors shut, but the O.U. ones were made with them open.

This model, which used slightly different assumptions about combining wind and temperature effects to those above, was extended to estimate the ventilation rates for the occupied houses, including measured window opening. These calculations are all described in detail in the main Linford report.

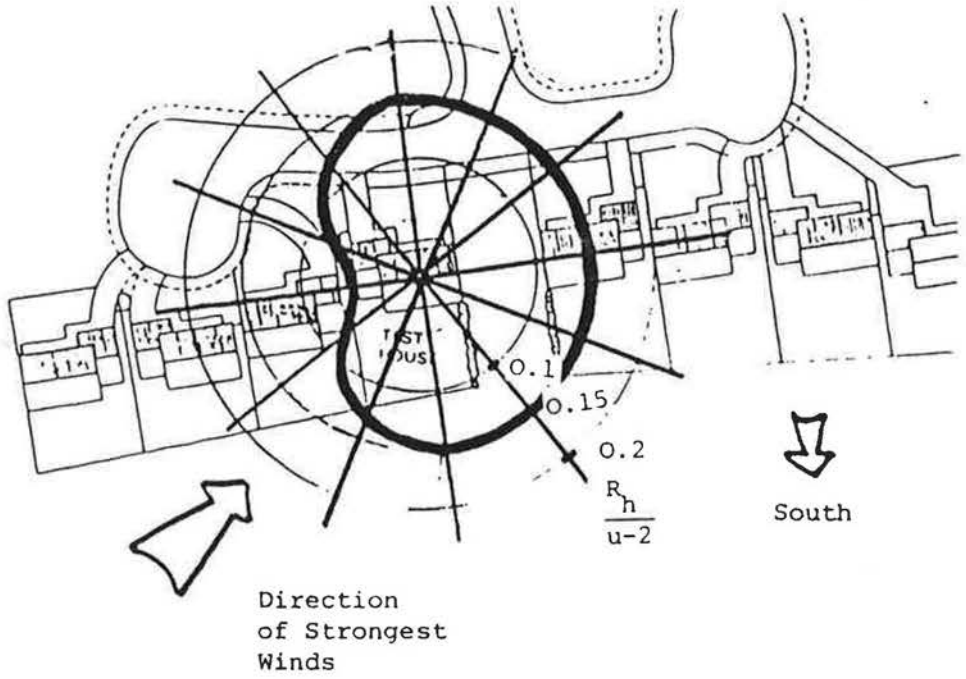

Figure 4.8 The response of the Linford test house to wind pressure showed a pronounced sheltering effect due to the house immediately adjacent to the west.

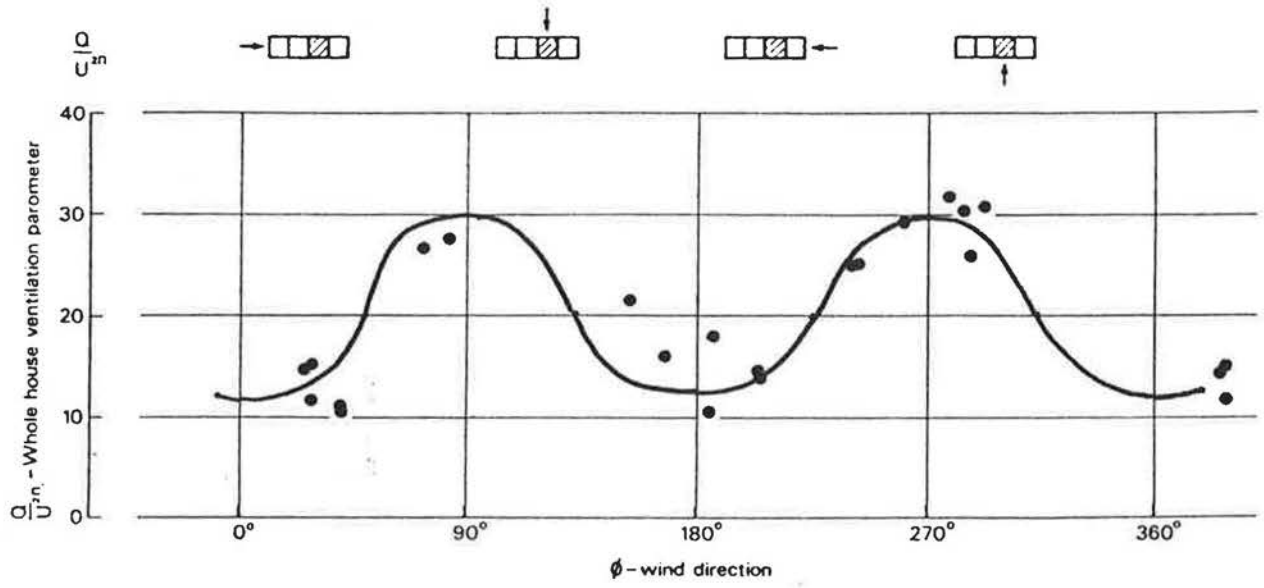

Figure 4.9 The response of a terrace house to wind pressure (ref.4.1)

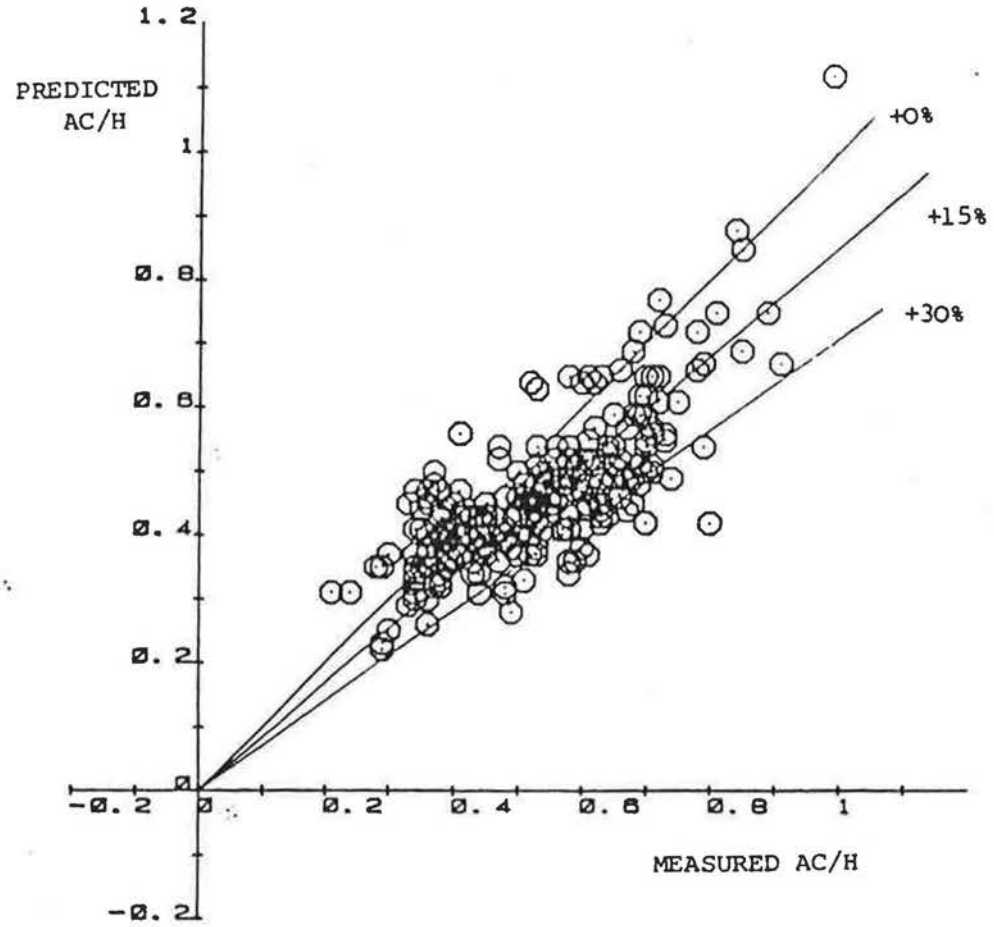

Figure 4.10. Comparison of measured Linford test house air infiltration rates with predictions from British Gas model.

4.4. Practical Measurements

There are several possibilities open to the researcher for practical infiltration measurements during the thermal calibration period. In order of decreasing effort, these are:-

A. Full continuous measurements

This is the most desirable situation, but implies the use of an automatic measurement rig. This is likely to be very expensive, but for the Linford project a normal manually controlled rig was converted to automatic operation (see Chapter 5).

B. Intermittent Measurements

This is basically what is likely to happen if (A) is attempted, given the normal interruptions in measurements for changing filters and attending to minor breakdowns in the infiltration rig. Figure 4.11 shows a typical sequence of measurements, showing missing gaps of one or two days. For a manually controlled rig, the samples would be even more sporadic. Given the importance of the measurements and the rapidity with which the infiltration rate can increase with wind speed, it is necessary to fill in missing values by generating a crude model of infiltration as a function of wind speed, direction and ΔT (see below).

C. Pressure tests alone, or no measurements

This is certainly the cheapest option. Here it would be best to assume that the infiltration rate is constant, but to discard days from the data set with wind speeds greater than about 4 m/s for a significant proportion of the time, especially when the wind is broadside on to the house. No infiltration rate measurements were made during the thermal calibration test on the Spencer St. house, but fortunately the winds were both light and end on to the terrace over the period. It is thus very likely that the house was firmly operating in a stack dominated mode over the whole time.

4.4.1. Filling in Missing Values

Given the brief theory described so far, it is possible to build up plots of infiltration vs. ΔT, wind speed and direction using fairly minimal amounts of data. The measurements in figure 4.11 tend to take the form of an almost constant base level value of about 0.5 ac/h determined largely by ΔT, punctuated with short wind-induced peaks rising up to 1 ac/h. The problem is that of how far the infiltration model described above can be built up using only a limited number of data points.

Over a short data set of a couple of weeks, ΔT is not likely to vary very much. Plotting air change rate, R_h, against ΔT for low wind speeds (<1 m/s) for this sample measurement period (see figure 4.12) is really no more informative than using the larger number plotted in figure 4.5. It is really up to the experimenter to decide how to fit a line between the cluster of points and the origin. A line of the form $R_h = K.\ \Delta T^{0.7}$ is probably the best from the point of view of the physics involved.

Like ΔT, the wind direction over this short data set does not vary very much either. The wind response of infiltration is thus best determined by splitting plots of infiltration against wind speed into wind direction

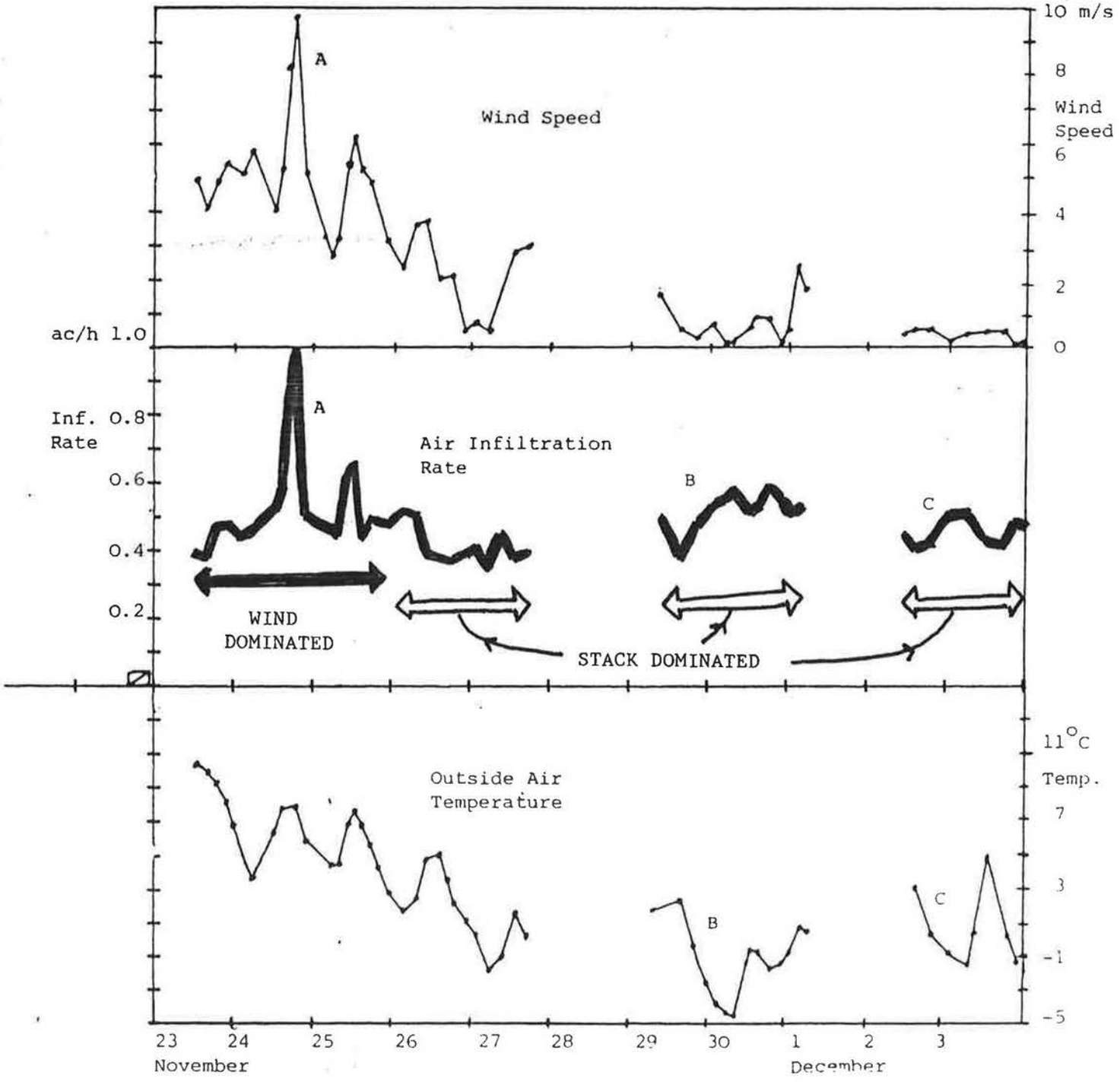

Fig.4.11. Effect of wind and stack effect on air infiltration rates

Test House measurements 1982
Internal temperature = 25°C
Wind dominated - Point A
Stack dominated - Points B and C

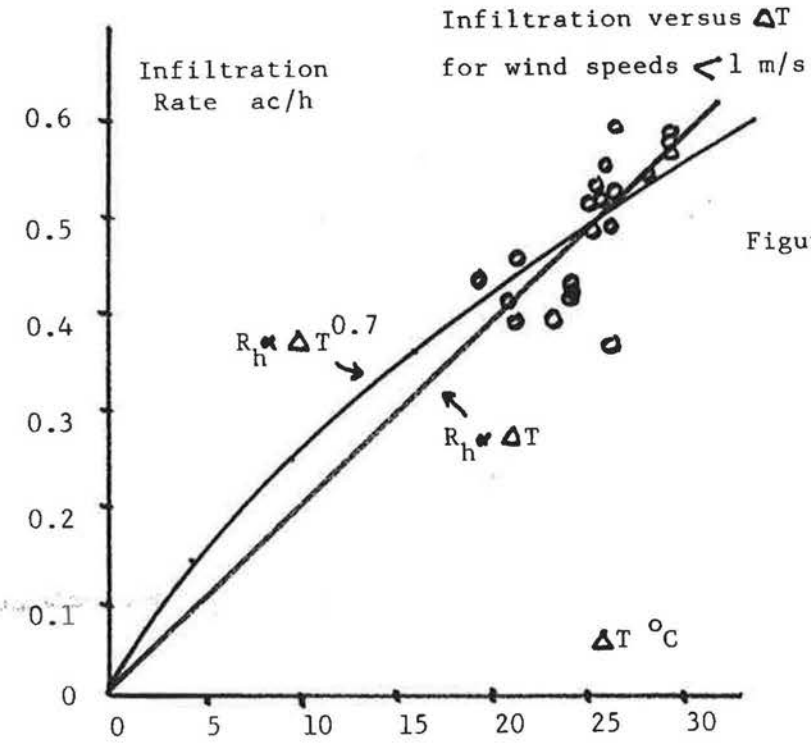

Figure 4.12

Figure 4.13.

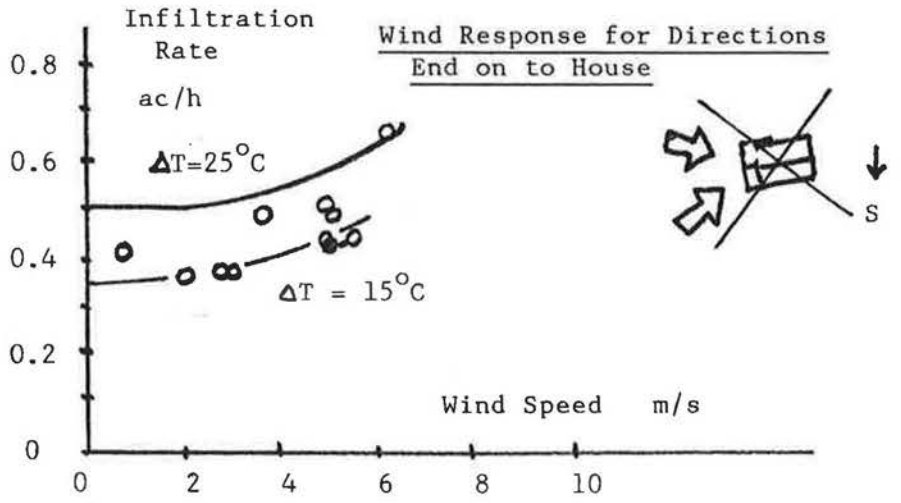

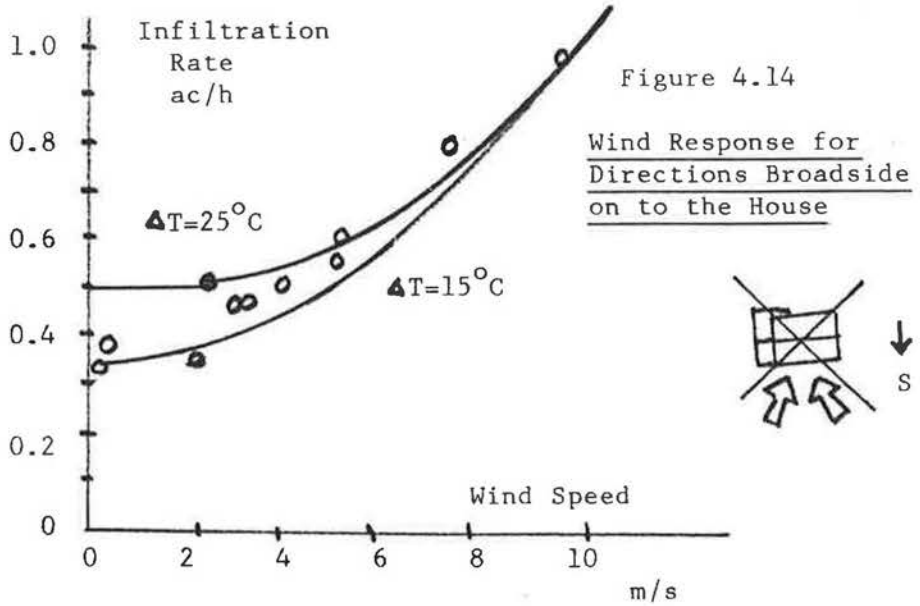

Figure 4.14

Wind Response for Directions Broadside on to the House

sectors, the size being chosen to contain a reasonable number of points. In this case the sectors can be quadrants broadside on and end on to the houses.

Figures 4.13 and 4.14 show plots of R_h vs. wind speed for the two quadrants containing data points with high wind speeds (directions at low wind speeds obviously do not matter so much). Figure 4.14 clearly shows the transition from stack dominated to wind dominated response and thus could be used to fill in missing data points to an accuracy of about $\pm$ 0.2 ac/h given measured values for ΔT, wind speed and direction within this quadrant. Figure 4.13, on the other hand, lacks enough data points at high wind speeds and so can only be used up to about 5 m/s.

Thus this limited data set can give a partial descriptive model of infiltration rates that can be used to fill in missing measurements. Although it would be reasonable to extrapolate beyond the actual measurements as far as ΔT is concerned, doing so for the wind response would be rather risky. It would be better to discard days from the thermal calibration data set that have high wind speeds from previously unmeasured directions.

4.5. Relation of Pressure Tests and Average Infiltration Rates

A pressure test essentially determines the total number and size of cracks in a building structure. The average infiltration rate over a heating season, which is a figure that is meaningful in terms of heat loss calculations involves also the distribution of cracks in the building, the sheltering of the building by others adjacent and obstacles such as trees and hills, average wind speeds and directions plus average internal and external temperatures.

As such, there is obviously no simple relation between pressure test results and average infiltration rates.

By making extensive assumptions, some researchers have produced rough answers. The main problem is that of mutual sheltering of houses from the wind and the related problem of assessing actual wind speeds in built-up areas from 'meteorological' wind speeds (usually measured in such places as airfields). This has led to studies of house models in wind tunnels to assess the wind effects.

Calculations for the Linford test house, using the fitted infiltration model and a whole heating season's weather data, show that the seasonal average infiltration rate is strongly dependent on the assumed house orientation and sheltering. It may vary from 0.28 ac/h with the house essentially in a terrace, end on to the prevailing wind, up to 0.41 ac/h with the house facing the prevailing wind with no sheltering from other houses.

The 50 pa pressure test air leakage for the house was 8.9 ac/h and taking the infiltration figure of 0.41 ac/h implies that the seasonal average air infiltration rate is about 1/20th that of the pressure test leakage. This is in reasonable agreement with the values from figure 4.15, showing 'typical' house infiltration rates at 3.5 m/s wind speed plotted against their 50 pa leakage rates. The figure of 1/20th is thus a good rule of thumb, but obviously can vary by 30% either way.

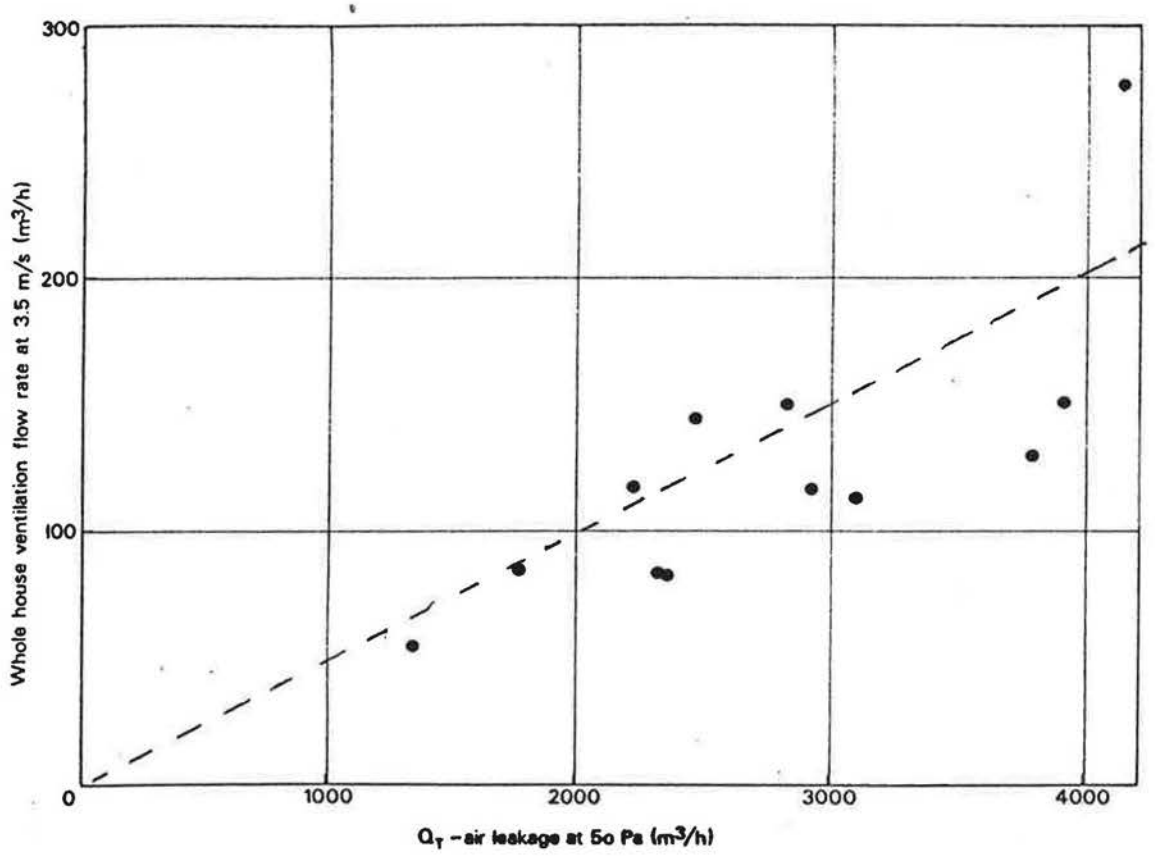

Figure 4.15. Variation of 'typical' winter air infiltration rate at 3.5 m/s wind speed with measured pressure test leakage at 50 pa pressure. (ref. 4. 3).

References

4.1 Ventilation Measurements in Housing, P.Warren & B.Webb, C.I.B.S. 'Natural Ventilation by Design' Conference, Dec. 1980

4.2 Leakages of 4 houses in the Linford 8b Scheme, Milton Keynes, D.W.Etheridge & J.P.Smart, British Gas, June 1981.

4.3. Natural Infiltration Routes and their Magnitude in Houses, P.Warren, Building Research Establishment, 1976.

4.4 Ventilation Measurements in an O.U. Test House, D.W.Etheridge & J.P.Smart, British Gas, December 1982.

4.5 An Instrumented, Microprocessor-Assisted Residential Energy Audit, R.Sonderegger, D.Grimsrud & D.Krinkel, Colloquium Comparative Experimentation of Low Energy Houses, University of Liege, 1981.

4.6 Relationship between Tracer Gas and Pressurisation Techniques in Dwellings, P.Warren & B.Webb, Building Research Establishment, 1980.

5. MEASURING AND ANALYSIS EQUIPMENT

CONTENTS

This chapter describes the equipment needs for both measurement and analysis and describes some of the equipment found useful in the three projects in this report.

CHAPTER 5

MEASURING AND ANALYSIS EQUIPMENT

This report is not the place to launch into a full description of all possible monitoring techniques. Much of this area is exhaustively covered in the S.E.R.C. Field Trial Monitoring Notebook (ref. 5.1). There have, however,been advances in certain areas since this was compiled in 1981 and so this chapter contains descriptions of equipment that has been specially developed for the projects covered in the report, or found especially useful.

Also the Field Trial Notebook did not fully address itself to the equipment needs of analysing data. The Linford and Pennyland projects have provided plenty of experience in data analysis and it is worth spelling out the equipment needs and the processes involved.

5.1. Analysis Equipment and Methodology

Time and again researchers set forth to do monitoring with the idea that if only they can get their datalogger to read in some temperatures all will be well and the project answers will fall out by magic (and the final report will be written in the next week!). In practice, a whole project has a large number of processes that have to be gone through. They can be summarised as:-

A. Measurement
B. Storage
C. Display
D. Cleaning
E. Description
F. Understanding
G. Calculation
H. Explanation

There are also various feedback loops in the process that are shown in figure 5.1.

5.1.1 Measurement

This is the topic that usually gets the most thought. It requires datalogging equipment that actually works in the field and not just in the laboratory. Since technicians who are prepared to leave the cosy laboratory are rather rare, it is best to test everything in the lab. before starting. Since projects always run late (the precise details of how the funding process guarantees this are spelt out in the Field Trial Notebook) there is usually pressure to install untested equipment in order to create the illusion of progress. This simply creates more work for the future when the equipment breaks down on site. Be warned!

5.1.2 Storage

The best way of storing measured data is on one enormous computer disk. This gives instant access to any bit of data for checking and comparison. Having data on separate bits of tape (or paper) creates endless problems. For the small calibration projects envisaged here about 1 megabyte of storage is adequate.

Figure 5.1 MEASUREMENT AND ANALYSIS PROCESS

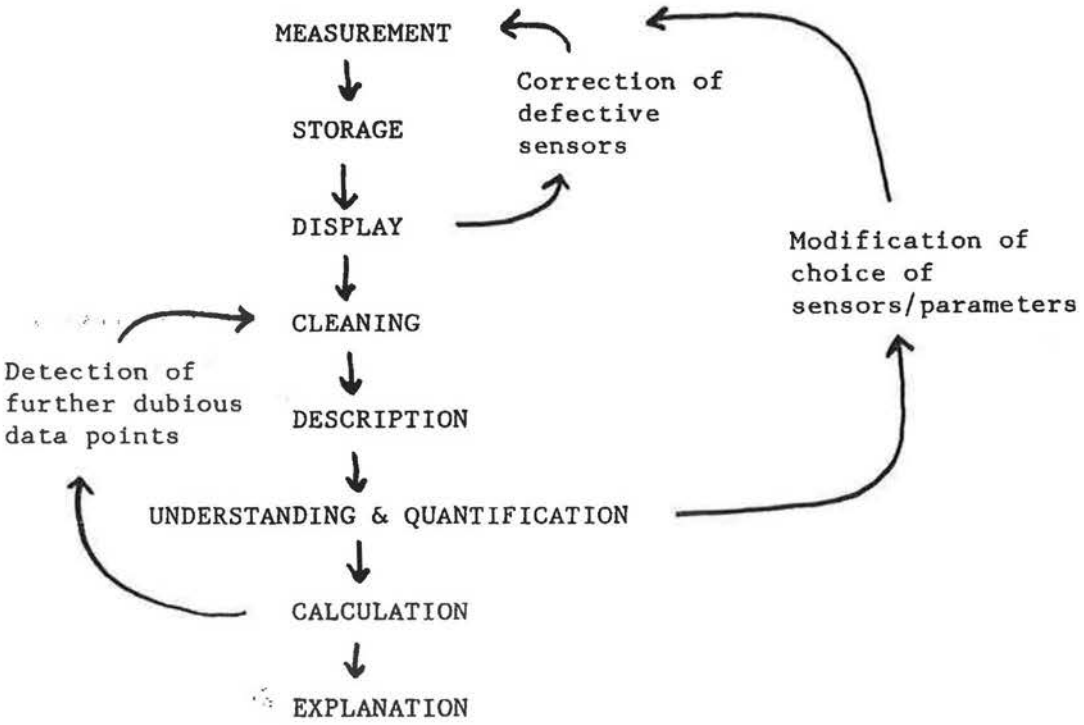

Since all the data is in one place, it does create the possibility that all of it might get lost at once. Keeping backup disks is, of course, vital, but massive computer failures do happen. It is thus a good idea to keep digests of daily data on paper, so that even if the worst happens, something can be produced in the way of results.

The adequate management of a disk database requires a computer of a certain level of sophistication, but it isn't very high and is well within the capabilities of most medium-sized micros.

5.1.3 Display

This is a rarely discussed topic, but is absolutely vital for both checking the data and understanding it.

The raw data should be checked as soon as possible after measurement to see whether any sensors have broken down. Preferably this should be done on the same day.

For this, it is vital that the computer has a V.D.U. with proper graphics. Most large university computers are hopeless in this respect, the V.D.U. being regarded as just a fast Teletype. Small micros with their video games heritage are ideal, especially since the display process is likely to be programmable with a high degree of user-friendliness. A large mainframe computer may have a graphics package, but it probably requires a friendly system programmer to actually get it to do what you want.

The best solution is either to use a large micro for the whole job or possibly to use a micro as a display terminal inspecting data stored in a large mainframe computer. Either way it is a vital area that must be thought about in a project.

5.1.4. Cleaning

Before the data can be fed into regression processes or even tidy graphs plotted, it must be made sure that there are no equipment errors, recording errors, or in the case of occupied houses, periods of anomalous occupant behaviour, such as holidays, in the data sets. This requires an enormous amount of data inspection. Basically every recorded bit of data has to be inspected to see if it is credible. This requires good fast access to all the data and good graphics. It is very tedious work, which can to a certain degree be automated, but the quality of final results is highly dependent on it.

5.1.5. Description

Much of the value of the Spencer St. and Linford projects has been in simply describing what is going on, without necessarily quantifying things. This qualitative information is very valuable in assessing how heating systems are working or thermal mass responding to solar radiation, etc. This requires a lot of use of computer graphics to display the data and many hours just spent inspecting it.

5.1.6. Understanding and Quantification

This follows on from description. It is a process during which data is summed in various different ways, according to different theories in the case of such topics as air infiltration, and plotted out in order to see which method makes the best sense. This requires an enormous amount of time just spent plotting graphs. This in turn requires good computer graphics and a fast printer/plotter. The graphs in this report, for instance, only represent about 1% of the total number plotted out over the course of the various projects.

The understanding process is also likely to make it clear that different measurements are required or that some measurements that have been regarded as unimportant are in fact quite vital and that the sensors should be checked for accuracy.

5.1.7. Calculation

Although the understanding and quantification process requires a certain amount of calculation, at the end of the day the graphs that make the best 'sense' are subjected to statistical analysis to extract the important parameters and to quantify the quality of fit. This requires that the computer has a statistics package. Although these are standard for large main-frame computers, they are sometimes expensive to get hold of for a micro. In the case of the O.U. mainframe used for the Linford project, a Vax, the statistics package simply never arrived from the USA and one had to be written specially, so it is wise to check that one is actually available.

The calculation process is also likely to throw up data points that do not fit with the rest and it may be necessary to return to the data cleaning stage to see if these are not just due to equipment errors.

5.1.8. Explanation

While the researchers may think they understand the final numbers coming out of a project, it can be guaranteed that very few other people will. Actually explaining the results is a whole task in itself. This requires good quality plots of graphs,which in turn requires a good understanding of the software of the printer/plotter driver, especially as regards putting the labels on graphs, automatically drawing best-fit lines through data, etc. For a micro this seems to require many hours reading the fine print of the computer and printer manuals. For a main-frame machine it usually requires a long-suffering system programmer to do it for you.

5.1.9. Conclusions

From this description, it can be seen that over and above a datalogger and appropriate sensors there are other vital equipment needs for data handling and analysis:-

1. A computer capable of handling a reasonable disk database
2. About 1 megabyte of disk storage
3. A V.D.U. capable of handling good computer graphics.
4. A statistics software package
5. A graphics printer.
6. Intelligible software to drive it.
7. For a main-frame computer, a long-suffering system programmer.

Given that most projects have enough problems with the houses themselves and the measurement equipment, there is probably a real need for a house analysis/display software package incorporating data cleaning and statistics routines, to ease the computing burden.

5.2. Automatic Air Infiltration Rig - Design by John Butler

The continuous measurement of air infiltration is a vital part of the thermal calibration process. Manual operation of a gas analyser is slow and tedious. Commercial automatic systems such as the 'Autovent' system used by British Gas are very expensive although extremely versatile. Thus a conventional manual system was modified for automatic operation for the Linford project and used for several months in the test house.

The process consisted of injecting nitrous oxide gas into the house and measuring the rate at which the gas concentration was diluted by normal infiltration. The equipment also went through an automatic calibration cycle at the end of each measurement cycle.

The overall system is shown as a diagram in figure 5.2 and a photo in figure 5.3. The primary sensing instrument used was an IRGA 120 infra-red gas analyser made by Sieger Gasalarm. This instrument draws the sample gas through the sensing process at about 1 l/min and gives a continuous voltage output proportional to the gas concentration.

In order to reduce the time lag between the sample being drawn into tubes situated in various parts of the house and it arriving at the analyser, two pumps were used to increase the velocity of the sample air through the tubes. Most of the sample air was exhausted into the room containing the gas analysis apparatus (which was situated in the test house) via a tee piece connected to the analyser intake.

The gas concentration was recorded against time using a Pointax chart recorder measuring 0-100 mV and fitted with high and low alarm relays. These were used to initiate and terminate the calibration and gas injection cycle. This process was controlled by a timing circuit using three relays. Two of the relays were of the time delay type (RS 347-927) which only turn on after a preset time has elapsed from the application of the switching voltage. Override switches (not shown in figure 5.2) also allowed the various solenoids to be operated for setting up and test purposes.

Gas flows were selected by three solenoid valves, two 3-way (RS 348-380) and one simple on-off type (RS 348-396). One three-way valve (SOL 3) selected sample air or calibration gas, the other (SOL 2) selected zero concentration (outside air) or a calibrated sample, a certified cylinder of N_2O,N_2 and O_2 mixed to known concentrations, 375 ppm N_2O. The on-off solenoid valve (SOL 4) controlled gas injection to the house.

As the calibrated sample gas was stored in a pressure cylinder and had to be reduced to atmospheric pressure before being drawn into the gas analyser, a fourth valve (SOL 1) was used to feed calibrated sample gas through a regulator into a rubber bladder from which the gas could be drawn into the analyser. The bladder was kept full, but not under pressure using a hinged arm connected to a microswitch controlling the solenoid valve.

Nitrous oxide was injected into the various rooms of the house from a pressure cylinder via a gas regulator and control solenoid valve (SOL 4) and through a system of $\frac{1}{4}$" plastic hoses. Each N_2O outlet was fitted with a hose clamp which was adjusted so that the flow out of each outlet was roughly proportional to the volume of the room into which it was injecting gas. Each hose outlet was fixed to a normal office type fan which was kept running continuously to ensure good mixing of the gas and air. It also helps in maintaining a good constant uniform house internal temperature.

Air was sampled through a system of hoses from a number of points throughout the house, at least one per room. Once again each sample intake point was fitted with a hose clamp which was adjusted so that the flow rate into the hose was proportional to the volume of the room from which it was sampling (see figure 5.5).

One hose was fitted through a small hole in a window frame so that outside air could be drawn into the analyser for a zero reference.

The full operating cycle and a truth table for the various components is given in Table 5.1.

A typical chart recorder trace is shown in figure 5.6 showing both the calibration cycle and the exponential gas decay. The actual house infiltration rate is calculated as follows:-

If v is the flow rate of ventilating air into (and therefore out of) the house of volume V, then the change in tracer concentration in time interval dt is:

$$dc = \frac{-vc}{V}\,dt = -Acdt$$

where A is the air change rate in house volumes per unit time,

therefore $\quad \frac{dc}{c} = -Adt$

and $\quad [\ln c]_{co}^{ct} = -A[t]_{o}^{t}$

and $\quad \ln\left(\frac{ct}{co}\right) = -AT$

and $\quad A = -\frac{\ln\left(\frac{ct}{co}\right)}{T}$

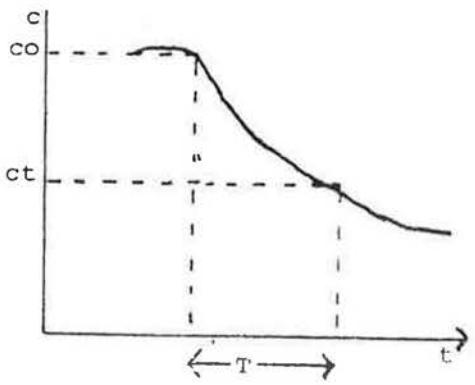

The air change rate can simply be calculated from two points on the decay curve, as shown above.

Figure 5.2 AUTOMATIC INFILTRATION RATE MEASUREMENT RIG

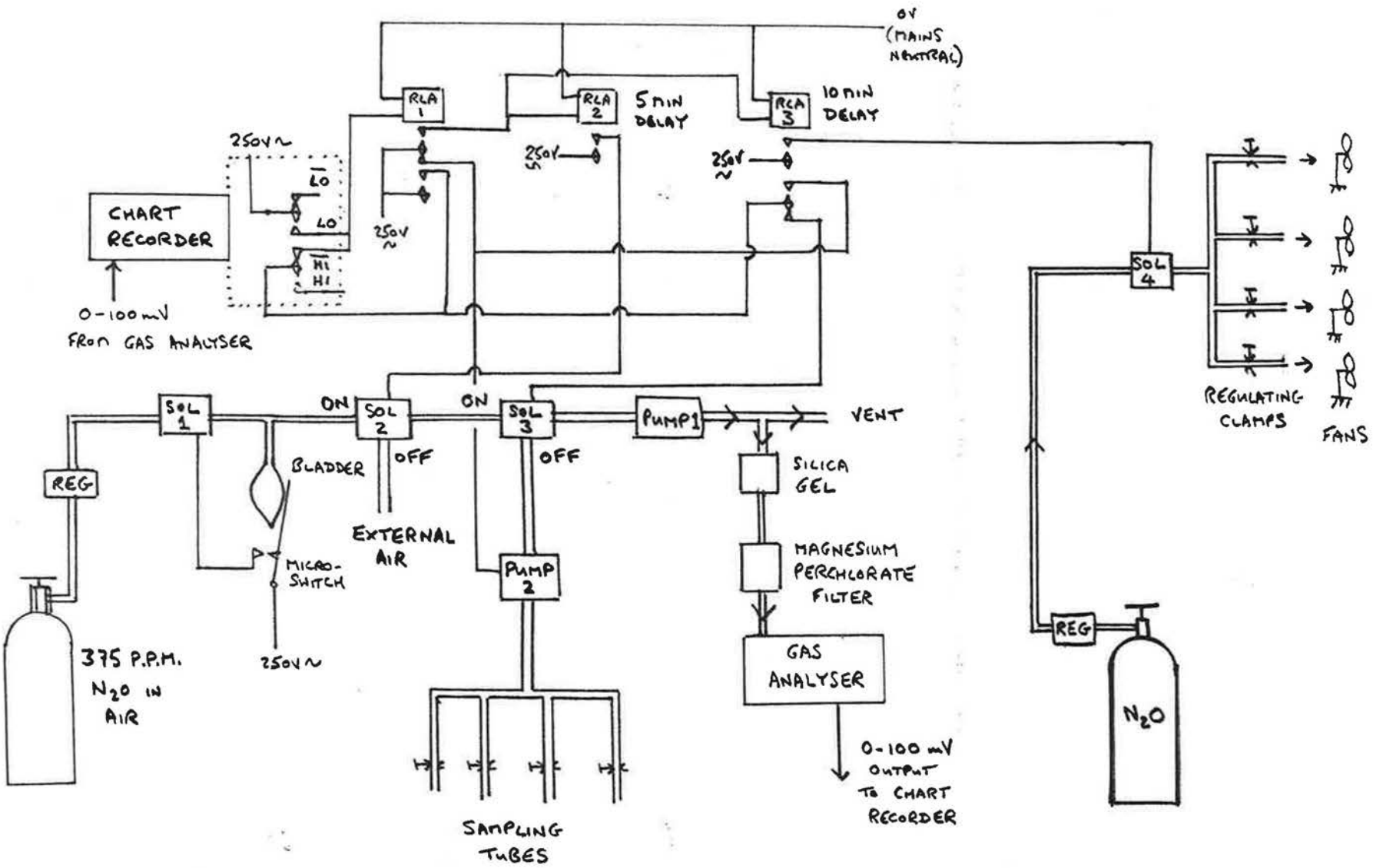

Fig.5.3 The Infra-Red Gas Analyser

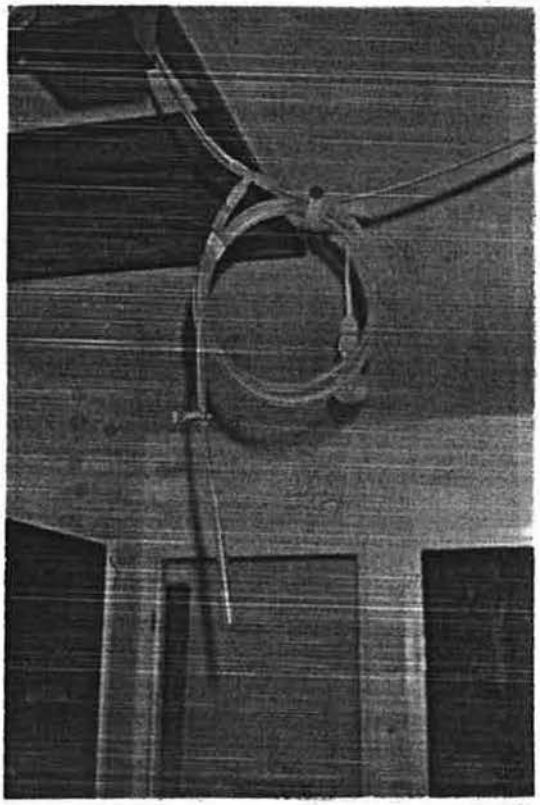

Fig 5.5 Air is sampled through nylon tubes in each room. This one has a small flow meter attached

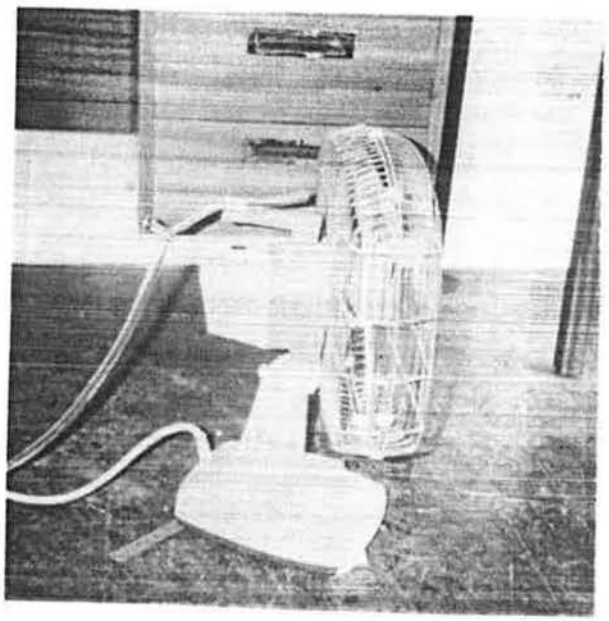

Fig. 5.4 N_2O gas is injected into the house using a fan to ensure good mixing.

TABLE 5.1. CALIBRATION AND MEASUREMENT CYCLE

Step	Action	Truth Table							
		LO ALARM	RLA1	RLA2	RLA3	SOL2	SOL3	SOL4	PUMP2
1.	N_2O level in house below LO limit. Air drawn from outside to analyser to record zero setting.	1	1	0	0	0	1	0	0
2.	After 5 mins. Calibrated gas mixture fed to analyser for 5 mins.	1	1	1	0	1	1	0	0
3.	After 10 mins. Internal house air fed to analyser. N_2O fed to house until HI alarm limit (set 400 ppm) reached.	1/0	1	1	1	1	0	1	1
4.	Measurement period. No more N_2O fed to house. Level decays until LO limit (set 50 ppm) reached and cycle repeated.	0	0	0	0	0	0	0	1

1 = ON 0 = OFF

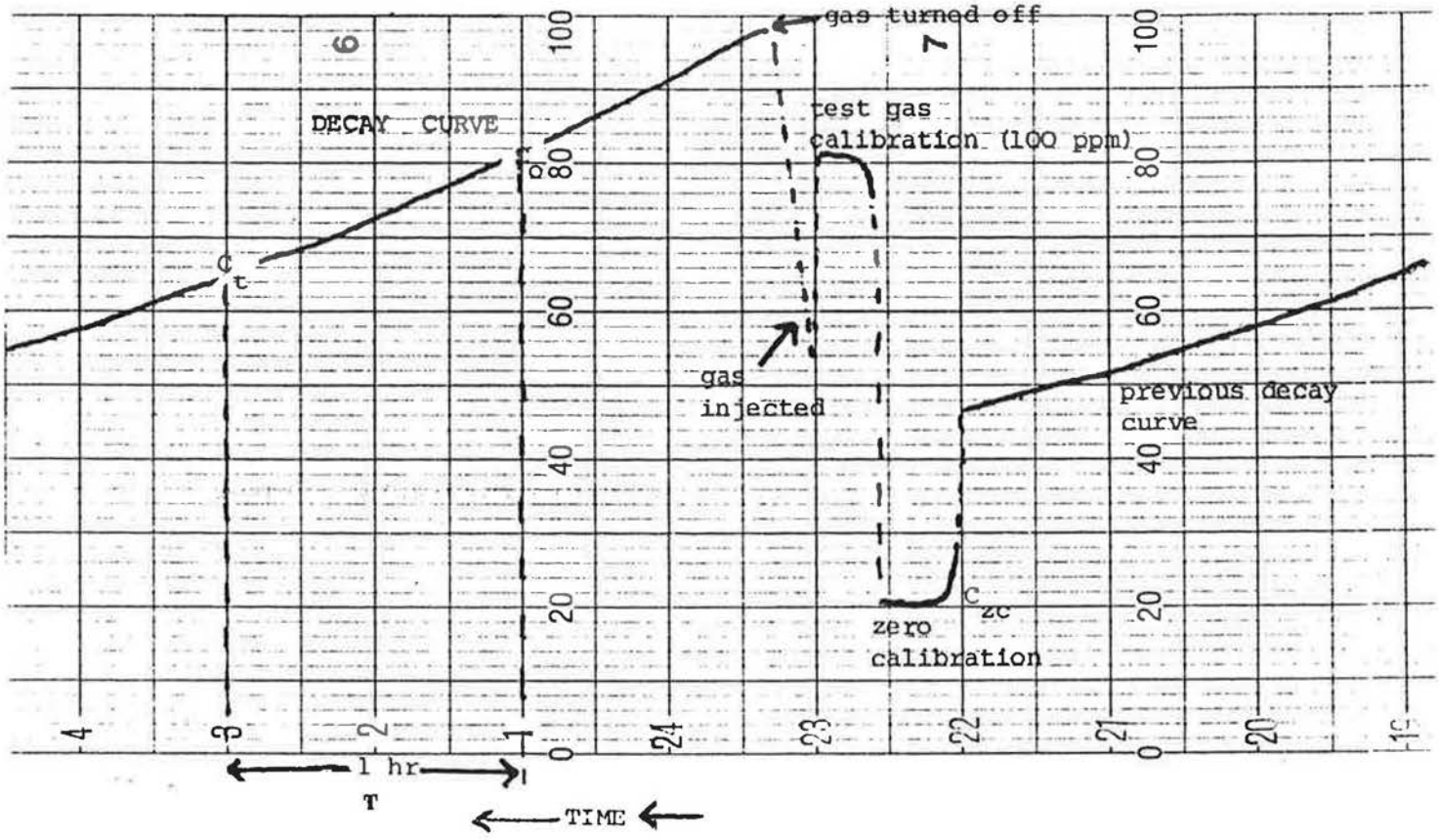

$$\text{Air change rate} = \frac{-\ln\left[\frac{(C_t - C_{zc})}{(C_o - C_{zc})}\right]}{T} = \frac{-\ln\left[\frac{(65 - 21)}{(82 - 21)}\right]}{1}$$

$$= 0.33 \text{ air changes per hour (ac/h)}$$

Figure 5.6 Typical decay curve from ventilation rate measurements

Setting Up and Maintenance

The IRGA 120 requires the sample gas mixtures to be clean and dry. It was therefore necessary to pass the sample through a drying agent and filter before allowing it to be drawn into the analyser. Two drying agents were used, silica gel followed by magnesium perchlorate. These needed to be changed every two days. One of the manufacturer's representatives cast some doubts on the use of silica gel as a drying agent but this was communicated too late to be acted upon.

The signal output of the gas analyser was provided with a potentiometer which could be adjusted to give a 75 mV output for 375 ppm concentration delivered from the calibration mixture cylinder and 0 mV for outside air. It was found useful to offset the chart recorder amplifier by about 5 mV downwards so that drifts of the gas analyser output below zero could be detected.

The gas analyser output persistently tended to drift despite attention from the manufacturers. However, since the proportional rate of decrease in concentration is the significant factor being measured and the system was calibrated every few hours, good data was obtained despite these shortcomings.

It can be seen from this description that the sheer complexity of gas input and output tubes and the need to balance them to get a reasonable whole house air change rate, requires a lot of time to set up, probably two days at least. Also, the need to change the drying filters every day or two means that the system has to be continually 'nursed', despite its 'automatic' nature.

Although constructed using relay logic, the essential timing functions could easily be acheived using simple logic circuits. In fact, the whole measurement process including the calculation of the air change rates and corrections for analyser drifts could be much better carried out now using the simplest of microcomputers.

5.3 Thermographic Survey

No thermal assessment of a house can be regarded as complete without a survey with an infra-red camera. This can quickly spot particular building defects such as missing insulation and cold bridges, though it cannot really quantify them. This is the function of the thermal calibration process. The survey is also useful in making sure that the heat flux sensors are not located in the middle of some defect and are hence not representative of what they are attempting to measure. It is thus suggested that a thermographic survey be carried out before the start of any thermal calibration measurements.

Infra-red cameras are expensive (£10,000 - £40,000) and temperamental pieces of equipment and the mere possession of a camera does not guarantee pictures. During the course of the Linford project the Open University acquired two such cameras, neither of which could be persuaded to work in the field despite many hours of laboratory testing. Finally an outside company were called in for two evenings work with a skilled operator. Despite rates of £150/hour, the value for money was exceptional.

The Linford test house was examined thoroughly in about two hours. This included looking at floor edge heat losses and window lintels from both inside and out, checking the uniformity of the wall insulation and looking at the cold bridges formed by the roof joists through the insulation, both from above and below. Examination of the losses around the windows entailed blanking some of them off thoroughly with thick insulation to avoid the interfering effects of the large heat flows through the glass. Some of the Linford photographs are shown in figures 5.7 to 5.9 .

It also proved possible to check uniformity of insulation and such things as floor edge heat loss on a number of other estates from the outside, proceeding at a respectable walking pace. The best weather for exterior work is cold, dry weather, since rain has the effect of coating houses with a uniform temperature film of moisture. The work also has to be done well after sunset, to avoid the effects of solar heat stored in the fabric surface. Given the cold conditions, the limits to what could be acheived in an evening were mainly determined by the freezing point of the researchers.

Given the experience of the Linford project, it would thus seem best to use an outside contractor to do the thermographic survey work and it is advisable to have possibly three or four houses available for inspection to get the best value from an evening's work. Infra-red cameras are currently under extensive development, mainly for military applications, but they should be regarded with great suspicion as to their reliability until proven otherwise.

See also Appendix 1 for E.C.R.C. experience with thermographic survey work.

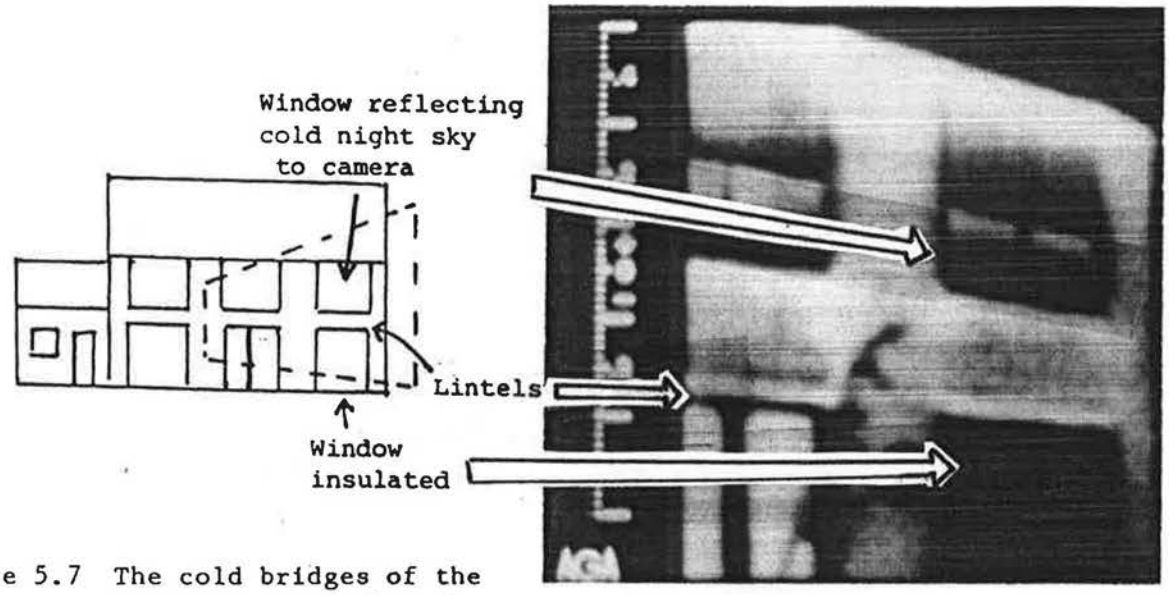

Figure 5.7 The cold bridges of the window lintels show white.

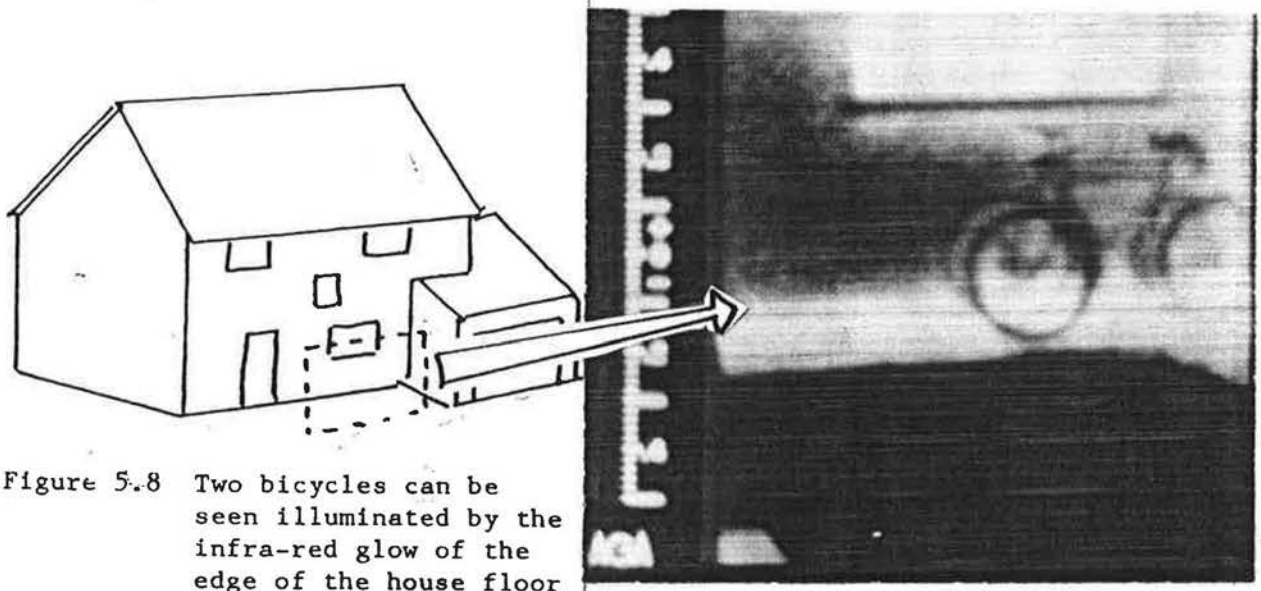

Figure 5.8 Two bicycles can be seen illuminated by the infra-red glow of the edge of the house floor slab.

HOT = WHITE
COLD = BLACK

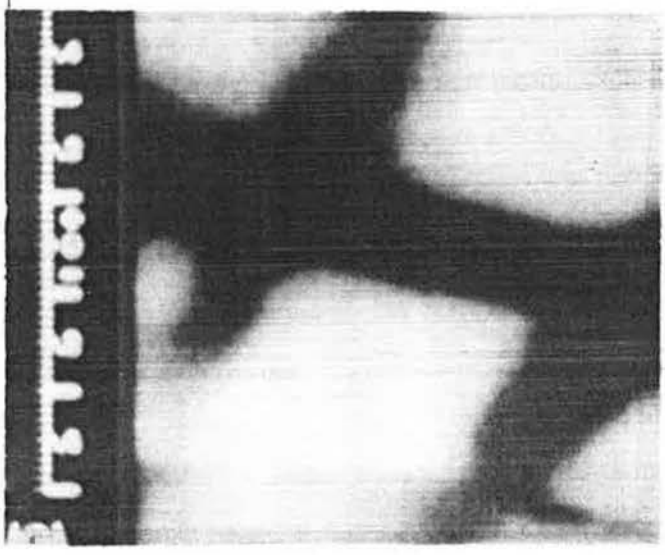

Figure 5.9 Bedroom ceiling seen from below shows cold patches under joists and missing insulation patch.

5.4. Heat Flux Sensors - Design by Alan Horton

Given the large number of heat flux sensors needed and the high cost of commercial ones, much effort was devoted to manufacturing them for the Linford project. The result was the production of quite successful sensors whose material cost was about £10 and could be tailored to the material into which they were to be set, compared to a cost of £300 each for those bought from T.P.D.(Technische Physische Dienst) in Delft, in the Netherlands.

The principle of heat flux measurement is to measure the temperature difference between the two opposing faces of a thin slab of material with a uniform thermal conductivity. The perpendicular heat flow through the slab is then proportional to the temperature difference, as shown in figure 5.10.

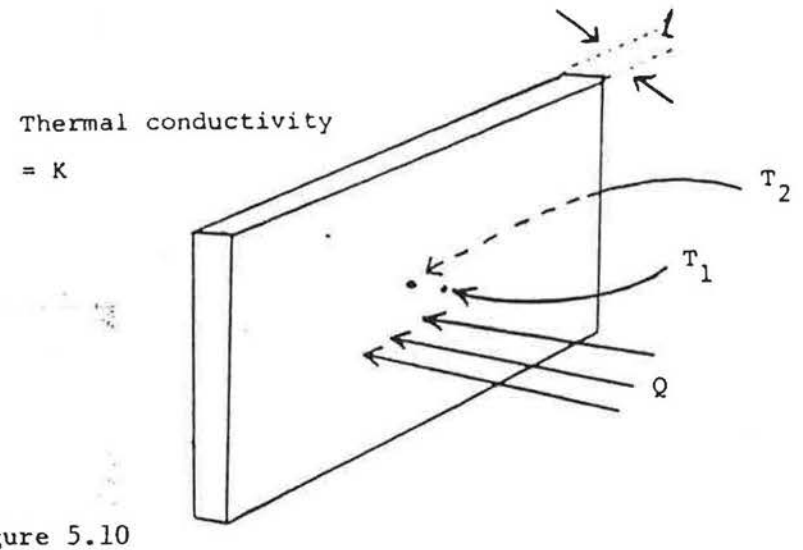

Figure 5.10

$$\text{Heat flow } Q = \frac{K}{l} (T_1 - T_2)$$

5.4.1 Construction

Approximately 150 turns of 28 SWG constantan wire were wound in a coil fashion around a thin slab of plastic material such as polythene, P.V.C. or perspex (see figure 5.11). The slab was then immersed edge-on in a bath of copper sulphate solution, so that the liquid reached half-way up the face of the slab. The constantan coil was then plated with copper to a thickness of approximately 0.025 mm. This was done by connecting the positive side of a low-voltage d.c. power supply to two pieces of copper plate immersed in the solution, one on each side of the slab. The constantan coil was connected to the negative side of the power supply, using a large bulldog clip to ensure electrical contact at the same point of each turn, for as many turns as possible. The constantan coil thus became the cathode and the copper plates the anode of an electrolytic cell. The power supply was set to provide a current of about one amp and the coil plated for 4-5 minutes.

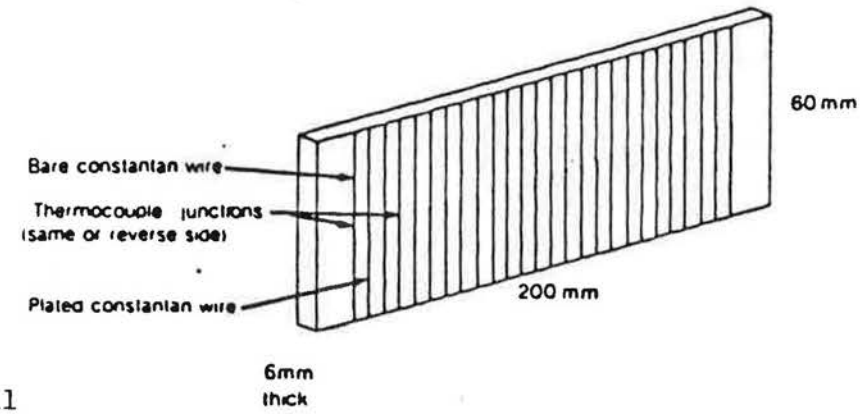

Figure 5.11

Heat flux meter construction.

The half-plated coil resembles a thermopile with as many thermojunctions as there are turns in the coil, successive junctions being on either side of the coil. A small e.m.f. is generated between successive junctions if a temperature difference exists across the faces of the slab, typically of the order of 1/100 th of a degree. Each full turn of the coil contains two junctions and if there are 150 turns the total voltage output will be 150 times that of a single pair. The voltage output is not as high as that of more conventionally constructed thermocouples since each pair is partially short-circuited by the constantan wire running through the copper. The copper plating thickness is thus fairly critical to make sure that most of the current flows through it, rather than the higher resistivity constantan.

Finally, the entire construction was potted in epoxy resin to protect the delicate wire coil and then plastered into the test house walls or set into the concrete surface of the floor. This rather drastic step is not necessary for short thermal calibrations, but meant that the sensors themselves had to be made of a material with the same thermal conductivity as the surrounding building fabric. This is to ensure that the lines of heat flux do not take an easier path around the sensor through the building fabric. The higher the total thermal resistance of the structure, the less important this is, but for thin poorly insulated structures, significant errors can arise.

For sensors used in the walls and floor, polythene was used, with a thermal conductivity of 0.35 $W/m^{o}C$. This compares with about 0.48 $W/m^{o}C$ for the plaster of the walls and 1.0 for the concrete floor. For the ceilings, P.V.C. was used with a conductivity of 0.16 $W/m^{o}C$, identical to the quoted value for the plasterboard into which they were set.

For short-term measurements it is better to use the mounting method suggested in Appendix 1. The heat flux sensor is mounted on the fabric surface with a layer of heat-conducting grease to ensure good thermal contact. The sensor should be surrounded by a guard ring of the same slab material to ensure that the heat flux flows thourgh the sensor rather than around it. Finally a screen of paper should be mounted in front of the sensor to protect it from any radiative effects (hot researchers, sunshine, etc.). This was not done in the Linford test house, leading to measurements that are 'realistic' from the point of view of the actual radiation environment of the house, but somewhat difficult to interpret in terms of plain U-values.

5.4.2 Calibration of Sensors

The heat flux sensors were calibrated against some commercially available ones bought from T.P.D. Figure 5.12 shows the two types of sensor.

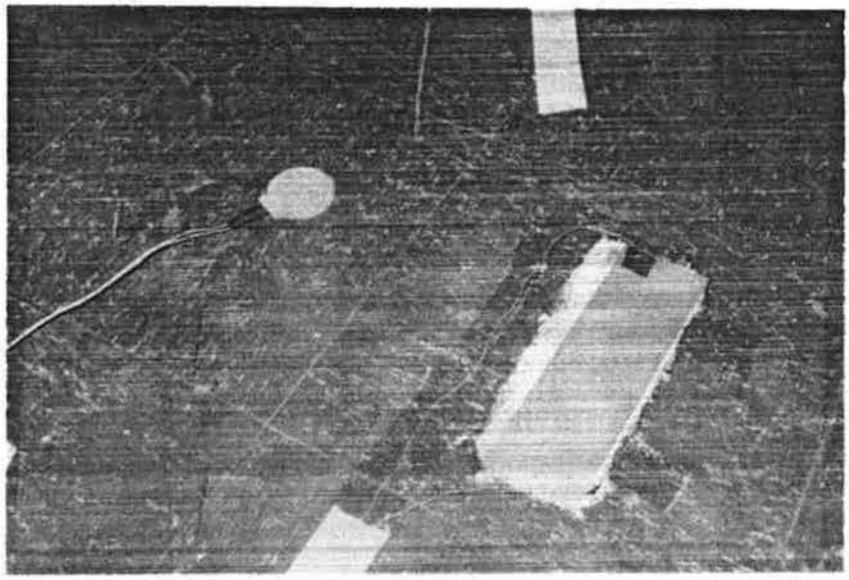

Figure 5.12

Commercial (left) and OU-constructed (right) heat flux meters, surface mounted on a floor for illustration only. Actual measurements were obtained from the OU devices embedded in the walls and floor etc.

The apparatus used for calibration is shown in figure 5.13. The two types of sensor were slotted into holes cut in sheets of material of similar thermal conductivities to each type. For the O.U. devices, the slab material from which they were made was used, perspex was used for the T.P.D. ones.

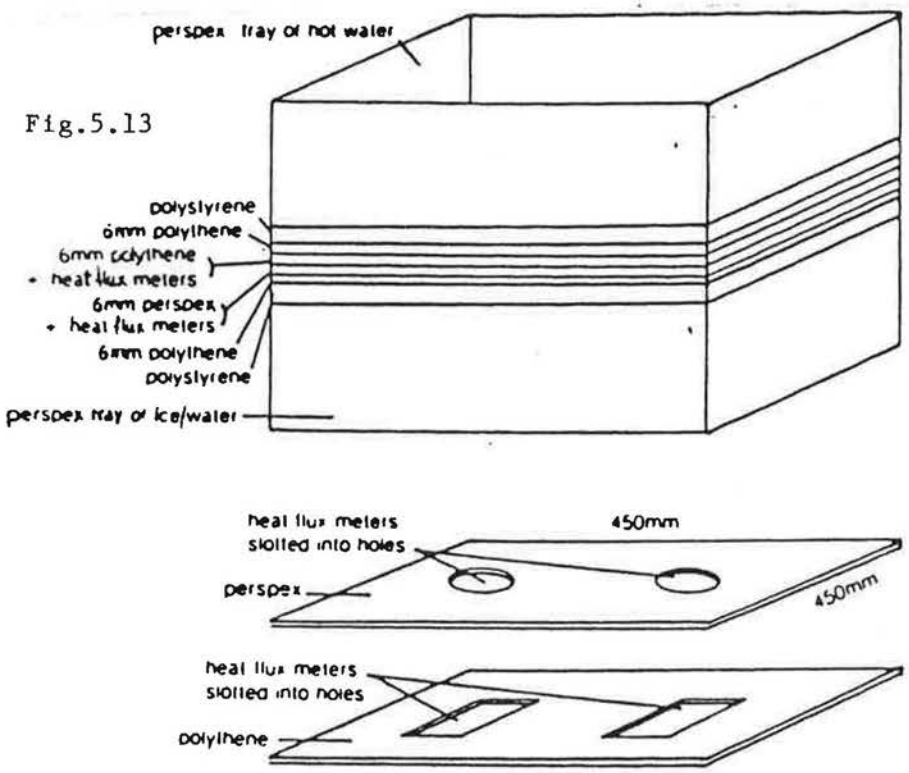

Fig.5.13

The top tray was filled with water at 60°C, and the bottom tray filled with an ice/water mixture at 0°C. This arrangement established a uniform heat flow field around the centre of the apparatus where the heat flux sensors were situated. The entire construction was surrounded by 100 mm thick polystyrene insulation to reduce edge effects.

This apparatus enabled calibration of the O.U. sensors against those from T.P.D. with reasonable accuracy. The calibration of the T.P.D. meters is quoted as being ± 5%. It is likely that the corresponding accuracy of the O.U. ones would be ± 10%.

The O.U. meters gave outputs of about 20 W/m^2 per mV compared with about 15 W/m^2 per mV for the commercial ones. This meant that for a temperature difference of about 15°C across a wall of U-value 0.3 $W/m^2°C$ would give rise to a heat flow of 4.5 W/m^2. For this the O.U. meters would give a voltage output of 0.23 mV.

5.4.3. Amplification

The drift-free amplification of voltages this small is somewhat of a problem and requires special amplifiers. ICL 7600 CAZamps (commutating auto-zero amplifiers) were used. These cost about £10 each and were capable of providing an amplification of up to 1000 times. The amplifier actually consists of two halves which continually swop over, one measuring the signal while the other measures and corrects its own drift.

This rapid alternation, at about 30 khz did create r.f. interference problems and it was not possible to operate a radio tuned to long wave close to the sensors.

As well as radiating interference, the coil nature of the heat flux sensor, together with its large surface area, made it quite good at picking up mains hum from the surroundings. The situation seemed to be rather bad in the Linford test house, where the sensors were set into the building fabric and there appeared to be large earth currents actually flowing through the ground.

It was thus necessary to incorporate a filter in the input of the amplifier to remove this hum. The peculiar properties of the CAZamp meant that it was not possible to use the normal Miller feedback capacitor approach of connecting a smoothing capacitor between the output and inverting input of the amplifier. The filter had to be put right at the input. Also, given the minute D.C. voltage in the presence of a larger a.c. signal it is advisable to use the best quality polyester capacitors for this purpose, to avoid any rectification or electrolytic effects.

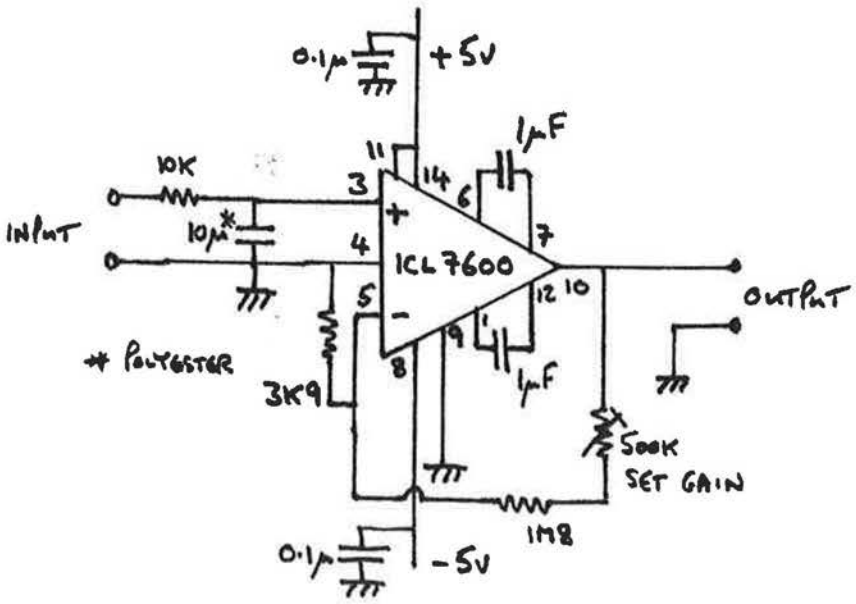

Figure 5.14 Ultra-low drift gain-of-500 amplifier

5.5. Electronic Thermostat

In order to maintain a constant internal temperature in the test house an electronic thermostat was used for each fan heater. This unit was designed to control a 2 kW heater (usually only set to 1 kW) in response to the signal from a platinum resistance thermometer suspended in the centre of the room being heated.

The circuit is shown in figure 5.15 . It uses an LM324 quad op-amp with three of the amplifiers making up a low drift instrumentation amplifier and using the fourth as a comparator comparing the output voltage of the P.R.T. amplifier with a voltage set on a potentiometer representing the thermostat setting. The comparator drives a switching transistor operating a relay, which in turn switches the mains supply to the heater.

The sensing platinum resistance thermometer has a resistance of 100 ohms at 0°C and increases at the rate of 0.385 ohms/°C. It is fed with a constant current of 3.2 mA. The voltage across the P.R.T. is compared with a similar voltage produced across a standard 0.1% 100 ohm resistor (Radiospares 158-086). This voltage difference is then amplified up to a level of 100 mV/°C with 20°C being at 2 volts output. This level can be set by plugging in a 0.1% 110 ohm resistor in place of the P.R.T. and setting the amplifier output to 2.60 volts with the offset trimpot. The amplifier output should be accurate enough without any trimming. The amplifier cannot be checked at 0°C with a 100 ohm resistor because the system has only one power rail (+ 5 volts) and so the amplifier can only pull the output down to a minimum of +300 mV. The two 1 K resistors to ground from pins 8 and 14 of the LM 324 allow those stages to operate down to output voltages of +100 mV.

The thermostat setting pot should cover the range +15°C to +25°C with +20°C in the centre. The pot can be calibrated by plugging in a P.R.T., measuring the amplifier output voltage, i.e. the recorded temperature and checking where the relay operates by turning the pot. There should be about 0.3°C hysteresis on the pot between the relay switching one way or the other. The large electrolytic capacitor on pin 6 of the LM 324 is necessary to slow down the cycling rate of the system in order to preserve the relay contacts. Without this capacitor and the filter capacitors across the relay contacts there tends to be relay chatter, resulting in short relay life and mains interference.

The output to the logger swings between about 0 volts and +4 volts when the relay operates. This signal can be used to operate and elapsed time meter in the logger giving the rough average power output of the heater. Alternatively it can be heavily integrated using a very long time constant CR filter and fed to a chart recorder to give an instantaneous recording of the average heating power.

On balance the digital method is simpler to carry out though a long time constant filter was used to produce the traces of figure 2.7.

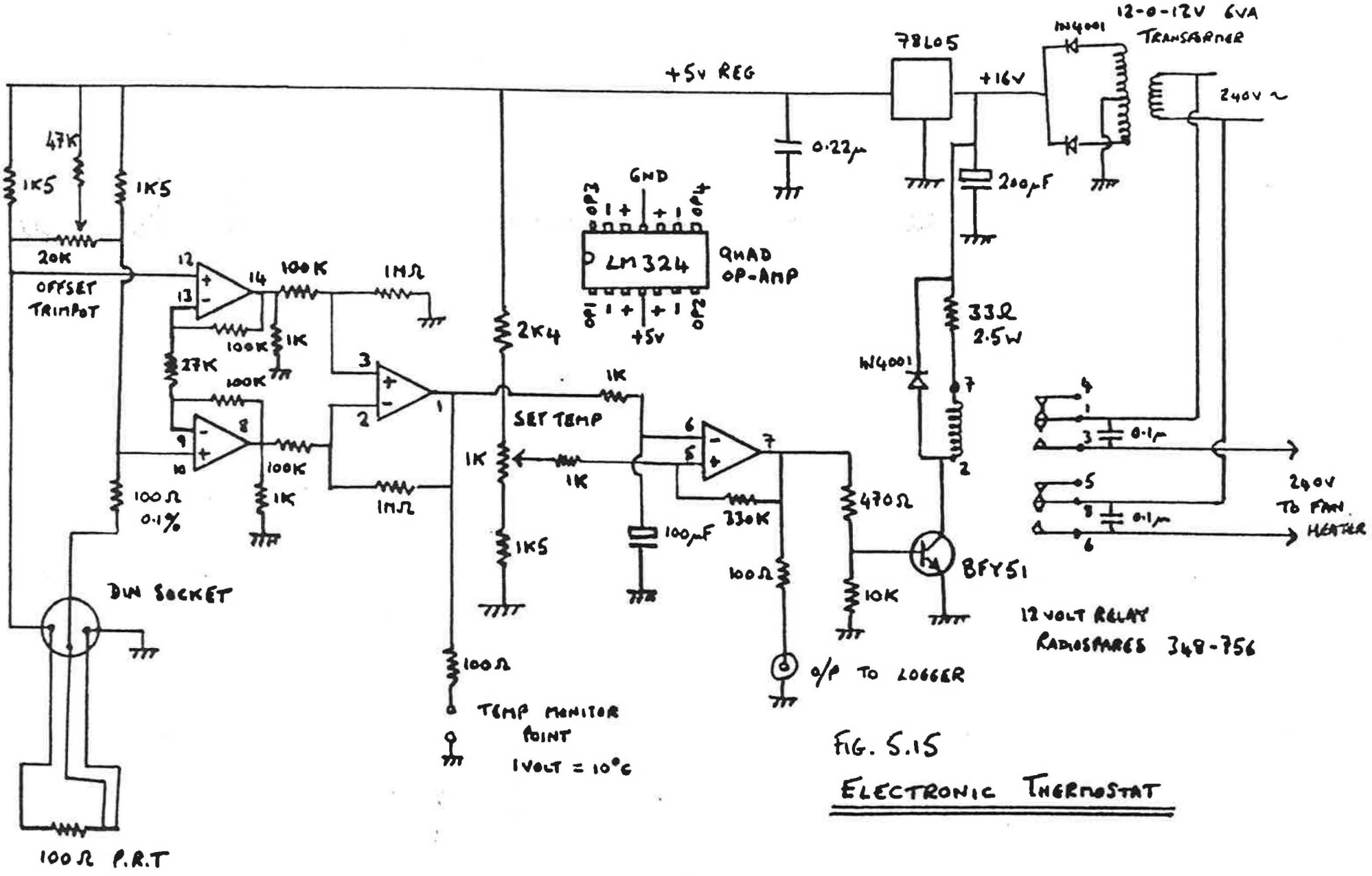

FIG. 5.15

ELECTRONIC THERMOSTAT

5.6. Wind Measurements

5.6.1. Wind Speed

For both the Spencer St. and Linford projects wind speed was measured using a normal cup anemometer. This has a pulse output of either a microswitch or optoswitch type and the task of the logger is simply to count pulses. This should be no problem for modern equipment, though the logger used at Spencer St. perversely only accepted analogue inputs and had to have a special interface made.

There is a lot of controversy as to where to properly measure wind speed. 'Meteorological' wind speeds are measured at a height of 10 m. This was done at Linford, requiring a cumbersome tall mast. Fortunately, a naval technician was to hand. The measurements should also be made as far away from obstructing buildings as possible, preferably at least five house heights. This in practice is almost impossible to acheive without straying onto someone else's land.

In practice, wind speed is of relatively small interest and mainly useful for assessing and filling in missing air infiltration values. Therefore there has to be some compromise between 'accurate' wind speeds and the trouble required to locate the anemometer in the right place and get it to work properly once installed, especially if time is limited. The positioning of the anemometer at Spencer St. seems about right from this point of view - mounted on the fence at the bottom of the garden, about 10 m from the house at a convenient step-ladder height.

5.6.2. Wind Direction

This parameter is really only of any use at high wind speeds and except for very detailed air infiltration work only required to a low accuracy ($\pm$ 30^{o}). Thus the effort of installing a wind vane, interfacing it to the datalogger and the effort of writing a computer program to unscramble the output (usually binary or an analogue voltage) and 'average' the wavering result is hardly worth all the effort. The wind vane for the Linford project probably consumed at least two man-weeks to achieve all this. It is far simpler just to wave a wet finger in the air twice a day and write it in a notebook.

5.7. Air Temperatures

These are fairly straightforward to measure by several methods. Thermocouples were used at Spencer St. and platinum resistance thermometers at Linford and Pennyland. Generally, in terms of volts/^{o}C output, the best buy currently are precalibrated thermistors (such as Radiospares 151-215). The S.E.R.C. Field Trial Notebook contains a full discussion of the merits and disadvantages of the different types of sensors.

Internal temperatures are best measured by hanging the sensor in the centre of the room at least two feet from the ceiling. This avoids

the puddle of hot air that tends to accumulate close to the ceiling especially when the electric lights are on. The Linford measurements were made using sensors mounted in commercial heating thermostat housings, in the interests of tidiness, but this is likely to give a wall surface temperature rather than a true air temperature.

External air temperatures are probably best measured using an aspirated sensor, essentially with the sensor mounted in the inlet of a small fan. This gurantees getting a true air temperature. Normal 'meteorological' temperatures are measured in a Stevenson Screen, a louvred wooden box. As pointed out in Appendix 2, this can be thought of as a rather poor efficiency passive solar test cell, with solar gains of its own. Thus the screen temperature may not give the right answer for the solar aperture of the house.

The external temperature sensors used at Pennyland were also deficient from this respect, being mounted about 100 mm out from the external wall of the house, about 3 m from the ground. Some of the sensors on west facing walls exposed to direct unlight registered temperatures $5^{o}C$ or more above the true air temperature on sunny days. Shielding the sensor from the direct sunlight did not improve matters much since under sunny conditions the whole wall was bathed in a warm boundary layer of air rising up the external surface. The sensor would have had to be at least 1 m from the wall surface to be totally free of this effect. Although the average effect of these solar gains is likely to be small (perhaps $0.5^{o}C$) they have caused some confusion in the analysis of the Pennyland data in the comparison of two house types, where one house type may have all the external temperature sensors mounted on the south side and the other type may have them all mounted on the north. It thus becomes impossible to tell whether the experiment is one of comparing house designs or of monitoring systems.

5.8 Electricity Consumption

This is straightforward to measure. A reflective optoswitch mounted over the disc of a normal electricity meter will register one pulse per revolution if a black stripe is painted on the disc. (see fig.5.16) This represents usually 1/300th or 1/250th kWh depending on the type. Logging is simply a matter of counting pulses.

It should be stressed that the 'electric heating' measured in the thermal calibration process includes any electric lights, fans and monitoring equipment actually inside the house at the time.

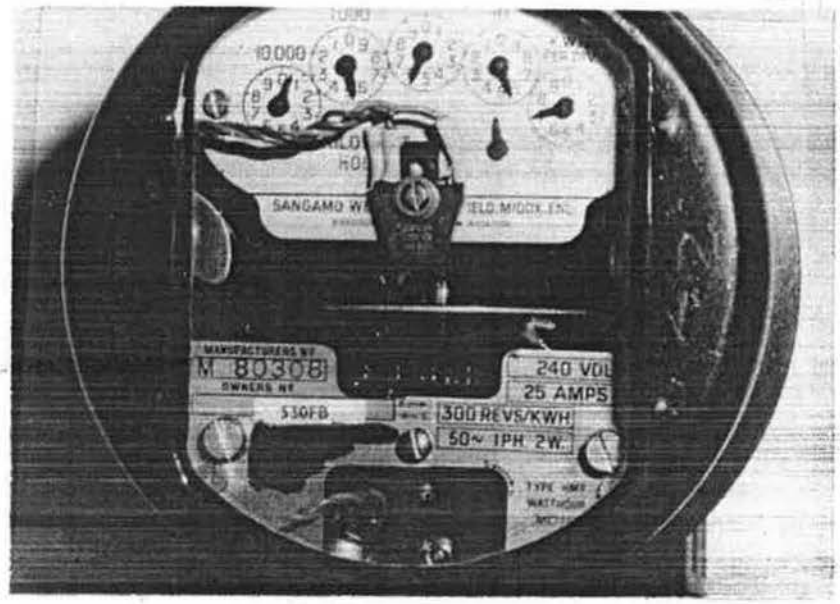

Figure 5.16 Electricity Meter with Reflective Optoswitch Mounted Over Disc.

6. STATISTICS OF WEATHER

CONTENTS

This chapter looks at the statistical problems of carrying out the analysis, the availability of a suitable mix of sunny and dull days and the comparability of successive results. It also looks at the spectrum of results obtainable ranging from synthetic computer-generated data through test house emperiments to crudely monitored occupied houses.

CHAPTER 6

STATISTICS OF WEATHER

6.1 Availability of Suitable Weather

As described in chapter 2, the determination of the building fabric heat loss is really dependent on the availability of dull days in a data set, while the determination of the effects of solar gains requires a mixture of dull and sunny ones. The question is 'What is the maximum amount of time that we are likely to have to wait in order to be sure of getting suitable weather to perform a good thermal calibration?'.

In order to answer this, sunshine data from two locations at opposite ends of the U.K. has been analysed, from Bracknell, near London (lat. 51° 21' N) and Lerwick in the Shetlands (lat 60° 08' N). The particular solar variable that has bee tested is the daily total solar radiation on the south-facing vertical surface, since this is a reasonable indicator of solar gains into the house, whether south-facing or not.

Figure 6.1 shows the relation between daily totals of solar radiation on various planes for clear sky days, calculated for approximately the latitude of Bracknell. At this latitude, the total radiation on the south-facing surface on a sunny winter day is not very different to that on a sunny summer one. The low solar altitude in the winter means that the sun shines square on to the south surface. In summer the sun shines obliquely from a higher altitude, but for a longer period. At the more northerly latitude of the Shetlands, the pattern is slightly different, with a pronounced drop in solar radiation in the mid-winter months.

Not all days are sunny, though. Figures 6.2 and 6.3 show scattergrams of daily solar radiation throughout the year 1982 for the two locations. For ease of printing the daily totals have been rounded to the nearest 0.5 $kWh/m^2/day$ and printed in columns of one week each.

For Lerwick the pattern is of a large number of very dull days in mid-winter, a good mixture of sunny and dull days in spring and autumn and a mixture of sunny and moderately dull ones in summer but with a distinct lack of very dull days. For Bracknell there is a good mixture of sunny and dull days for most of the year but again with a lack of very dull days in summer.

In order to estimate the worst-case length of continuous monitoring time to acheive a thermal calibration, the weather data has been analysed using two criteria. One is a 'non-solar' one requiring continuous monitoring until three very dull days (i.e. $S < 0.5$ $kWh/m^2/day$) have occured. This is subject to a further constraint that the day before each dull day should not have been a sunny one (i.e. $S > 3$ $kWh/m^2/day$). This is to avoid problems of stored solar gains being carried over into the dull day. This kind of weather data would give a thermal calibration plot as shown in figure 6.5, allowing estimation of $\leq$A.U, but not the solar aperture R.

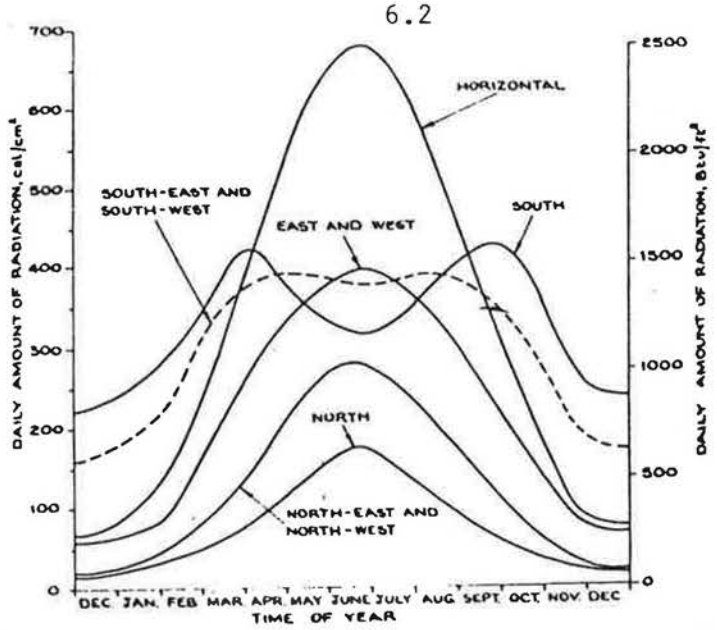

Figure 6.1

Clear Sky Daily Totals of Solar Radiation on Various Planes for Latitude 51.7°N

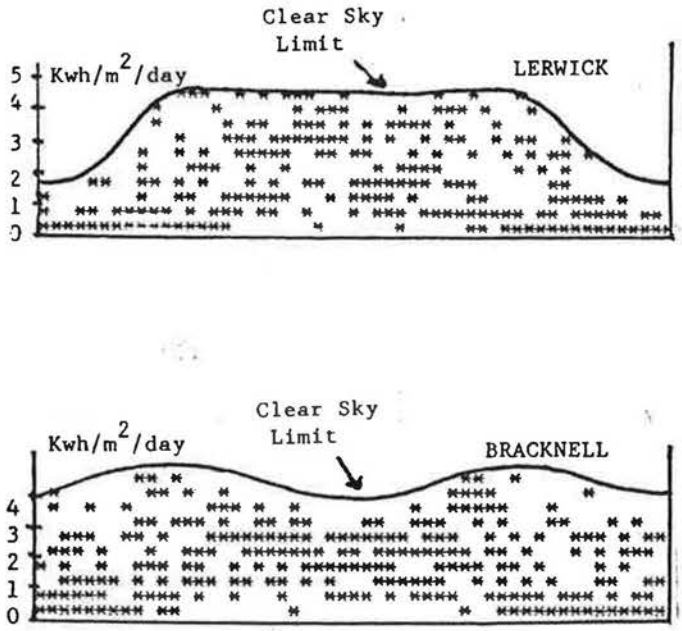

Figures 6.2 and 6.3

Scattergrams of Daily Total Solar Radiation on the South-facing Vertical Surface for Lerwick and Bracknell

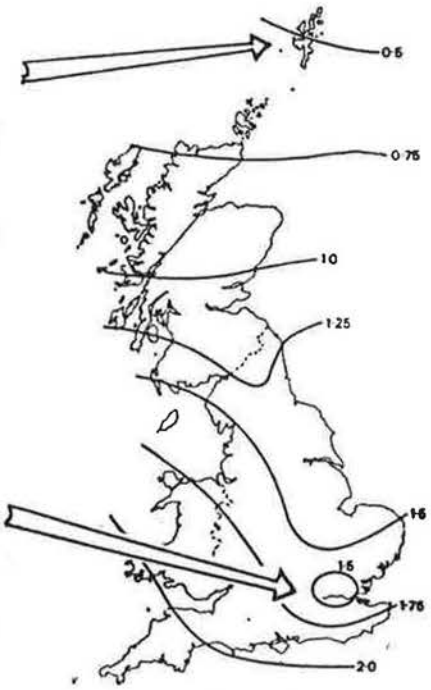

Figure 6.4
Daily Totals of Solar Radiation on the Horizontal Plane for December (MJ/m^2)

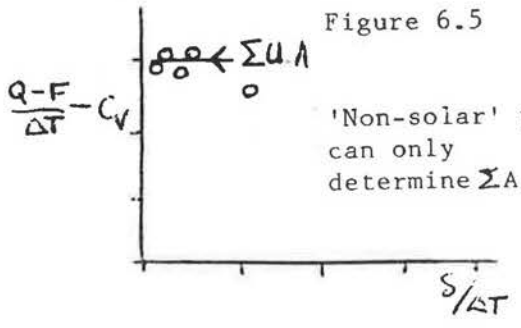

Figure 6.5

'Non-solar' plot can only determine ΣA.U.

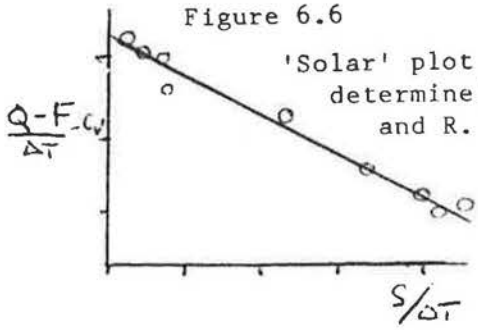

Figure 6.6

'Solar' plot can determine ΣA.U and R.

The second criterion is a 'solar' one, requiring two moderately dull days ($S < 1$ kWh/m^2/day), again not preceeded by a sunny day, plus two sunny days ($S > 3$ kWh/m^2/day) to fix the solar aperture. This would give a regression plot as shown in figure 6.6.

Just over two years data from each site has been analysed, from November 1980 to December 1982. For each day over this period, the analysis algorithm has been set to count forward the number of days until each criterion is satisfied. The results for the 'solar' and 'non-solar' criteria for each location are shown in figures 6.7 and 6.8. The data has been printed out on a weekly basis with the worst-case number of required days starting from any day in a given week. Rough overall worst-case lines have been drawn on these plots.

These rather confusing scattergrams do show the general patterns of the availability of suitable weather. For the 'non-solar' mode in Lerwick the high density of dull days in mid-winter makes it very easy to achieve an estimate of ΣU.A in 10 days or less during the period mid-November to mid-January. The availability of very dull days in mid winter at Bracknell, though, is considerably less, requiring a worst-case 20 days to obtain three very dull days during this period. These are 'worst-case' figures, though, and typical measurement times are more like 5 days for Lerwick and 10 for Bracknell. The 'non-solar' mode completely breaks down for both locations during the months February to October because the weather is just too sunny to ignore the solar effects and there aren't enough very dull days.

The 'solar' mode is applicable over a much longer period of the year. For Bracknell, the criterion can be met in under a month from September through to March, with typical required measurement times of about two weeks. The method breaks down in the sunnier summer weather from April through to August because of the lack of dull days.

For Lerwick, the 'solar' mode also breaks down in mid-winter, from mid-October through to mid-January, for want of sunny days.

The typical required measurement periods for the two locations and two modes are summarised in Table 6.1 below. Worst-case periods are likely to be about twice the typical values.

Month	Lerwick		Bracknell	
	'Solar'	'Non-solar'	'Solar'	'Non-solar'
Jan.	-	5	12	12
Feb.	12	15	15	15
Mar.	15	-	18	-
Apr.	-	-	-	-
May	-	-	-	-
June	-	-	-	-
July	-	-	-	-
Aug.	12	-	20	-
Sept.	12	15	15	-
Oct.	-	15	12	18
Nov.	-	5	12	12
Dec.	-	5	12	10

TABLE 6.1. Typical required measurement periods to satisfy criteria

Figure 6.7 Number of Days Required to Acheive a Calibration - LERWICK

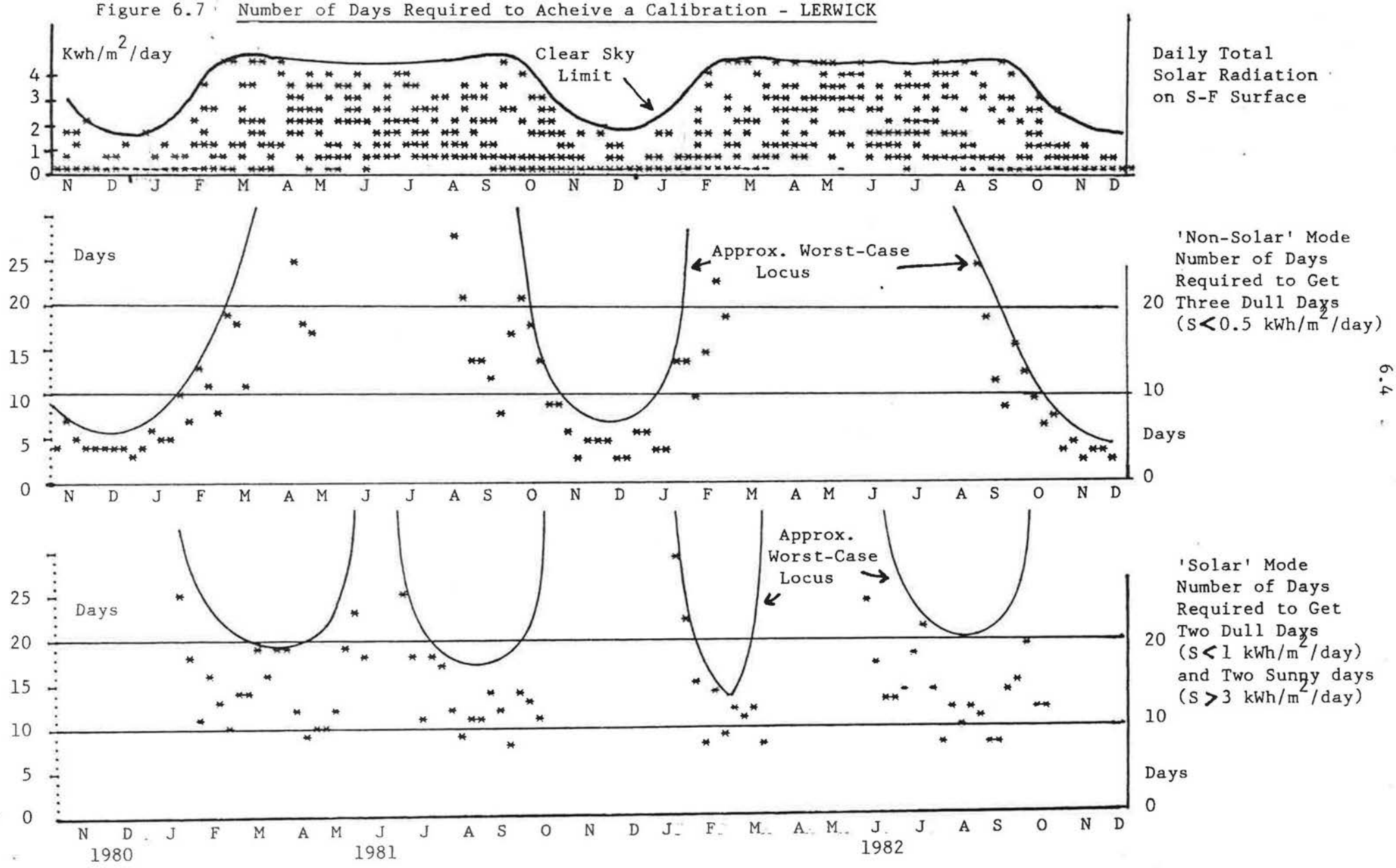

Figure 6.8 Number of Days Required to Acheive a Calibration - BRACKNELL

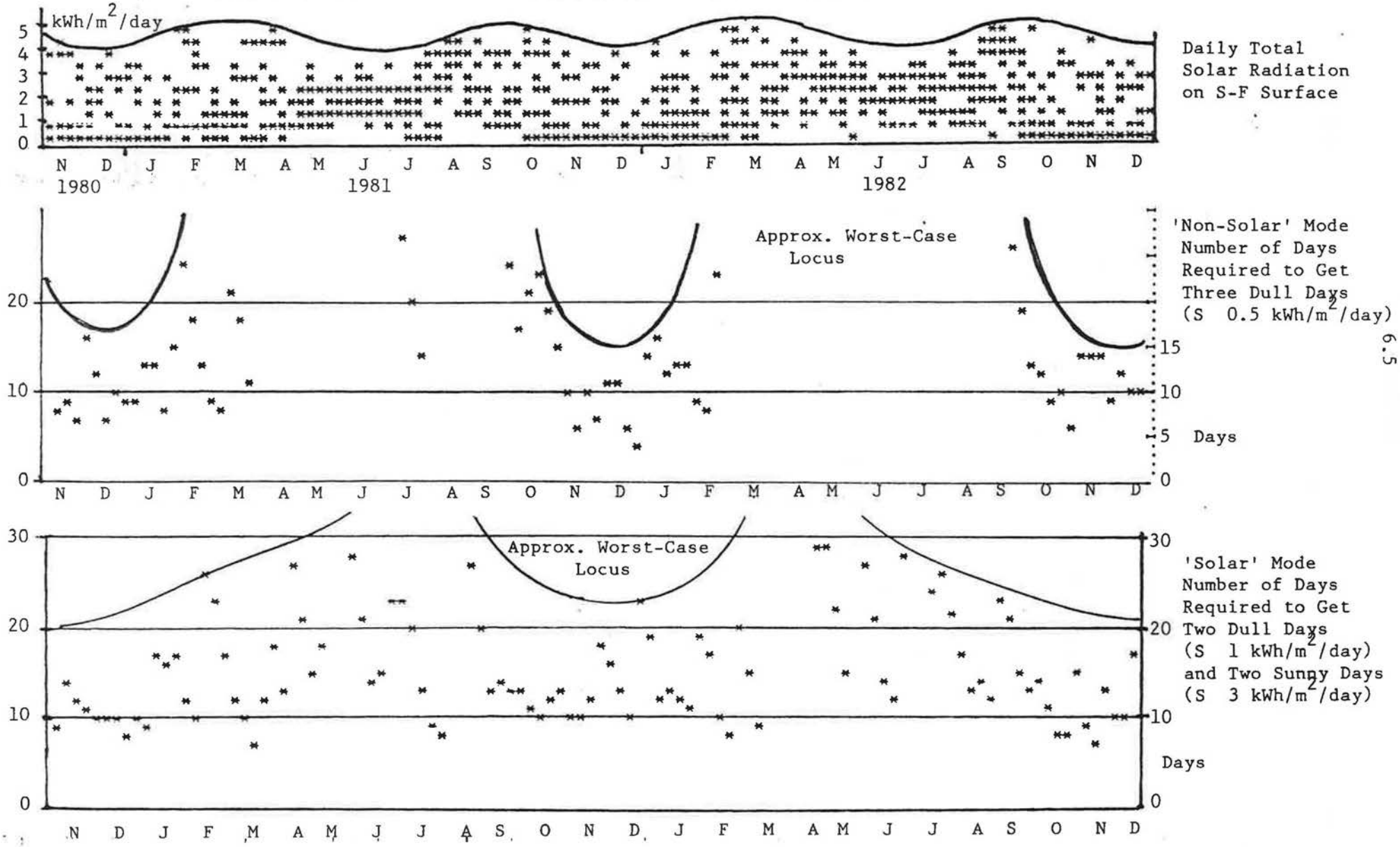

6.1.1 Conclusions

From Table 6.1 we can deduce a distinct thermal calibration 'season'. This runs from August through to March, though calibrations run in August might require a rather uncomfortably high internal temperature ($30^{o}C$?) to get a large enough ΔT.

The best period for the determination of $\Sigma A.U$ for both locations is between September and February when good results can be expected with typically 15 days data or less. For the more southerly latitudes this can be expected to produce a good estimate of the solar aperture as well.

For northerly latitudes the solar aperture is best determined during September, February or March.

Although the weather is still rather cold in April and sometimes in May, there are too few dull days to make much sense of the data. The measurements on the Linford test house for April 1982 and April 1983 have been of little use, except in comparison with measurements from earlier in the year.

6.2. Effects of Inadequate Available Time

Although the previous section has used terms of 'success' and 'failure', in practice matters are more indistinct. The process is more one of progressively increasing error bars as the time scale is reduced. This can be illustrated by taking the six week long data set of figure 2.4 and splitting it up into its three two week periods and then into six separate weeks.

These plots are shown in figures 6.9 to 6.17. The resultant values for $\Sigma A.U$ and R and their respective error bars are shown in figures 6.18 and 6.19 as a function of the number of weeks measurement.

The overall result is one of basically consistent answers but with increasing error bars that decrease roughly as $1/\sqrt{n}$ where n is the number of weeks measurement.

Even in the weekly data sets the average error of interpretation on $\Sigma A.U$ is typically only 6 $W/^{o}C$, significantly less than the probably measurement errors in floor loss and infiltration rate, which are likely to amount to 15-20 $W/^{o}C$. The picture for the solar aperture is not so good, though. The worst of the data sets has error bars of $\pm$ 2.8 m^2 at the 68% confidence interval. While this is sufficiently accurate to tell us that a house does respond to solar radiation, it is certainly not good enough to distinguish one solar variant from another.

There is also a downward trend in the successive values of both $\Sigma A.U$ and R produced in figures 6.18 and 6.19, though barely at a level of statistical significance. This may be due to the effects of errors in determining the floor heat loss and problems of covariance between solar radiation and ΔT, which are dealt with later in this chapter.

(Q-F)/Delta T - Cv

Kwhr/Day/DegC

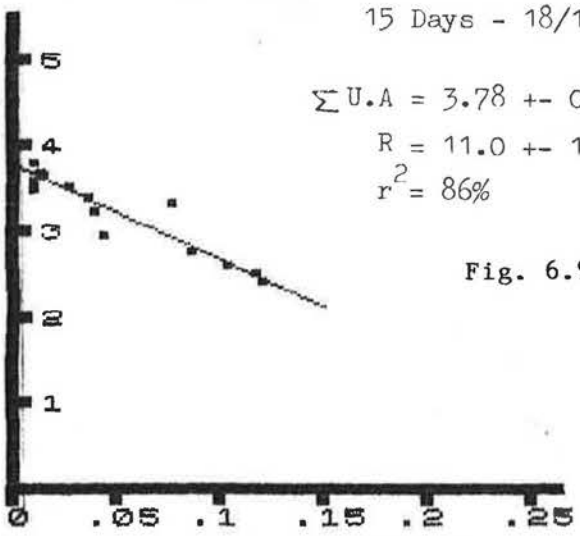

15 Days - 18/12/82 - 2/1/83

Σ U.A = 3.78 +- 0.07 Kwhr/day/°C

R = 11.0 +- 1.2 m^2

r^2 = 86%

Fig. 6.9

(Q-F)/Delta T - Cv

Kwhr/Day/DegC

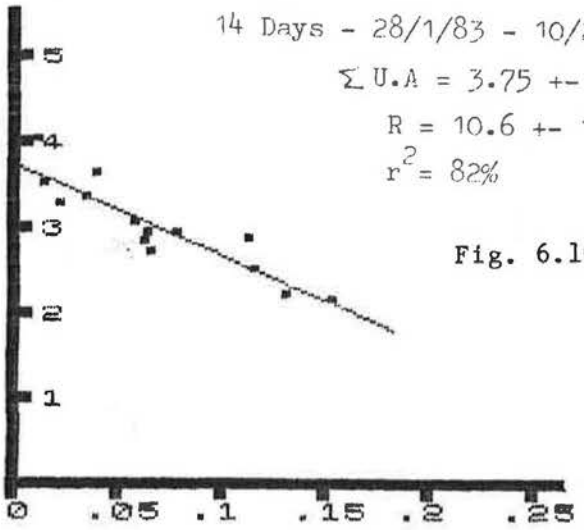

14 Days - 28/1/83 - 10/2/83

Σ U.A = 3.75 +- 0.11 Kwhr/day/°C

R = 10.6 +- 1.4 m^2

r^2 = 82%

Fig. 6.10

(Q-F)/Delta T - Cv

Kwhr/Day/DegC

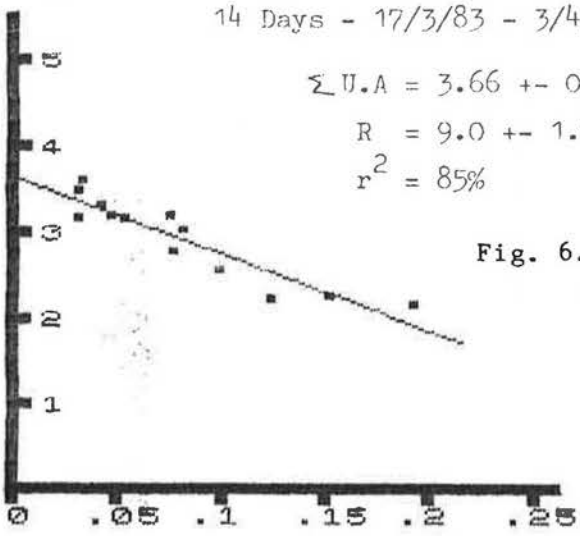

14 Days - 17/3/83 - 3/4/83

Σ U.A = 3.66 +- 0.09 Kwhr/day/°C

R = 9.0 +- 1.0 m^2

r^2 = 85%

Fig. 6.11

(Q-F)/Delta T - Cv

Kwhr/Day/DegC

7 Days 18/12/82 - 24/12/82

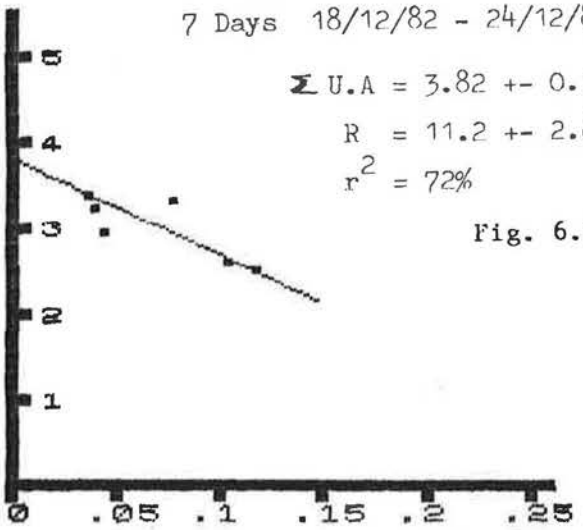

Σ U.A = 3.82 +- 0.19 Kwhr/day/^{o}C

R = 11.2 +- 2.8 m^2

r^2 = 72%

Fig. 6.12

(Q-F)/Delta T - Cv

Kwhr/Day/DegC

8 days 26/12/82 - 2/1/83

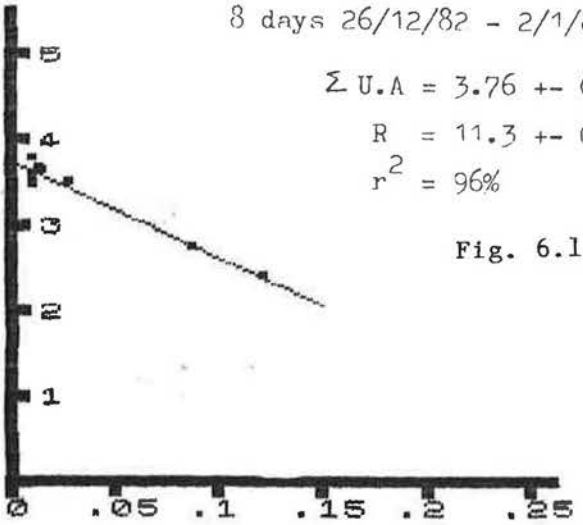

Σ U.A = 3.76 +- 0.05 Kwhr/day/^{o}C

R = 11.3 +- 0.9 m^2

r^2 = 96%

Fig. 6.13

(Q-F)/Delta T - Cv

Kwhr/Day/DegC

7 Days - 24/3/83 - 3/4/83

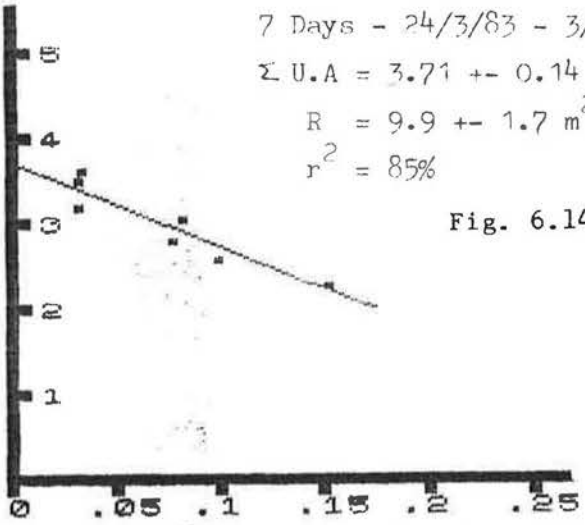

Σ U.A = 3.71 +- 0.14 Kwhr/day/^{o}C

R = 9.9 +- 1.7 m^2

r^2 = 85%

Fig. 6.14

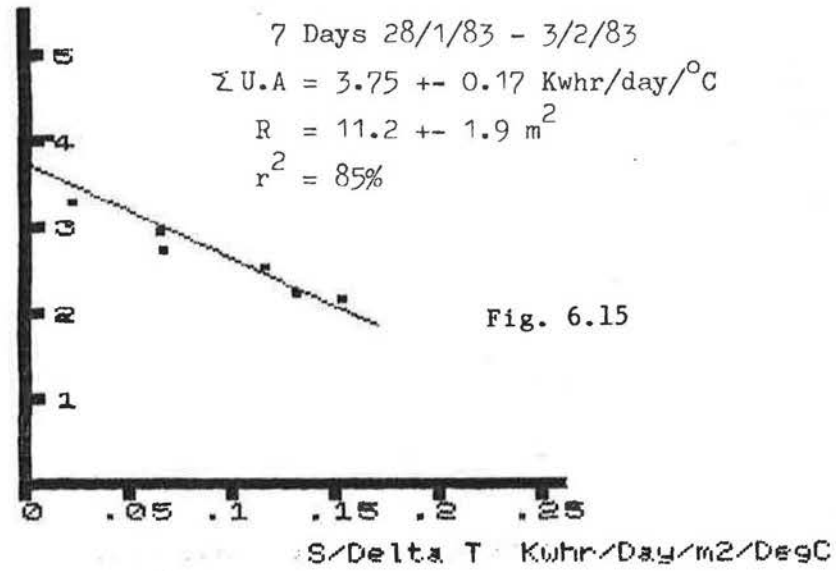

Fig. 6.15

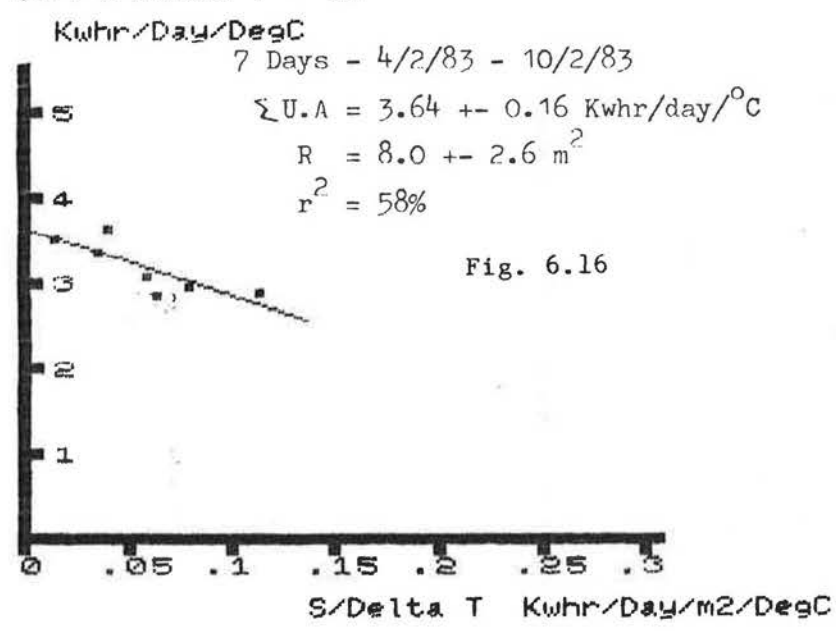

Fig. 6.16

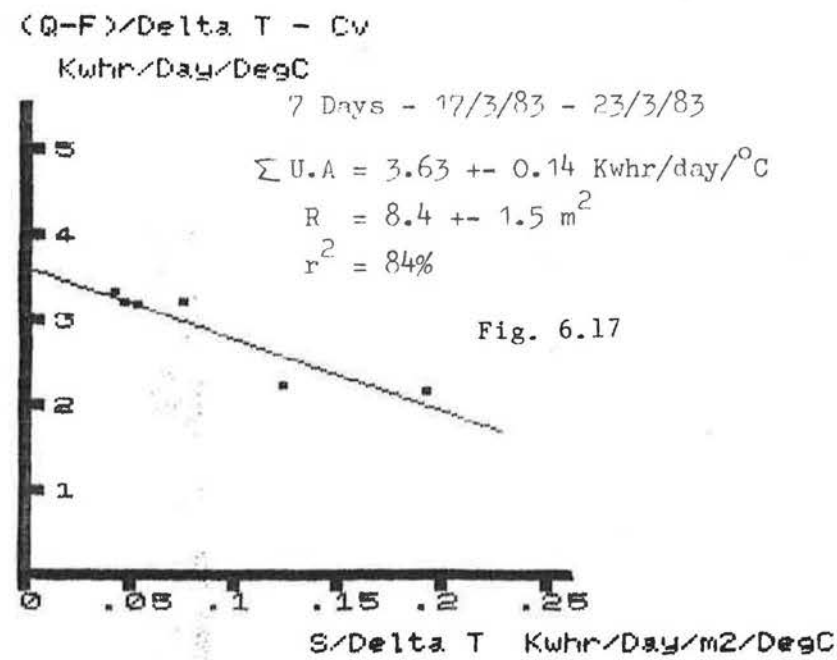

Fig. 6.17

Figure 6.18. ESTIMATES OF ERRORS OF INTERPRETATION ON ΣA.U VS. NO. OF WEEKS

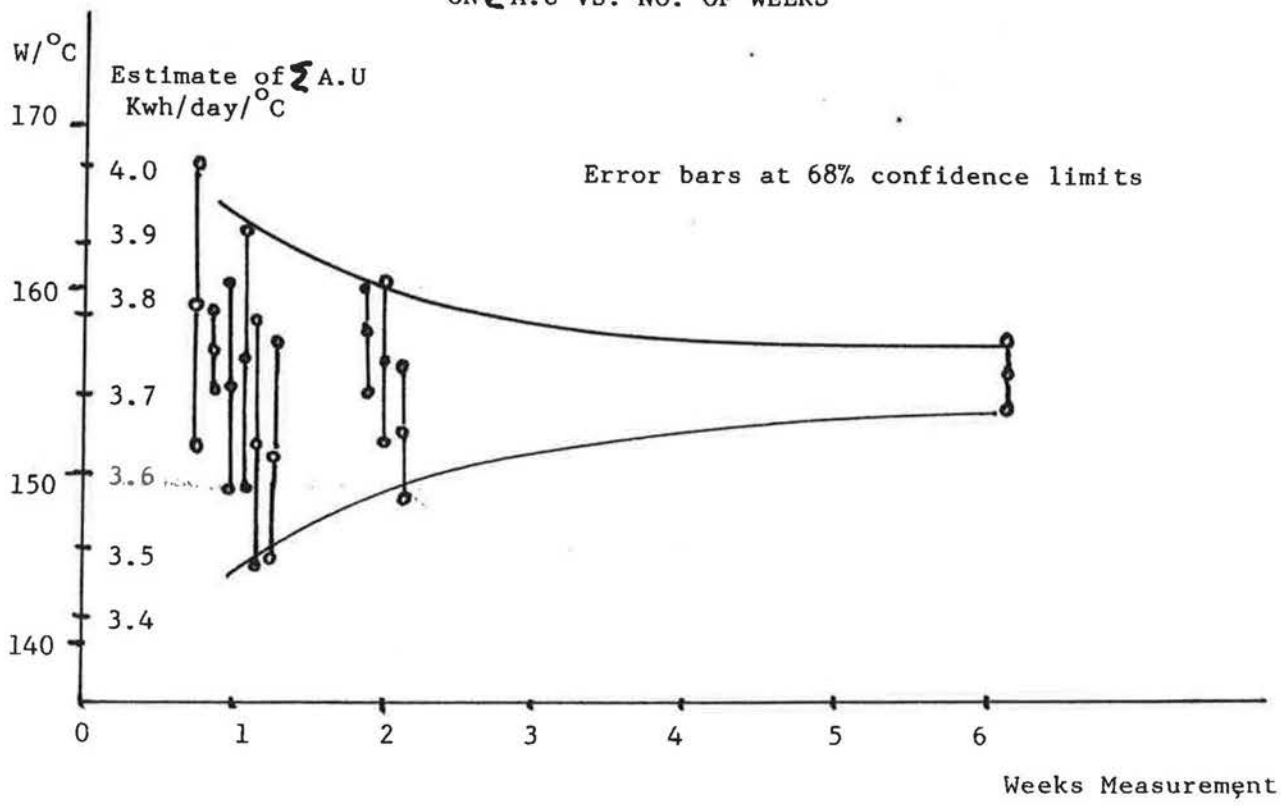

Figure 6.19 ESTIMATES OF ERRORS OF INTERPRETATION ON R VS. NO. OF WEEKS

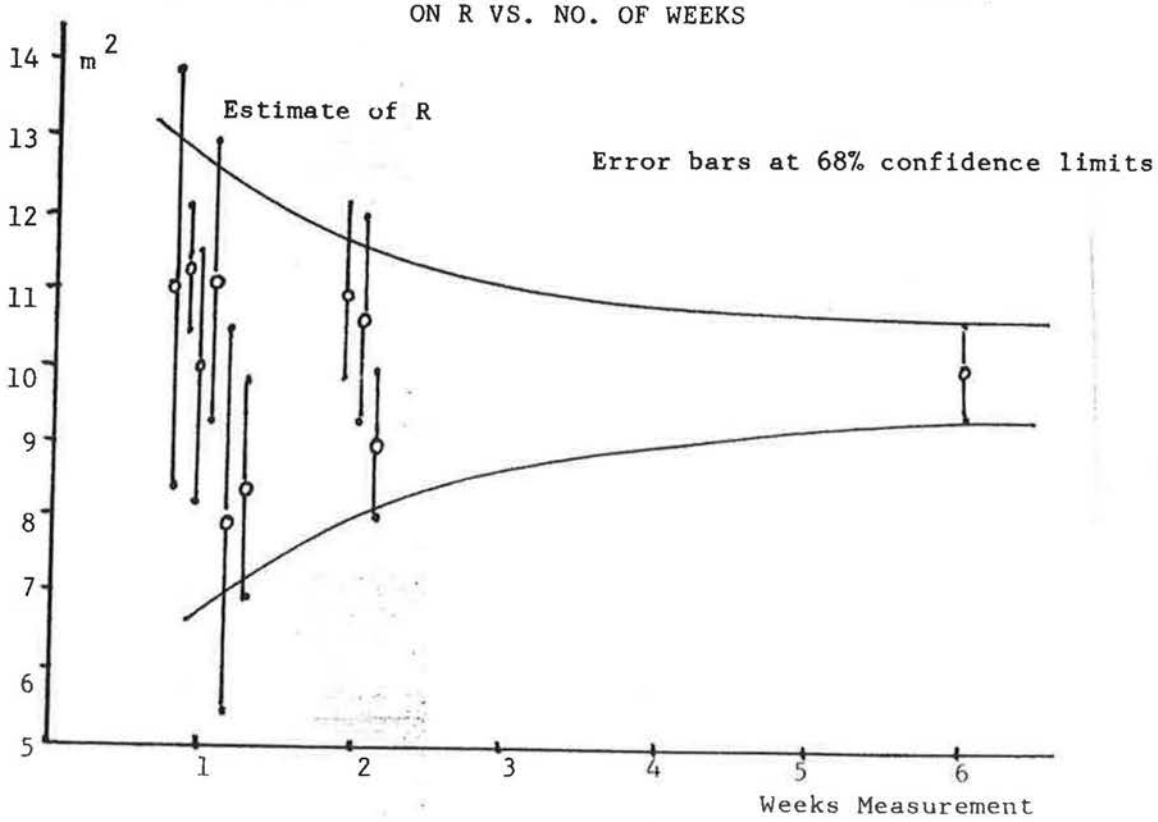

The basic conclusion that can be drawn from this comparison of different time periods is that as long as there are sufficient dull days in a data set, no matter how short, some kind of estimate of ΣA.U is likely to emerge that is more limited by air infiltration and floor heat loss measurement errors than by interference from the effects of solar gains.

In order to get good reliable estimates of the solar aperture, a good mixture of sunny and dull days is necessary, but if the measurement period has to be limited for one reason or another so that there is a lack of sunny days, then there will just be larger error bars on the estimate of solar aperture.

6.3 Self-consistency of Method

If the thermal calibration method is to be of practical use, successive tests should produce similar answers. Figure 6.18 has shown that this is true to a certain extent, but does indicate a slow fall in the estimate of ΣA.U with time. This can be seen more clearly in figure 6.20 plotting 12 successive estimates of ΣA.U from March 1982 to May 1983. The data periods are each of approximately two weeks each except for the last, where the lack of dull days has required 20 days measurement.

The data covers the period immediately before and after the floor of the Linford test house was insulated over with 50 mm polystyrene. This was estimated to produce about a 40 W/^{o}C reduction in total house heat loss. The estimates of ΣA.U, though show a clear jump of about 20 W/^{o}C, though since the floor heat loss is estimated separately there should be no change.

The two estimates before the floor insulation are consistent with each other. The estimate from March 1982 is also just consistent at about a 10% probability level. The four estimates immediately afterwards are also consistent with each other, but thereafter there is a fall in successive values (accompanied by increasing error bars as well as the weather becomes more unsuitable).

The most likely reason for these results is that the floor heat loss has not been estimated properly. It was determined using only two heat flux sensors located at one corner of the house (see figure 3.3). It seems most likely that the extrapolation of the floor heat loss from these two sensors was reasonable before insulation, but probably not so afterwards. The sensors were then covered with 50 mm polystyrene, but there was a very large cold bridge in this floor insulation in the form of the partition walls, made of dense concrete blockwork.

It is likely that the floor heat loss after insulation is as shown in the dashed line in figure 6.21 rather than as estimated from the two sensors. This illustrates the importance of accurately measuring the floor heat loss, especially if as in this case it amounted to almost 20% of the total house heat loss.

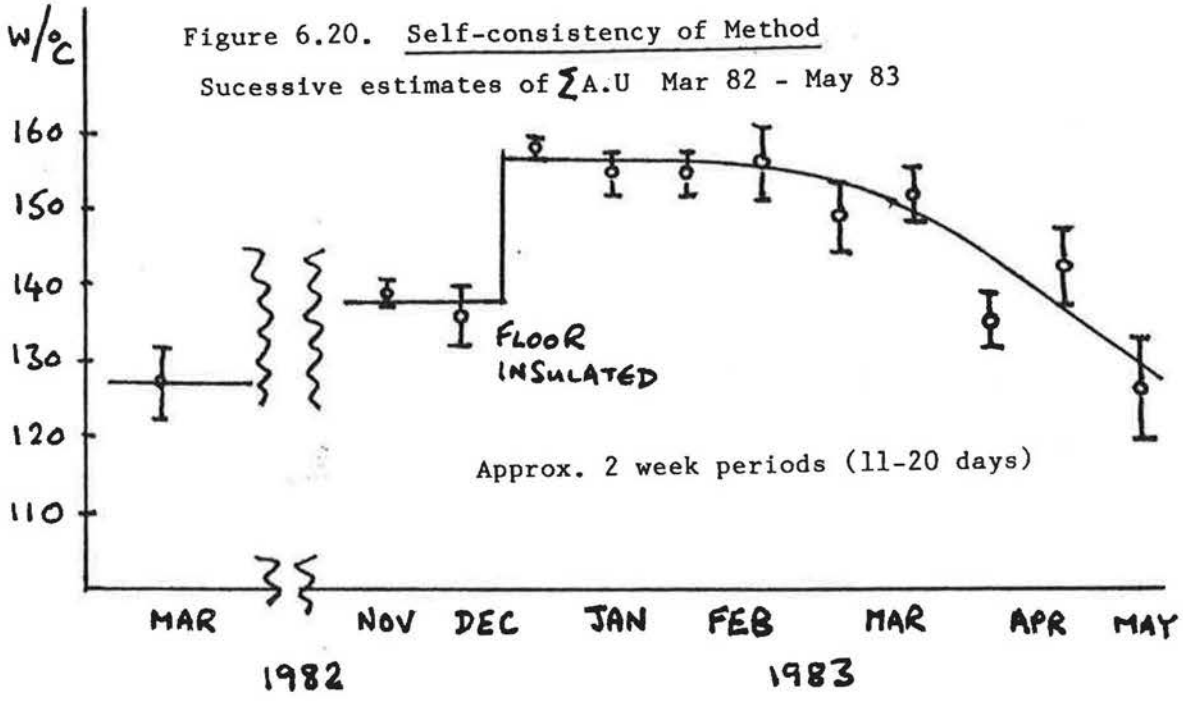

Figure 6.20. Self-consistency of Method

Sucessive estimates of $\sum$A.U Mar 82 - May 83

Figure 6.21 Variation of Floor Heat Loss

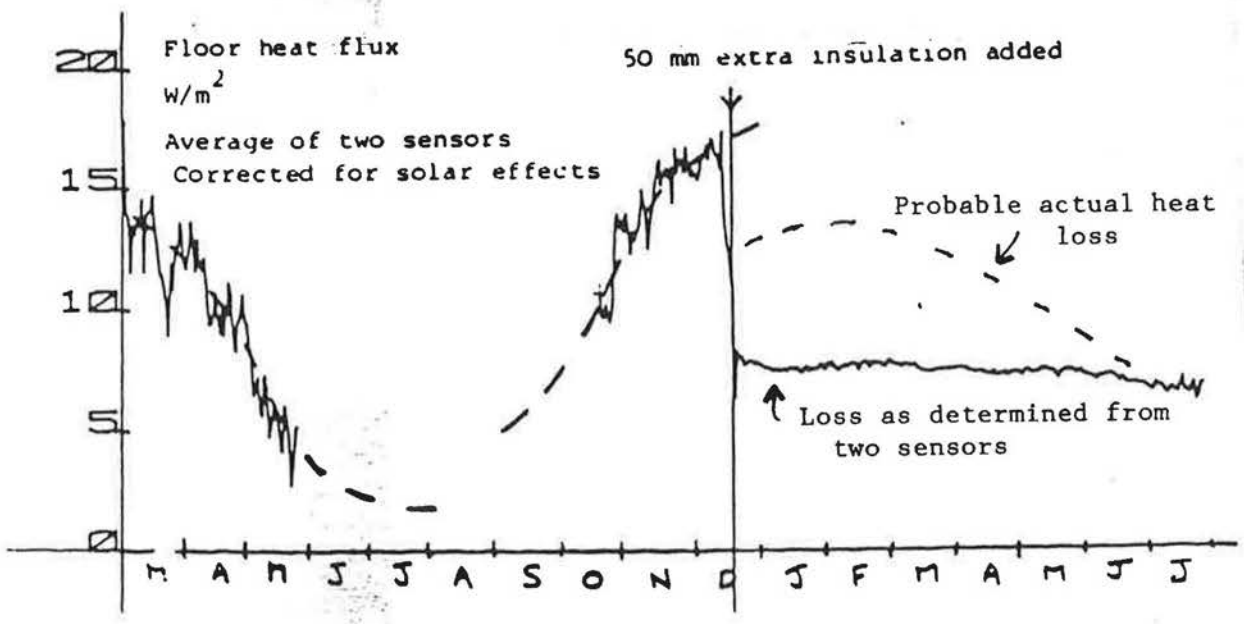

6.4 Regressions on Occupied House Data

As mentioned in chapter 2, the thermal calibration test results for the Linford test house seem to agree with data from three of the four occupied Linford houses analysed in detail. This was totally unexpected and especially the quality of the occupied house results. This agreement seems to forge the link between 'thermal calibration', essentially 'scientific tests' and 'house characterisation' or the analysis of monitored occupied houses with a view to extracting some information about the level of insulation, temperatures and solar gains, etc.

Both the triaxial and two-dimensional regression methods were suggested in 1978 as ways of analysing the fuel consumptions of passive solar houses by the U.S.Solar Energy Research Institute (S.E.R.I.) (see reference 6. 1). However, no actual results appear to have been published to date.

6.4.1 Triaxial Regressions

Monitoring of the Pennyland estate was carried out with a view to 'characterisation', especially the extraction of a solar aperture. A large number of houses were equipped with simple temperature monitoring equipment, sampling three internal temperatures and one external one and essentially calculating a continuous cumulative house average ΔT. The houses were also fitted with electronic heat meters in the central heating systems, measuring space and water heating energy. These two pieces of equipment, together with normal gas and electricity meters including an extra gas meter for cooking, were all read on a weekly basis. Solar radiation on the south-facing vertical surface was measured at the Linford weather station.

A weekly energy balance could then be drawn up for each house:-

$$Q + K = (\Sigma U.A' + C_v) . \Delta T - R.S$$

where Q = Weekly space heating energy
K = Free heat gains from cooking, lights, etc.
$\Sigma U.A'$ = Total fabric heat loss (including floor)
C_v = Ventilation loss (assumed constant)
ΔT^v = Whole house average weekly inside-outside temperature difference
R = Solar aperture
S = Weekly total south-facing vertical solar radiation

By correlating Q with ΔT and S, it was hoped that the three unknowns K, $\Sigma U.A + C_v$ and R could possibly be extracted.

This is equivalent to fitting a plane surface through data points lying in three-dimensional space between the Q, ΔT and S axes (see figure 6.22).

Figure 6.22

$$Q = (\Sigma u.A + C_v).\Delta T - K - R.S$$

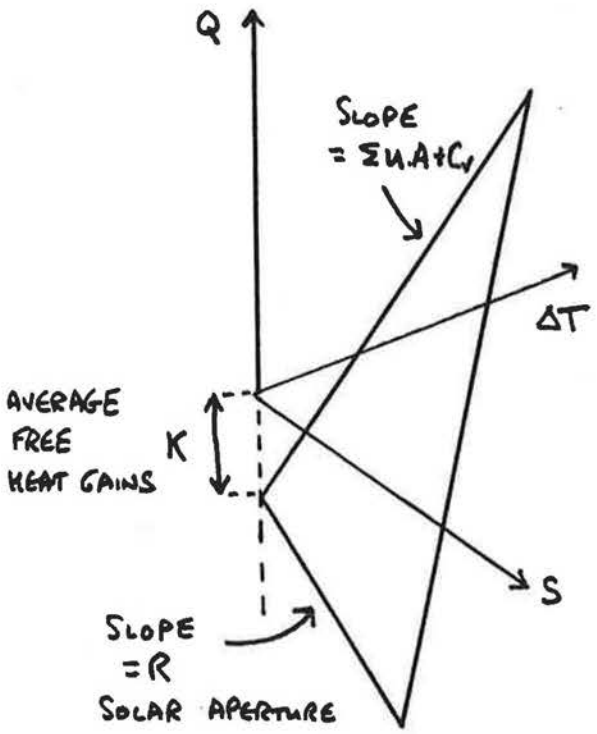

Triaxial Data Plot for Occupied House Data

The slope of the intersection of this plane with that of the Q and ΔT axes should give the total house heat loss term $\Sigma A.U' + C_v$ and that with the Q and S axes should give the solar aperture R.

In practice, in assessing the performance of the house, we are at the mercy of available winter weather conditions to fix the various data points. As such, fitting a practical plane to them is not so easy.

One of the easiest problems to grasp is that of the relatively small spread of values of ΔT over a heating season. A well insulated house with a reasonable level of internal free heat gains may not actually need any appreciable space heating energy until the weekly average ΔT has risen above $6^{o}C$ or more. Given typical midwinter weekly average internal temperatures of $18^{o}C$ and external temperatures of about $2^{o}C$* (in central and southern England), the maximum weekly average ΔT is likely to be only $16^{o}C$. Thus the spread of values of ΔT over a heating season may be only $10^{o}C$ or less, which is not very large considering that temperature measurement errors can easily be $\pm 1^{o}C$.

This low spread in values of ΔT is likely to give very uncertain values for K in a regression. This can be seen by considering just weeks with low values of solar radiation (essentially that portion of the plane close to the Q - ΔT plane (see figs. 6.23 and 6.24). Typical measurement errors combine with the long 'lever' effect of having data a long way removed from the Q axis to give very poor estimates for K (see figure 6.24).

* The 1981/82 dataset used in the Pennyland project was rather exceptional in having some very cold weather with several weeks having average temperatures of below $0^{o}C$.

$$Q = (\Sigma u.A + C_v).\Delta T - K - R.S$$

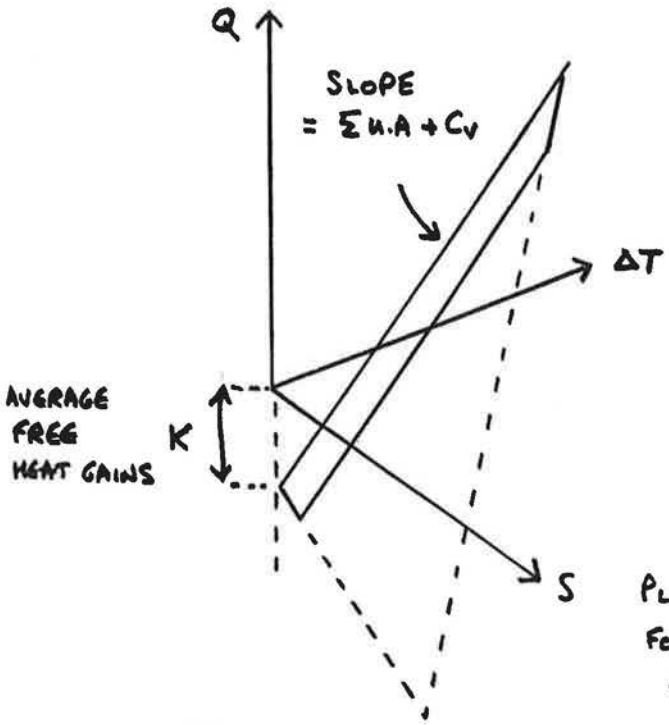

Figure 6.23

PLOTTING DATA POINTS FOR DULL WEEKS ONLY .....

Figure 6.24

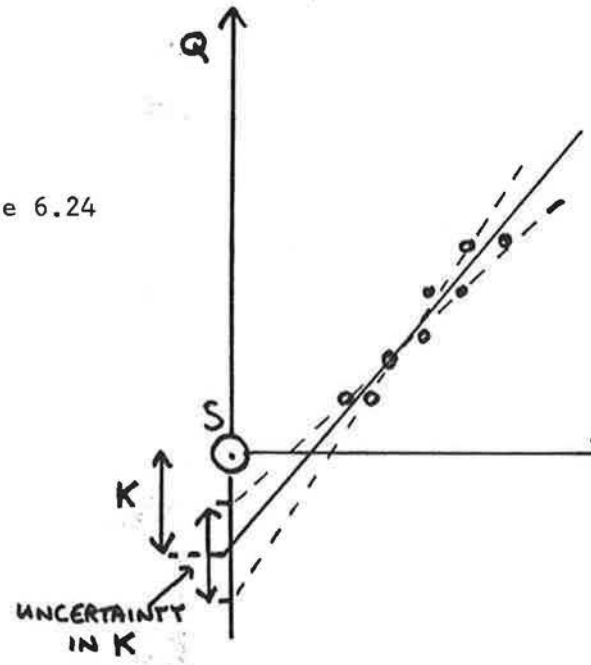

THE UNCERTAINTY OF FIT OF A LINE THROUGH THESE POINTS COUPLED WITH THE LONG 'LEVER' EFFECT BACK TO THE Q AXIS .....

LEADS TO VERY POOR ESTIMATES OF K, THE AVERAGE FREE HEAT GAINS FROM COOKING, LIGHTING, ETC.

In practice, the estimates of K, the free heat gains, are so bad that any credible estimate made by a researcher from other information, such as electricity consumption, measured cooking gas, etc., would be better.

Once K is treated as known, rather than unknown, the regression can immediately be rearranged into the two-dimensional form.

There are several other reasons why the three dimensional regression is should be treated with care:-

1) The least squares regression method is very sensitive to 'outliers' or extreme data points. It is thus essential that 'clean' data is used, i.e. any obvious measurement or recording errors or periods of anomalous occupant behaviour (holidays or even wholesale removal), are identified and removed. This, in practice, requires careful data inspection, which becomes a little difficult with data in three dimensional space.

2) The least squares regression method is potentially a 'biassed estimator'. The regression theory assumes that all measurement errors are in one variable (Q in this case). Thus regressing Q against ΔT and S will give different answers to regressing ΔT against S and Q. Practical measurement errors are likely to be in all three terms (and in generally unknown quantities). These in practice mean that the regression will become a biassed estimator, i.e. it can be almost guaranteed to underestimate the $\Sigma U.A' + C_v$ term, for instance.

3) If the regression package made a wrong estimate of one parameter (say $\Sigma U.A' + C_v$) it is also likely to make a compensating error in another, such as R. Experiments with computer generated data, using a house computer model and real weather data, showed that the regression process was incapable of determining R to within 10% despite an almost perfect fit of the data to a plane surface ($r^2 > 0.995$). Worse still, the uncertainty was not reflected in the quoted error bars for the results. Changing the internal temperature in the house model would produce a different plane fit to the data, whose coefficients $\Sigma U.A'+C_v$, K and R differed from the previous set by more than the quoted errors for individual coefficients. This effect did not appear to depend on the covariance of values of S and ΔT, but seems to be rooted in the mathematics of the regression process. Thus although the regression was able to fit a plane through the data that is a 'good explanation', this is no guarantee that this is the 'right explanation'.

These statistical problems are currently being investigated in several parameter extraction projects. Pennyland and Linford data is being assessed using ARIMA statistics (Auto-Regressive Moving Average) with a view to getting an energy model that can 'lock-on' to the monitored performace of a house in real time. This would be of great use both for predictive purposes and also for 'before and after' savings estimates for various measures.

Hopefully some advice on the 'right kind of statistics' will emerge from these projects.

6.4.2. 2-Dimensional Regressions

Once the free heat gain term, K, has been taken to be a known, rather than unknown quantity, the energy balance equation can be rewritten:-

$$Q + K = (\Sigma U.A' + C_v).\ \Delta T - R.S$$

Taking just dull weeks ($S < 1$ kWh/m^2/day) and plotting Q+K against ΔT for three separate houses of different types, as shown in figure 6.25, clearly distinguishes the different heat loss coefficients $\Sigma U.A' + C_v$, as the slope of the graph. This plot is essentially the same as figures 6.23and 6.24 except that K has beenadded to Q to give the total useful heat input to the house. For this, the free heat gains have been taken to be the total house electricity consumption plus total cooking gas consumption.

Using the phrase coined in the U.S. Twin Rivers field trial, this plot gives the 'Energy Signature' of a particular house, its energy response to external temperature.

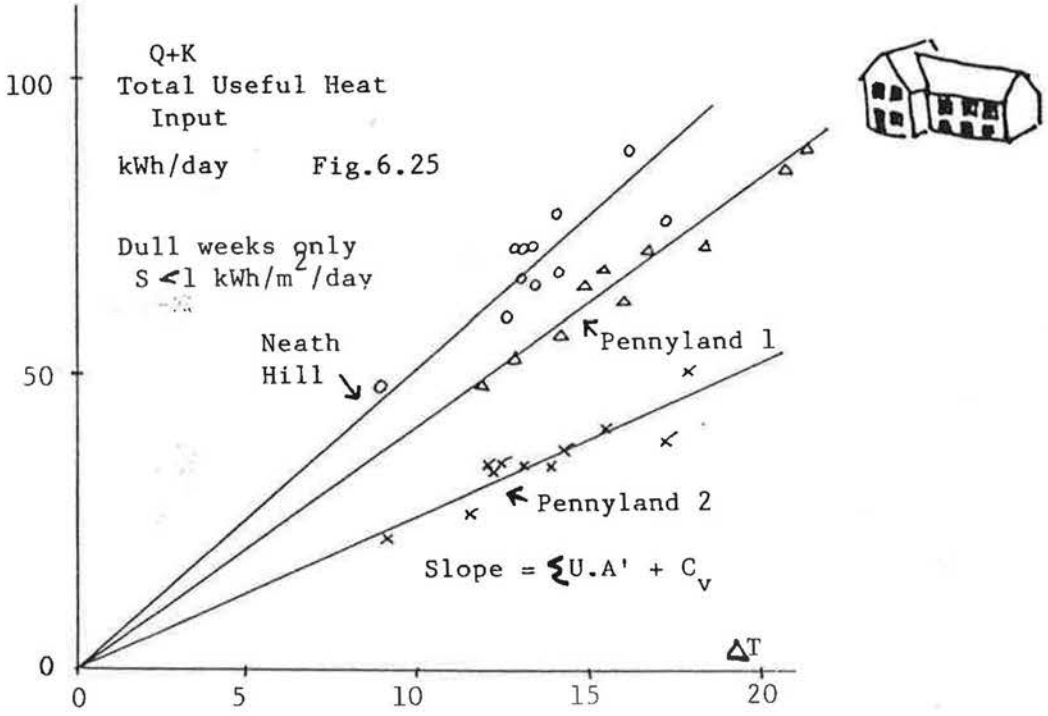

Figure 6. 'Energy Signatures' of 3 different individual houses

Although the Pennyland 1 and Neath Hill houses are likely to have similar fabric heat losses, they are likely to have a 0.5 ac/h difference in air change rate. Thus it is the difference in C_v that alters the slope. he Pennyland 1 and Pennyland 2 houses are likely to have the same air change rate, but a difference in fabric heat loss, $\Sigma U.A'$.

Figure 6.26shows estimated values for $\Sigma U.A' + C_v$ produced from measured energy consumption for a large number of houes, compared with heat loss figures calculated from actual wall areas and text-book U-values. This shows a basic general agreement but with a spread of about +10%-30% This may reflect actual genuine constructional variations or may simply be due to defects in the assumptions, such as heat losses through party walls, etc.

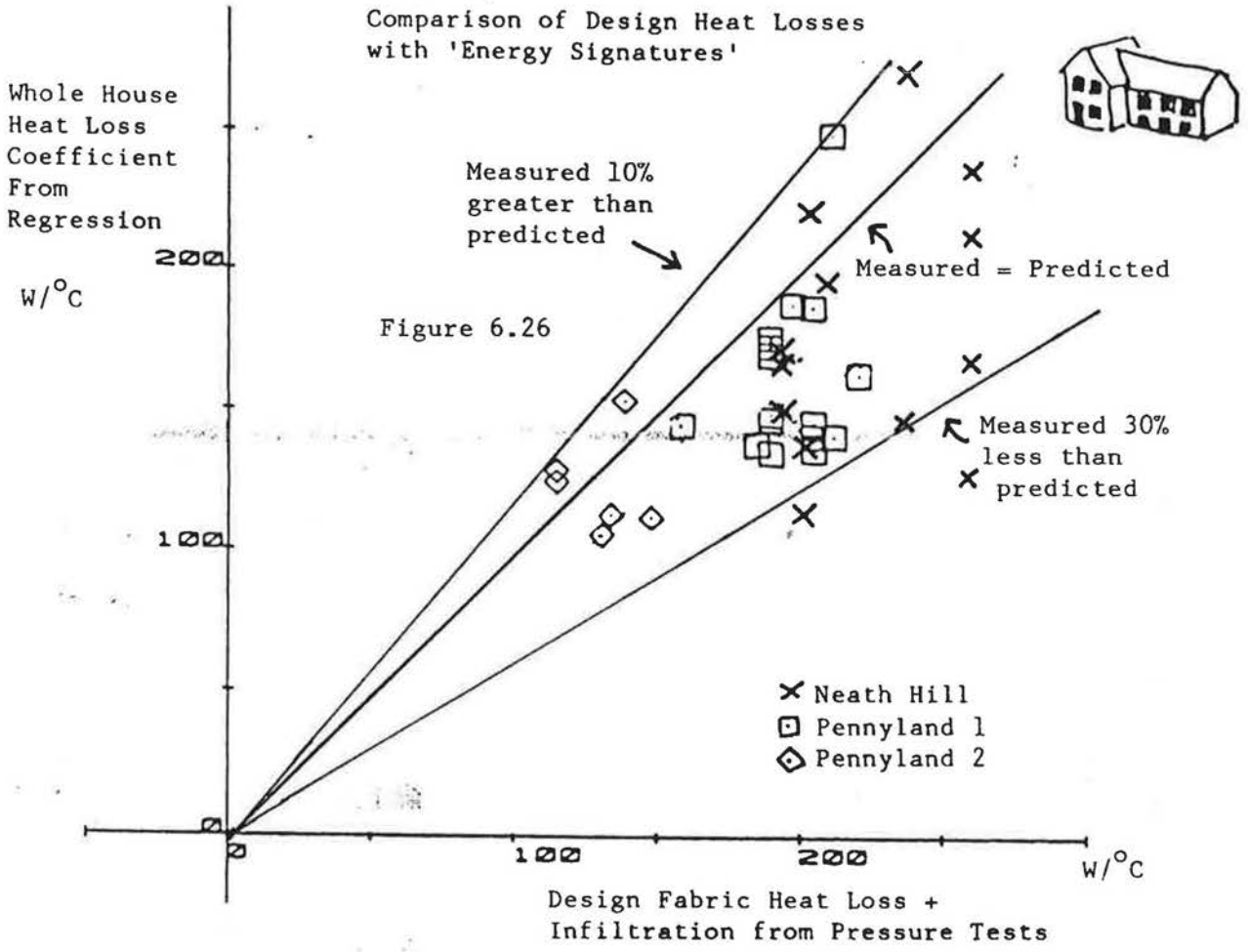

Figure 6.26

We perhaps expect a slight underestimate since there are still some solar gains into the house that we have ignored.

The basic conclusion here is that simple monitoring of this type (space heating energy, gas and electricity consumptions and ΔT, all on a weekly average basis) is only sufficient to <u>detect</u> relatively large differences in house heat loss for individual houses. It can thus show the difference between a 150 W/°C house and a 200 W/°C one, but not accurately enough to really quantify the difference. For <u>groups</u> of houses, though the Pennyland project has shown that energy savings calculated with average heat loss figures produced by this method and simple degree-day type calculations agree quite well with results derived in other ways (such as simple comparisons of annual space heating consumption).

Assessing the performance of individual houses seems to require more detailed monitoring.

6.4.3. Detailed Monitoring

Bringing together the Pennyland and Linford occupied house results, the Linford test house experiments and computer modelling gives a spectrum of results ranging from relative vagueness to extreme precision as more factors are brought under control. This is illustrated in figures 6.27 to 6. 32.

First for the Pennyland and Linford occupied houses, we can take the energy balance equation:-

$$Q + K = (\Sigma U.A' + C_v).\Delta T - R.S$$

where $\Sigma U.A'$ is the fabric heat loss <u>including</u> the floor

This can be rearranged into the two-dimensional form:-

$$\frac{Q + K}{\Delta T} = \Sigma U.A' + C_v - R.S/\Delta T$$

Plotting $(Q+K)/\Delta T$ against $S/\Delta T$ gives a graph with a Y-intercept of $\Sigma U.A'+C_v$ and a slope R.

Figures 6.27and 6.28 show this kind of plot for a sample Pennyland house and a Linford occupied house. Both use essentially weekly average data, although in the Linford case it has been compiled from hourly measurements. The Linford graph is compiled from much more detailed measurements, with temperatures measured in every room and a very careful appraisal of free heat gains, including estimates of occupants body heat, boiler casing heat losses, etc.
The results are rather similar with correlation ratios r^2 of 0.75 and 0.68 respectively.

In the next figure more detail is added by incorporating a separate estimate for the floor heat loss on the basis of an assumed U-value derived from test house measurements referred to an assumed ground temperature, rather than air temperature (see chapter 3).

In the heat balance equation the term $\Sigma A.U'$ is expanded to $\Sigma A.U$ and a separate floor loss term F, though F is expressed in energy terms rather than $W/^{o}C$ related to ΔT.

The heat balance equation can now be expressed:-

$$\frac{Q + K - F}{\Delta T} = \Sigma A.U + C_v - R.S/\Delta T$$

This gives an intercept of $\Sigma A.U + C_v$ and a slope of R, as before.
The effect of including this floor heat loss correction is to improve the quality of fit further with r^2 rising from 0.68 to 0.80. The value of R remains much the same but the intercept falls by about 1 $kWh/day/^{o}C$ which is the floor heat loss (i.e. about 20% of the total house heat loss).

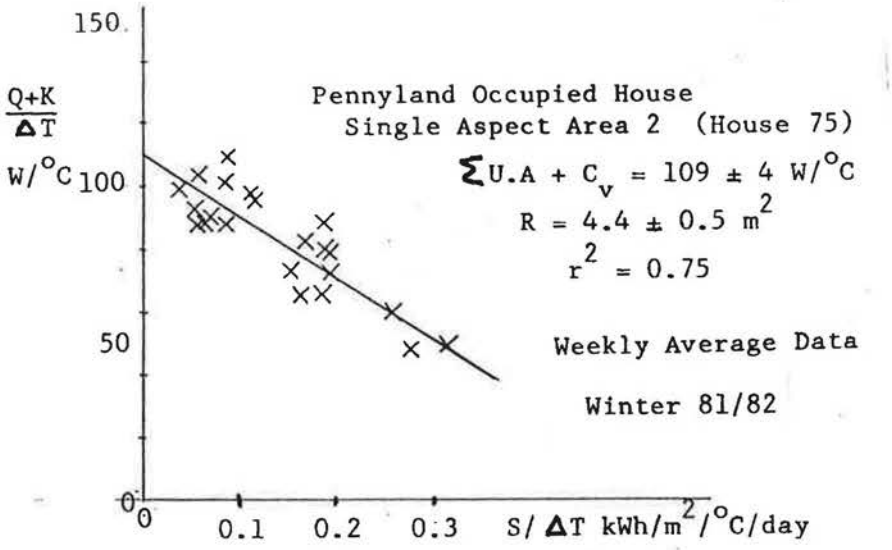

Figure 6.27

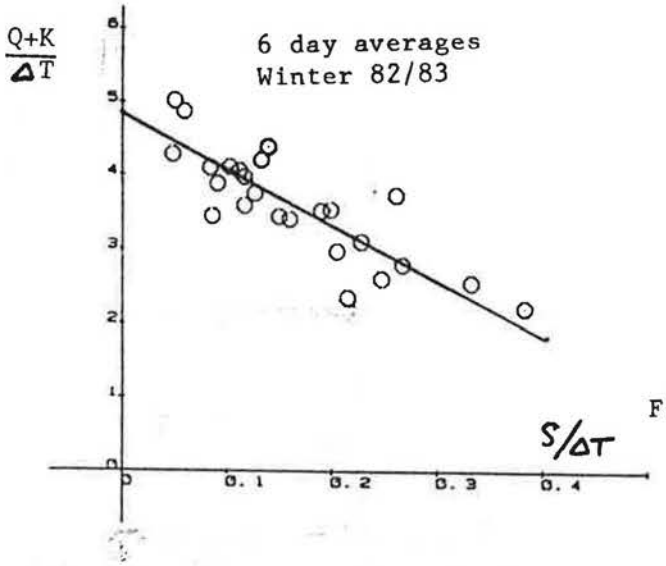

Linford House 35

$\Sigma A.U' + C_v = 4.80 \pm 0.18$ kWh/d/°C

$R = 7.2 \pm 1.0$ m²

$r^2 = 0.68$

Figure 6.28

Linford House 35

$\Sigma A.U' + C_v = 3.70 \pm 0.13$ kWh/day/°C

$R = 7.4 \pm 0.7$ m²

$r^2 = 0.80$

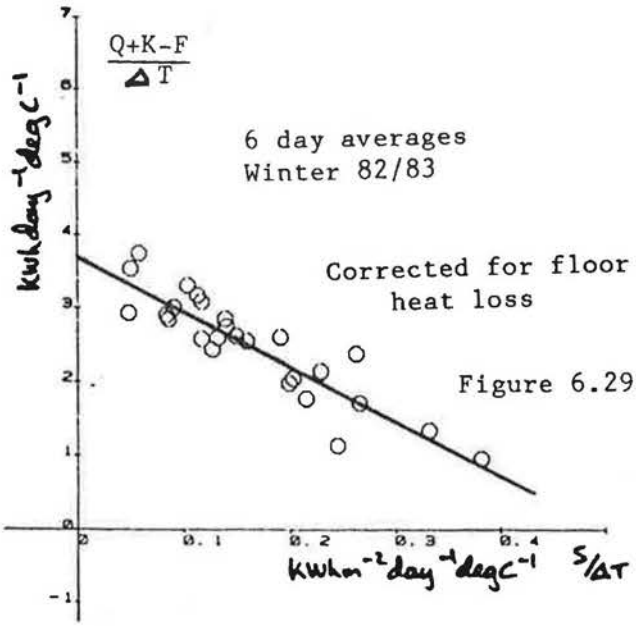

Figure 6.29

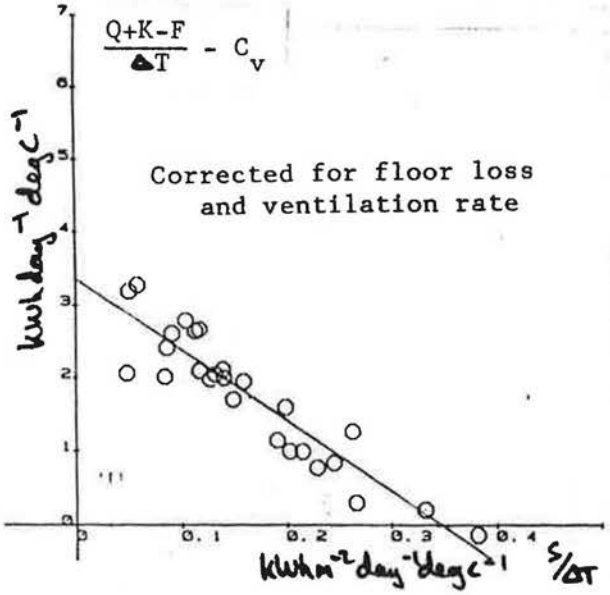

Figure 6.30

Linford House 35

$\Sigma A.U = 3.35 \pm 0.15$ kWh/day/°C

$R = 9.8 \pm 0.8$ m²

$r^2 = 0.85$

Linford Test House

$\Sigma A.U = 3.1 \pm 0.1$ kWh/day/°C
$= 127 \pm 5$ W/°C
$R = 9.8 \pm 0.6$ m²
$r^2 = 96\%$

Corrected for floor heat loss and measured air infiltration

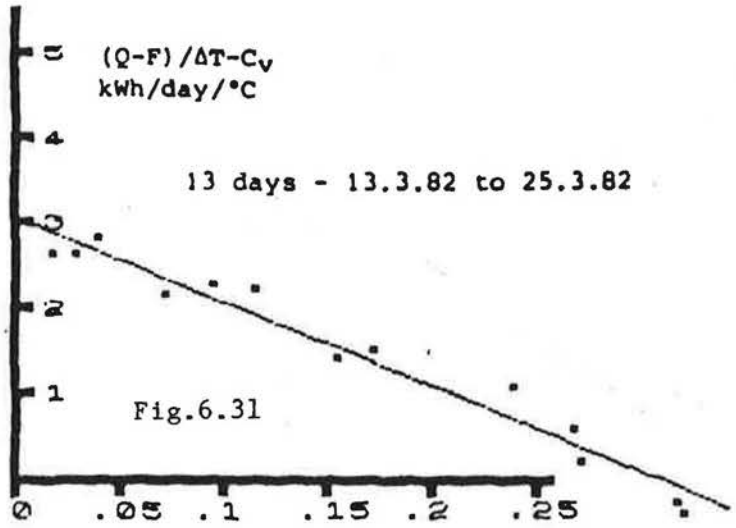

Fig.6.31

Figure 6.32

Computer model of occupied Linford house

$\Sigma A.U + C_v = 3.75 \pm 0.05$ kWh/day/°C

$R = 12.1 \pm 0.5$ m²

$r^2 = 0.97$

Weekly average data

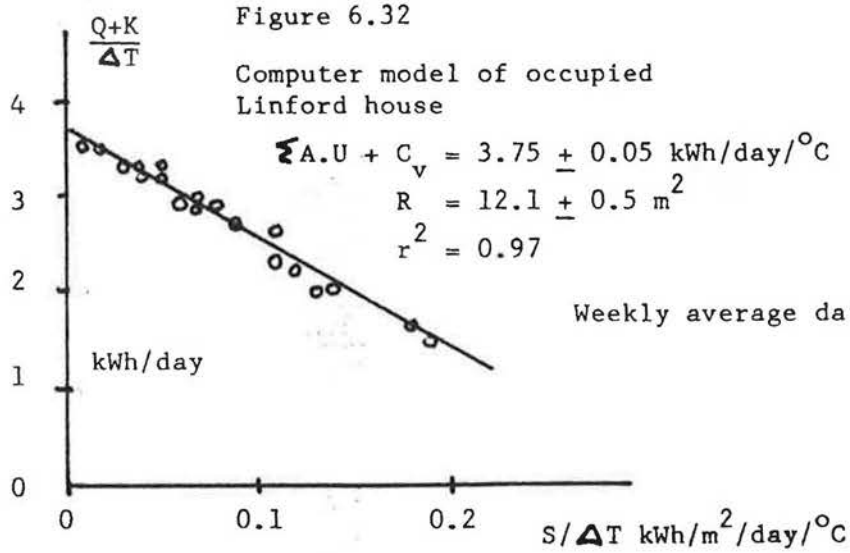

The next improvement that can be made is to include variations in ventilation rate. This has been done by extrapolating the air infiltration model derived for the test house, described in chapter 4, to the occupied houses, using measured wind speed and direction information and measured internal and external temperatures, also taking the measured pressure test leakages into account and measured window opening. This rather complex process is described in full in the main Linford project report.

The heat balance equation can now be rearranged:-

$$\frac{Q + K - F}{\Delta T} + C_v = \Sigma A.U - R.S/\Delta T$$

This improves the quality of fit even further, with r^2 rising to 0.85. The intercept falls further since it is now just the fabric heat loss $\Sigma A.U$, excluding the floor. The estimate of the solar aperture rises to 9.8 m^2 (see figure 6.30).

The estimate of the solar aperture rises as the quality of fit improves because the regression process assumes that all errors are in the dependent variable (Q).
of the slope.

Next comes the step to test house measurements. In figure 6.31, the internal temperature is controlled to be constant, the air infiltration is measured, as is the floor heat loss. There are no free heat gains, only electric space heating energy. The quantities are all daily values, summed from dawn to dawn, with slight corrections to ΔT for thermal timelags.
This graph is thus a plot of:-

$$\frac{Q - F}{\Delta T} - C_v = \Sigma A.U - R.S/\Delta T$$

The actual results here are very similar to those of the previous figure, though it only contains two weeks data rather than five months.

The degree of fit is very good, with $r^2 = 0.96$, though other data sets using air infiltration predicted from the model described in chapter 4 have lower values around 0.85.

Finally figure 6.32 shows a plot of weekly space heating demands calculated by a dynamic computer model. This includes specified free heat gains and a specified constant air infiltration rate. The floor heat loss, in this model has been treated as responding to the same ΔT as the rest of the building fabric.

The graph as drawn is a plot of

$$\frac{Q + K}{\Delta T} = \Sigma A.U' + C_v - R.S/\Delta T$$

This is the same as that used for figures 6.27 and 6.28.

This has a better fit still, with $r^2 = 0.97$. It is not a perfect fit since the model does have some non-linearities (curtains are drawn at night, windows open if the internal temperature gets too high and solar gains are not a perfectly linear function of south-facing vertical solar radiation).

The plot does show, though, that the results of a complex computer model running with hourly timesteps, can be reduced to an equivalent simple U-value type model.

The value of solar aperture produced, $12.1 \pm 0.5\ m^2$ is compatible with the ratio of solar gains calculated into the house to the solar radiation on the south-facing vertical surface, which gives a value of $13\ m^2$ (see figure 2.1).

The intercept, $\Sigma A.U'+C_v$, is slightly different to that in figure 6.28 because of different assumed heat loss values in the model.

This sequence of six graphs does demonstrate the spectrum of possible results ranging from the rather fuzzy plots of raw Pennyland and Linford occupied house data, through more detailed occupied house analysis, to test house data and finally a computer model.

As a result of the Linford test house experiments, the computer model was adjusted in terms of solar absorption to give a better agreement in solar aperture. This model was then used to calculate the project solar energy savings.

6.5 Covariance of S and ΔT

It has already been pointed out that for the triaxial regression method to work it is desirable to have a wide spread of values of both solar radiation and ΔT. It is also desirable that there be little covariance. The regression process is not going to be able to make much sense of the data in separating solar and temperature effects if all sunny days or weeks are equally warm and all the dull ones equally cold.

Fortunately, this does not seem to be too much of a problem in practice. While on a monthly average basis solar radiation and external temperature are strongly correlated (see figure 6.33), on a weekly basis over the heating season there is plenty of scatter. There are dull weeks occuring in warm weather, and some moderately sunny ones occuring in cold weather (see figure 6.34).

For short-run daily data there is a much reduced spread in values of external temperature (figs. 6.35 & 36). There is, on average, a tendency for mid-winter weather to have a slight negative covariance between solar radiation and air temperature (i.e. sunny days are cold). In summer, the pattern is reversed and sunny days are hot. For the spring and autumn there is little relation (ref. 6.2).

However, individual data sets may exhibit strong covariance either way and it is just as well to know what the likely effects are.

Predominantly, they seem to be second order effects, relating how errors in determining the constant term in a regression (floor loss or free heat gains) effects errors in estimating the temperature related coefficient ($\Sigma A.U + C_v$) and the solar coefficient, R.

The process is a little difficult to illustrate and perhaps the best way is as a triaxial plot but with the constant term inserted as a known quantity (see figures 6.37 and 6.38).

These show that if solar radiation is positively covariant with ΔT, i.e. sunny days are cold, an overestimate of the constant term will give:-

a) an underestimate of $\Sigma A.U + C_v$
b) an underestimate of R

If solar radiation is negatively covariant with ΔT, i.e. sunny days are warm, an overestimate of the constant term will give:-

a) an underestimate of $\Sigma A.U + C_v$
b) an overestimate of R

This state of affairs is likely to be true not only if the researcher inserts the constant term (as in the two-dimensional regression form) but also if we let the triaxial regression process work it out.

These findings have been tested using sample data in the two-dimensional regression format.

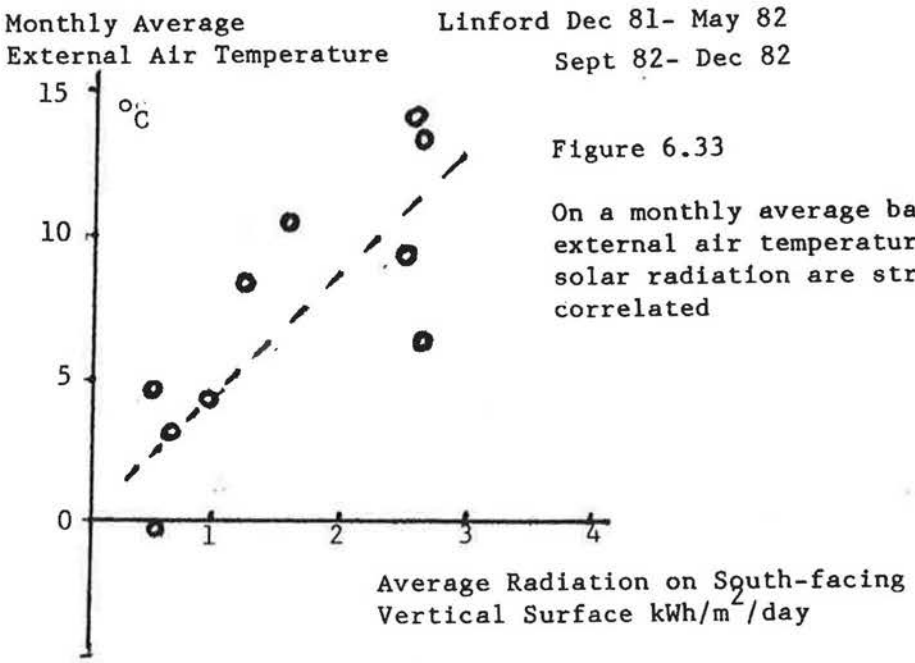

Figure 6.33

On a monthly average basis external air temperature and solar radiation are strongly correlated

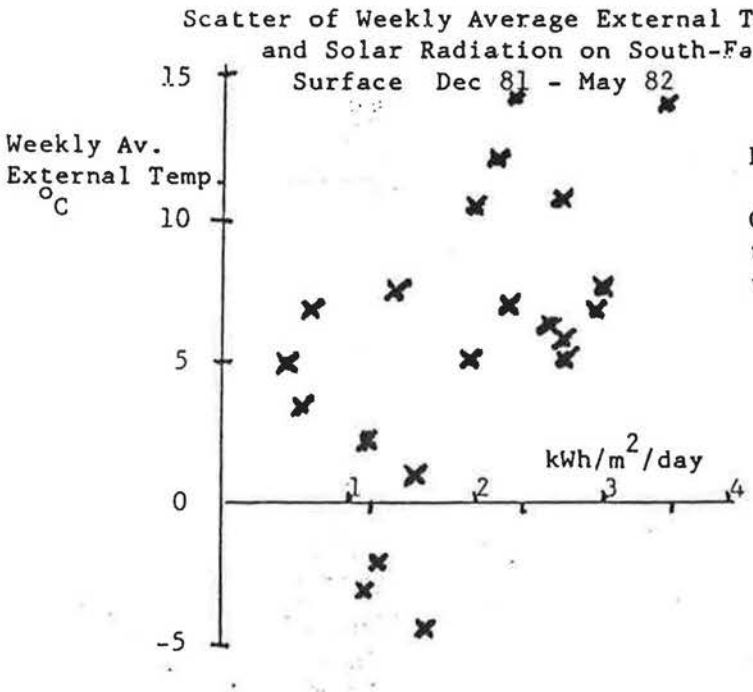

Figure 6.34

On a weekly average basis there is more scatter and the correlation is weaker.

ON A DAILY AVERAGE BASIS THE RANGE OF VALUES OF EXTERNAL AIR TEMPERATURE IS MUCH REDUCED.

SOLAR RADIATION AND TEMPERATURE CAN BE STRONGLY NEGATIVELY CORRELATED.....

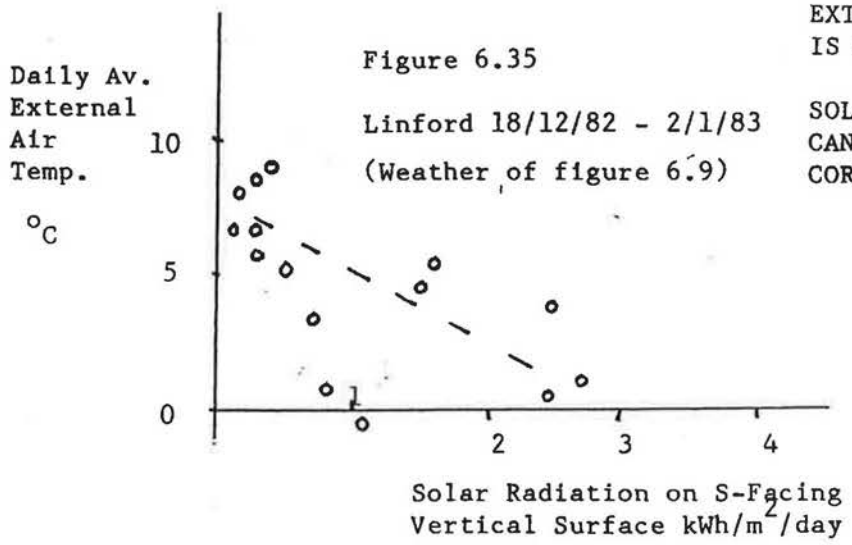

Figure 6.35

Linford 18/12/82 - 2/1/83

(Weather of figure 6.9)

... OR HARDLY CORRELATED AT ALL.

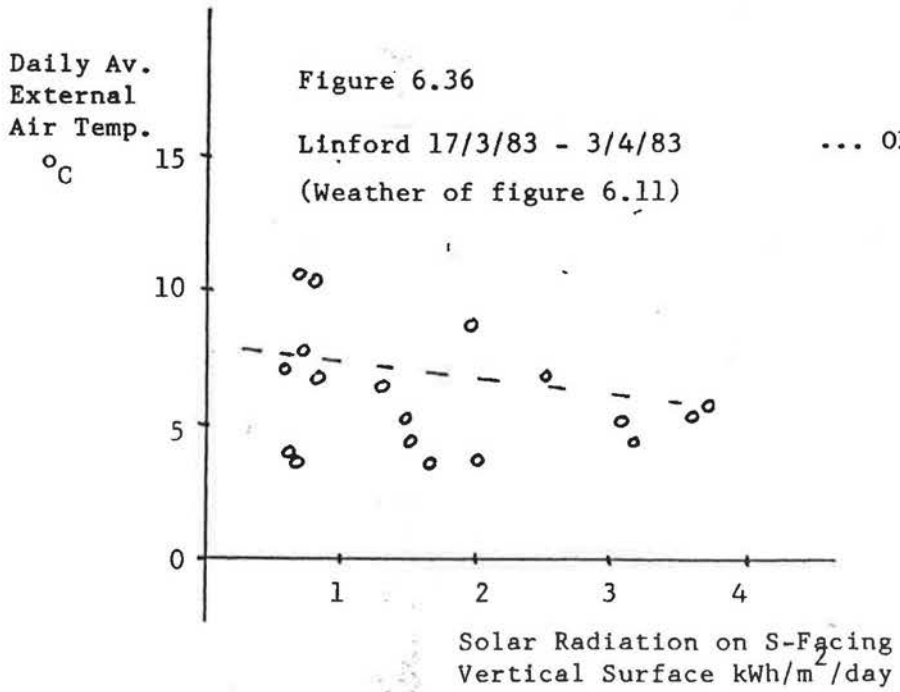

Figure 6.36

Linford 17/3/83 - 3/4/83

(Weather of figure 6.11)

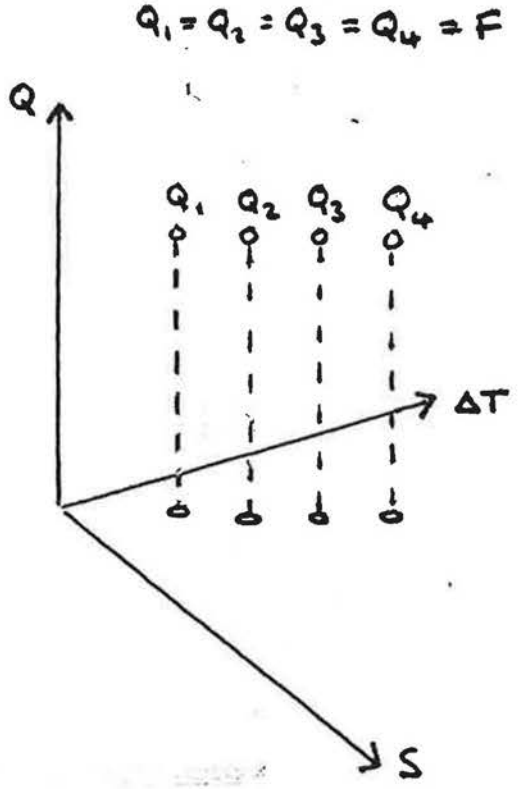

Figure 6.37 Effects of Covariance of S and ΔT

IMAGINE A DATA SET IN WHICH S WAS POSITIVELY COVARIANT WITH ΔT AND ALL VALUES OF Q WERE EQUAL TO A CONSTANT F.

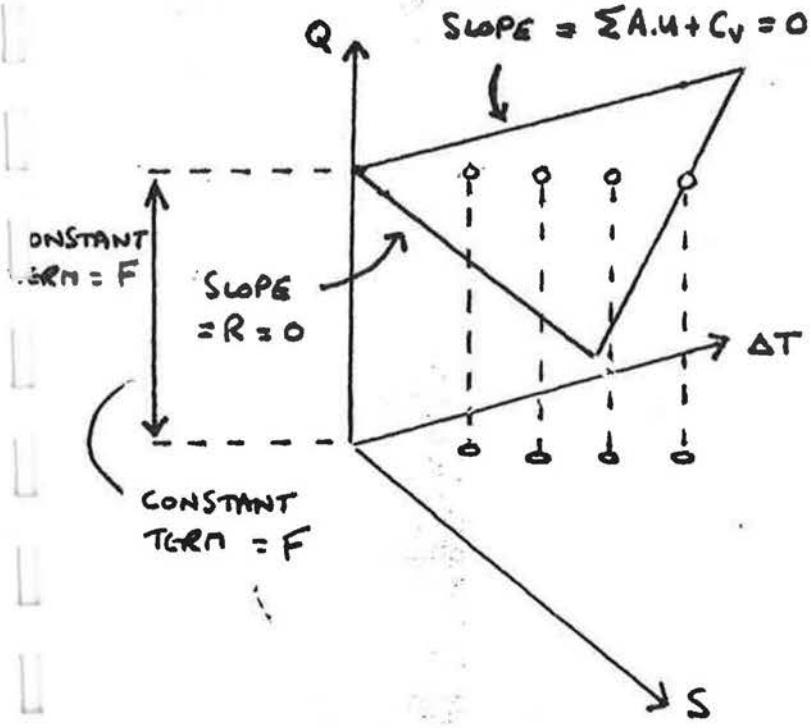

IN A TRIAXIAL PLOT WE COULD 'EXPLAIN' THIS DATA BY FITTING A HORIZONTAL PLANE THROUGH IT SHOWING NO VARIATION WITH EITHER TEMPERATURE OR SOLAR RADIATION.

THIS WOULD MEAN THAT $\Sigma A.U + C_V = 0$ AND $R = 0$.

Figure 6.38

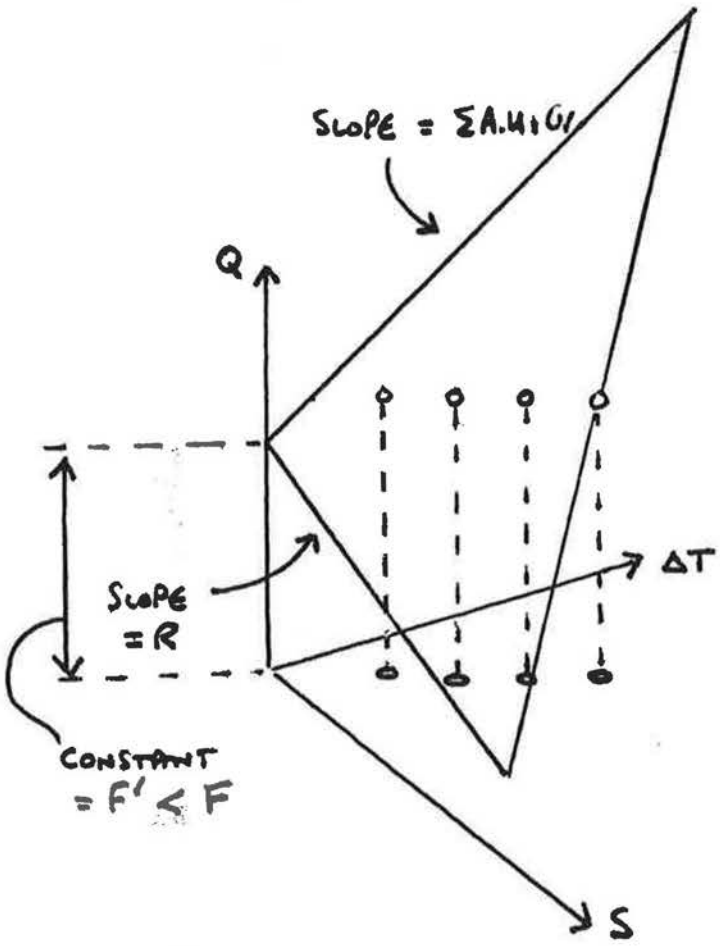

ALTERNATIVELY WE CAN 'EXPLAIN' THE DATA BY A PLANE WITH A LARGE POSITIVE VALUE OF $\Sigma A.U+C_v$ AND A POSITIVE VALUE OF R.

THUS IF S IS POSITIVELY COVARIANT WITH ΔT, I.E. SUNNY DAYS ARE COLD, THEN AN OVERESTIMATE OF THE CONSTANT TERM, F, WILL GIVE:-
AN UNDERESTIMATE OF $\Sigma A.U + C_v$
AN UNDERESTIMATE OF R

Experience with the Linford data set has shown that plotting out graphs with good video computer graphics can work wonders. Plots can be made split into different 'bands' of ΔT's to see if the answer varies. Similarly it is wise to check if there is any time variation (such as due to the changing floor heat loss).

BE WARNED --- STATISTICS PACKAGES CAN DAMAGE YOUR UNDERSTANDING.

References

6.1. L.S.Palmiter, L.B.Hamilton & M.J.Holtz, 'Low cost performance evaluation of passive solar buildings', Solar Energy Research Institute, S.E.R.I./RR 63-223, 1979.

6.2. M.G.Davies, Useful Solar Gains through a South-Facing Window in the U.K.Climate, Building and Environment, Vol.15, pp 252-272., (1980).

7. THERMAL WEIGHTING FUNCTIONS

CONTENTS

This chapter describes a response factor based method for correcting for day-to-day thermal timelags in the building fabric. It is highly mathematical and (fortunately) probably not very important.

CHAPTER 7

THERMAL WEIGHTING FUNCTIONS

These are an attempt to correct for thermal timelags in the fabric of a building. The 'external' weighting factor corrects for lags in the response of the building to changes in external temperature. The 'internal' weighting factor attempts to correct for day-to-day energy storage effects caused by variations in internal temperature, in particular short temperature rises at around midday caused by excessive solar gains.

These two functions are produced by considering a simple response factor model of the house. This does imply some knowledge of the thermal properties of the building in advance and it may seem that this is what is supposed to be being measured. However, all that is being predicted with these weighting functions is the phase of response of the building, with a view to improving the accuracy of determination of the magnitude.

As mentioned in chapter 2, these mathematical niceties do tend to take second place in practice to the problems of errors of measurement, especially in infiltration rate. Also, the complexity of the mechanisms of storage of solar energy in the building fabric seem to have made the internal weighting factor, with its assumptions about the nature of the total thermal mass of a house, rather a dubious proposition, but it is included here for completeness.

7.1. External Weighting Factor

In evaluating the heat balance equation

$$(Q-F)/\Delta T = \Sigma U.A + C_V - R.S/\Delta T$$

if we use values of Q, S and ΔT summed over the same period of 24 hours it implies that the house has no thermal mass. A particular day's space heating is dependent not only on that day's ΔT but also on that of the previous day and even the day before. It would thus be better to use a value of ΔT calculated on a weighted average of temperatures stretching back in time. This has the effect of keeping the heat balance equation a straightforward linear function of ΔT and S, rather than introducing extra terms for the previous day's ΔT, etc.

In order to explain the derivation of the weighting function, it is necessary to describe a bit of theory of response factors, in particular the Y-response function. A more general description will be found in reference 7.1.

The Y response function is a way of splitting up the U-value of a piece of building fabric, or even the whole house itself as a history of responses to past values of external temperature. Thus, if the inside temperature is kept constant, the heat loss at the

inside surface, Q_t, at time t can be expressed as

$$Q_t = U.T_{in} - Y_j \cdot T_{out\ t-j+1}$$

where T_{in} is a constant.

Normally the time steps would be of one hour, though longer or shorter ones can be used.

The various terms of Y have the property that

$$\sum_{j=1}^{\infty} Y_j = U$$

i.e. the Y response function is a way of disaggregating the total U-value of the fabric in time.

Figure 7.1 shows some typical Y response functions for the Linford test house. The walls have a very long time response extending back for two days. The roof is much more 'immediate' with a response only lasting for five hours or so. Components such as windows and, if included, the ventilation loss have no thermal mass and so have only one term.

The Y response functions of the various building components can be added together when multiplied by their respective areas to give a total Y response function for the whole house. This is the same as generating U.A from the individual U-values but incorporating an extra dimension of time.

The Y response function of a building element is the heat flow response at the inside surface to a unit temperature impulse (i.e. an increase in external temperature of 1°C lasting for one hour) on the outside. This property can be used to check practical values.

For example, figure 7.2 shows the response of the inside surface temperature of the house/conservatory wall of the Spencer St. house to a massive temperature impulse produced in the conservatory by solar gains. The wall surface temperature is an indication of the inside surface heat flux flowing into the living room, which is maintained at a constant 20°C by the fan heater.

The response shows a peak after about 9 hours, decaying away slowly into the next day. Initial calculations based on a description of the building fabric predicted a peak after 5 hours, but this was subsequently found to be due to assuming too high a density for the brick. The plot at the top of the diagram shows the computed wall surface heat flux based on the measured conservatory temperatures and the revised Y response function.

LINFORD HOUSE COMPONENT Y-RESPONSE FUNCTIONS

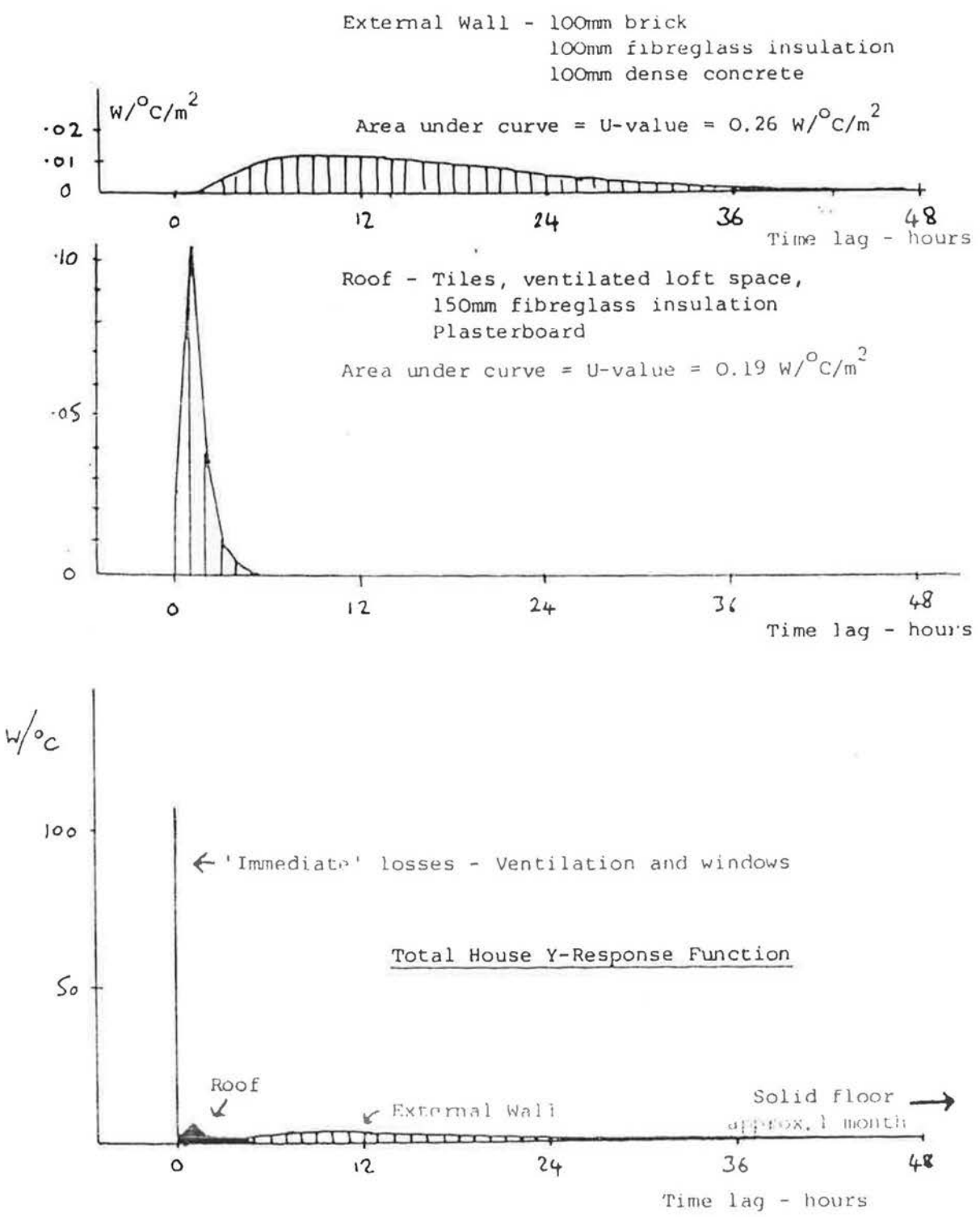

Figure 7.1

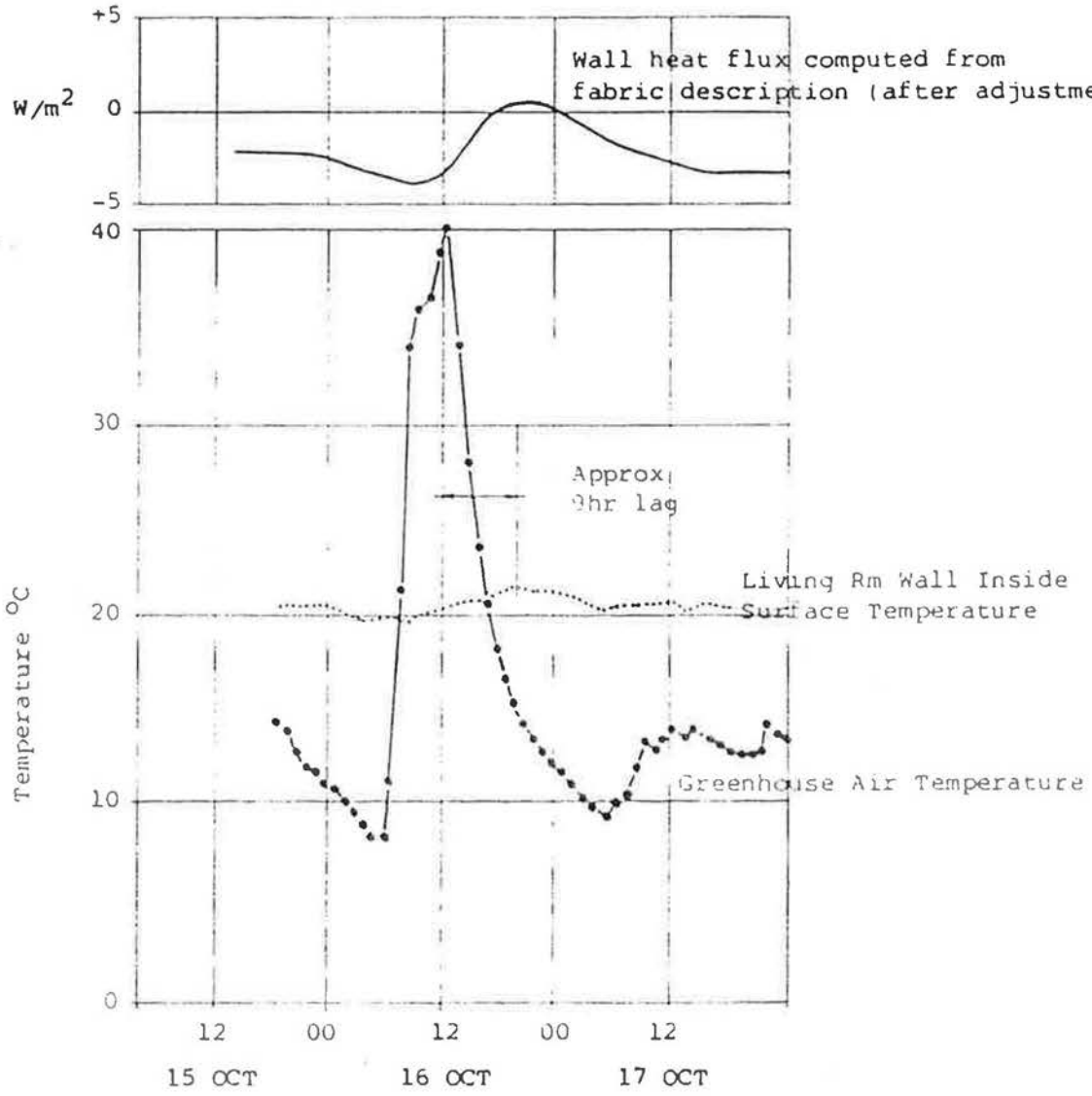

Response of Wall Heat Flow to a Temperature Impulse

Figure 7.2

Given a constant internal temperature, a single hour's heating demand from fabric components can be determined by convolving the Y response function with past values of outside temperature (figure 7.3).

This is the process described by the equation

$$Q_t = U.T_{in} - \sum_{j=1}^{\infty} Y_j . T_{out_{t-j+1}}$$

A whole day's heating can thus be seen as the sum of 24 of these hourly convolutions, each displaced by one hour:-

$$\sum_{n=1}^{24} Q_n = 24.U.T_{in} - \sum_{n=1}^{24}\left[\sum_{j=1}^{\infty} Y_j . T_{out_{t-j+1}}\right]$$

The 24 Y series can be summed before convolving with temperature to give a new series and effectively normalised to 1 by dividing by the total heat loss:-

$$\sum_{n=1}^{24} Q_n = 24.U \cdot \left[T_{in} - \sum_{k=1}^{\infty}\left[\frac{\sum_{n=1}^{24} Y_{k-n+1}}{24.U} \cdot T_{out_{25-k}}\right]\right]$$

The series $\sum_{k=1}^{\infty}\left(\sum_{n=1}^{24} Y_{k-n+1}\right) / 24.U$ is the <u>external temperature weighting function</u>.

For massless house or building element this series would only have 24 terms. For a practical house it is likely to have significant terms stretching back for two days or more.

The weighting function is used to build up a weighted 'average' daily external temperature for use in the regressions. A range of sample Y response functions for common building elements are given in Appendix 3.

Although the convolution integrals do look rather daunting, in practice 48 terms are sufficient and the calculations themselves reduce to a few lines of simple computer program.

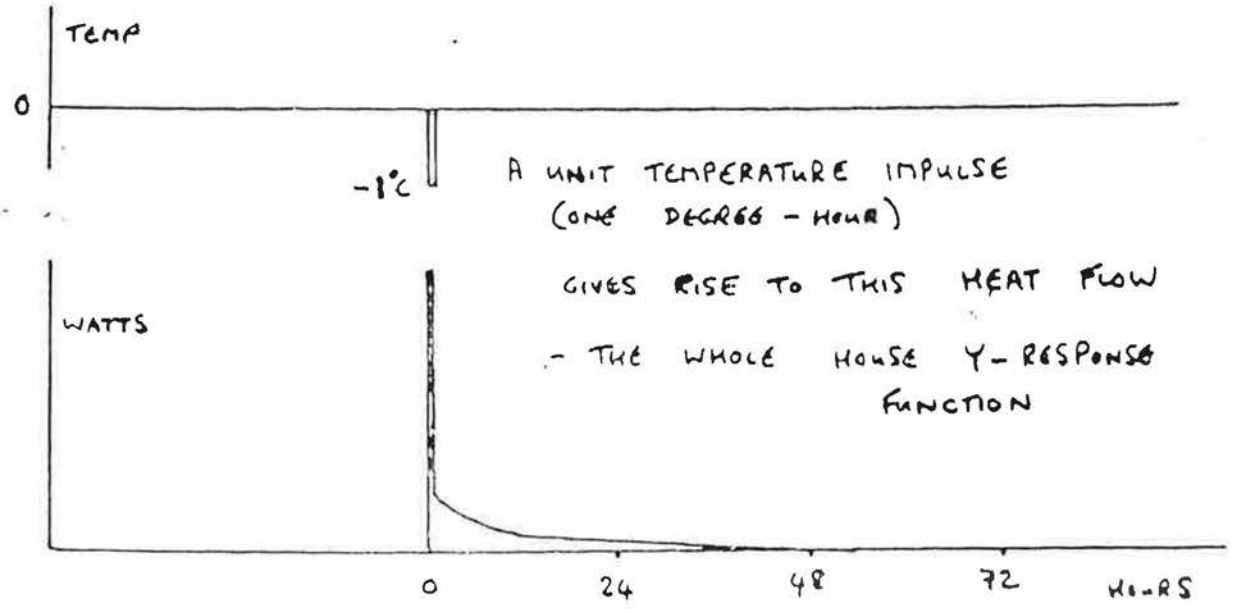
TEMP
0
-1°C
A UNIT TEMPERATURE IMPULSE
(ONE DEGREE - HOUR)
GIVES RISE TO THIS HEAT FLOW
- THE WHOLE HOUSE Y-RESPONSE FUNCTION
WATTS
0
24
48
72
HOURS

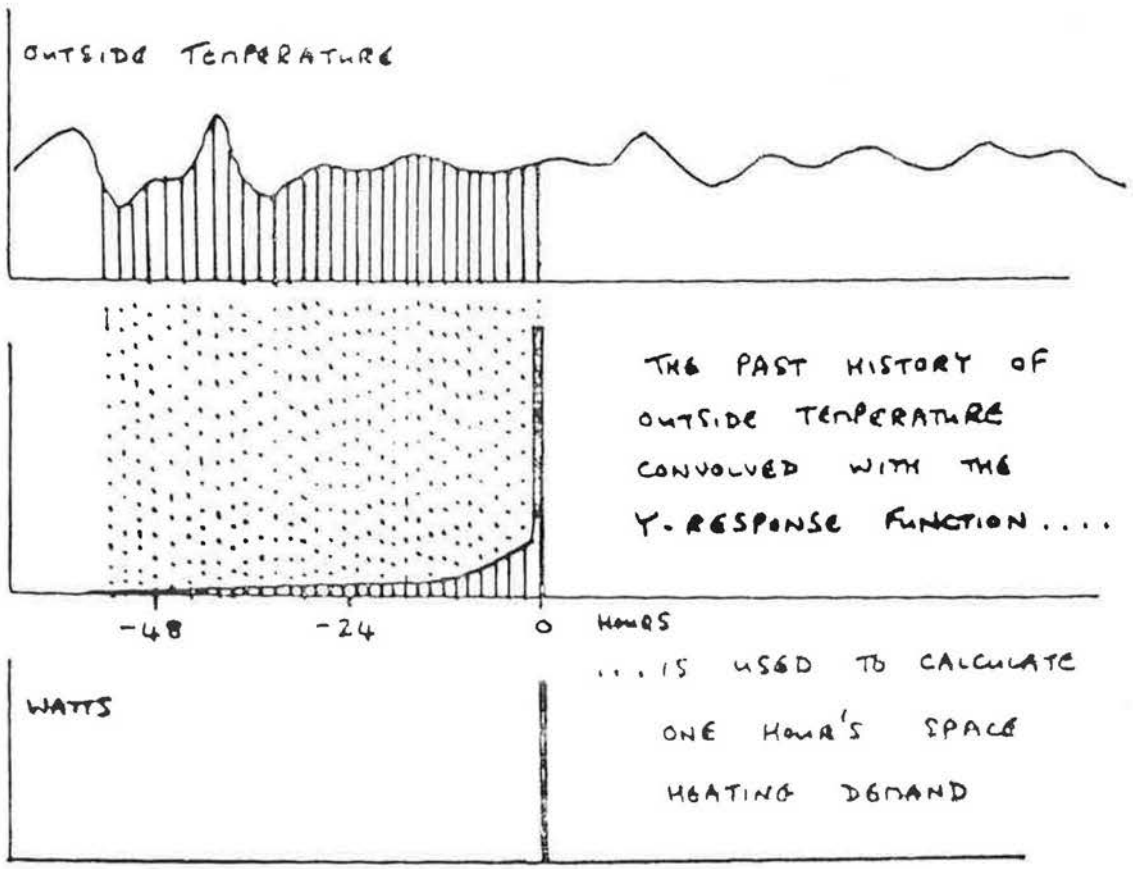
OUTSIDE TEMPERATURE
THE PAST HISTORY OF OUTSIDE TEMPERATURE CONVOLVED WITH THE Y-RESPONSE FUNCTION....
-48
-24
0
HOURS
...IS USED TO CALCULATE ONE HOUR'S SPACE HEATING DEMAND
WATTS

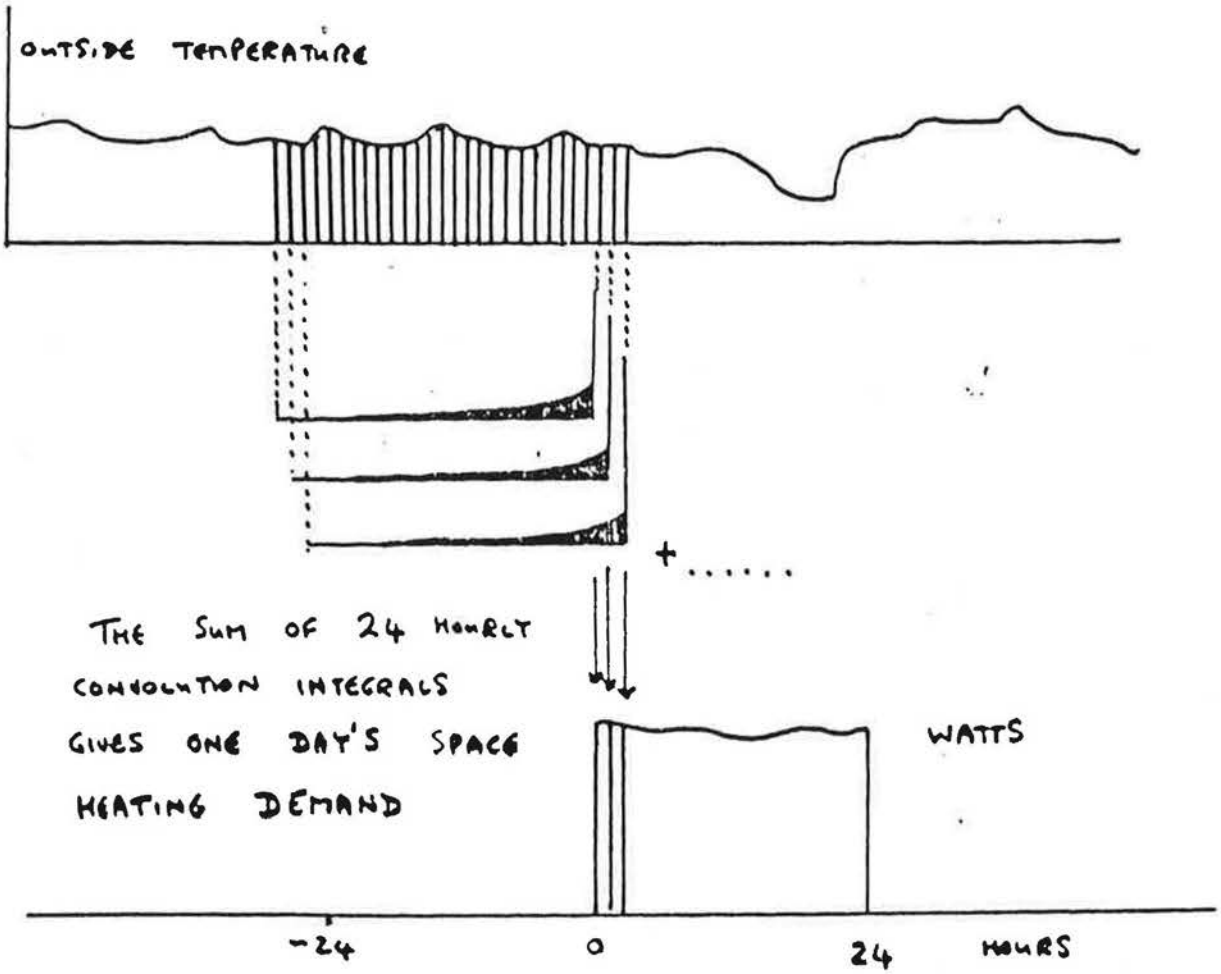

THIS IS EQUIVALENT TO CONVOLVING THE TEMPERATURE WITH A SINGLE FUNCTION WHICH IS THE SUM OF 24 Y-RESPONSE FUNCTIONS EACH DISPLACED BY 1 HOUR

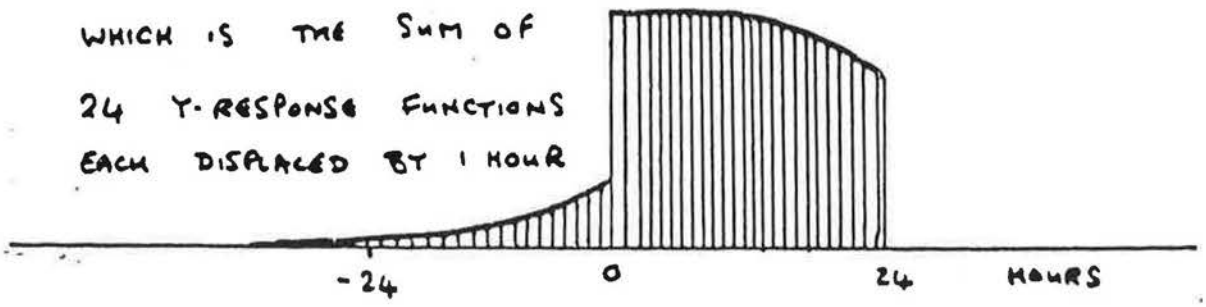

THIS CURVE, WHEN NORMALISED TO HAVE AN AREA OF UNITY, IS THE HOUSE OUTSIDE TEMPERATURE WEIGHTING FUNCTION

Figure 7.4.

7.2. Internal Temperature Weighting Function

We can extend this theory to cope with energy storage effects due to changes in internal temperature. To do this we must use the X-response function of the response factor method. This is defined as the heat flow response at the inside surface of a building element in response to a unit temperature impulse, also at the inside surface.

A typical response is shown in figure 7.5. If the internal temperature is raised suddenly, there will be a large flow of heat into the fabric surface. When the temperature is lowered again there is a large flow of heat out again, quickly dying down to a long exponential tail as the fabric approaches thermal equilibrium again. As with the Y response function, the integral of all the terms is equal to the U-value of the element:-

$$\sum_{j=1}^{\infty} X_j = \sum_{j=1}^{\infty} Y_j = U$$

It is difficult to explain in physical terms what an X response function represents, since it is a combination of both U-value and thermal mass. The long exponential tail of the function is a good indicator of potential thermal storage, while the first few terms are indicative of the surface 'warmth' or 'coldness' to the touch. A 'cold' surface could perhaps either be uninsulated glass, or a slab of marble with insulation behind. Both would have high values for X_1 but they would have completely different U-values.

As with Y response functions they can be added, like U-values to give a single X response series for the whole house (considered as a one room box). Partition walls, furniture, internal floors and even the air in the house all contribute to a whole house X response function even though they do not have a U-value. Also a solid ground floor may have a well defined short term thermal mass as given by the properties of the first few feet of construction, though the U-value and long term properties may be almost unknown. Equivalent X response functions for all these components can be estimated. Details of the mathematics are given in reference 7.2.

Having built up a whole house X response function we can calculate the hourly heat demand produced by the building fabric in terms of past values of internal and external air temperatures:-

$$Q_t = \sum_{j=1}^{\infty} X_j . T_{in_{t-j+1}} - \sum_{j=1}^{\infty} Y_j . T_{out_{t-j+1}}$$

Figure 7.5

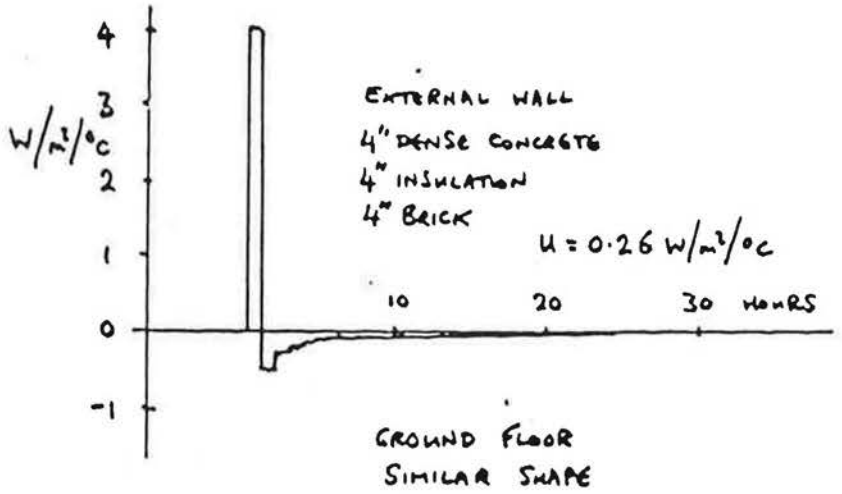
4
3
2
1
0
-1
W/m²/°C
EXTERNAL WALL
4" DENSE CONCRETE
4" INSULATION
4" BRICK
U = 0·26 W/m²/°C
10
20
30 HOURS
GROUND FLOOR
SIMILAR SHAPE

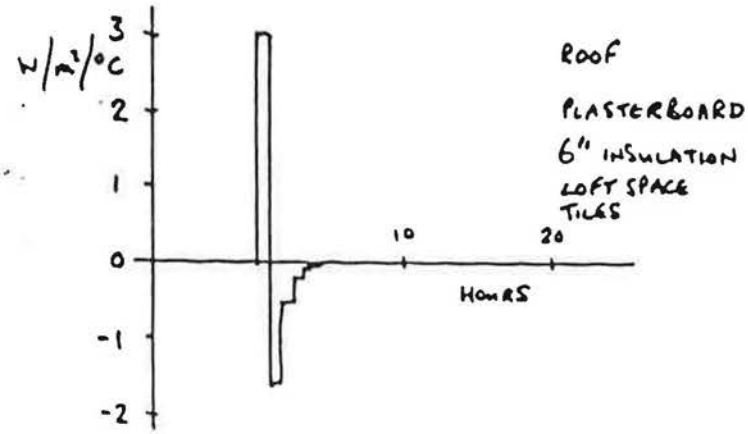
3
2
1
0
-1
-2
W/m²/°C
ROOF
PLASTERBOARD
6" INSULATION
LOFT SPACE
TILES
10
20
HOURS

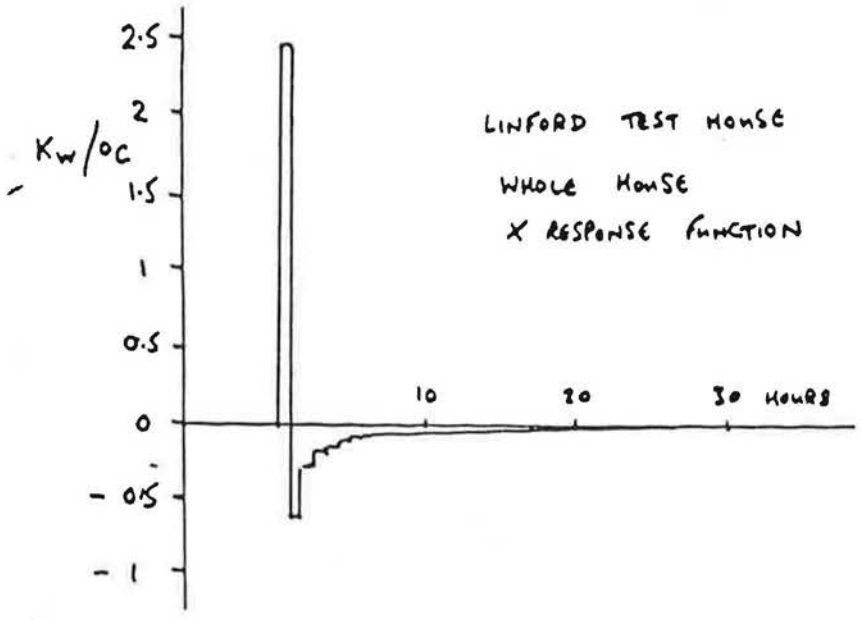
2·5
2
1·5
1
0·5
0
- 0·5
- 1
Kw/°C
LINFORD TEST HOUSE
WHOLE HOUSE
X RESPONSE FUNCTION
10
20
30 HOURS

This can be summed over 24 hours to obtain a day's total space heating requirement:-

$$\sum_{t=1}^{24} Q_t = \sum_{t=1}^{24} \left(\sum_{j=1}^{8} X_j . T_{in_{t-j+1}} \right) - \sum_{t=1}^{24} \left(\sum_{j=1}^{8} Y_j . T_{out_{t-j+1}} \right)$$

or changing the order of summation and normalising with the total heat loss U :-

$$\sum_{t=1}^{24} Q_t = 24.U . \left[\sum_{j=1}^{8} \left(\frac{\sum_{t=1}^{24} X_j . T_{in_{t-j+1}}}{24.U} \right) - \sum_{j=1}^{8} \left(\frac{\sum_{t=1}^{24} Y_j . T_{out_{t-j+1}}}{24.U} \right) \right]$$

The series in X is the internal temperature weighting function and the series in Y the external weighting function.

The summation of the individual X response functions is shown diagramatically in figures 7.6 and 7.7.

Attempts to use the internal weighting function to improve the quality of Linford regressions were not very fruitful but this may be due to the problem of defining an 'average' instantaneous house internal temperature, given six spot values, rather than defects in the mathematics. A major problem appears to be the 'differential' nature of the function, i.e. a small difference in internal temperature between one day and the next is translated into a large amount of energy being stored from one day to another. Thus small errors in internal temperature measurement become large energy errors. The Y response function is by contrast 'integrative' and small errors in external temperature are smoothed out over a long timescale.

References

7.1 R.Everett, Passive Solar in Milton Keynes, ERG 031, June 1980

7.2 T.Kusuda, NBSLD, The Computer Program for Heating and Cooling Loads in Buildings, N.B.S. Building Science Series 69, Dec.1978, U.S. Dept. of Commerce.

GIVEN A CONSTANT EXTERNAL AIR TEMPERATURE

A UNIT IMPULSE OF INTERNAL TEMPERATURE :-

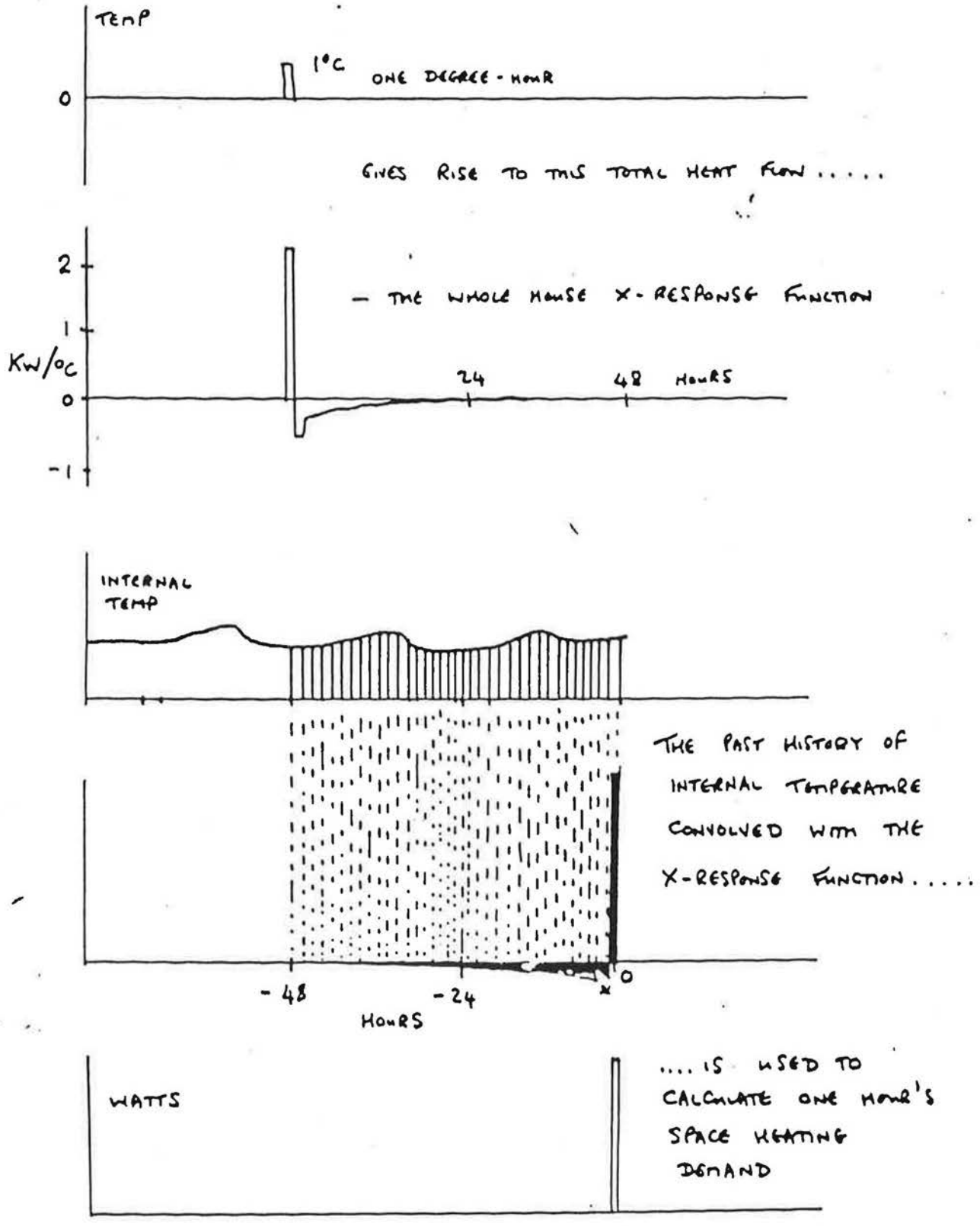

FIGURE 7.6

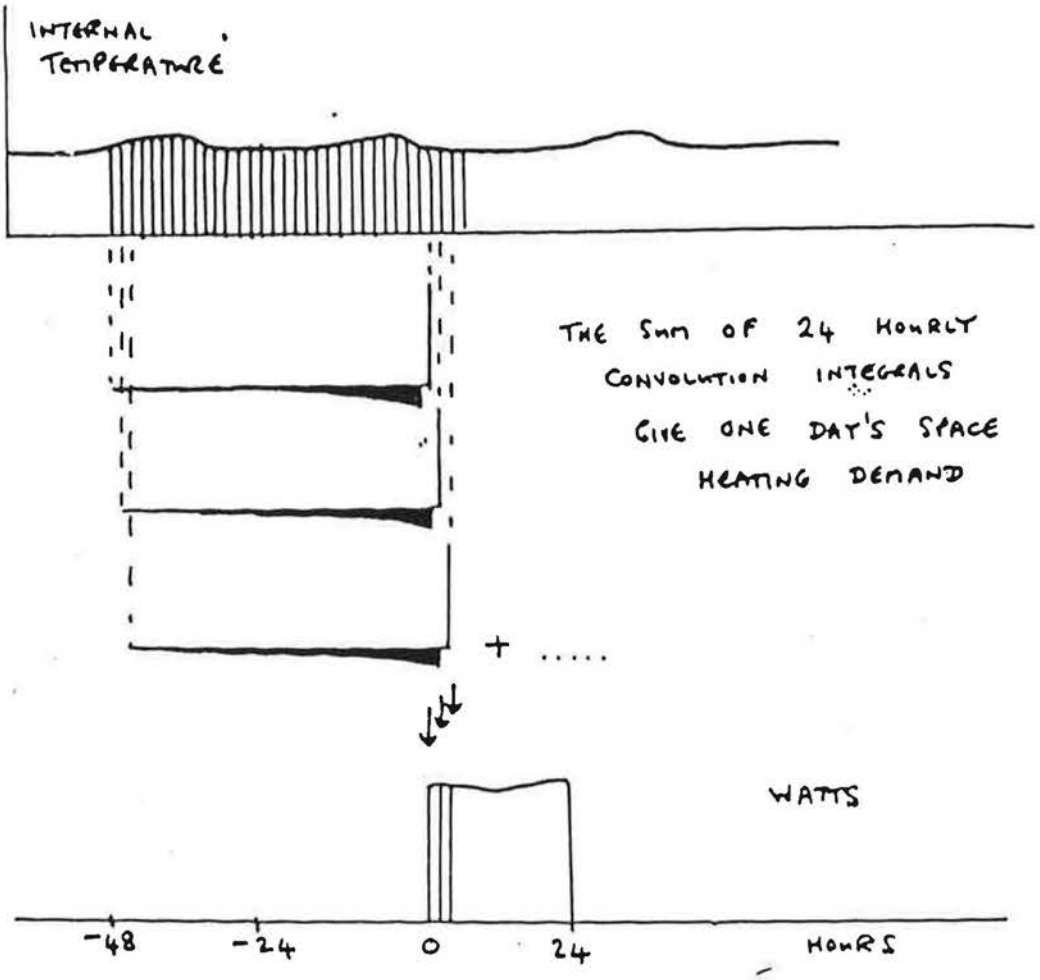

THIS IS EQUIVALENT TO CONVOLVING THE TEMPERATURE WITH A SINGLE FUNCTION WHICH IS THE SUM OF 24 X-RESPONSE FUNCTIONS EACH DISPLACED BY 1 HOUR.

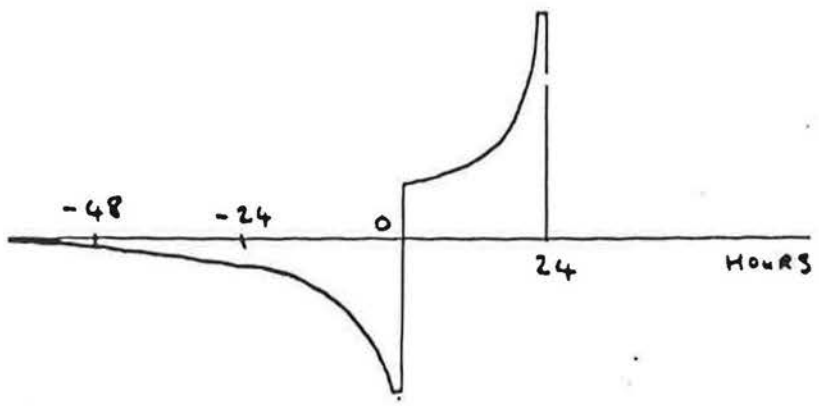

FIGURE 7.7.

THIS CURVE IS THE HOUSE INTERNAL TEMPERATURE WEIGHTING FUNCTION

8. CONCLUSIONS

CONTENTS

This chapter gathers together the main finding of this study and suggests how the rather capital-intensive equipment could be put to good use.

CHAPTER 8

CONCLUSIONS AND FUTURE POSSIBILITIES

8.1 Conclusions

Behind this study initially was the hope that the current improvements in monitoring equipment and computing power would enable thermal measurements in houses to be simplified and speeded up to such a point that it might be possible for architects or even architecture students to actually test a house design, rather than relying totally on book learning. Unfortunately, the apparent need for detailed air infiltration measurements and the temperamental nature of infra-red cameras seem to have put the process back firmly in the hands of the scientists.

However, given the right equipment, this study has shown that a reasonably rapid assessment of the thermal properties of a house can be achieved. In weather conditions similar to those in London (i.e. England and Wales) the fabric heat loss and the response to solar gains can be determined in typically two weeks measurements during the months of September to March, though three to four weeks should be allowed for worst-case conditions. The method tends to break down during the summer months for want of dull days.

At the most northerly latitudes of the U.K., around 60°N, the method also breaks down in mid-winter, from October to January, for want of sunny days, though during these months an estimate of the fabric heat loss can be achieved very rapidly indeed, in typically a week, by ignoring solar effects.

Although the Linford results have shown that the answers from one two-week period are reasonably consistent with another, the case is not totally proven because of a lack of adequate floor loss measurements. It is a pity that the analysis was carried out so long after the measurements were carried out, since the installation of more sensors could have produced conclusive answers. The solution is to try again with new test houses with a clear idea of what can be achieved.

Study of the data sets has shown that the time requirements for measurement are fairly flexible and if the researchers do not have a full two weeks to spare then all that will result is slightly less well-defined answers.

Good air infiltration measurements seem to be a major requirement in order to get good answers. Obtaining reasonably continuous measurements and filling in any missing values seems to be the most technically difficult part of the whole thermal calibration process. The results are of great interest in themselves and a lot more work is needed in this area both in terms of equipment and understanding.

Full floor heat loss measurements would also be of great interest, though measurements from a short thermal calibration would only represent a 'snapshot' of heat flows with time constants of many months.

A thermographic survey is a vital part of any thermal testing. However, the mere possession of an infra-red camera is no guarantee of results. For the Linford project an external contractor who was well trained was brought in. This was far more fruitful than attempts by researchers to operate two inferior cameras bought by the Open University.

Pressure testing of houses has been very useful in both the Linford and Pennyland projects and has given a lot of information for only a few hours work per house. The equipment is bulky, but not expensive or difficult to operate.

The Linford occupied house results have shown good agreement with those from the test house, though many assumptions have had to be made extrapolating test house floor losses and air infiltration rates. This good agreement has been a considerable surprise and indicates that occupied house energy use can make 'sense' if enough care can be put into the analysis.

Analysis of the more crudely monitored Pennyland project has shown that
a) The total house heat loss ($\Sigma A.U + C_v$) can be roughly determined (+10%-30%) for individual houses using measured data for dull weeks only. Results for groups of houses are likely to be more accurate.
b) Solar apertures for individual houses cannot reliably be determined. Answers for groups of houses of 10 or more are still only marginally significant statistically.
c) other important factors such as boiler efficiency and pressure test air leakage can be determined very easily with a minimum of monitoring effort.

Thus we have a picture that the full assessment of a group of houses (and their occupants) should perhaps take the form of a Pennyland-style monitoring scheme (weekly averages of energy use, temperatures, etc. on a fairly crude basis, plus a social survey) with brief intensive measurements on an unoccupied sample of each house type and possibly intensive monitoring of just a few occupied houses. This would be very similar to the combined Pennyland and Linford projects, though with less concentration on the intensive monitoring, which is very expensive.

Although there has been much written on the hardware needs for the actual measurement of temperatures and energy consumptions, there are also particular needs for data analysis which are rarely discussed. These seem to amount to:-

1. A computer capable of handling a reasonable disk database
2. About 1 megabyte of disk storage
3. A V.D.U. capable of handling good computer graphics.
4. A statistics software package
5. A graphics printer.
6. Intelligible software to drive it.
7. For a main-frame computer, a long-suffering system programmer.

Given that most projects have enough problems with the houses themselves and the measurement equipment, there is probably a real need for a house analysis/display software package incorporating data cleaning and statistics routines, to ease the computing burden.

8.2 The Travelling Laboratory

The thermal calibration/house assessment process requires the use of complex equipment that requires careful nursing, viz. an air infiltration measurement rig and an infra-red camera. In the past data-logging equipment has also required considerable nursing and data analysis has been incredibly tedious and slow.

The whole process of testing house designs has been extremely laborious and the Linford project has been no exception. Expertise in the various aspects has had to be gathered together, equipment bought and coaxed into operation just to test one house design, after which all the expertise and equipment is wasted.

Given a serious government commitment to energy conservation and a genuine interest in testing houses (we test cars every year!), it would not seem impossible to envisage a group of researchers going on tour with a travelling laboratory. This kind of thing has been in various 'house doctor' and retrofit programmes using thermographic surveys, pressure testing and crude monitoring (see refs. 8.1 & 8.2). The suggestion here is that the process can be taken a step further to give hard quantitative answers for fabric heat losses and solar gains with more intensive measurement.

The team would consist of four or five researchers who, armed the appropriate equipment could tour the country carrying out thermal calibrations on about five houses over the winter plus pressure tests and thermographic surveys on many more (in Sweden every other new house has to be pressure tested). This would build up a considerable body of knowledge on the performance of different house types, all tested with the same equipment.

This would require a certain amount of equipment development. An air infiltration rig of the complexity of the British Gas 'Autovent' system does not travel well. Fitting out a house with the necessary gas injection and sampling tubes is a messy business, as is wiring up temperature and heat flux sensors to a datalogger. However, with practice, this need not consume more than a day or two per house.

The important thing is that equipment and expertise should be carried from house to house, rather than being accumulated and dissipated as has been the case in past projects.

The equipment costs are not cheap, probably around £80-100,000, with running costs of as much again per year. However, with new house construction running at 150,000 per year (it will have to rise to 250,000 in the near future to replace the gently decaying U.K. housing stock [ref.8.3]), with accompanying fuel bills of £50-100 million/yr, it seems ludicrous not to have adequate tools to test the product.

References

8.1 A.Hildon, L.J.Heap, M.Trollope, R.Watkins, Case Studies of Retrofits to Existing Energy Typical Dwellings, CIB W67 Energy Conservation in the Built Environment, Dublin 1982.

8.2 R.A.Grot, Field Techniques for Measuring the savings of Energy Improving Retrofits in Single Family Dwellings, Colloquium Comparative Experimentation of Low-Energy Houses, University of Liege, 1981 (C.E.C. EUR 7419 EN).

8.3 M.Hillman, A.Bollard, Less Fuel More Jobs, Policy Studies Inst. Pub. No. 644.

Experimental Thermal Calibration of Houses

J.B. Siviour, B.Eng., Ph.D., Electricity Council Research Centre, Capenhurst, Chester, CH1 6ES, United Kingdom.

Paper presented at the Colloquium 'Comparative Experimentation of Low Energy Housing', University of Liege, 1981.

Abstract

A comprehensive thermal calibration procedure has been developed to measure the transmission and ventilation heat losses of unoccupied houses and their solar heat gain. It covers both whole house testing, and detailed measurements for surface temperature distribution and local heat flows through any component. Places where air leakage occur may also be identified.

Introduction

The calibration procedure for unoccupied houses described in this paper covers whole house testing, individual component measurements for surface temperatures and heat flow, and tests for airtightness.

The period of testing depends on the information required. Airtightness tests can be carried out in a day or less, including setting up and removing the apparatus. Ventilation tests require a minimum of a few days and usually longer if a calibration is required in terms of wind speed, direction and temperature difference to cover a range of these variables.

Surface temperature measurements using an infra-red camera are instantaneous, although several hours or even a day may be needed for temperatures to stabilise when heating the house from cold. Using colour photography to record infra-red pictures of all surfaces takes a few days.

For whole house thermal calibration the shortest period is a week, preferably in mid-winter when solar heat gain is small because it has to be calculated. For greater accuracy, and to obtain solar heat gain experimentally from the same measurements as for transmission and ventilation heat losses, would require a period of 6 weeks in late autumn or early spring.

Testing outside the heating season would be less accurate. Solar heat gain would be high and lead to inaccuracies in the determination of the transmission heat loss. Internal temperatures would have to be higher than during the heating season to maintain a suitable temperature elevation above the outside, and this can have an effect on timber moisture content, its shrinkage and house airtightness.

Calibration equipment is installed for the period of tests only. It

comprises heaters, thermostats, temperature recorders, tracer gas supply and sampling tubes and mixing fans in each major room for whole house tests. Additional equipment is required for detailed component measurements and for recording weather data.

Whole house calibration theory

The whole house calibration is based on the fact that under steady conditions the heat input to the house equals the heat lost by transmission and ventilation. With no occupancy and electric heating the only other heat input is from the sun, and the energy balance can then be expressed as:

electric heating (EEN) + solar heating (SEN)
= transmission heat loss (TEN) and ventilation heat loss (VEN) (1)

The balance strictly applies only when there is no change in heat stored in the structure and heat lost by evaporation. With steady internal temperatures, experience and simple calculations show that changes in external temperatures have negligible effects when measurements are averaged over periods of seven consecutive days.

It is convenient to work in terms of kWh/day averaged over these seven day periods. Electric heating (EEN) is measured directly. Ventilation heat loss is obtained from measurements of ventilation rates (V) and temperature elevation of the ventilation air:

$$VEN = V\Delta T \rho c \ 24 \ vol/3600 \qquad (2)$$

Ventilation rate V is in house volume air changes per hour and ΔT in K, ρ is the air density (kg/m^3) c is the air specific heat (kJ/kg K) and vol the house volume (m^3). The 24/3600 is needed to give the value of VEN in kWh/day.

Substituting 1.2 kJ/m^3K for ρc and simplifying gives:

$$VEN = V\Delta T \ vol/125 \quad kWh/day \qquad (3)$$

The theoretical transmission heat loss (TEN) is calculated from component areas (A), thermal transmittance values (U) and internal to external temperature differences (ΔT):

$$TEN = \Sigma AU\Delta T \ 24/1000 \text{ or } 0.024\Sigma AU\Delta T \quad kWh/day \qquad (4)$$

Substituting equations (3) and (4) into equation (1), rearranging and dividing by ΔT gives:

$$\frac{EEN}{\Delta T} - \frac{V.vol}{125} = 0.024 \ \Sigma AU - \frac{SEN}{\Delta T} \qquad (5)$$

The left-hand side can be evaluated from measurements. The only unknown variable is then SEN, since 0.024 ΣAU is constant and ΔT is measured. By plotting the left-hand side against known solar values representative of SEN/ΔT both 0.024 ΣAU (the intercept) and SEN/ΔT can be obtained. Figure 1 shows this using the theoretical solar heat gain through the glazing (SENG) calculated in the way described later.

The value of the intercept and therefore 0.024 ΣAU is around 2.58 kWh/day K, varying slightly with the three correlations given in the figure. Those with 18 data sets exclude the sunnier results, and there is

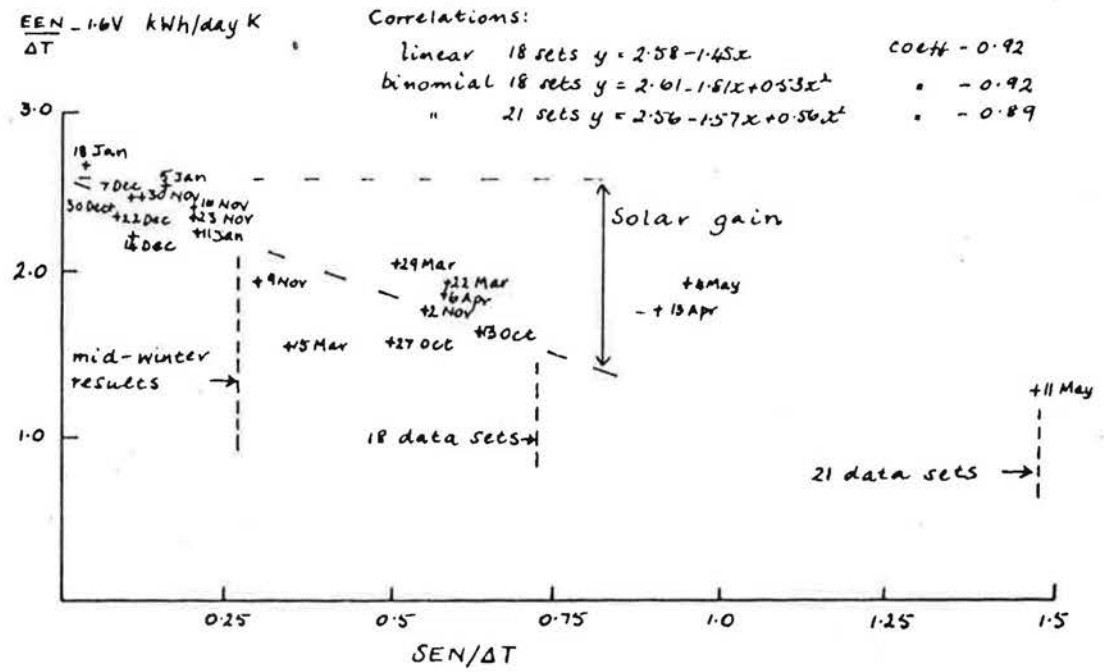

Figure 1. Graph for determining whole house experimental transmission heat loss and solar heat gain. Seven day periods are identified by the middle day date.

insignificant difference between linear or binomial correlation in either intercept or correlation coefficient. The value of the intercept can now be used in equation (5) with the experimental results to evaluate SEN.

Mid-winter results (16 November to 18 January in figure 1) cluster because the values of the weekly average insolation are similar. Six weeks of testing during this period would not produce a reliable intercept value. The minimum six-week test period needed to obtain a reliable intercept needs to include sunnier weather, for example, from 2 November to 7 December.

If tests are restricted to within the mid-winter period then it may be best to depend on a calculated value of SEN, to use in equation (5). A week of testing may be long enough. Fortunately, solar heating during mid-winter is small (~5 kWh/day), ΔT is large (15 K or more) and relatively large errors (±20%) in calculating SEN will have little effect on the value of 0.024 ΣAU.

The first step in calculating SEN is to calculate the solar heat gain through the glazing (SENG) and then add to it the effective solar heating (SENS) through the non-glass area. The curves (1) in figure 2 can be used to obtain insolation on vertical surfaces from insolation measurements on the horizontal plane. Values of SENG are then calculated using the glass areas for each orientation, making allowances for shading and ground reflectance, and solar gain factors for example for plain glass of 0.76 for single glazing and 0.65 for double glazing (2).

For SENS test results (3,4) have shown that it varies as a percentage of SENG from about 33% for a well insulated house with double glazing ($\bar{U}$ elsewhere <0.5 W/m^{2}K) to 50% for a poorly insulated house with single

glazing ($\tilde{U}$ elsewhere >1.5 W/m^{2}K). Put another way then this variation in SENS is 1% to 2% of the insolation on the whole of the exterior surface.

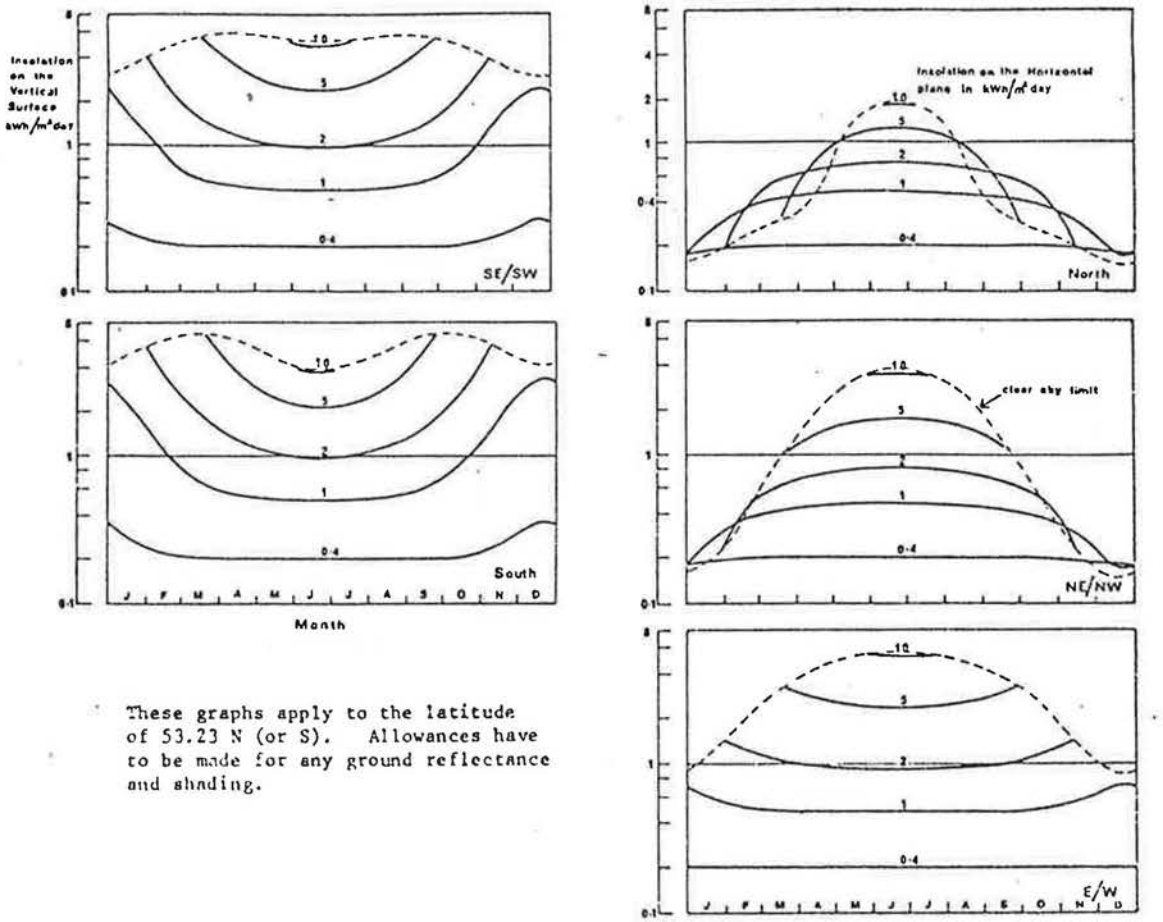

Figure 2. Graphs for obtaining insolation on vertical surfaces from measurements on the horizontal plane (1).

One way of obtaining SEN separately is to test with no heating other than the sun (EEN = 0) and use the theoretical value of $0.024\Sigma AU$ in equation (5). Difficulties arise from the small temperature elevation ($\sim$1 or 2 K) of the inside above the outside. Temperature variations around the house may be significant. Errors in measuring temperatures of ± 0.25 K may give an acceptable percentage error in ΔT when this exceeds 10 K, but not when $\Delta T = 1$ K. There is also theoretical evidence (5) that with small temperature elevations the effect of radiation to the cold sky at night is to increase transmission heat losses by 50 to 100% in mid-winter which would mean SEN is underestimated.

Whole house calibration instrumentation and equipment

The theory outlined above shows the measurements which have to be made. The house has to be heated and internal temperatures measured. Ventilation rates have to be measured and also external weather data. Ventilation rates are best measured continuously during the whole period of tests, then the weather data needed are external temperature and insolation on the horizontal plane. For a ventilation calibration, perhaps for later use, in terms of wind speed, wind direction and temperature difference then wind velocity is needed as well.

Checks on all instrumentation and test equipment should be carried out daily. Recorded data should be analysed daily for the first few days and then no more than a week in arrears. Unless this is done errors,

omissions and malfunctions could make much of the data useless over a significant proportion of the few weeks allowed for the calibration.

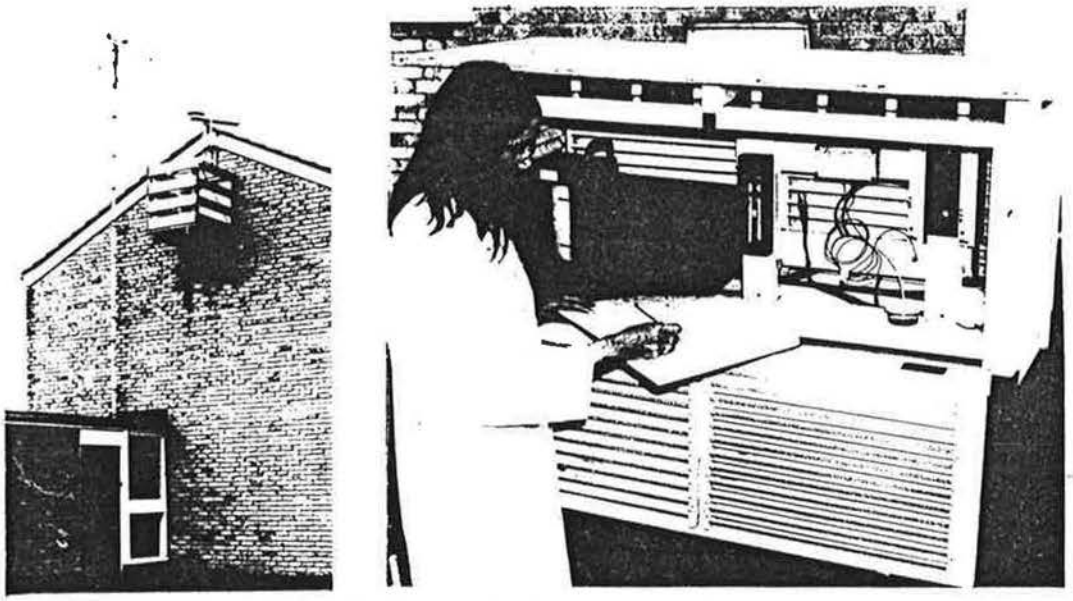

Figure 3. Weather station comprising anemometer, solarimeter and screen

Weather data can be recorded on site, figure 3, with a solarimeter mounted at ridge level, a Stevensen screen for temperature measurements, and an anemometer for wind velocity. The anemometer should be sited to obtain representative wind velocities on to the house by exposing them equally to the prevailing wind. The standard requirement for siting an anemometer, of open ground and 10m high may not be available locally, and may not be representative.

It is generally accepted that weather data recorded 10 km or even 15 km distant is sufficiently accurate when averaged over a week, although it is not known whether this has been checked. The main problem with distant weather stations is in having the data quickly enough, especially if the weather station is owned by others.

A typical set of equipment for one room is shown in figure 4. Each major room and the hall has a thermostatically controlled heater. Electricity measurements are made at each heater and for the whole house. Temperatures are recorded in each major room and the hall and landing. Analysis of results is made easier if the temperature in the house is uniform and constant to within say ± 0.5 K, because then simple averaging measured temperatures gives a satisfactory whole house average. Internal doors are left open to help in this temperature requirement. To measure ventilation rates supply tubes for tracer gas are put in front of the mixing fans* which are in the doorways blowing into each major room. Tubes are also needed from each room to sample air to measure the tracer gas concentrations.

Inside temperature measurements may be made continuously using thermograph or thermocouple on to chart recorder, with some check on their accuracy using, for example, a calibrated mercury-in-glass thermometer. Data loggers using thermocouples would normally scan hourly and then record a near instantaneous temperature. The measurements are a mix of

---

*In houses with ducted warm air heating or ventilation single point supply and sampling may suffice in the main supply and return ducts (6).

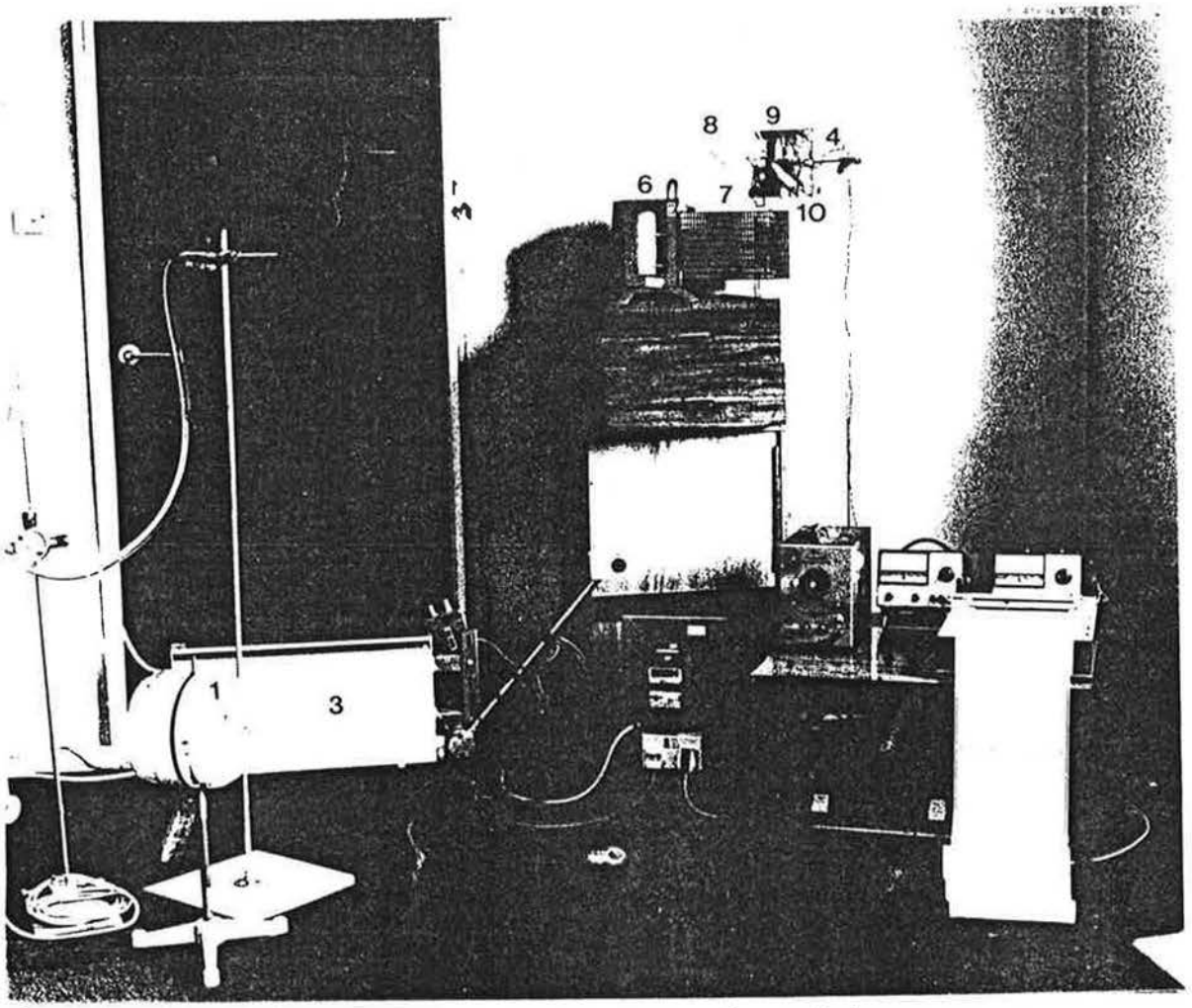

Figure 4. Experimental set up for one room (repositioned for the purpose of photograph)

(1) tracer gas supply + mixing fan, (2) tracer gas sampling, (3) electric heater, (4) heater control sensor, (5) electricity meter, (6) thermohygrograph, (7) calibrated thermometer, (8) surface mounted heat flow sensor, (9) embedded heat flow sensor, (10) differential thermocouple, (11) selector switch, (12) microvolt amplifiers, (13) chart recorder.

air (Ta) and mean radiant (Tr) temperatures. Transmission heat losses from a room are generally less influenced by Ta than Tr in the ratio Ta/Tr:0.33/0.67. People on average are about equally sensitive, i.e. Ta/Tr:0.5/0.5 (7). Instruments can be made to cover a wide range as the following list shows:

	Ta/Tr
thermocouple (aspirated, radiation shielded)	0.9/0.1
freely exposed thermocouple (bead diameter of 1.5 mm)	0.84/0.16
mercury-in-glass thermometer	0.67/0.33
bimetallic thermograph	0.67/0.33
single black globe 30 mm diameter	0.5/0.5
single black globe 150 mm diameter	0.4/0.6
double black globe	0.2/0.8

The globe instruments are particularly sensitive to air speeds (8).

In practice, errors arising from measuring the wrong mix of Ta/Tr can be

made negligible, even with air heating, under steady temperature conditions. The sensor should be placed in the centre of the room away from direct effects of the heating system, sun and radiation draughts from the windows. Then it is easy to calculate that in a well insulated house (double glazing and $\bar{U}$ <0.5 W/m^{2}K) Ta would be less than 0.4 K higher than Tr for a temperature elevation of 15 K above the outside. The difference between the mix controlling heat loss (0.33 Ta/0.67 Tr) and that of a sensor (0.67 Ta/0.33 Tr) is then only 0.1 K, an error of less than 1% of ΔT. Even in a poorly insulated house (single glazing, $\bar{U}$ of 1.5 W/m^{2}K) the error rises to only 3 to 4% with Ta 2 K higher than Tr. These small differences have been confirmed by measurements (9) in a poorly insulated house with air heating. Heating by hot water radiator eliminated the difference between Ta and Tr.

Ventilation measurements by continuous and decay methods have been used with carbon dioxide and nitrous oxide. The principles are simple (10). For the continuous method tracer gas is supplied at a measured rate continuously through each supply tube to be mixed by the fans. Each supply is adjusted separately (figure 5) so that the concentration is about uniform throughout the house as indicated by the continuous sampling from each room. Then the separate samplings can be mixed and a bulk concentration measured.

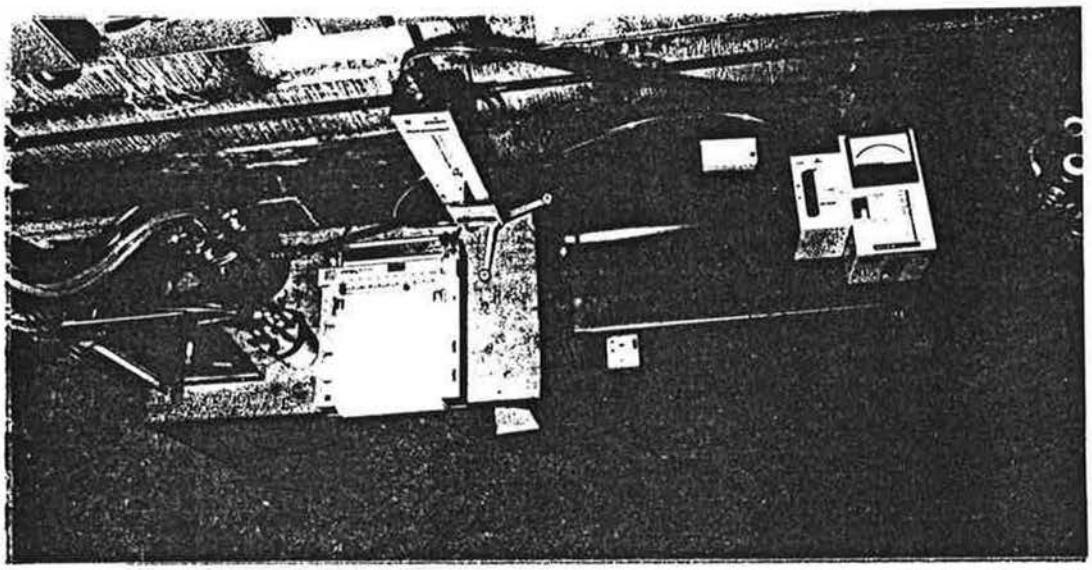

Figure 5. Apparatus for measuring ventilation rates.

(1) tracer gas flow meter, (2) tracer gas supply distribution box, (3) sampling control and mixing box, (4) sampling rate flow meter, (5) analyser, (6) chart recorder.

The ventilation rate is determined from the rate of supply of tracer gas divided by the measured bulk concentration for a gas not present in outside air. For a tracer gas such as carbon dioxide which is present in outside air the extra concentration is used as the divisor.

The tracer gas supply rate is governed by the concentration needed for analysis which itself is influenced by the ventilation rate. The relatively high concentration of CO2 in outside air ($\sim$0.033%) means that relatively large quantities of it are needed, typically 0.5 to 1.0 m^3/day to give a bulk concentration of around 0.06%. Far less N_2O is needed, $\sim$0.1 to 0.15 m^3/day because a bulk concentration of 50 ppm is suitable.

A cylinder of N_2O would therefore last weeks compared with days for a similar cylinder of CO_2.

A continuous recording of the bulk concentration gives a continuous record of ventilation rate. Hourly or 2-hourly averages with corresponding values of ΔT gives ventilation heat loss. To be exact, the value of ΔT should be calculated from the temperatures at which the air leaves and enters the house, but with steady and uniform temperatures the average of the room temperatures can be used, with the external screen temperature.

The decay method of measuring ventilation rates uses the same equipment. Tracer gas is introduced and mixed to give a uniform concentration. The supply of tracer gas is stopped and the bulk rate of decay of concentration measured. Thorough mixing makes the rate of decay the same in each room. For a tracer gas not present in outside air, ventilation rate is deduced from the relationship:

$$\text{concentration (time t)} = \text{concentration (time zero)}^{-Vt}$$

where V is the ventilation rate in house volumes per hour. A graph of ln concentration against ln t will have a slope of -V.

Changes in wind speed, direction and ΔT alter the routes of air infiltration and therefore the required rate of supply of tracer gas to each room to maintain near uniform concentration throughout the house. Adjustment to each supply rate is needed at times according to the measured concentrations from each sampling point. A correlation of ventilation in terms of wind speed, direction and ΔT is useful for use at other times but there is evidence of summer to winter variations in airtightness arising probably from expansion and contraction of timber due to changes in moisture content (6).

Component measurements

Detailed measurements on the components separately may be required if the whole house calibration is unsatisfactory to show experimentally:

(a) the thermal performance of each component.
(b) local areas of high transmission heat loss, for example, due to thermal bridging, missing insulation, and at corners.
(c) places of air leakage.

The equipment needed is an infra red camera, preferably with a colour monitor and colour film camera, small contact heat flow sensors, and a smoke generator with pressurisation equipment. Some examples are given here where the equipment has been used.

The equipment used for measuring heat flow is shown in figure 6 in use on an insulated wall (11). The sensing head is shown held in place with adhesive tape with a thin layer of grease between the sensor and wall surface for good thermal contact. The sensor is very responsive and sensitive and it is best to record its output continuously, rather than depend on spot readings, as the record will show fluctuations. The paper screen is used to eliminate the effects of radiation onto the sensor from people running the tests. A human face 0.5m away increases the sensor output by around 25%, taking about a minute to reach the new output. The heating needs to be either at a constant input or very closely controlled, for example, using a thermistor. The normal bi-metallic thermostat controlling the fan heater gives an air temperature swing of ±2K and a heat

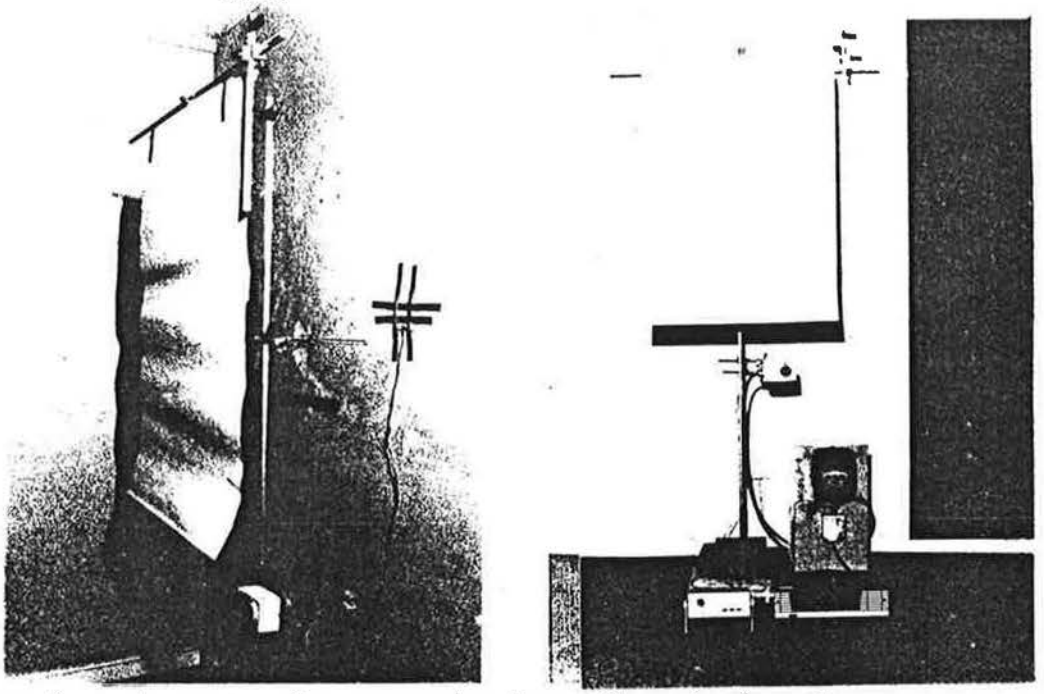

Figure 6. Apparatus for measuring heat flow showing the sensor on a wall screened from direct human radiation by a sheet of paper. The thermostat acts as a high temperature cut-out rather than control.

flow swing of ±70% (30% to 170%). Temperature stabilisation is also important. Room and wall temperatures have to be steady so the heating needs to be on for at least 6 hours before taking measurements. Fitting the sensor disturbs temperatures locally and readings should not be taken for at least an hour. This period should allow the temperature of the instrumentation to stabilise.

The effects of external changes in temperature and insolation on the outer surface on heat flow at the inner surface are delayed by several hours. Again a continuous recording of heat flow would be useful to see the changes and for making a 24 hour average.

Results of some measurements are shown in figure 7. An average heat flow rate of 9.8 W/m^2 was measured at the inner surface of the plasterboard and 7.9 W/m^2 on the inner surface of the insulating block. One explanation for this difference is that air flow in this cavity gives it a negative thermal resistance. The theoretical heat flow is 4.9 W/m^2, which means that there is an additional flow of 2.9 W/m^2. Measurements of temperatures through the wall show this to be because the foam insulation works far less well than predicted, corresponding to a k value of 0.08 W/mK rather than the value of 0.038 W/mK used in calculating the theoretical flow.

For measuring surface temperatures, the infra-red camera would be used. Insulated walls have warm surfaces internally and cold surfaces outside, provided of course the buildings are heated. A composite inside photograph is produced in figure 8. It is of the wall in figure 7. There are significant changes of 2 K over the wall. The outline of the insulated door to an outside porch is clearly visible and the threshold is very cold. The cold corner to the right of the picture is at the abutment to a timber-framed outside wall.

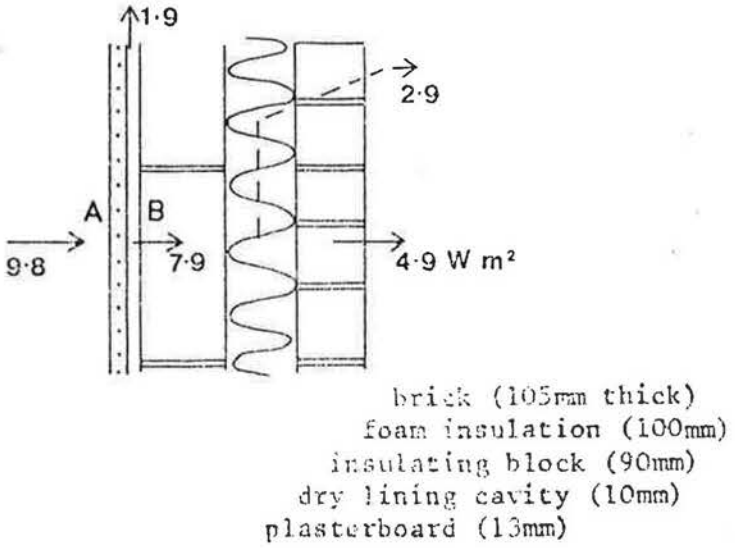

Figure 7. Thermal analysis of an external house wall based on heat flow measurements at surfaces A and B.

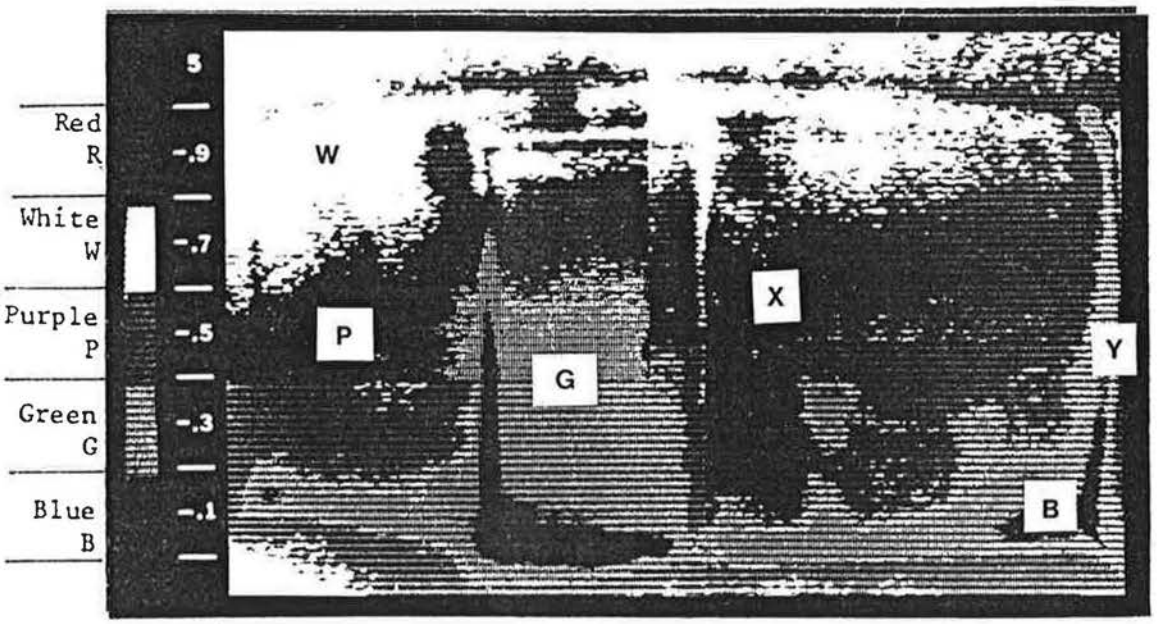

Figure 8. Infra-red composite photograph of an insulated wall. The original photograph was in colour as indicated, with each colour representing 1 K difference. Positions measuring representative (X) and local heat flows (Y) are shown.

Such a picture shows where to put heat flow sensors for both representative measurements (at X) and at cold spots (at Y). It is important to measure heat flow at cold spots because they may not be places where local heat flows are high, but where cold outside air is infiltrating which would reduce heat flow.

External surface temperatures may also be measured using the infra-red camera. Figure 9 shows this for a pair of houses, with a normal photograph included. The house on the left of the picture is well insulated

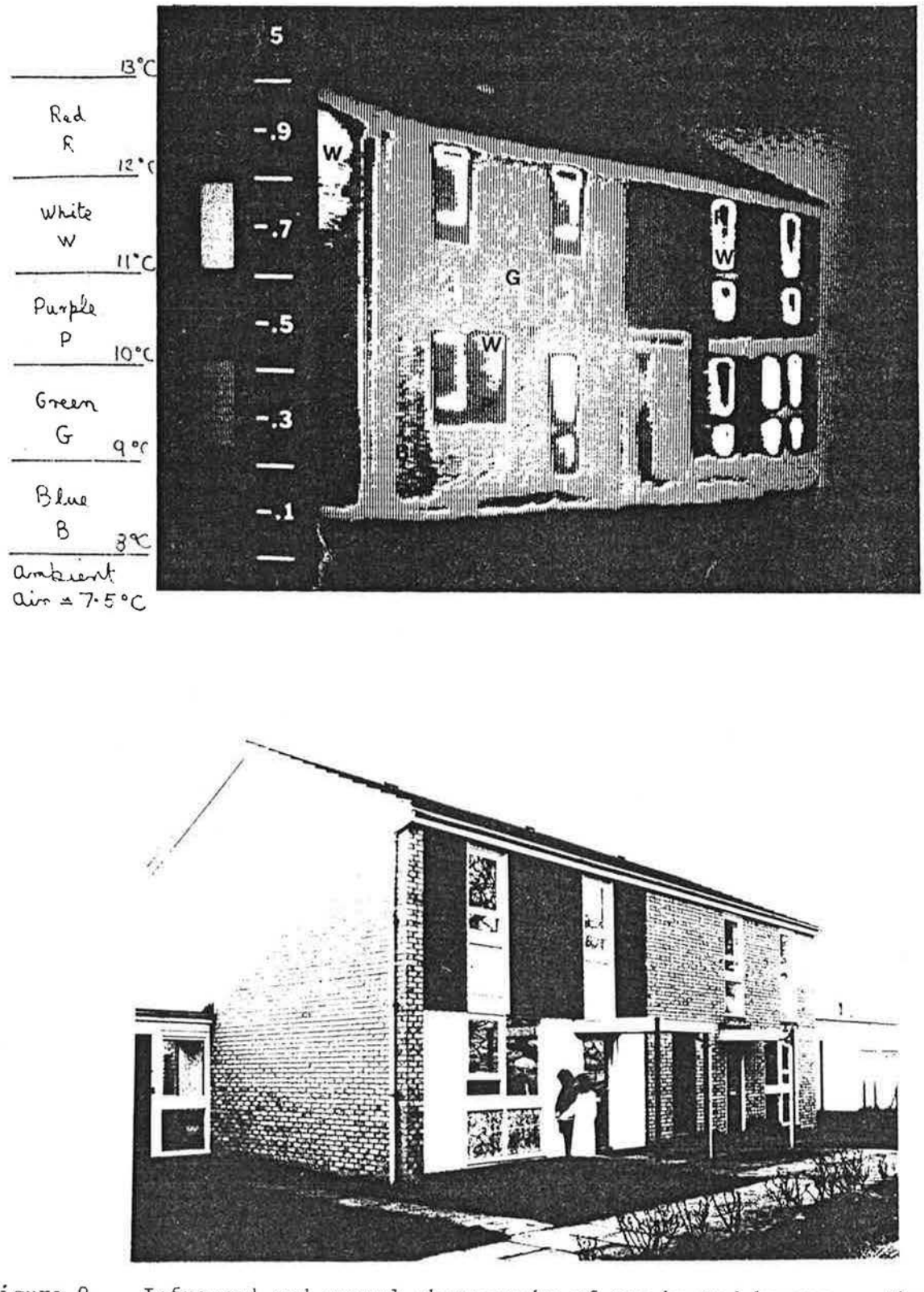

Figure 9. Infra-red and normal photographs of two heated houses. The one on the left is well insulated (wall $U < 0.5$ W/m^{2}K) and the one on the right poorly insulated (wall $U \approx 2.0$ W/m^{2}K). The original infra-red photograph was in colour as indicated.

(U ∿0.3 to 0.5 W/m^2K, double glazed) and the one on the right poorly insulated (U ∿2.0 W/m^2K, single glazed) and the colder outer surfaces of the insulated house show this. The lower sections of the windows of the left hand house have been insulated internally, explaining why their surface appears at the same temperature as the rest of the front wall. The left-hand wooden cladding is the coldest part of the front wall, suggesting that it is better insulated than the rest, but it could be that cold outside air is getting behind the cladding.

The surface of most of the double glazing is in fact purple and white compared with white and red for single glazing, except for two red strips at the top of the openable upstairs windows. Here the explanation is warm air leaking from inside.

The gable wall is insulated, yet its colour, purple and white, suggests otherwise. The explanation is the residual effect of the sun. The IR photograph was taken about 4 hours after sunset on a sunny November day. The normal photograph was taken mid-afternoon.

The roof looks uniformly blue and cold, even though the loft insulation was 300 mm thick in the insulated house and 20 mm thick in the other. What is being seen is the reflection of the cold night-time sky.

Air leakage paths could be identified by slight pressurisation of the house or room, using a fan in a false door (10). Smoke generated in figure 10 shows clearly leakage around the window frame.

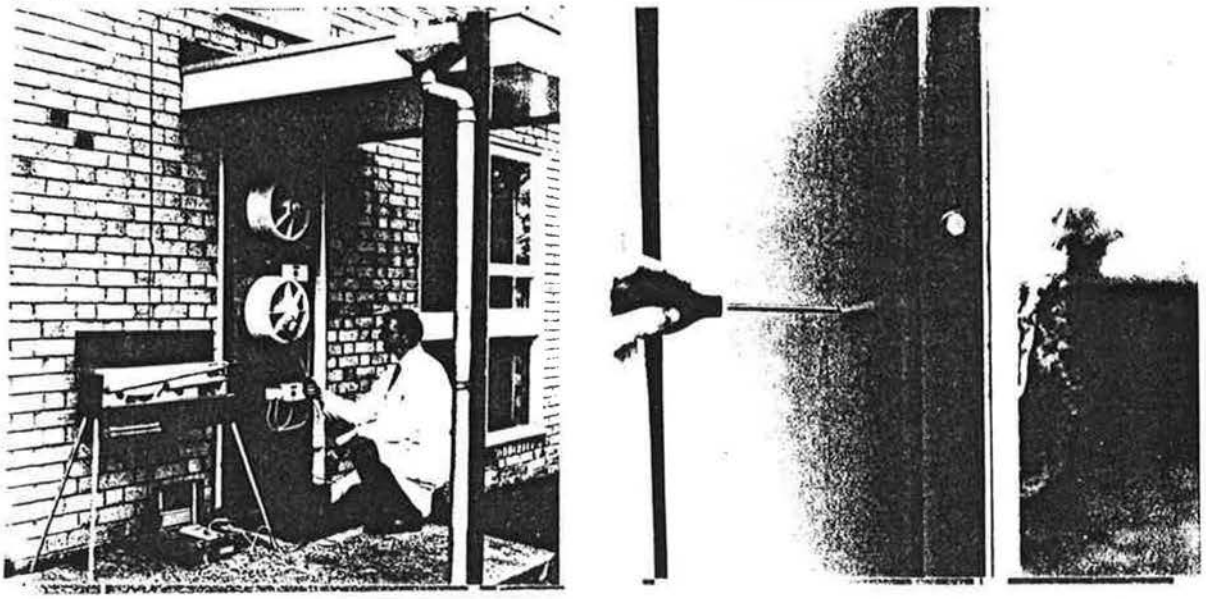

Figure 10. Pressurisation testing revealing air leakage between wall and window frame.

Concluding remarks

The results obtained using the procedure presented in this paper depend very much on the skill of the people operating it and on their familiarity with the equipment. Setting up in a test house is essential to gain experience and check the equipment before on-site testing. The extent of testing must be defined clearly because in many cases not all the tests may be needed, afforded, or carried out in the time available.

References

1. P. Basnett. Curves for Determining Solar Radiation Incident on Vertical Surfaces. ECRC/1199, 1978.

2. CIBS Guide A6. Chartered Institution of Building Services, 1970.

3. J.B. Siviour. Theoretical and Experimental Heat Losses of a Well Insulated House. ECRC/ , 1981.

4. J.B. Siviour. Houses as Passive Solar Collectors. ECRC/1070, 1977.

5. J.B. Siviour. A Simplified Theoretical Assessment of the Effects of Sky Radiation Temperature on Building Heat Loss. Temperature without heating of buildings. Symposium held in Brussels and Liege, May, 1979, 255-258.

6. J.B. Siviour & A.E. Mould. A Tracer Gas Method for the Continuous Monitoring of Ventilation Rates. CIB S17, Holzkirchen, 28-30 September, 1977.

7. D.A. McIntyre. Indoor Climate. Architectural Science Series. Applied Science Publishers Ltd., Barking, Essex, England, 1980.

8. D.A. McIntyre. A Polyethylene Shielded Globe Thermometer. ECRC/940, 1976.

9. J.B. Siviour. The Effects of Weather on House Heating Requirements. An Interim Report on Unoccupied Houses. ECRC/710, 1974.

10. D.J. Dickson. Methods of Measuring Ventilation Rates and Leakage of Houses. ECRC/1419, 1981.

11. D.A. McIntyre & J.B. Siviour. U-value Meters in Theory and Practice. ECRC/1455, 1981.

Appendix 2 Air Temperatures and High Solar Flux

The modelling of house energy use has assumed that heat is lost to the external air temperature, T_a, though no allowance has been made for the effects of solar radiation on the external wall and roof surfaces. The air temperature which has been used for thermal calibration purposes has been measured inside a Stevenson screen. This is essentially a white-painted box fitted with louvred sides (see figure A.2.1). . The problem is the degree to which this arrangement actually measures trueair temperature on sunny days, and the resulting errors that this may cause in determining the solar aperture.

For crude calculation purposes we can assume that the box is made of some perfectly conducting substance so that at any time it has the same temperature all over. We can also assume it to be a 1 metre cube, for simplicity. If we work on a daily average basis and take a typical spring day with a daily total of south-facing solar radiation of 1 kWhr/m^2, then the radiation on the top, east and west faces will also be approximately 1 kWhr/m^2. The radiation on the north face will be about 0.4 kWhr/m^2. Assuming a solar absorptivity of 50%, this gives a daily total solar absorption of 4.4 x 0.5 = 2.2 kWhr.

This absorbed solar radiation will raise the daily average box temperature above the true air temperature T_a by an error amount e_1. The energy will be conducted back to the external air through surface resistances assumed to be 0.055 $m^2{}^oC/W$ on the outside of the box and 0.13 $m^2{}^oC/W$ on the inside.

$$\text{Solar Absorbed} = \text{Heat Lost to Air Outside Box} + \text{Heat Lost to Air Inside Box}$$

$$\frac{2.2 \times 1000}{24} = \frac{e_1 \times 6}{0.055} + \frac{e_1 \times 6}{0.13}$$

$$e_1 = 0.59\ ^oC$$

i.e. the daily average screen temperature is raised by 0.59°C for every kWhr/m^2 day of south-facing solar radiation.

The actual temperature sensor is mounted inside the box. It is coupled to the box temperature by a radiation resistance and by a convection resistance to the internal air, assumed to be at the same temperature as the external air.

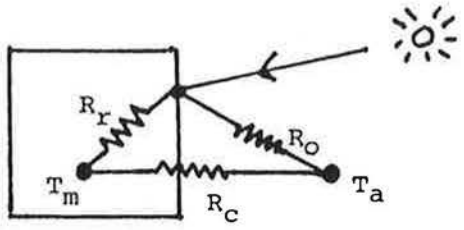

Assuming a high surface emmisivity of 0.9 and a value of the radiation coefficient h_r of 5.1 $W/m^2{}^oC$ gives the radiation resistance R_r = 0.22 $m^2{}^oC/W$.

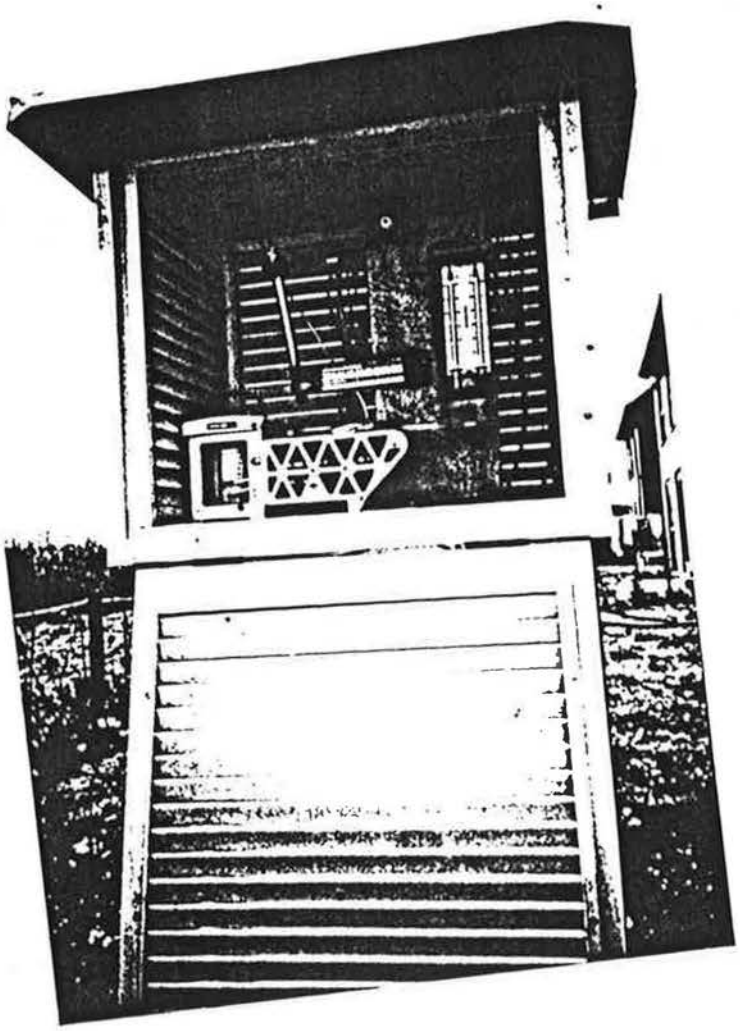

Figure A.2.1. Stevenson Screen containing various temperature sensors.

The convection resistance R_c has been taken as 0.13 $m^2{}^oC/W$, assuming an internal air movement of 0.5 m/sec. The average measured air temperature T_m would thus lie somewhere between the true air temperature T_a and the box surface temperature $T_a + e_1$. If $T_m = T_a + e_2$ then:-

$$e_2 = e_1 \cdot \frac{R_c}{R_r + R_c} = 0.59 \cdot \frac{0.13}{0.35}$$

$$e_2 = 0.22^oC$$

Thus for every kWhr/m^2day of south-facing solar radiation, the average daily temperature is in error by 0.22°C.

While this is not very important for most purposes it can have an effect on the determination of the solar aperture by regression.

If we take the house heat balance equation:-

$$Q + K = (\Sigma U.A + C_v).(T_{in} - T_a) - R.S$$

and substitute for T_a the measured air temperature $T_m = T_a + e_2.S$:-

$$Q + K = (\Sigma U.A + C_v).(T_{in} - T_m + e_2.S) - R.S$$

$$= (\Sigma U.A + C_v).(T_{in} - T_m) - (R - e_2.(\Sigma U.A + C_v)).S$$

We are thus likely to get a regression with the same value of house heat loss, but with a smaller solar aperture, the reduction being dependent on the magnitude of the heat loss. For the Linford houses with a total heat loss of about 5 kWhr/°C day this apparent reduction in solar aperture amounts to:-

$$e_2 . (\Sigma U.A + C_v) = 0.22 \times 5 = 1.1 \ m^2$$

This may go some way in explaining the discrepancy between the calculated solar aperture with clear windows of 13 m^2 and the measured value of 10 m^2.

This calculation is obviously very crude and the answers will vary enormously with wind speed. The basic tendency for the solar aperture to be cancelled out in proportion to the house heat loss has a curious consequence. It may mean that for a house with a high heat loss and a small window area it will be impossible to detect any response to solar radiation for the simple reason that the Stevenson screen is a better passive solar collector than the house.

It may be necessary in future passive solar projects to make sure that an aspirated air temperature sensor is used, although this will then no longer be a true 'meteorological' parameter.

Night sky radiation effects may slightly offset this solar problem, since sunny days are likely to have cloudless nights during which the radiation temperature will be less than the air temperature. Initial calculations suggest that these effects are at least a factor of three smaller than the basic solar effect.

Appendix 3

Weighting Function Data

Tables A1.1 to A1.3 give Y-Response functions of typical roof and wall constructions. These functions, when multiplied by the total area of the individual building component can be used to build up the whole-house Y-response function as described in Chapter 7. Items such as windows and (if included) ventilation loss are deemed to have no thermal mass and their Y-response function has one term, the U-value, at zero time.

Examination of Table A3.1, typical roof constructions, shows very little time lag, with the response functions peaking after only an hour or two. These small lags are not going to make much difference the whole house daily average temperature response, so for practical purposes they could be treated the same as for windows, with a single Y-response term equal to the U-value, at zero time.

Tables A3.1 and A3.2 show a similar response for lightweight timber-frame construction with lightweight cladding on the outside. However, once brick and blockwork is incorporated into the walls, appreciable time lags will occur. For the wall constructions used in the Linford and Pennyland houses, with a dense concrete inner leaf and brick outer leaf, the Y-response function peaks after about 10 hours and still has significant terms lasting well into the next day.

Comparison of similar wall structures at different insulation levels shows that the time lags are more related to the thickness and density of the brick and blockwork than the thickness of the insulation.

Tables A3.1 - A3.3 will at least give some idea of the scale of time lag problems in typical houses. Any researcher wishing to try the method on a particular house will probably have to calculate his own values, paying careful attention to the actual thickness and density of the wall construction. Since it is the nature of the long exponential tail of the response function that we are likely to be interested in, rather than the detailed short-term response, relatively crude finite-element modelling could be used, rather than the complex and rather time-consuming response factor calculation method of the NBSLD program.

Table A3.1

Typical House Roof Constructions - Y-Response Functions

Hours Delay	Plasterboard, 50 mm fibreglass, loft space, tiles U-value = 0.62 W/m^2/°C	Plasterboard, 80 mm fibreglass, loft space, tiles U-value = 0.45 W/m^2/°C	Plasterboard, 150 mm fibreglass, loft space, tiles U-value = 0.25 W/m^2/°C
0	0.0374	0.0231	0.0418
1	0.1811	0.1235	0.1384
2	0.1509	0.1083	0.0526
3	0.0944	0.0696	0.0116
4	0.0582	0.0440	0.0023
5	0.0358	0.0278	0.0004
6	0.0221	0.0176	0.0000
7	0.0136	0.0111	0.0000
8	0.0083	0.0070	0.0000
9	0.0051	0.0044	0.0000
10	0.0031	0.0028	
11	0.0019	0.0017	
12	0.0012	0.0011	
13	0.0007	0.0007	
14	0.0004	0.0004	
15	0.0002	0.0002	
16	0.0001	0.0001	
17	0.0001	0.0001	
18	0.0000	0.0000	

Table A3.2

Y-Response Functions - Sample Wall Constructions

Increasing Thermal Mass →

Hours Delay	200mm Brick U-value 1.98 W/m²/°C	100mm Lightweight Conc Unfilled cavity 100mm Brick U-value 1.0 W/m²/°C	Plasterboard 50mm Fibreglass Plywood U-value 0.57 W/m²/°C	Plasterboard 50mm Fibreglass 100mm Brick U-value 0.57 W/m²/°C	100mm Lightweight Conc 50mm Fibreglass 100mm Brick U-value 0.47 W/m²/°C	100mm Dense Concrete 50mm fibreglass 100mm Brick U-value 0.57 W/m²/°C
0	0.00008	0.00003	0.00629	0.00042	0.00000	0.00000
1	0.01451	0.00791	0.08308	0.01720	0.00078	0.00080
2	0.08615	0.05058	0.13687	0.05529	0.00768	0.00581
3	0.15851	0.09667	0.11851	0.07393	0.02008	0.01324
4	0.18823	0.11589	0.08430	0.07369	0.03041	0.01943
5	0.18855	0.11510	0.05491	0.06552	0.03636	0.02371
6	0.17522	0.10474	0.03407	0.05532	0.03866	0.02639
7	0.15703	0.09104	0.02051	0.04553	0.03845	0.02785
8	0.13814	0.07710	0.01211	0.03699	0.03666	0.02839
9	0.12033	0.06428	0.00706	0.02984	0.03397	0.02825
10	0.10425	0.05307	0.00407	0.02398	0.03082	0.02764
11	0.09006	0.04355	0.00233	0.01923	0.02754	0.02669
12	0.07768	0.03560	0.00133	0.01540	0.02430	0.02551
13	0.06694	0.02903	0.00075	0.01233	0.02124	0.02419
14	0.05765	0.02363	0.00043	0.00987	0.01842	0.02279
15	0.04965	0.01922	0.00024	0.00789	0.01587	0.02136
16	0.04274	0.01562	0.00013	0.00631	0.01359	0.01994
17	0.03680	0.01268	0.00007	0.00505	0.01159	0.01854
18	0.03167	0.01030	0.00004	0.00404	0.00985	0.01719
19	0.02727	0.00836	0.00002	0.00323	0.00834	0.01590
20	0.02347	0.00679	0.00001	0.00258	0.00703	0.01468
21	0.02020	0.00551	0.00000	0.00207	0.00592	0.01352
22	0.01739	0.00447	0.00000	0.00165	0.00497	0.01244
23	0.01497	0.00363	0.00000	0.00132	0.00417	0.01143
Continuation Common Ratio $Y_{t+1}=Y_t$. CR	0.861	0.811	0.562	0.800	0.823	0.911

Table A3.3.

Y-Response Functions - Sample Wall Constructions

Increasing thermal mass →

Hours Delay	Plywood 100mm fibreglass U-value 0.33 W/m^2/°C	Plasterboard 100mm fibreglass 100mm Brick U-value 0.33 W/m^2/°C	Plasterboard 100mm fibreglass 100mm Brick U-value 0.30 W/m^2/°C	100mm Lightweight Concrete 100mm Fibreglass 100mm Brick U-value 0.33 W/m^2/°C	100mm Dense Concrete, 100mm Fibreglass, 100mm Brick U-value 0.33 W/m^2/°C
0	0.00234	0.00013	0.00000	0.00000	
1	0.04011	0.00774	0.00032	0.00033	
2	0.07465	0.02812	0.00366	0.00273	
3	0.06918	0.04001	0.01035	0.00660	
4	0.05183	0.04142	0.01644	0.00997	
5	0.03531	0.03785	0.02033	0.01241	
6	0.02280	0.03264	0.02222	0.01402	
7	0.01424	0.02733	0.02265	0.01498	
8	0.00870	0.02253	0.02210	0.01545	
9	0.00522	0.01840	0.02092	0.01554	
10	0.00310	0.01495	0.01938	0.01536	
11	0.00182	0.01212	0.01766	0.01498	
12	0.00106	0.00980	0.01589	0.01445	
13	0.00062	0.00792	0.01415	0.01383	
14	0.00036	0.00640	0.01250	0.01314	
15	0.00020	0.00516	0.01096	0.01242	
16	0.00012	0.00417	0.00955	0.01169	
17	0.00006	0.00336	0.00828	0.01096	
18	0.00003	0.00271	0.00715	0.01025	
19	0.00002	0.00219	0.00615	0.00955	
20	0.00001	0.00177	0.00527	0.00888	
21	0.00000	0.00142	0.00450	0.00825	
22	0.00000	0.00115	0.00384	0.00764	
23	0.00000	0.00093	0.00326	0.00701	
Continuation Common Ratio $Y_{t+1}=Y_t.CR$	0.570	0.807	0.824	0.917	